

**Synthesis and Structural Analysis of Novel Bis(triazole) UDP Analogs as Potential
Glycosyl Transferase Inhibitors**

By

Steven E. Knapp

Submitted in Partial Fulfillment of the Requirements

for the Degree of

Master of Science

in the

Chemistry

Program

YOUNGSTOWN STATE UNIVERSITY

December, 2008

Synthesis and Structural Analysis of Novel Bis(triazole) UDP Analogs as Potential Glycosyl Transferase Inhibitors

Steven E. Knapp

I hereby release this thesis to the public. I understand that this thesis will be made available from the OhioLINK ETD Center and the Maag Library Circulation Desk for public access. I also authorize the University or other individuals to make copies of this thesis as needed for scholarly research.

Signature:

Steven E. Knapp

Date

Approvals:

Dr. Peter Norris
Thesis Advisor

Date

Dr. John A. Jackson
Committee Member

Date

Dr. Nina V. Stourman
Committee Member

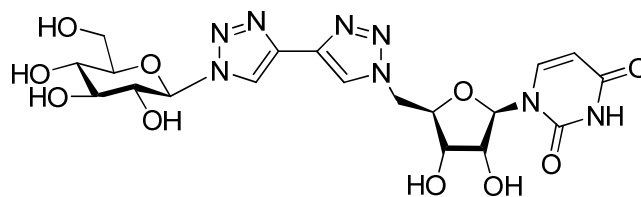
Date

Dr. Peter J. Kasvinsky
Dean of Graduate Studies and Research

Date

Thesis Abstract

The following details the synthesis of a novel bis(1,2,3-triazole), which is a potential glycosyltransferase inhibitor. A glycosyltransferase is an enzyme that is involved in the synthesis of polysaccharides, for example the capsule that protects *Staphylococcus aureus*. Bis(1,2,3-triazoles) may mimic the UDP conjugates of aminosugars (D-ManNAcA, D-FucNAc, and L-FucNAc) found in the capsular polysaccharide of *S. aureus*, and may prevent the formation of the capsular polysaccharide leaving the bacteria open to attack by phagocytosis or antibiotics. Bis(1,2,3-triazole) groups will be used to replace the phosphate linkages in the UDP-parent aminosugars. Bis(1,2,3-triazoles) may mimic the diphosphate linkage in binding to a transferase due to the N-3 lone pairs on the heterocycles.



Potential bis(triazole) transferase inhibitor.

Acknowledgements

I would like to thank the Youngstown State University Department of Chemistry and the School of Graduate Studies for allowing me the opportunity to pursue the Master of Science degree. I would also like to thank my committee members, Dr. John Jackson and Dr. Nina Stourman for their help and suggestions. Dr. Matthias Zeller has been very helpful, especially with his help solving numerous X-Ray crystal structures.

I would especially like to thank Dr. Peter Norris for allowing me into his research group and allowing me to work on a very interesting research project. I would also like to thank him for his guidance and support throughout my academic career; he has been tremendously helpful and has taught me to understand Organic Chemistry.

I would like to thank Jen, Dave, Ashley, Mike, Lucas, and Brian as well as other members of the Norris group for their support and friendship. You all made my graduate school experience very entertaining and fun.

I would also like to thank my parents Jean and Don and my girlfriend Ember for their tremendous support throughout graduate school. I would not have been able to complete this without their love, encouragement and support.

Table of Contents

Title Page	i
Signature Page	ii
Abstract	iii
Acknowledgements	iv
Table of Contents	v
List of Tables	vii
List of Schemes	vii
List of Equations	vii
List of Figures	ix
Introduction	1
Statement of Problem	16
Results and Discussion	17
Experimental	45
References	60
Appendix A	64

Appendix B 144

List of Tables

Table 1:	Reactions of sulfonyl chlorides to yield sulfonyl azides	28
Table 2:	Variations of the attempted synthesis of 10 from Roth's one-pot method.....	31

List of Schemes

Scheme 1:	Protection of β -D-Glucose.....	5
Scheme 2.	Deprotection of acid-labile protecting groups	7
Scheme 3.	One-pot conversion of aldehyde to alkyne	11
Scheme 4.	Synthesis of D-glucosyl azide.	18
Scheme 5.	Postulated catalytic cycle for azide-alkyne coupling.....	22
Scheme 6.	Mechanism of the formation of α,β -unsaturated methyl ketone 16	28
Scheme 7.	Synthesis of dimethyl(diazomethyl)phosphonate (27)	34
Scheme 8.	Mechanism of the aldehyde to alkyne conversions using dimethyl(diazomethyl)phosphonate (27).....	37
Scheme 9.	Synthesis of 5'-azido-5'-deoxy-2',3'- <i>O</i> -isopropylidene uridine (40).....	38
Scheme 10.	Deprotection of glucosyl-bis(1,2,3-triazole)-uridine 41	40

List of Equations

Equation 1.	1,2,3-Triazole formation <i>via</i> Huisgen 1,3-dipolar cycloaddition	8
Equation 2.	Synthesis of the 1,4-isomer.....	9

Equation 3.	Synthesis of a 1,2,3-triazole with propargyl alcohol	10
Equation 4.	Synthesis of triazole 8	20
Equation 5.	Synthesis of aldehyde 9 from alcohol 8	23
Equation 6.	Synthesis of aldehyde 9 via DMP oxidation.....	25
Equation 7.	Synthesis of aldehyde 9 via Swern oxidation	25
Equation 8.	Synthesis of aldehyde 9 via 2 mol % PCC with periodic acid...	26
Equation 9.	Attempted synthesis of alkyne 10 from aldehyde 9	27
Equation 10.	Synthesis of <i>p</i> -toluenesulfonyl azide 13	29
Equation 11.	Synthesis of <i>o</i> -nitrobenzenesulfonyl azide 19	30
Equation 12.	Synthesis of <i>p</i> -nitrobenzenesulfonyl azide 21	30
Equation 13.	Synthesis of 4-chlorophenylacetylene (25) from 4-chlorobenzaldehyde (24) utilizing a one-pot synthesis published by Roth <i>et. al.</i>	33
Equation 14.	Synthesis of alkyne 10 from aldehyde 9 using 27 as a reagent .	36
Equation 15.	Synthesis of 4-chlorophenylacetylene (25) from 4-chlorobenzaldehyde using 27 as a reagent.....	36
Equation 16.	Synthesis of glucosyl-bis(1,2,3-triazole)-uridine 41 from alkyne 10 and 5'-azido-5'-deoxy-2',3'- <i>O</i> -isopropylidene uridine (40)	39
Equation 17.	Deprotection of the acetyl groups of triazole 8 to yield 44	41
Equation 18.	Deprotection of the acetyl groups of aldehyde 9 to yield deprotected aldehyde 45	42
Equation 19.	Deprotection of the acetyl groups of triazole 46 to yield triazole 47	42

Equation 20.	Deprotection of the acetyl groups of glucosyl azide 3 to yield deprotected glucosyl azide 48	43
Equation 21.	Attempted synthesis of <i>tert</i> -butyl-diphenylsilyl-protected glucosyl azide 49	43

List of Figures

Figure 1.	Structures of simple “D” monosaccharides.....	2
Figure 2.	L- and D-Glucose.....	2
Figure 3.	Different anomers of glucose.....	3
Figure 4.	Sucrose and lactose.....	4
Figure 5.	Two types of triazoles.....	8
Figure 6.	Antifungal drug Pramiconazole.....	8
Figure 7.	Structures of Type 5 (top) and Type 8 (bottom) capsular polysaccharides of <i>S. aureus</i>	12
Figure 8.	Potential bis(1,2,3-triazole) transferase inhibitor (bottom) and UDP-L-fucNAc (top).....	15
Figure 9.	Structures of gauche (left) and anti-periplanar (right) conformations in 2 and 3	19
Figure 10.	X-Ray crystal structure of triazole 8	21
Figure 11.	X-Ray crystal structure of aldehyde 9	24
Figure 12.	X-Ray structure of <i>o</i> -nitrobenzenesulfonyl azide (19).....	30
Figure 13.	X-Ray structure of <i>p</i> -toluenesulfonamide (22).....	32
Figure 14.	X-Ray structure of <i>p</i> -acetamidobenzenesulfonamide (23).....	32
Figure 15.	X-Ray structure of deprotected glucosyl phenyl triazole 47	42

Figure 16.	X-Ray structure of <i>tert</i> -butyldiphenylsilanol tetramer 50	44
Figure 17.	400 MHz ^1H spectrum of glucosyl bromide 2	65
Figure 18.	100 MHz ^{13}C spectrum of glucosyl bromide 2	66
Figure 19.	400 MHz ^1H - ^1H COSY spectrum of glucosyl bromide 2	67
Figure 20.	400 MHz ^1H - ^{13}C HSQC spectrum of glucosyl bromide 2	68
Figure 21.	Mass spectrum of glucosyl bromide 2	69
Figure 22.	400 MHz ^1H spectrum of glucosyl azide 3	70
Figure 23.	100 MHz ^{13}C spectrum of glucosyl azide 3	71
Figure 24.	400 MHz ^1H - ^1H COSY spectrum of glucosyl azide 3	72
Figure 25.	400 MHz ^1H - ^{13}C HSQC spectrum of glucosyl azide 3	73
Figure 26.	Mass spectrum of glucosyl azide 3	74
Figure 27.	Infrared spectrum of glucosyl azide 3	75
Figure 28.	400 MHz ^1H spectrum of glucosyl triazole 8	76
Figure 29.	100 MHz ^{13}C spectrum of glucosyl triazole 8	77
Figure 30.	400 MHz ^1H - ^1H COSY spectrum of glucosyl triazole 8	78
Figure 31.	400 MHz ^1H - ^{13}C HSQC spectrum glucosyl triazole 8	79
Figure 32.	Mass spectrum of glucosyl triazole 8	80
Figure 33.	400 MHz ^1H spectrum of aldehyde 9	81
Figure 34.	100 MHz ^{13}C spectrum of aldehyde 9	82
Figure 35.	400 MHz ^1H - ^1H COSY spectrum of aldehyde 9	83
Figure 36.	400 MHz ^1H - ^{13}C HSQC spectrum of aldehyde 9	84
Figure 37.	Mass spectrum of aldehyde 9	85
Figure 38.	400 MHz ^1H spectrum of alkyne 10	86

Figure 39.	100 MHz ^{13}C spectrum of alkyne 10	87
Figure 40.	400 MHz ^1H - ^1H COSY spectrum of alkyne 10	88
Figure 41.	400 MHz ^1H - ^{13}C HSQC spectrum alkyne 10	89
Figure 42.	Mass spectrum of alkyne 10	90
Figure 43.	Mass spectrum of dimethyl-2-oxopropylphosphonate (11)	91
Figure 44.	400 MHz ^1H spectrum of <i>p</i> -toluenesulfonyl azide (13).....	92
Figure 45.	100 MHz ^{13}C spectrum of <i>p</i> -toluenesulfonyl azide (13).....	93
Figure 46.	400 MHz ^1H - ^1H COSY spectrum of <i>p</i> -toluenesulfonyl azide (13)	94
Figure 47.	400 MHz ^1H - ^{13}C HSQC spectrum of <i>p</i> -toluenesulfonyl azide (13).....	95
Figure 48.	Mass spectrum of <i>p</i> -toluenesulfonyl azide (13).....	96
Figure 49.	Infrared spectrum of <i>p</i> -toluenesulfonyl azide (13)	97
Figure 50.	400 MHz ^1H spectrum of α,β -unsaturated ketone 16	98
Figure 51.	100 MHz ^{13}C spectrum of α,β -unsaturated ketone 16	99
Figure 52.	400 MHz ^1H - ^1H COSY spectrum of α,β -unsaturated ketone 16	100
Figure 53.	400 MHz ^1H - ^{13}C HSQC spectrum of α,β -unsaturated ketone 16	101
Figure 54.	Mass spectrum of α,β -unsaturated ketone 16	102
Figure 55.	400 MHz ^1H spectrum of <i>o</i> -nitrobenzenesulfonyl azide (19)..	103
Figure 56.	100 MHz ^{13}C spectrum of <i>o</i> -nitrobenzenesulfonyl azide (19)	104

Figure 57.	400 MHz ^1H - ^1H COSY spectrum of <i>o</i> -nitrobenzenesulfonyl azide (19)	105
Figure 58.	400 MHz ^1H - ^{13}C HSQC spectrum of <i>o</i> -nitrobenzenesulfonyl azide (19)	106
Figure 59.	Mass spectrum of <i>o</i> -nitrobenzenesulfonyl azide (19)	107
Figure 60.	Infrared spectrum of <i>o</i> -nitrobenzenesulfonyl azide (19)	108
Figure 61.	400 MHz ^1H spectrum of <i>p</i> -nitrobenzenesulfonyl azide (21) ..	109
Figure 62.	100 MHz ^{13}C spectrum of <i>p</i> -nitrobenzenesulfonyl azide (21)	110
Figure 63.	400 MHz ^1H - ^1H COSY spectrum of <i>p</i> -nitrobenzenesulfonyl azide (21)	111
Figure 64.	400 MHz ^1H - ^{13}C HSQC spectrum of <i>p</i> -nitrobenzenesulfonyl azide (21)	112
Figure 65.	Mass spectrum of <i>p</i> -nitrobenzenesulfonyl azide (21)	113
Figure 66.	Infrared spectrum of <i>p</i> -nitrobenzenesulfonyl azide (21)	114
Figure 67.	400 MHz ^1H spectrum of 4-chlorophenylacetylene (25)	115
Figure 68.	Mass spectrum of 4-chlorophenylacetylene (25)	116
Figure 69.	400 MHz ^1H spectrum of dimethyl(diazomethyl)phosphonate (27)	117
Figure 70.	100 MHz ^{13}C spectrum of dimethyl(diazomethyl)phosphonate (27)	118
Figure 71.	161 MHz ^{31}P spectrum of dimethyl(diazomethyl)phosphonate (27)	119

Figure 72.	400 MHz ^1H - ^1H COSY spectrum of dimethyl(diazomethyl)phosphonate (27).....	120
Figure 73.	400 MHz ^1H - ^{13}C HSQC spectrum of dimethyl(diazomethyl)phosphonate (27).....	121
Figure 74.	Mass spectrum of dimethyl(diazomethyl)phosphonate (27)....	122
Figure 75.	Infrared spectrum of dimethyl(diazomethyl)phosphonate (27).....	123
Figure 76.	400 MHz ^1H spectrum of 5'-azido-5'-deoxy-2',3'- <i>O</i> -isopropylidene uridine (40).....	124
Figure 77.	100 MHz ^{13}C spectrum of 5'-azido-5'-deoxy-2',3'- <i>O</i> -isopropylidene uridine (40).....	125
Figure 78.	400 MHz ^1H - ^1H COSY spectrum of 5'-azido-5'-deoxy-2',3'- <i>O</i> -isopropylidene uridine (40).....	126
Figure 79.	400 MHz ^1H - ^{13}C HSQC spectrum of 5'-azido-5'-deoxy-2',3'- <i>O</i> -isopropylidene uridine (40).....	127
Figure 80.	Mass spectrum of 5'-azido-5'-deoxy-2',3'- <i>O</i> -isopropylidene uridine (40).....	128
Figure 81.	Infrared spectrum of 5'-azido-5'-deoxy-2',3'- <i>O</i> -isopropylidene uridine (40).....	129
Figure 82.	Mass spectrum of bis(1,2,3-triazole) 41	130
Figure 83.	Mass spectrum of deprotected triazole 44	131
Figure 84.	Mass spectrum of deprotected aldehyde 45	132
Figure 85.	400 MHz ^1H spectrum of phenyl triazole 46	133

Figure 86.	100 MHz ^{13}C spectrum of phenyl triazole 46	134
Figure 87.	400 MHz ^1H - ^1H COSY spectrum of phenyl triazole 46	135
Figure 88.	400 MHz ^1H - ^{13}C HSQC spectrum of phenyl triazole 46	136
Figure 89.	Mass spectrum of phenyl triazole 46	136
Figure 90.	400 MHz ^1H spectrum of deprotected phenyl triazole 47	138
Figure 91.	100 MHz ^{13}C spectrum of deprotected phenyl triazole 47	139
Figure 92.	400 MHz ^1H - ^1H COSY spectrum of deprotected phenyl triazole 47	140
Figure 93.	400 MHz ^1H - ^{13}C HSQC spectrum of deprotected phenyl triazole 47	141
Figure 94.	Mass spectrum of deprotected phenyl triazole 47	142
Figure 95.	Mass spectrum of deprotected glucosyl azide 48	143
Figure 96.	X-Ray crystal structure of glucosyl triazole 8	145
Figure 97.	X-Ray crystal structure of aldehyde 9	153
Figure 98.	X-Ray crystal structure of <i>o</i> -nitrobenzylsulfonamide (19) ...	162
Figure 99.	X-Ray crystal structure of <i>p</i> -toluenesulfonamide (22)	168
Figure 100.	X-Ray crystal structure of <i>p</i> -acetamidobenzenesulfonamide (23)	176
Figure 101.	X-Ray crystal structure of 4-chlorobenzoic acid (26)	182
Figure 102.	X-Ray crystal structure of 2,2,2-trifluoroethyl acedamidobenzenesulfonate (37)	187
Figure 103.	X-Ray crystal structure of 2',3'- <i>O</i> -isopropylidene uridine (38)	196

Figure 104.	X-Ray crystal structure of 47	204
Figure 105.	X-Ray crystal structure of <i>t</i> -butyl-diphenylsilanol tetramer 50	212

Introduction

Carbohydrate Structure

Carbohydrates are the most abundant type of biological molecules.¹⁻⁶ The process of photosynthesis produces 4×10^{14} kg of carbohydrates each year.⁷ They are necessary components for life, and the name means “carbon hydrate”, which comes from the chemical composition of $C(H_2O)_n$, where n is greater or equal to 3. They are the basis of many important industries, including the manufacturing of sugar, starch, paper, textile fibers, plastics, foods, fermentation, and pharmaceuticals.⁸ There are five different general classes of carbohydrates: monosaccharides, disaccharides, trisaccharides, oligosaccharides, and polysaccharides.

Monosaccharides are the fundamental units of carbohydrates; they are synthesized in the body *via* gluconeogenesis and are also an important element of nucleic acids. They are classified by the chemical nature of their carbonyl group and the number of carbon atoms they contain. Carbohydrates derived from aldehydes are called *aldoses* and those derived from ketones are called *ketoses*. The smallest monosaccharides have 3 carbons, and are referred to as trioses. Monosaccharides with four, five, six, etc. carbons are called tetroses, pentoses, hexoses, etc; the terms can be combined as well. Glucose, with the chemical formula $C_6H_{12}O_6$, is an aldohexose, while ribulose, with the chemical formula $C_5H_{10}O_5$, is a ketopentose.¹



Figure 1: Structures of simple “D” monosaccharides.

Stereochemistry within carbohydrates is important; aldoses tend to have $2^{(n-2)}$ stereoisomers, while ketoses tend to have $2^{(n-3)}$ stereoisomers (n being the number of carbons in the molecule). Glucose, for example, has 2^4 (sixteen) different stereoisomers. Aldoses and ketoses differ in the number of stereoisomers because of the position of the carbonyl groups.

Figure 1 shows the structures of D-glucose and D-ribulose. The D prefix is used when the hydroxyl on the last chiral carbon that is farthest from the carbonyl group, in a Fischer projection, is on the right hand side; L is used when the hydroxyl is on the left hand side, as shown in Figure 2. Enantiomeric L- and D-glucose are mirror images of each other. D-Glucose is the only aldose that commonly occurs in nature as a monosaccharide. The L-sugars are much less abundant biologically than are D-sugars.¹



Figure 2: L- and D-Glucose.

Alcohols and aldehydes on straight-chain monosaccharides react to give hemiacetals, while alcohols and ketones react to give hemiketals. These reactions form a heterocyclic ring, which is a ring that contains non-carbon atoms in addition to carbon. Sugars can thus react intramolecularly to yield cyclic hemiketals and hemiacetals. During these reactions, the anomeric carbon, which is the carbonyl carbon in the straight chain form, becomes a chiral center with two different anomers that exist in equilibrium, alpha and beta. Figure 3 shows the difference between the two anomers. With the alpha anomer, the alcohol substituent on the anomeric carbon is *trans*, pointing opposite of the CH₂OH on carbon five. The beta anomer arises when the alcohol substituent is *cis*, pointing in the same direction as the CH₂OH group on carbon five. Monosaccharides with six-membered rings are called *pyranoses* while those with a five-membered ring are called a *furanose*. A cyclic glucose molecule, in the six-membered ring form, is called a glucopyranose.

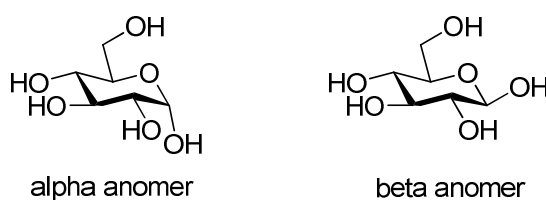


Figure 3: Different anomers of glucose.

Disaccharides are monosaccharides joined by covalent bonds, called a glycosidic bond. Sucrose, common table sugar, and lactose, milk sugar, are two common disaccharides (Figure 4). The glycosidic bond is formed from the loss of a hydrogen atom from one monosaccharide and a hydroxyl group from another. This dehydration

reaction allows for the formation of complex polysaccharides, such as, glycogen, cellulose, and starch.

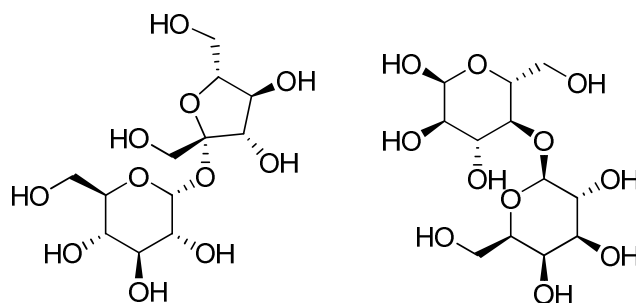


Figure 4: Sucrose and lactose.

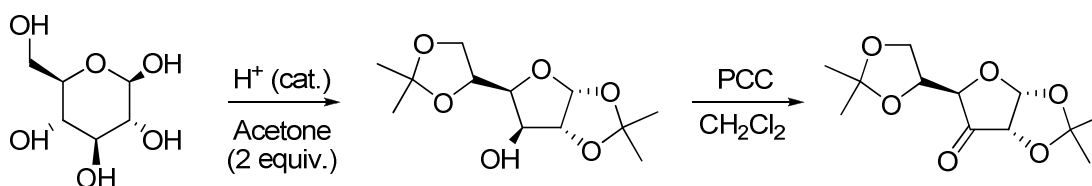
Oligosaccharides and polysaccharides consist of many monosaccharides linked by glycosidic bonds. Starch and glycogen are both polysaccharides that are found in nature. The majority of naturally occurring polysaccharides contain 80 to 100 residues.⁹ Starch is used as a source of energy in plants, while glycogen is used for energy storage in animals. Cellulose is another example of a polysaccharide that is important in nature. It is the most common organic molecule found on Earth and is found in the cell walls of plants. Cellulose is important for the production of paper; it can be used for insulation, and even to produce biofuels.

Carbohydrates, due to their biological function at the molecular level, can be of great use for development of antibiotics and other drugs. Carbohydrate constituents of glycoconjugates on cell surfaces often act as elements for signaling, for transport, and for molecular recognition that are critical in cellular communication.² However, it is often difficult to build large carbohydrate structures due to issues of stereoselectivity in

glycosidic bond formation and the need to manipulate the hydroxyl groups in donor and acceptor molecules using protection and deprotection strategies.²

Protecting Group Chemistry

In the synthesis of large molecules such as pharmaceuticals many steps are required and certain parts of the molecule being built need to be “blocked” to prevent unwanted reactions. Protecting groups are an essential key behind building large molecules. Protecting groups are introduced onto a functional group to block its reactivity under the experimental conditions needed to make modifications elsewhere.¹⁰ Glucose has five hydroxyl groups. If the intent is to oxidize one of them, the other four must be protected, for example, with cyclic ketals (Scheme 1).¹⁰ Acetone will react with four of the hydroxyls in the presence of an acid catalyst to form a derivative containing two cyclic ketals. Pyridinium chlorochromate (PCC) in dichloromethane can then be used to oxidize the remaining alcohol into a ketone.



Scheme 1: Protection of β -D-Glucose.

A molecule must be studied carefully in order to select the right protecting group(s). When adding or removing a protecting group, one must know if it is acid- or base-labile. Acid-labile protecting groups may be cleaved in the presence of an acid,

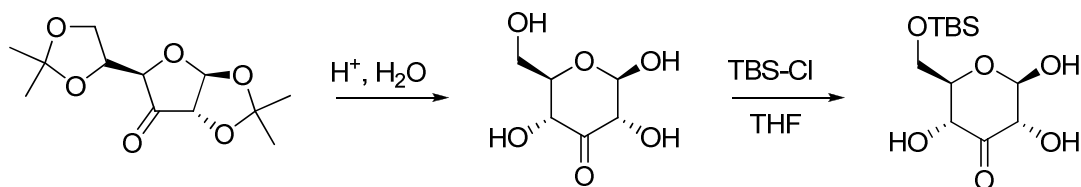
base-labile in the presence of a base. If, for example, a base is used in a reaction with a molecule with acetyl protecting groups, they will be cleaved. Therefore, it is necessary to understand the molecule and what is going to be done to it, mechanistically, before choosing protecting groups.

If acids and bases are used on a molecule with protecting groups that are acid- or base-labile, protecting groups can be changed, to avoid cleavage. To change protecting groups from, for example, an acid-labile to a non acid-labile protecting group, one must cleave it with the appropriate acid and then add a base-labile protecting group. Scheme 2 shows the acid-labile cyclic acetal protecting groups being removed by water and catalytic acid, followed by the addition of a non-acid-labile protecting group, *tert*-butyldimethylsilyl (TBDPS), introduced at the primary alcohol. If more equivalents are added, the TBDPS group will add to the secondary groups as well. TBDPS reacts at the primary hydroxyl over the secondary hydroxyls due to the steric environment. TBDPS protecting groups can be removed with tetra-*n*-butylammonium fluoride (TBAF) or any other source of fluoride ion; it is also possible to remove them with boron trifluoride in MeOH or HCl in MeOH.¹⁰

One of the major problems within carbohydrate chemistry is the need for highly selective functional group interconversions. Carbohydrates contain many reactive hydroxyl groups which need to be protected while other functional group interconversions take place. A protection group strategy must be well thought out before one begins a synthesis with carbohydrates. The most common protecting groups for carbohydrates with single hydroxyls are acetyl (Ac), benzoyl (Bz), and allyl (All), while

the most common protecting groups for a pair of hydroxyl groups are benzylidene and isopropylidene acetals.¹⁰

In our project, different types of protecting groups will be applied to our sugars, primarily acetyl protecting groups. One step in the planned synthesis may require non-base-labile protecting groups, so the base-labile acetyl groups present on the sugar may have to be replaced.



Scheme 2: Deprotection of acid-labile protecting groups.

Triazole Chemistry

Triazoles are heterocycles containing three nitrogen atoms and two carbon atoms, with the molecular formula $C_2H_3N_3$. There are two types of triazoles, 1,2,3- and 1,2,4-triazoles, differing in the positioning of a nitrogen atom (Figure 5). Triazoles are found to be useful in drug synthesis, and various antifungal drugs, such as Pramiconazole (Figure 6), contain them. 1,2,3-Triazoles have a strong affinity for metal ions,¹¹ which could prove to be useful in drug synthesis.¹² The construction of triazoles from an azide and an alkyne was discovered by Dimroth in the early 1900's, however this reaction wasn't fully understood mechanistically until the 1960's with the work of Rolf Huisgen.^{13,14}



Figure 5: Two types of triazoles.

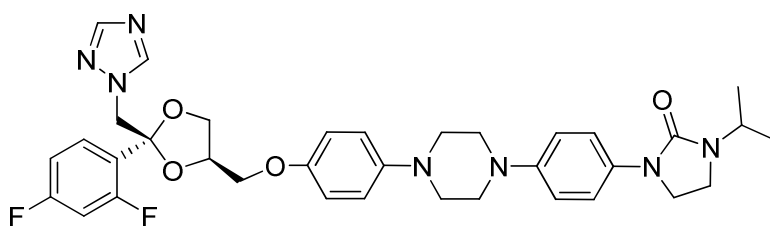
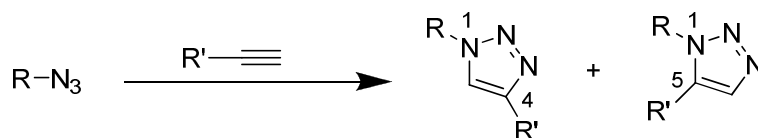


Figure 6: Antifungal drug Pramiconazole.

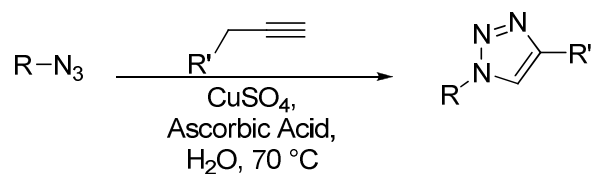
Huisgen developed a 1,3-dipolar cycloaddition between an azide and terminal alkynes to yield 1,2,3-triazoles;¹³ usually the reaction yields 1,4- and 1,5-triazole isomers. This cycloaddition has been referred to recently as the “cream of the crop” of “click chemistry” by K. Barry Sharpless.¹¹ Click chemistry uses simple reaction conditions and is used to synthesize compounds simply, quickly, and stereospecifically with readily available starting materials and benign solvents with no need of column chromatography for purification.¹¹ The Huisgen cycloaddition reaction yields two isomers, 1,4- and 1,5-, which is a problem when only one of the isomers is desired (Equation 1).



Equation 1: 1,2,3-Triazole formation *via* Huisgen 1,3-dipolar cycloaddition.

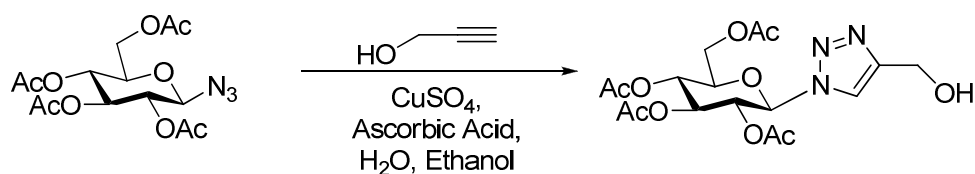
Meldal *et. al.* found a method to avoid the 1,5-isomer, yielding only the 1,4-isomer.¹⁵ Adding a copper (I) catalyst to the reaction allows for only the 1,4-isomer by coordinating to N-1 of the azide. Around the same time as Meldal, Sharpless *et. al.* did extensive research with Cu(I)-catalyzed 1,2,3-triazole reactions.¹¹

The 1,4-isomer can be synthesized by adding an alkyne to an azide with CuSO₄ and ascorbic acid. (Equation 2).¹⁵ The R' group can then be functionally interconverted to produce many different molecules. CuSO₄ is a source of Cu(II), which is reduced to a Cu(I) catalyst by ascorbic acid. The Cu(I) catalyst drives the reaction forward at 70 °C in approximately eight hours. Fokin *et. al.*, expanded triazole research by synthesizing 1,2,3-triazoles in a microwave in 15 minutes.¹⁷



Equation 2: Synthesis of the 1,4-isomer.

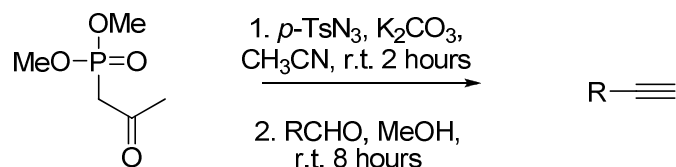
In our synthesis, 1,2,3-triazoles will be produced using propargyl alcohol (Equation 3). Through several functional group interconversions, the corresponding aldehyde will be converted to an alkyne, which can then be expanded upon to form bis(triazoles), which ultimately may be useful in the treatment of antibiotic resistant *S. aureus* strains.



Equation 3: Synthesis of a 1,2,3-triazole with propargyl alcohol.

The conversion of aldehydes to alkynes has historically been a tedious, multi-step process. Seyfreth *et. al.* reported a five-step procedure to make diazoalkanes, which were then used to convert aldehydes to alkynes.¹⁹ Gilbert and Weerasooriya expanded upon Seyfreth's research.²⁰ Callant *et. al.* later developed a useful method to synthesize diazoalkanes in one step.²¹

Roth *et. al.* reported a simple, one-pot synthesis to convert aldehydes into alkynes.^{22, 23} Their method avoids the use of strong bases, such as *n*-butyllithium, inert gas techniques, and below freezing temperatures. They also make use of a commercially available reagent that can be used directly in the one-pot synthesis, avoiding a multiple step process to synthesize a diazoalkane. Scheme 3 shows the conversion of aldehyde to alkyne, which produces yields of 65-89%, reported by Roth *et. al.* They combined dimethyl-2-oxopropylphosphonate with *p*-toluenesulfonyl azide and K_2CO_3 in MeCN and let it react for two hours at room temperature, leading to the formation of a diazoalkane; an aldehyde and methanol were added to the flask, which was left to react for eight hours at room temperature, yielding an alkyne.²²



Scheme 3: One-pot conversion of aldehyde to alkyne.

Staphylococcus aureus

Staphylococcus aureus (*S. aureus*) is a pathogenic bacterium that is responsible for a number of diseases in humans and animals. *S. aureus* is responsible for minor infections, such as boils and abscesses, to life-threatening infections, such as endocarditis and bacteremia.²⁴⁻³⁰ The bacterium is prevalent in approximately 30% of people,²⁵ colonizing the nasal passage and/or skin. Problems arise when the bacteria enter the body, usually *via* skin or mucosal cuts.

Because of the prevalence of antibiotic resistant strains of *S. aureus*, along with the emergence of clinical isolates resistant to vancomycin, the bacterium has become more difficult to control.²⁵ There is a growing problem with more virulent strains of the pathogen. *S. aureus* has historically affected people with weak immune systems, particularly in hospitals, where the bacterium is rampant. Recently there have been a growing number of community-acquired infections occurring in otherwise healthy people.²⁶

There exist a number of factors as to why *S. aureus* has become increasingly difficult to control, one of them being the production of a capsular polysaccharide, which protects the bacteria from phagocytosis by interfering with opsonization. Eleven different capsule types have been discovered from eighteen different strains of capsule-positive *S. aureus*. Type 5 and 8 capsular polysaccharides are the most common strains

of the bacteria found in people. Type 5 and 8 capsular polysaccharides are similar in structure with each containing 16 genes, labeled *cap5A-cap5P* and *cap8A-cap8P*, and the same three sugars *N*-acetyl-D-mannose uronic acid (D-ManNAcA), *N*-acetyl-D-fucosamine (D-FucNAc), and *N*-acetyl-L-fucosamine (L-FucNAc) (Figure 7). Twelve of the sixteen genes are nearly identical.²⁷ O’Riordan and Lee proposed a pathway for the biosynthesis of *S. aureus* capsular polysaccharide type 5. They reported that *cap5H* encodes a protein with a high degree of homology to a family of bacterial *O*-acetyltransferase genes. They also explained the function of many of the other genes involved in type 5 capsular polysaccharide.

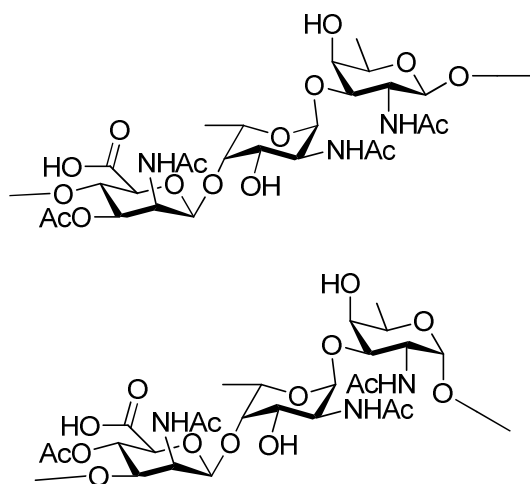


Figure 7: Structures of Type 5 (top) and Type 8 (bottom) capsular polysaccharides of *S. aureus*.

“The staphylococci have been studied as much as any Gram-positive bacterium, and yet the distinction between their interaction with man as a commensal and as a pathogen is still a mystery.”³¹

Antibiotics

The first uses of antibiotics date back 2500 years ago, in which the Chinese would apply the moldy curd of soybeans to infectious areas. The first modern antibiotic effect was discovered by Louis Pasteur, when he noticed that certain saprophytic bacteria kill anthrax germs.³² Sir Alexander Fleming was the first to biologically discover an antibiotic, penicillin, in 1928. Penicillin was discovered by accident. Fleming noticed that *staphylococcus* bacteria, contaminated with mold from the air, were being killed. The mold belonged to the genus *Penicillium*.³² Fleming then showed that penicillin was effective in inhibiting a number of different bacteria. Penicillin was not used on humans until 1940. The first antibiotic used on humans, tyrothricin, turned out to be too toxic for use.

The problem with antibiotics arises when bacteria evolve, by genetically mutating, and build resistance to certain drugs. Infections caused by *S. aureus* were treated with penicillin in the 1940s. By 1950, 40% of *S. aureus* isolates were resistant to penicillin; by 1960 this number grew to 80%.³³ Today, in the United Kingdom, only 2% of *S. aureus* isolates are sensitive to penicillin.³⁴ *S. aureus*' resistance to penicillin is mediated by an enzyme, penicillinase, which breaks down the β -lactam ring that is found in penicillin. Methicillin is able to resist the cleavage of the β -lactam ring by the penicillinase enzyme.

Methicillin is used to treat penicillin-resistant *S. aureus*, however the bacterium has become increasingly resistant to methicillin. This resistance is caused by the *mec* operon of *S. aureus*, which leads to resistance to all β -lactam antibiotics. *S. aureus* that are resistant to β -lactam antibiotics, termed Methicillin-resistant *S. aureus* (MRSA), are

treated with clindamycin and co-trimoxazole and linezolid. Vancomycin is a glycopeptide antibiotic that is used to treat very serious MRSA infections; vancomycin is given intravenously, and because of its high toxicity, it is considered a last resort drug in treating MRSA.

Vancomycin-resistant *S. aureus* (VRSA) were discovered in 2002,³⁵ and VRSA has built resistance to glycopeptides antibiotics. There have only been a handful of cases of VRSA reported in the United States, but one can assume that the number will grow as they have with other antibiotics. The CDC estimated that MRSA was linked to 18,650 hospital-related deaths in the U.S. in 2005,³⁶ which means MRSA is now responsible for more deaths than AIDS in the U.S. annually.³⁷

In our project, the synthesis of a potential glycosyltransferase inhibitor will be attempted. Glycosyltransferase inhibitors mimic the UDP-conjugate of the parent aminosugar, L-FucNAc, found in the capsular polysaccharide of *S. aureus*. Inhibition of the transferase enzyme, responsible for the introduction of L-FucNAc, may prevent the formation of the capsular polysaccharide, leaving the bacterium open to attack by phagocytosis.

For model studies, acetyl-protected β -D-glucose will be converted to the bis(triazole) derivative shown in Figure 8 by a series of synthetic steps. The lone pairs on the nitrogen atoms of triazoles have been shown to coordinate to metal atoms, which indicate that the proposed molecule may be able to imitate the diphosphate linkage in UDP-L-FucNAc in binding to the transferase enzyme (Figure 8). If inhibition of glycosyl transferase enzyme is successful with the bis(1,2,3-triazole) different analogs will be constructed, including the desired L-FucNAc derivative.

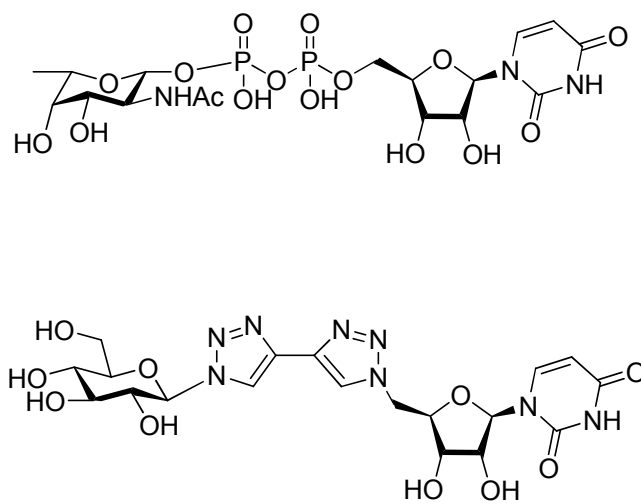


Figure 8: Potential bis(1,2,3-triazole) transferase inhibitor
(bottom) and UDP-L-fucNAc (top).

Statement of Problem

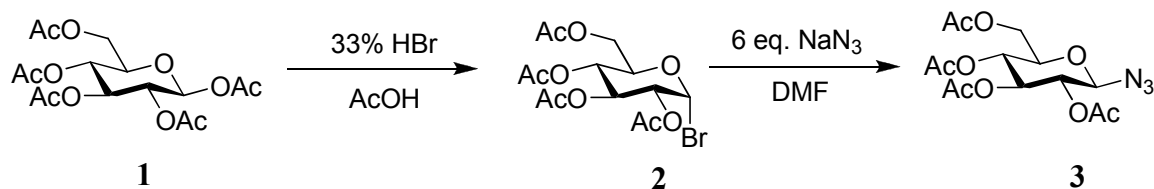
The primary goal of this research is to synthesize potential glycosyltransferase inhibitors which will mimic the UDP conjugates of aminosugars (D-ManNAcA, D-FucNAc, and L-FucNAc) found in the capsular polysaccharide of *S. aureus*. This may prevent the formation of the capsular polysaccharide leaving the bacteria open to attack by phagocytosis. 1,2,3-Triazole heterocycles will be used to replace the phosphate groups in the UDP-parent aminosugars. Bis(triazoles) may mimic the diphosphate linkage in binding to a transferase due to interaction with the N-3 lone pairs on the heterocycles.

Results & Discussion

1. Synthesis of D-glucosyl azide 3 from D-glucose pentaacetate 2.

The primary goal of this research was to develop a bis(1,2,3-triazole) that may mimic the diphosphate linkage in binding to a glycosyl transferase, due to the N-3 lone pairs on the heterocycles. Another important factor was to use inexpensive starting materials. Acetylated D-glucose was selected as the starting material with which to begin the synthesis.

The initial step in the synthesis (Scheme 4) involved the treatment of 1,2,3,4,6-penta-*O*-acetyl- β -D-glucose (**1**) with 33% HBr in acetic acid, which undergoes a simple S_N1 reaction to yield a bromide in place of an acetyl group on the anomeric carbon. Stereochemistry is alpha because the bromine prefers the axial position due to the anomeric effect, which can be explained by the overlap of one of the lone pairs of electrons on the ring oxygen with the antibonding σ^* orbital of the C-Br bond. TLC showed complete consumption of starting material after 3 hours and formation of a new spot with a higher R_f value than the starting material. ¹H NMR data showed the disappearance of the doublet signal at 5.71 ppm and the appearance of a doublet at 6.62 ppm with a coupling constant of 4.03 Hz; it also showed the disappearance of a singlet around 2 ppm, signaling the disappearance of the acetyl group on the anomeric carbon. The reason for the doublet appearing further downfield is due to the electronegative effect and the size of the bromine atom. Electrospray Ionization (ESI) mass spectrometry provided a mass of 433.0 which corresponds to the addition of sodium to the calculated mass of 410.02 amu. Bromine is a very good leaving group and the next reaction took full advantage of that fact.



Scheme 4: Synthesis of D-glucosyl azide.

Following the completion of the glucosyl bromide **2** reaction, sodium azide was immediately added to a solution of **2** in DMF and allowed to stir for eight hours. This reaction is a simple S_N2 reaction, resulting in 100% inversion of stereochemistry, stereospecifically yielding glucosyl azide **3** in 80% yield. TLC showed complete consumption of starting material and appearance of a new spot burning at a lower R_f value than the starting material. ^1H NMR showed the absence of the doublet signal at 6.62 ppm, which corresponds to the anomeric proton of the α -glucosyl bromide, and a new doublet signal at 4.66 ppm. The azide shields the anomeric proton, pushing it upfield in the NMR spectrum. ^{13}C NMR verified the compound by indicating 14 carbon signals, with the signals for the methyl groups of the acetyl protecting groups between 20.5-20.6 ppm, and the carbonyl carbon of the acetyl protecting groups between 169.4-170.5. ESI mass spectrometry provided a mass of 396.1 amu which corresponds to the addition of sodium to the calculated mass of 373.11 amu.

In addition to the anomeric proton being further downfield with the α -glucosyl bromide, relative to the anomeric proton on the β -glucosyl azide, the coupling constants for the anomeric proton also differ. The β -glucosyl azide has a coupling constant of 8.88 Hz, while the α -glucosyl bromide has a coupling constant of 4.03 Hz. With the α -glucosyl bromide, the protons on C1 and C2 are gauche to each other, which

gives them a lower coupling constant. In the β -glucosyl azide, the protons on C1 and C2 are anti-periplanar, resulting in a higher coupling constant (Figure 9).³⁸



Figure 9: Structures of gauche (left) and anti-periplanar (right) conformations in **2** and **3**.

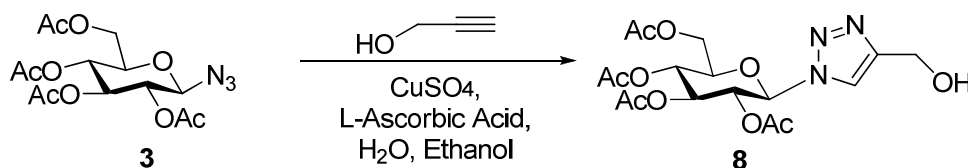
2. Conversion of β -D-glucosyl azide **3** into 1,2,3-triazoles.

The next step in the synthesis involves the formation of a 1,2,3-triazole. The mechanism for this reaction is a Cu(I)-catalyzed cycle (Scheme 5)³⁹ in which azide reacts with an alkyne, yielding a 1,2,3-triazole. CuSO_4 is a Cu(II) salt that is reduced to Cu(I) by interaction with L-ascorbic acid. The purpose of the Cu(I) catalyst in this reaction is to yield the 1,4-triazole isomer specifically. This reaction can take place without a Cu(I) catalyst, however without the Cu(I) catalyst the reaction, called the Huisgen addition, would yield a 1,5-triazole isomer in addition to the 1,4-triazole isomer.

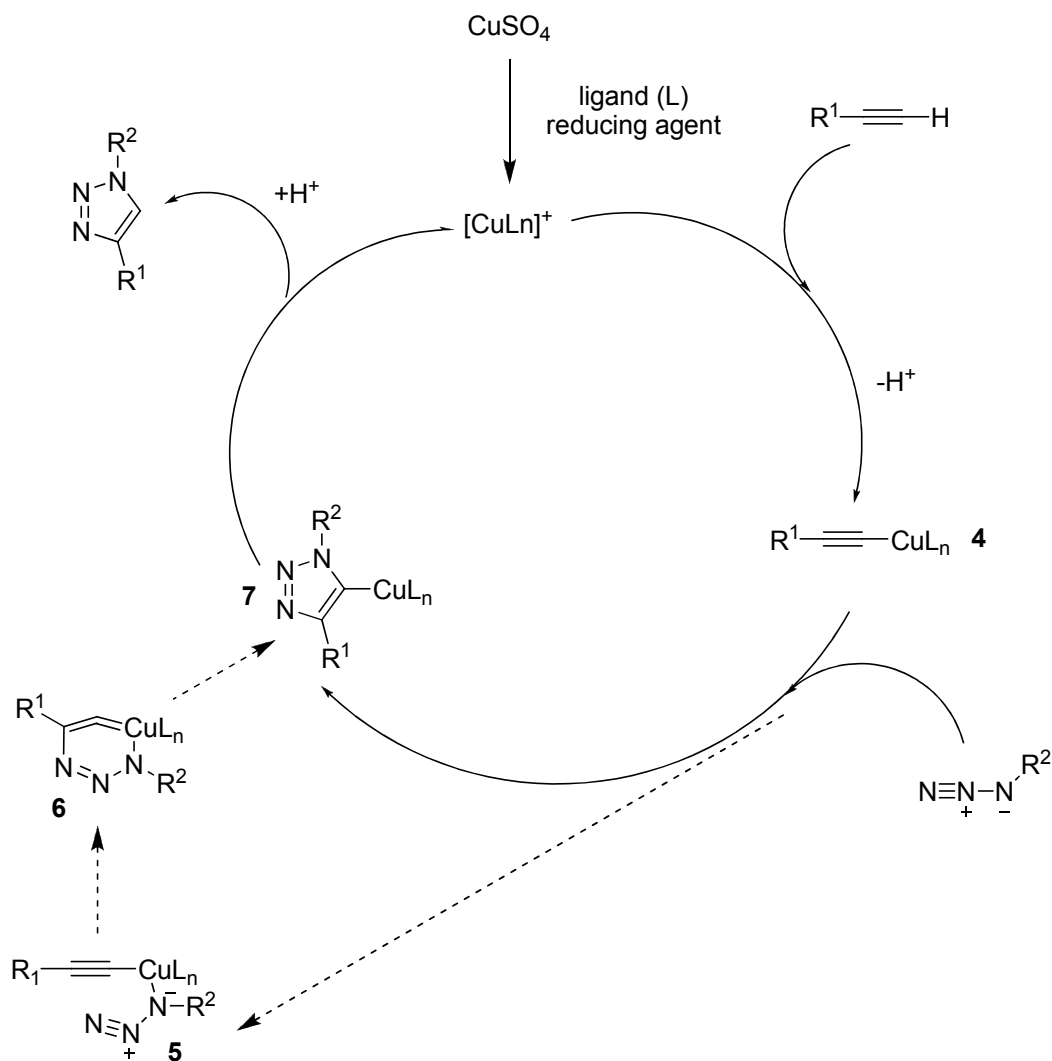
In an attempt to explain the mechanism of the Cu(I)-catalyzed reaction, Patton reported that density functional theory calculations show a preference for the stepwise addition (**4** \rightarrow **5** \rightarrow **6** \rightarrow **7**) over the concerted cycloaddition (**5** \rightarrow **8**) by approximately 12 to 15 kcal mol⁻¹, leading to a six-membered metallocycle **7**, as shown in Scheme 5.³⁹

The next step in our synthesis involved converting β -glucosyl azide **3** into triazole **8** (Equation 4) with propargyl alcohol, CuSO_4 , and L-ascorbic acid in 1:1 water / ethanol. TLC showed complete consumption of starting material after 48 hours and formation of a new spot with a lower R_f value than the starting material. The triazole **8** is not soluble in water at room temperature, which allows for easy isolation. The ethanol was allowed to

evaporate leading to precipitation of a white solid. The copper salt was washed out of the product with water over vacuum filtration and the product was recrystallized with hot methanol. ^1H NMR data showed the formation of a singlet at 7.82 ppm, which corresponds to the triazole proton. ^1H NMR data also showed two other new signals at 3.49 ppm, corresponding to the hydroxyl proton, and 4.81 ppm, corresponding to the CH_2 triazole substituent. It also showed the anomeric proton to have moved downfield from 4.66 ppm to 5.90 ppm; this is due to the electron-withdrawing effects of the triazole heterocycle. ^{13}C NMR showed new carbon signals at 56.6 ppm, 120.0 ppm, and 148.6 ppm while ESI mass spectrometry gave a mass of 452.2 amu which corresponds to the addition of sodium to the calculated mass of 429.14 amu. Single crystal X-Ray data (Figure 10) was obtained for triazole **8** to confirm the structure and conformation of the compound.



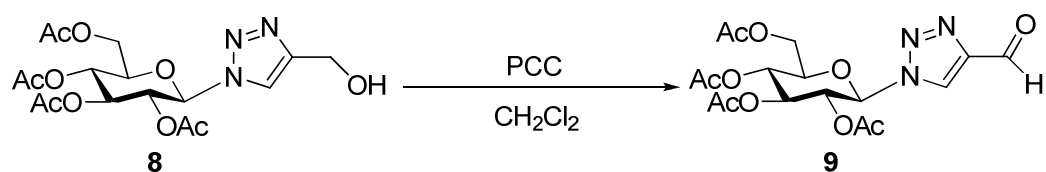
Equation 4: Synthesis of triazole **8**.



Scheme 5: Postulated catalytic cycle for azide-alkyne coupling.³⁹

The next step in the synthesis involved converting triazole **8** into aldehyde **9** (Equation 5). Under a nitrogen atmosphere, 6 equivalents of pyridinium chlorochromate (PCC) and an equivalent amount of 4 Å molecular sieves in methylene chloride were allowed to stir. TLC showed complete consumption of starting material after 2 days and formation of a new spot with a higher R_f value than the starting material. ^1H NMR data showed the formation of a singlet at 10.15 ppm, indicating the appearance of an aldehyde in place of the alcohol branching off of the triazole. ^1H NMR signals for aldehydes

generally appear between 9 and 10 ppm; this aldehyde is pushed further downfield because the triazole heterocycle acts as an electron-withdrawing group (EWG) and pulls the electron density away from the aldehyde proton. ^1H NMR data also showed the loss of the hydroxyl proton signal at 3.49 ppm. ^1H NMR data also showed that the proton on the triazole ring was pushed further downfield; this is due to the aldehyde being more electron-withdrawing than the hydroxyl. ^{13}C NMR showed a new carbon signal at 184.4 ppm corresponding to the formation of aldehyde and the disappearance of a signal at 56.6. ESI mass spectrometry gave a mass of 450.2 amu which corresponds to the addition of sodium to the calculated mass of 427.12 amu. Single crystal X-Ray data (Figure 11) was obtained for the aldehyde **9** to confirm the structure and conformation of the compound.



Equation 5: Synthesis of aldehyde **9** from alcohol **8**.

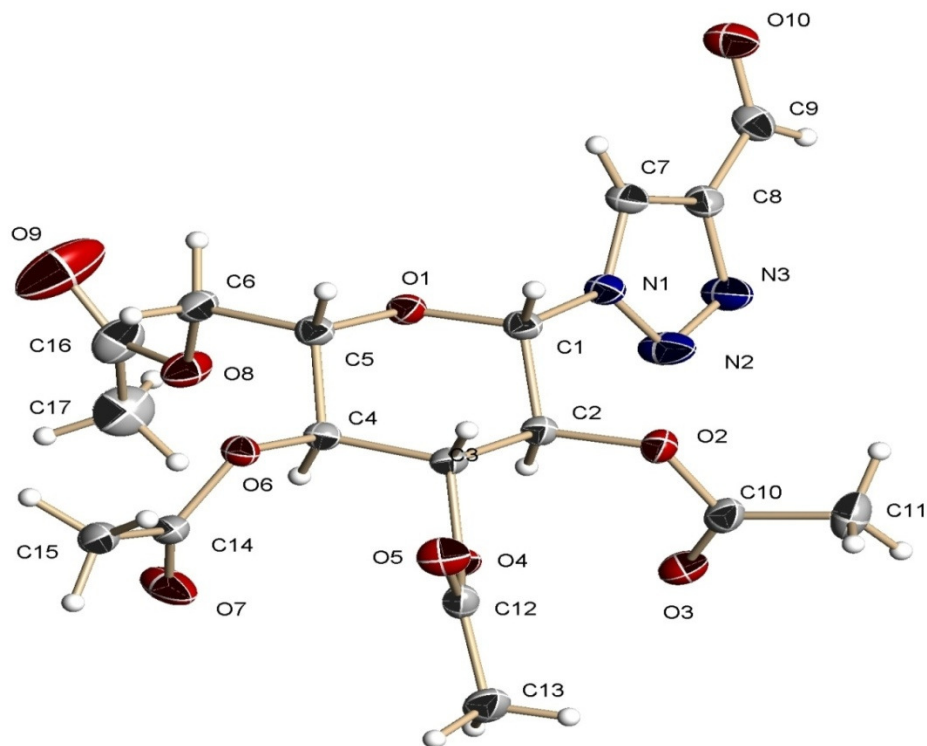
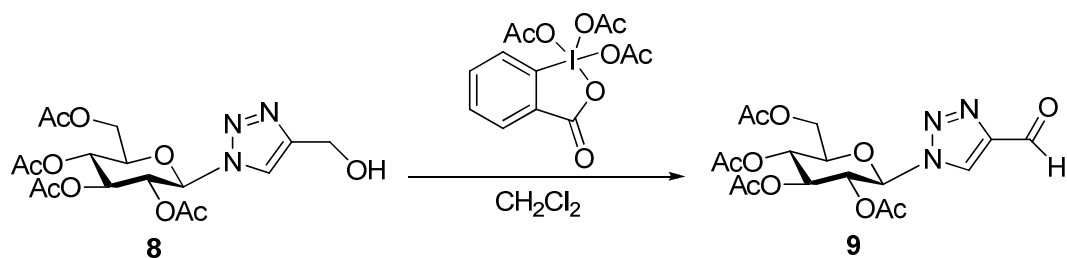


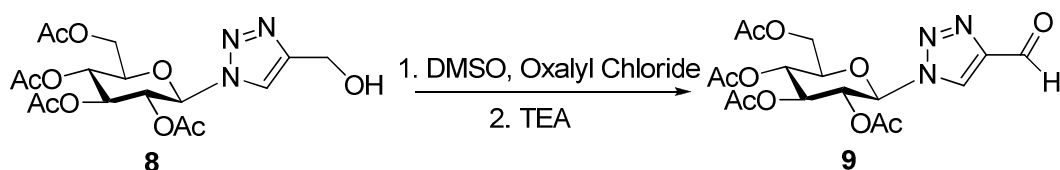
Figure 11: X-Ray crystal structure of aldehyde **9**.

Due to the toxicity of chromium compounds, other methods were used to synthesize aldehyde **9**. A large excess of Dess-Martin periodinane (DMP), which is a hypervalent iodine compound, was added to alcohol **8** in methylene chloride to afford **9** in high yield (Equation 6). This reaction is appealing because it gave high yields and avoided the use of toxic metals, such as chromium. However, due to the amount of reagent needed for this reaction to take place, this reaction wasn't used primarily and other methods were explored.



Equation 6: Synthesis of aldehyde **9** *via* DMP oxidation.

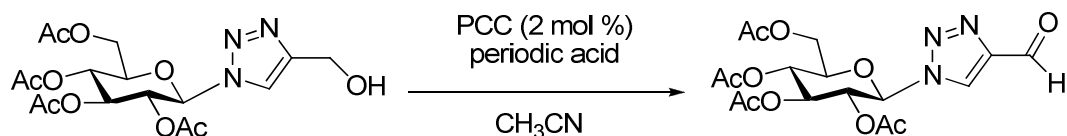
The Swern oxidation (Equation 7) also avoids the use of toxic metals. DMSO and oxalyl chloride were allowed to react to yield an alkoxy-sulfonium ion, then glucosyl alcohol **8** was dissolved in methylene chloride and added dropwise *via* addition funnel. To complete this reaction, triethylamine (TEA) was added dropwise *via* addition funnel to afford aldehyde **9** in low yield. This reaction was generally completed in three hours, however the problem with this reaction was not only the low yields that it produced, but the stench of a byproduct created in the reaction, dimethyl sulfide. This required the glassware to be kept in a fume hood at all times and then soaked in bleach after completion. There were also problems with the alcohol **8** desolvating from methylene chloride as it was being added *via* addition funnel.



Equation 7: Synthesis of aldehyde **9** *via* Swern oxidation.

The last oxidation explored was a PCC-catalyzed oxidation with periodic acid in acetonitrile (Equation 8), a method reported by Hunsen.⁴⁰ While using a toxic metal in

this reaction, it had a short reaction time of only two hours, and only a very small amount of PCC was necessary for completion of this reaction. The problem with this reaction was the very low yield; only 2% was afforded.



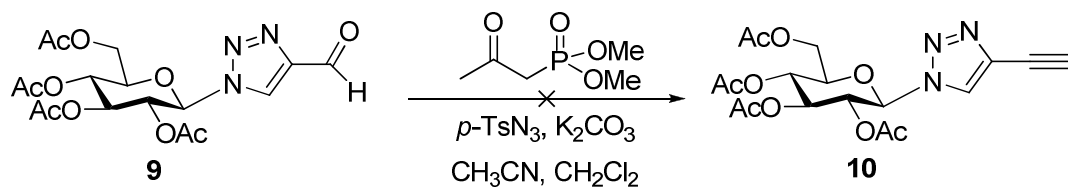
Equation 8: Synthesis of aldehyde **9** via 2 mol % PCC with periodic acid.

3. Synthesis of alkyne **10** from aldehyde **9**.

A necessary component in making a bis(1,2,3-triazole) is an alkyne substituent off of a triazole. There are several methods to afford an alkyne from an aldehyde, however most of them use a strong base which conflicts with the acetyl protecting groups present on **9**. Two methods were explored which didn't conflict with the acetyl protecting groups. Roth, *et. al.* utilized a weak base, potassium carbonate, while Hoyer, *et. al.* utilized potassium *tert*-butoxide with this functional group interconversion.

The next step in the synthesis involved converting aldehyde **9** into alkyne **10**. Several different variations of this functional group interconversion were utilized in an attempt to yield **10**. The initial methods attempted were those published by Roth *et. al.* Roth described two different methods to convert aldehyde to alkyne, the first being a one pot synthesis (Equation 9). Thus, under a nitrogen atmosphere, dimethyl-2-oxopropylphosphonate (DMOP) (**11**) was converted into dimethyl-1-diazo-2-oxopropylphosphonate (**12**) with K_2CO_3 and *p*-toluenesulfonyl azide (**13**) in acetonitrile. TLC showed complete consumption of starting material after 2 hours, and formation of a new spot with a higher R_f value than the starting material. Aldehyde **9** was then added

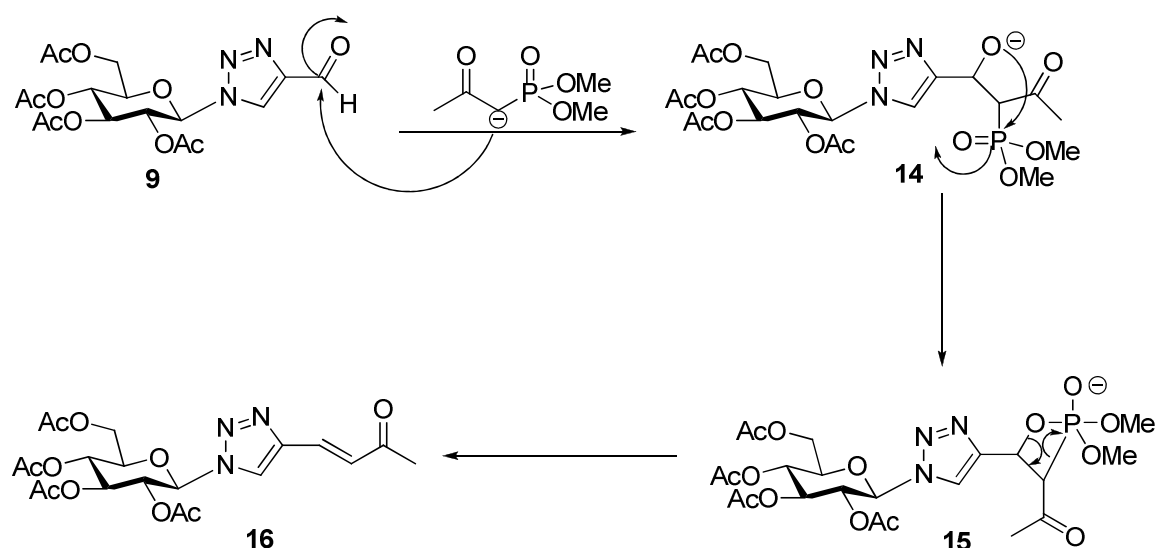
and allowed to stir for sixteen hours. TLC showed the complete consumption of starting material and formation of a new spot with a lower R_f value than the starting material.



Equation 9: Attempted synthesis of alkyne **10** from aldehyde **9**.

^1H NMR data showed the disappearance of the aldehyde singlet at 10.15 ppm, indicating that a reaction occurred at the carbonyl carbon of the aldehyde. ^1H NMR data also showed the appearance of a singlet at 2.36 ppm, and two doublets at 6.94 and 7.48 ppm, signaling that the product formed was not an alkyne, which would have yielded just one singlet from 2.00-3.00 ppm. Upon further investigation, it was concluded that a Horner-Wadsworth-Emmons reaction was occurring, yielding an α,β -unsaturated methyl ketone (**16**, Scheme 6) instead of an alkyne. This indicates that the diazotransfer reaction may have failed, or the diazo group was lost after the transfer, yielding an electron-deficient phosphonate, which reacted with the aldehyde **9**. ^1H NMR showed a singlet at 1.43 ppm and doublets at 6.97 and 7.49 ppm, while the ^{13}C NMR showed new carbon signals at 27.9, 129.1, 130.1, and 197.8 ppm corresponding to the α,β -unsaturated ketone **16**. ^{13}C NMR also showed the disappearance of the aldehyde signal, verifying that reaction occurred at the carbonyl carbon. ESI mass spectrometry gave a mass of 490.2 amu corresponding to the addition of sodium to the calculated mass of 467.15 amu, again

signaling that the α,β -unsaturated ketone was formed, rather than the alkyne target compound.



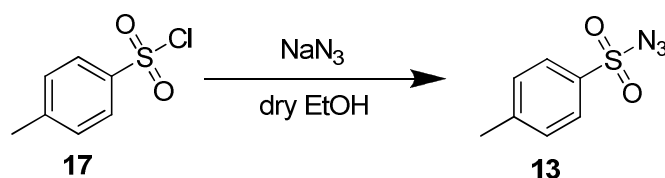
Scheme 6: Mechanism of the formation of α,β -unsaturated ketone **16**.

Table 1: Reactions of sulfonyl chlorides to yield sulfonyl azides.

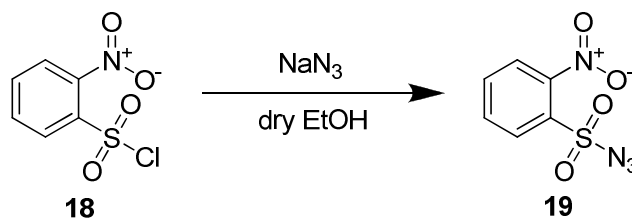
Starting Material	Sulfonyl Azide	R_f value	calculated m/z	m/z found
17	13	0.56	197.03	223.2
18	19	0.23	228.00	251.3
20	21	0.18	228.00	204.1

Aldehyde to alkyne functional group interconversions rely on the use of a sulfonyl azide; three different sulfonyl azides, *p*-toluenesulfonyl azide **13**, *o*-nitrobenzenesulfonyl azide **19**, and *p*-nitrobenzenesulfonyl azide **21** were synthesized from the sulfonyl chlorides *p*-toluenesulfonylchloride **17**, *o*-nitrobenzenesulfonyl chloride **18**, and *p*-nitrobenzenesulfonyl chloride **20** for use with this reaction (Table 1).

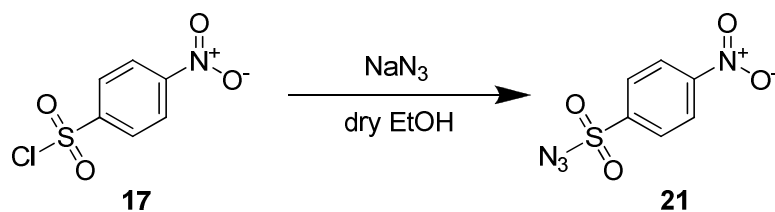
Under a nitrogen atmosphere, sulfonyl chlorides **17**, **18**, and **20** were mixed with sodium azide in dry ethanol and allowed to stir for 24 hours (Equations 10-12). TLC showed complete consumption of starting material and formation of new spots burning at lower R_f values than the starting materials. ^1H and ^{13}C NMR data verified the formation of the compounds, albeit showing no major difference from the starting materials. ESI mass spectrometry gave a mass of 220.0 amu for **13**, which corresponds to the addition of sodium to the calculated mass of 197.03 amu; 251.3 amu for **19**, which corresponds to the addition of sodium to the calculated mass of 228.00 amu; and 204.1 amu for **21**, which corresponds to the addition of sodium and loss of the nitro group to the calculated mass of 228.00 amu. Single crystal X-Ray data for *p*-toluenesulfonamide (Figure 13) helps to verify compound **13** because it is a known byproduct of the diazo transfer reaction. Single crystal X-Ray data (Figure 12) for compound **19** and a unit cell conformation for compound **21** verifies these compounds.



Equation 10: Synthesis of *p*-toluenesulfonyl azide **13**.



Equation 11: Synthesis of *o*-nitrobenzenesulfonyl azide **19**.



Equation 12: Synthesis of *p*-nitrobenzenesulfonyl azide **21**.

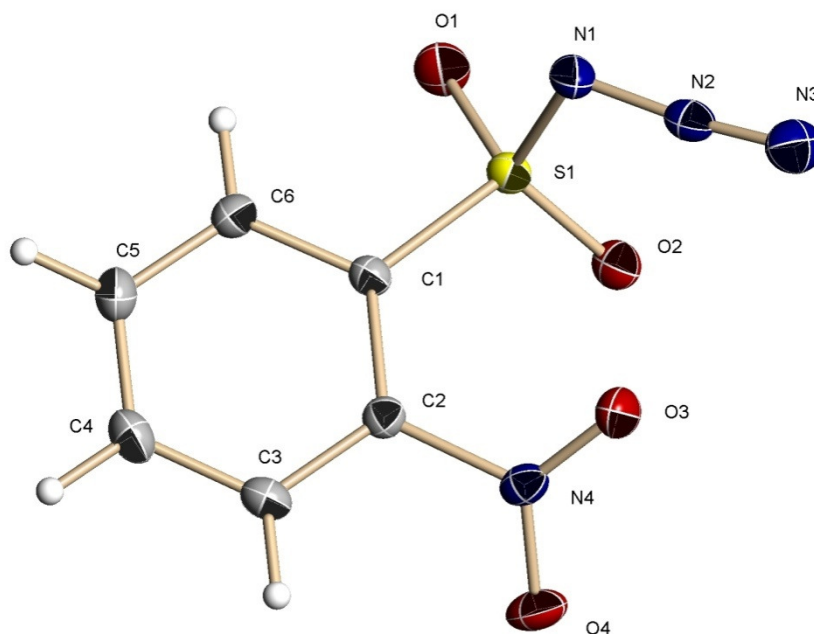


Figure 12: X-Ray structure of *o*-nitrobenzenesulfonyl azide **19**.

Different variations of Roth's method were attempted using sulfonyl azides **13**, **19**, **21**, and 4-acetamidobenzenesulfonyl azide (*p*-ABSA), temperature, solvent and 1,8-diazabicyclo[5,4,0]undec-7-ene (DBU) in place of K_2CO_3 (Table 2) with all yielding the α,β -unsaturated ketone **16** rather than alkyne **10**, except when methanol was used as the solvent at room temperature, which yielded an unknown compound. Single crystal X-Ray data (Figures 13 and 14) was obtained for *p*-toluenesulfonamide **22** and *p*-

acetamidobenzenesulfonamide **23**, byproducts of the reaction which hints that the diazo transfer reaction did not fail, and the diazo group is breaking off of the phosphonate after the diazo transfer occurs.

Table 2: Variations of the attempted synthesis of **10** from Roth's *et. al.* one-pot method.

Base	Sulfonyl Azide	Solvent	Temperature
K ₂ CO ₃	<i>p</i> -ABSA	Acetonitrile	RT
K ₂ CO ₃	13	Acetonitrile	RT
K ₂ CO ₃	19	Acetonitrile	RT
K ₂ CO ₃	21	Acetonitrile	RT
K ₂ CO ₃	13	Methanol	RT
K ₂ CO ₃	13	Methanol	0 °C
DBU	<i>p</i> -ABSA	Acetonitrile	RT
DBU	13	Acetonitrile	RT
DBU	19	Acetonitrile	RT
DBU	21	Acetonitrile	RT

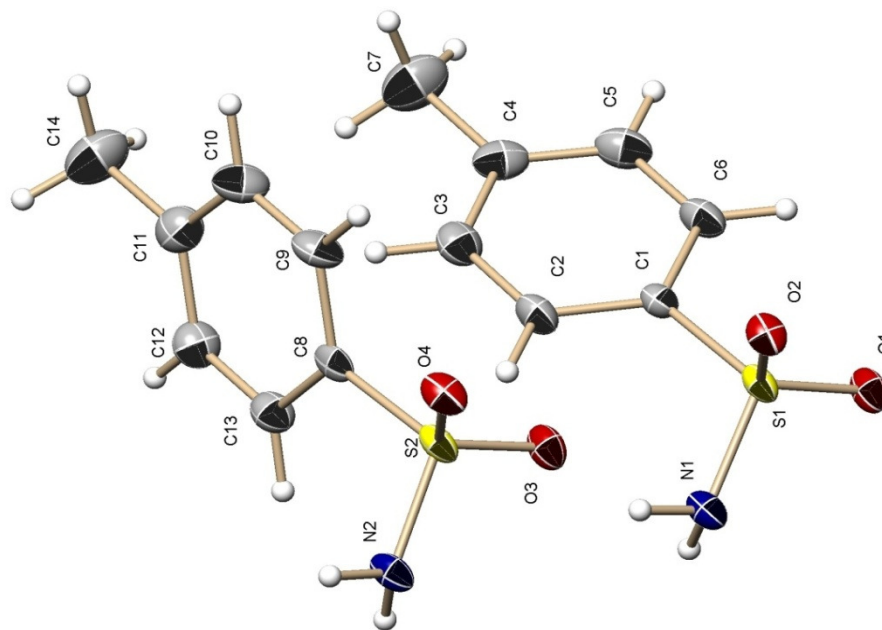


Figure 13: X-Ray structure of *p*-toluenesulfonamide (**22**).

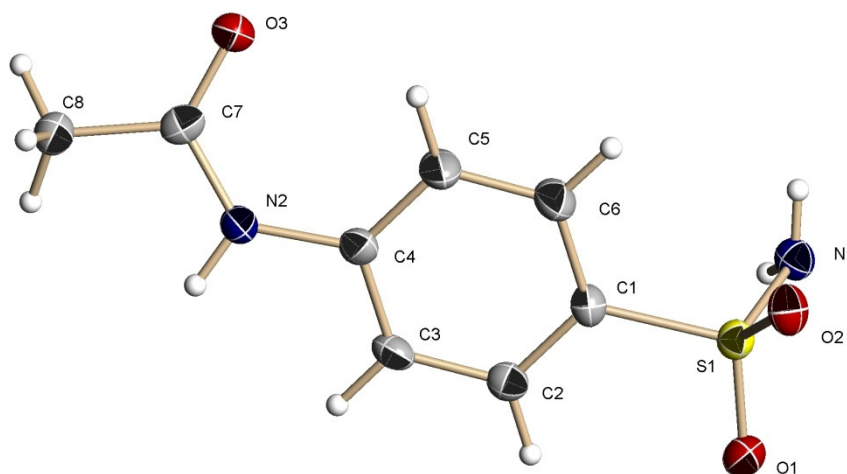
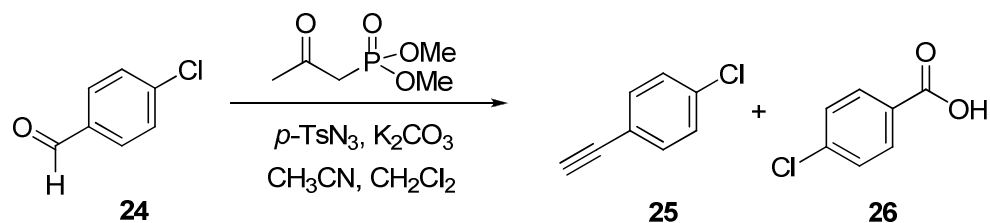


Figure 14: X-Ray structure of *p*-acetamidobenzenesulfonamide (**23**).

To verify if the diazo transfer reaction was occurring the reaction was attempted successfully on a compound, 4-chlorobenzaldehyde **24**, to produce 4-chlorophenylacetylene (**25**, Equation 13). This compound was successfully synthesized

previously by Roth *et. al.*²² TLC of the reaction mixture showed two spots, and column chromatography was used in an attempt to isolate **25**. The compound was not successfully purified *via* flash column chromatography, however NMR data showed signals reported in the literature for **25** and signals for the known byproduct, 4-acetamidobenzenesulfonylamide **23**. ¹H NMR showed the disappearance of the aldehyde signal at 9.99, the appearance of a singlet at 3.10, corresponding to the alkyne proton, and two doublets at 7.29 and 7.41 ppm corresponding to the aromatic protons, which agreed with the results published by Roth *et. al.* ¹³C NMR showed signals for the alkyne carbons at 78.1 and 82.4 ppm. ESI mass spectrometry provided a mass of 124.9 amu which corresponds to the addition of sodium and a proton and the subtraction of chlorine to the calculated mass of 136.01 amu. Single crystal X-Ray structure was found for a byproduct, 4-chlorobenzoic acid (**26**).

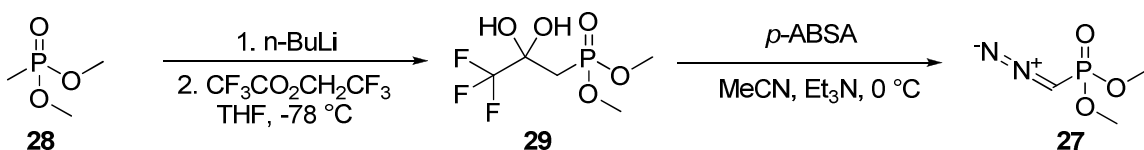


Equation 13: Synthesis of 4-chlorophenylacetylene (**25**) from 4-chlorobenzaldehyde (**24**) utilizing a one-pot synthesis published by Roth *et. al.*

The next approach attempted was the second method published by Roth *et. al.* which involved isolating dimethyl-1-diazo-2-oxopropylphosphonate (**11**) before adding it to aldehyde **9**. In a 100 mL round-bottom flask potassium carbonate (0.276 g, 2.0 mmol), aldehyde **9** (0.429 g, 1.0 mmol), and dimethyl-1-diazo-2-oxopropylphosphonate (**11**, 0.230 g, 1.20 mmol) were added to MeCN. This reaction was allowed to stir

overnight and then was diluted with methylene chloride (25 mL) and then washed with 5% NaHCO₃ (10 mL) and dried over MgSO₄. The solution was concentrated to leave an orange oil. TLC showed multiple spots that were very close together. Flash column chromatography, utilizing ethyl acetate as the solvent system, was performed in an unsuccessful attempt to cleanly isolate **11**. ESI mass spectrometry, set at 30% compound stability, gave a mass of 215.0 amu which corresponds to the addition of sodium to the calculated mass of 192.03 amu.

The next method attempted was the synthesis of dimethyl(diazomethyl)phosphonate (**27**, Scheme 7), also known as the Seyferth/Gilbert reagent, utilizing a procedure published by Hoye *et. al.*⁴⁴ This reagent is similar to dimethyl-1-diazomethyl phosphonate (**12**).



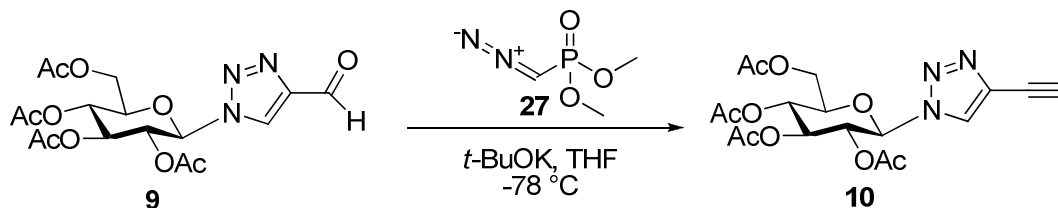
Scheme 7: Synthesis of dimethyl(diazomethyl)phosphonate (**27**).

To a flame-dried 250 mL round-bottom flask 40 mL of dry THF was added. Dimethyl methylphosphonate (**28**, 2.29 g, 2.00 mL, 18.4 mmol) was added and the mixture was cooled to -78 °C. *n*-Butyllithium (7.66 mL of a 2.40 M solution in hexanes, 18.4 mmol) was added over 5 minutes and the solution was allowed to stir at -78 °C for 30 minutes. 2,2,2-Trifluoroethyl trifluoroacetate (5.41 g, 3.73 mL, 27.6 mmol) was added rapidly, and the solution was allowed to stir at -78 °C for 15 minutes. The

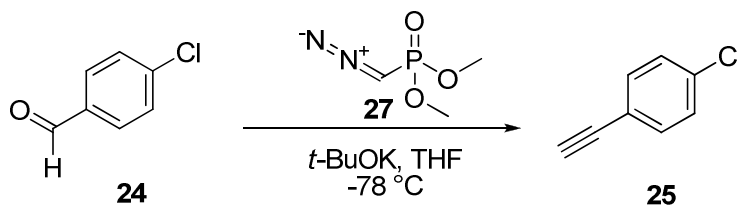
solution was warmed to room temperature and then partitioned between diethyl ether (250 mL) and 3% HCl (10 mL) and then washed with saturated NaHCO₃ (1 x 10 mL) and saturated NaCl (1 x 10 mL). The organic layer was separated, dried over MgSO₄, and concentrated to afford dimethyl (3,3,3-trifluoro-2,2-dihydroxypropyl)phosphonate (**29**). This crude sample was immediately dissolved in dry CH₃CN (40 mL). *p*-ABSA (3.97 g, 16.5 mmol) was added and the solution was cooled to 0 °C. Triethylamine (1.66 g, 2.29 mL, 16.5 mmol) was then added dropwise over 5 minutes. The mixture was warmed to room temperature and allowed to stir overnight. The solvent was reduced, chloroform was added, and 4-acetamidobenzenesulfonamide was filtered over a glass frit. TLC showed the formation of a new spot with a lower R_f value than the starting material. Column chromatography was used to purify the crude compound (ethyl acetate) to yield **27**. ¹H NMR data showed a doublet signal at 3.78 ppm corresponding to the protons on the methoxy groups. There was no signal for the diazo proton. ¹³C NMR showed a doublet at 28.5 ppm corresponding to the diazo carbon, and a doublet at 53.0 ppm corresponding to the methoxy carbons. ³¹P NMR showed one signal, corresponding to the lone phosphorus in the compound. IR spectrometry showed a signal at 2110 cm⁻¹, corresponding to the proton next to the diazo group. Single crystal X-Ray data was obtained for a byproduct of the reaction, 2,2,2-trifluoroethyl acedamidobenzenesulfonate (**37**).

Following the production of dimethyl(diazomethyl)phosphonate (**27**), another aldehyde to alkyne reaction was attempted. In a flame-dried 50 mL round-bottom flask, equipped with a magnetic stir bar, potassium *tert*-butoxide was added to dry THF. The solution was allowed to cool to -78 °C. Dimethyl(diazomethyl)phosphonate (**27**), in dry

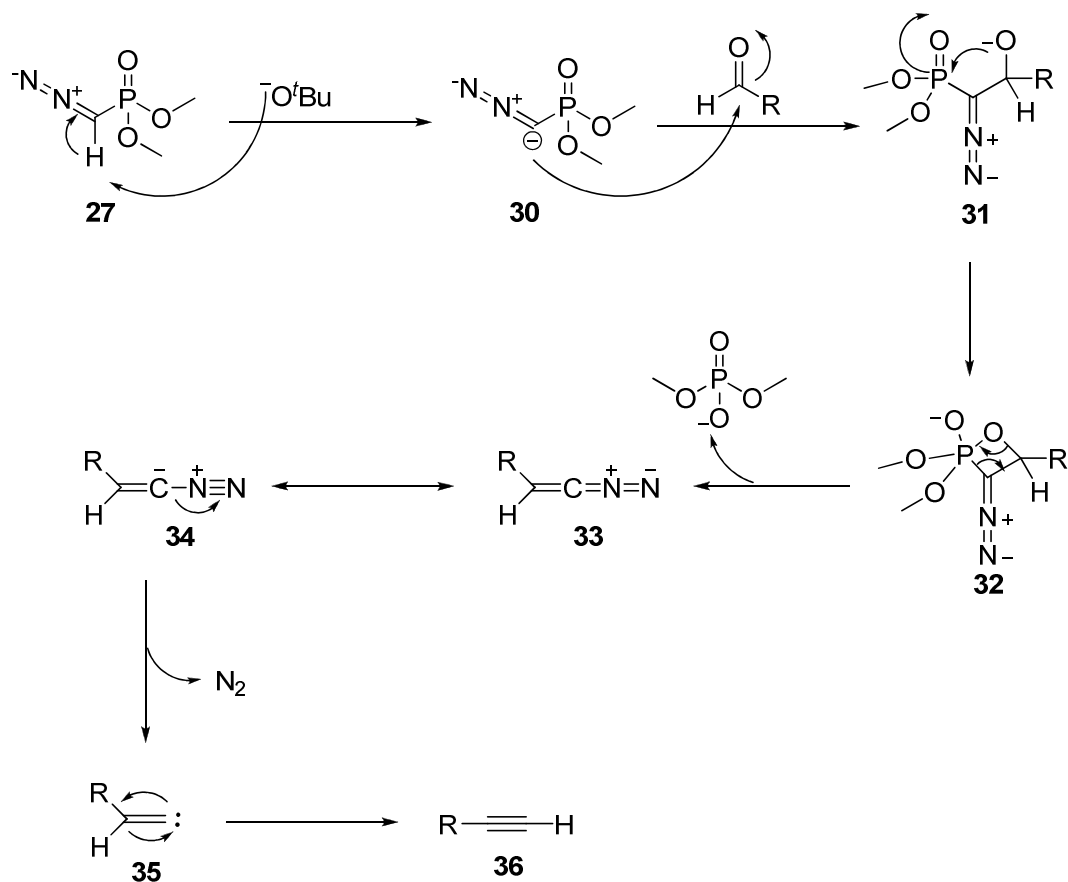
THF, was then added and allowed to react for 5 minutes, turning from orange to brownish-orange. Aldehyde **9** in dry THF was then added and allowed to stir for 12 hours at $-78\text{ }^{\circ}\text{C}$. TLC showed formation of a new spot with a higher R_f value than the starting material. ^1H NMR data showed a new signal at 3.27 ppm and the disappearance of the aldehyde signal at 10.15. The triazole proton appeared further upfield due to the loss of the electron-withdrawing aldehyde. ^{13}C NMR showed two signals at 72.5 and 81.82 ppm. This procedure was then repeated successfully using 4-chlorobenzaldehyde as the carbonyl source (Equation 15). ESI mass spectrometry provided a mass of 446.2 which corresponds to the addition of sodium to the calculated mass of 423.13 amu.



Equation 14: Synthesis of alkyne **10** from aldehyde **9** using **27** as a reagent.



Equation 15: Synthesis of 4-chlorophenylacetylene (**25**) from 4-chlorobenzaldehyde using **27** as a reagent.

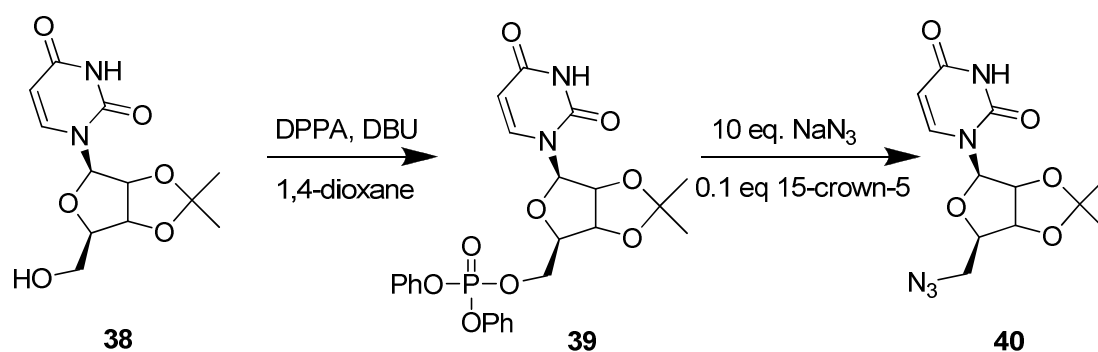


Scheme 8: Mechanism of the aldehyde to alkyne interconversion using dimethyl(diazomethyl)phosphonate (**27**).

4. Synthesis of 5'-azido-5'-deoxy-2',3'-*O*-isopropylidene uridine (**40**) from 2',3'-*O*-isopropylidene uridine (**38**).

Functional group transformation at the 5'-position of nucleosides has historically been an area of great interest due to the biological importance of these molecules.⁴¹ The primary difficulty in developing general and efficient methods for the synthesis of 5'-azido purine nucleosides lies mostly in the formation of undesired cyclonucleosides.⁴² Liu and Austin reported a general and efficient synthesis of 5'-azido nucleosides.⁴³

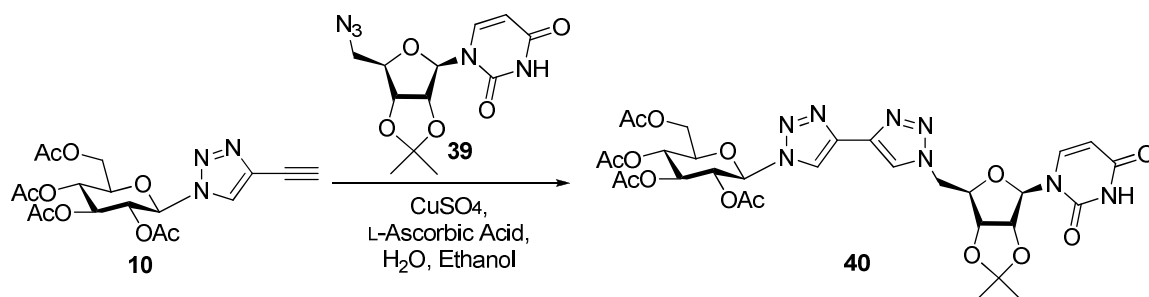
The next step in the overall synthesis involved taking 2',3'-*O*-isopropylidene uridine (**38**) and converting it to 5'-azido-5'-deoxy-2',3'-*O*-isopropylidene uridine (**40**) in a two step procedure (Scheme 9). Firstly, diphenylphosphoryl azide (DPPA) and DBU were allowed to react with **38** in 1,4-dioxane. TLC showed complete consumption of starting material after 16 hours, and formation of a new spot with a higher R_f value than the starting material. Upon completion of the first step, 15-crown-5 and sodium azide were added to the mixture, and it was left to react at 80 °C in an oil bath. TLC showed complete consumption of starting material after 18 hours, and formation of a new spot with a lower R_f value than compound **38**. The reaction was purified by flash column chromatography. The compound was verified by ^1H and ^{13}C NMR. ESI mass spectrometry provided a mass of 332.2 which corresponds to the addition of sodium to the calculated mass of 309.11 amu.



Scheme 9: Synthesis of 5'-azido-5'-deoxy-2',3'-*O*-isopropylidene uridine (**40**).

5. Synthesis of bis(1,2,3-triazole) 41 from alkyne 10 and 5'-azido-5'-deoxy-2',3'-*O*-isopropylidene uridine (40).

After the successful synthesis of **10** and **40** the two compounds were combined in 1:1 water / ethanol with CuSO_4 and L-ascorbic acid and were allowed to react for 48 hours (Equation 16). TLC showed complete consumption of alkyne **10** and the formation of a new spot with a lower R_f value than the starting materials. The ethanol was allowed to evaporate leading to precipitation of a white solid. The copper salt was washed out of the product with water over vacuum filtration and the product was subject to recrystallization with hot methanol. Clean NMR spectra were not obtained for **40** because of difficulty isolating it. ESI mass spectrometry gave a mass of 756.9 which corresponds to the addition of sodium to the calculated mass of 733.24 amu at 30% compound stability.

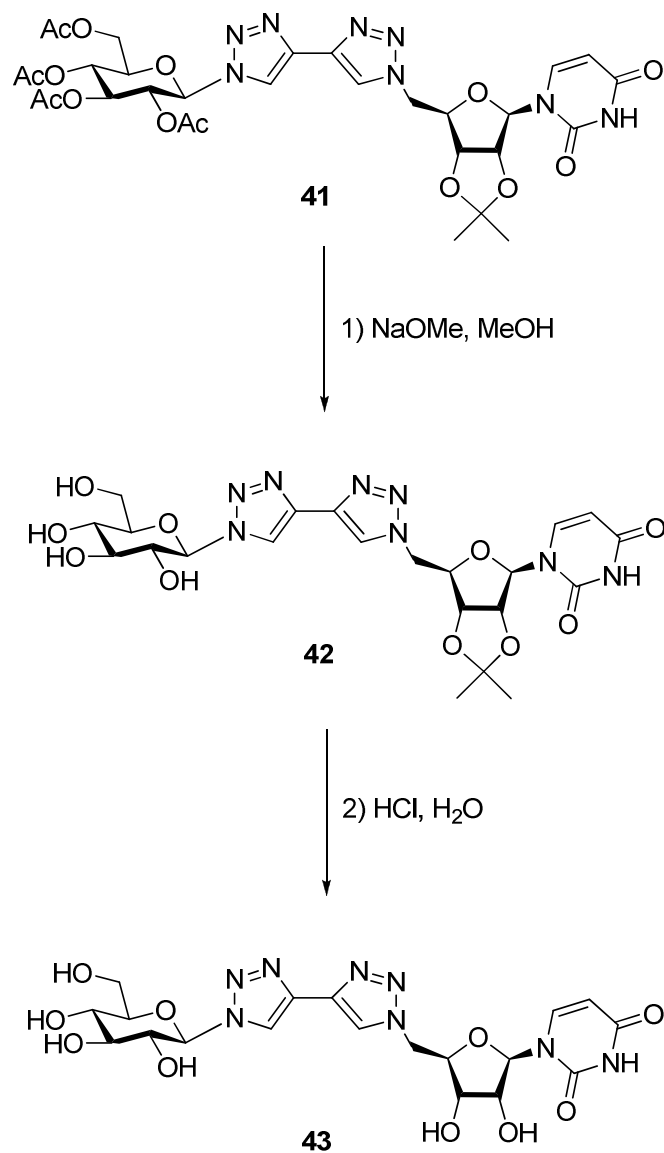


Equation 16: Synthesis of glucosyl-bis(1,2,3-triazole)-uridine **41** from alkyne **10** and 5'-azido-5'-deoxy-2',3'-O-isopropylidene uridine (**40**).

5. Future work.

While mass spectrum of the crude material showed a mass corresponding to the bis(1,2,3-triazole), the compound needs to be successfully isolated to get clean NMR spectra. Following the isolation of **41**, the protecting groups will need to be removed. There are two different kinds of protecting groups on **41**, acid- and base-labile. The acetyl groups

will be removed first with sodium methoxide in an excess of methanol. The isopropylidene protecting group will then be removed with HCl in water (Scheme 10).

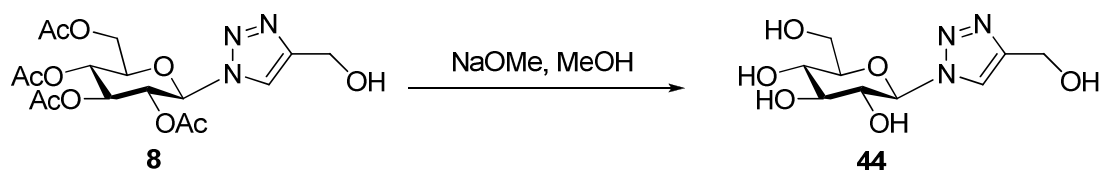


Scheme 10: Deprotection of glucosyl-bis(1,2,3-triazole)-uridine **41**.

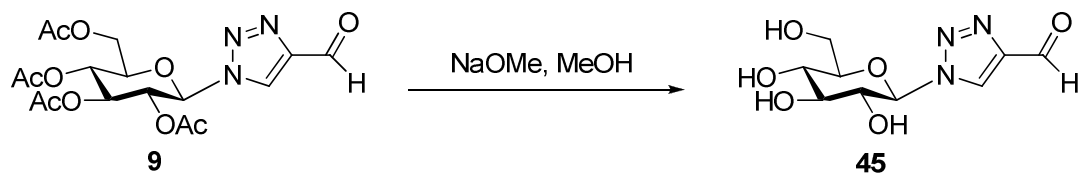
6. Deprotection of acetyl protected sugars

Glucosyl triazoles have the potential to inhibit carbohydrate-processing enzymes, and recently the ability to inhibit glucosidase enzymes were tested by biochemists for

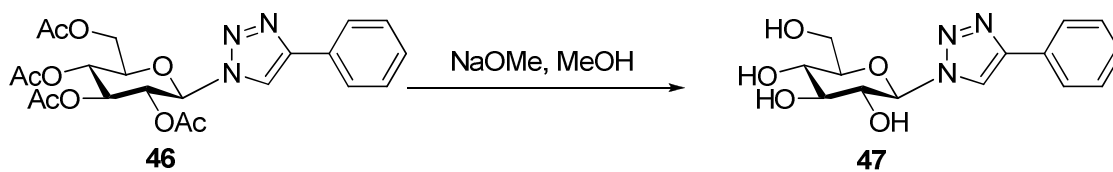
various glucosyl triazoles. Compounds **8**, **9** and **46** were deprotected with sodium methoxide in methanol to yield compounds **44**, **45**, and **47** (Equations 17-19). Glucosyl triazoles **7**, **8**, and **9** (1 mmol) were dissolved in MeOH. In a test tube with MeOH a sodium pellet was added to yield sodium methoxide; this was then added to the triazole solution and allowed to stir for an hour. The reaction was verified by TLC showing complete consumption of starting material. Acidic ion exchange resin was then added and allowed to stir for 30 minutes. Acidic ion exchange resin protonates the negative oxygens on the sugar. The product was concentrated and subject to recrystallization with *i*PrOH or H₂O, unfortunately ¹H and ¹³C NMR data were complicated for each compound, aside from deprotected phenyl triazole **47**. ESI mass spectrometry gave a mass of 284.1 for **44**, which corresponds to the addition of sodium to the calculated mass of 261.1 amu; 283.1 for **45**, which corresponds to the addition of sodium plus a proton to the calculated mass of 259.08 amu; and 330.2 for **47**, which corresponds to the addition of sodium and loss of the nitro group to the calculated mass of 307.1 amu. Single crystal X-Ray data (Figure 15) was obtained for the deprotected glucosyl triazole **47** to confirm the structure and conformation of the compound. Compound **47** was also reacetylated with acetic anhydride and pyridine to yield compound **46**.



Equation 17: Deprotection of the acetyl groups of triazole **8** to yield **44**.



Equation 18: Deprotection of the acetyl groups of aldehyde **9** to yield deprotected aldehyde **45**.



Equation 19: Deprotection of the acetyl groups of triazole **46** to yield triazole **47**.

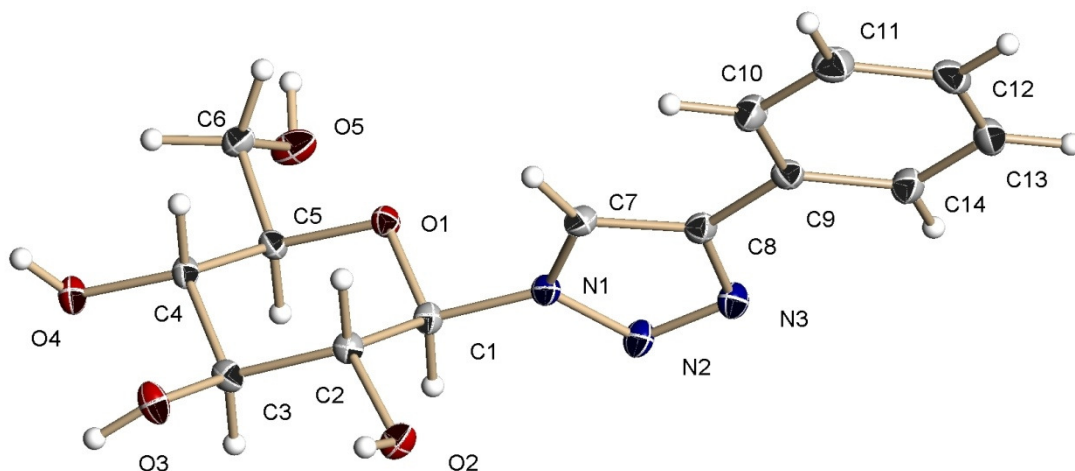
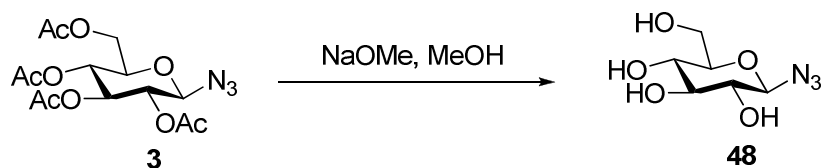


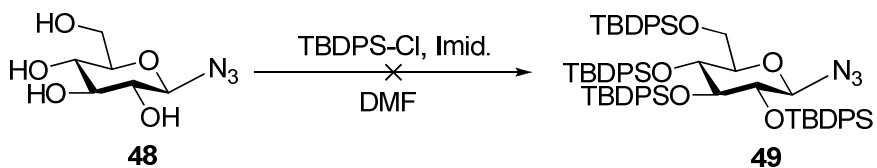
Figure 15: X-Ray structure of deprotected glucosyl phenyl triazole **47**.

Glucosyl azide **3** was also deprotected, to yield **48** (Equation 20). Azide **48** (1.70 g, 1 mmol) was mixed with *tert*-butylchlorodiphenyl silane (1.06 mL, 4.15 mmol) and imidazole (0.283 g, 4.15 mmol) in DMF (4.15 mL) in an attempt to add on the acid- and base-stable *tert*-butyldiphenylsilyl (TBDPS) protecting groups (Equation 21). This

reaction failed to give the desired product, but yielded a unique crystal structure of the silanol **50** with four crystallographically independent molecules that form a hydrogen bonded tetramer (Figure 16).



Equation 20: Deprotection of the acetyl groups of glucosyl azide **3** to yield deprotected glucosyl azide **48**.



Equation 21: Attempted synthesis of *tert*-butyl-diphenylsilyl-protected glucosyl azide **49**.

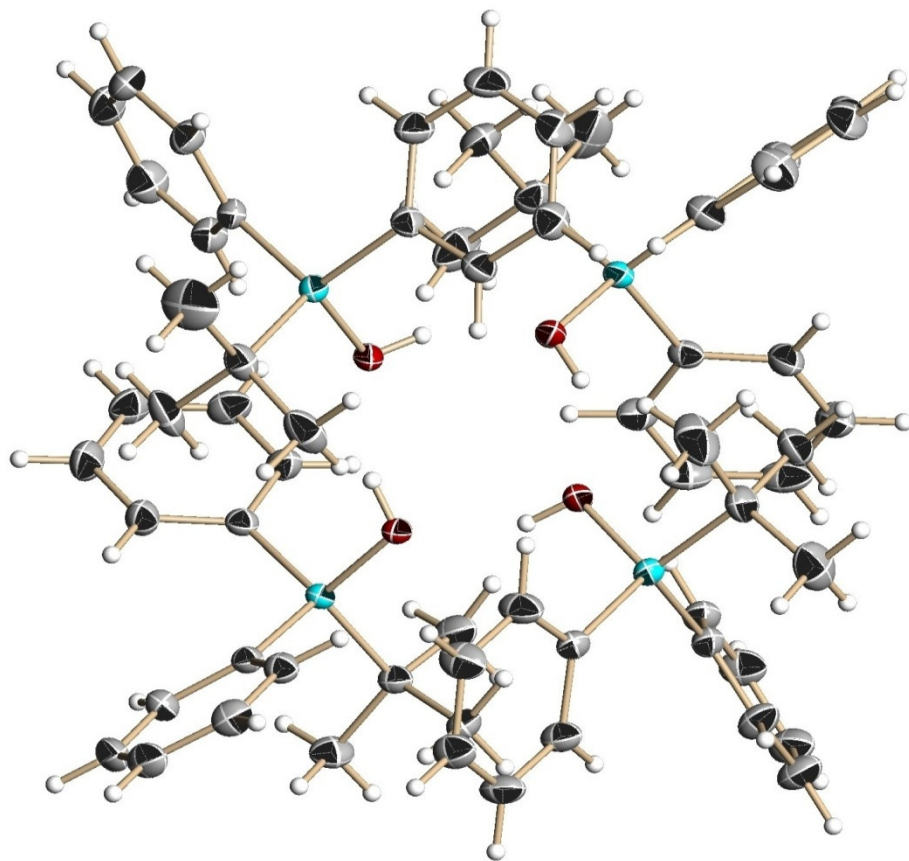


Figure 16: X-Ray structure of *tert*-butyldiphenylsilanol tetramer **50**.

Experimental

Preparation of glucosyl bromide **2** from 1,2,3,4,6-penta-*O*-acetyl- β -D-glucose (**1**).

In a 500 mL round-bottom flask equipped with a magnetic stir bar, 1,2,3,4,6-penta-*O*-acetyl- β -D-glucose (**1**, 30 g, 76.9 mmol) was dissolved in 33% HBr in acetic acid (120 mL). The mixture was allowed to react for 3.5 hours and reaction progress was monitored by TLC (2:1, hexane:ethyl acetate), which showed consumption of starting material and formation of a new product. The reaction was then diluted with methylene chloride (150 mL) and chilled to 0 °C. The mixture was neutralized with 10% NaOH (480 mL) and saturated sodium bicarbonate (50 mL). The product was extracted with methylene chloride (3 x 75 mL) and the organic layer was dried over anhydrous MgSO₄. After filtering, the solvent was reduced to yield **2** (31.6 g, 76.8 mmol, 99%) as a white solid.

¹H NMR (CDCl₃): δ 2.04, 2.06, 2.10, 2.11 (4s, 12H total, 4 x COCH₃), 3.70 (ddd, 1H, H-5, $J = 3.73, 6.34, 13.59$ Hz), 4.13 (dd, 1H, H-6, $J = 2.08, 12.97$ Hz), 4.33 (dd, 1H, H-6', $J = 4.14, 11.24$ Hz), 4.85 (dd, 1H, H-2, $J = 4.04, 10.07$ Hz), 5.17 (dd, 1H, H-3, $J = 10.03, 9.57$ Hz), 5.56 (dd, 1H, H-4, $J = 9.79, 9.79$ Hz), 6.62 (d, 1H, H-1, $J = 4.03$ Hz).

¹³C NMR (CDCl₃): δ 20.5, 20.5, 20.6, 20.6, 60.1, 67.1, 70.1, 70.5, 72.1, 86.6, 169.4, 169.7, 169.8, 170.5.

m/z calculated: 410.02

m/z found: 433.0 (+Na)

$R_f = 0.34$ (hexanes / ethyl acetate 2:1).

Melting Point: 59-62 °C.

Preparation of glucosyl azide 3 from glucosyl bromide 2.

In a 1000 mL round-bottom flask equipped with a magnetic stir bar, sodium azide (30 g, 470.8 mmol) was added to **2** (31.6 g, 76.8 mmol) and then dissolved in DMF (300 mL). The mixture was allowed to react overnight. The reaction was analyzed by TLC (2:1, hexanes / ethyl acetate, $R_f = 0.61$), which showed consumption of starting material and formation of new product. The reaction was then washed with 5% H₂SO₄ and then water. The aqueous layers were extracted with methylene chloride (3 x 100 mL) and the organic layer was dried over anhydrous MgSO₄. After filtering, the solvent was reduced to yield **3** (23.0 g, 61.5 mmol, 80%), which was subject to recrystallization with isopropyl alcohol to afford colorless crystals.

¹H NMR (CDCl₃): δ 2.02, 2.04, 2.09, 2.11 (4s, 12H total, 4 x COCH₃), 3.80 (ddd, 1H, H-5, $J = 2.32, 4.73, 10.04$ Hz), 4.17 (dd, 1H, H-6, $J = 2.30, 12.47$ Hz), 4.29 (dd, 1H, H-6', $J = 4.78, 12.50$ Hz), 4.66 (d, 1H, H-1, $J = 8.88$ Hz), 4.96 (dd, 1H, H-2, $J = 8.90, 9.53$ Hz), 5.11 (dd, 1H, H-3, $J = 9.98, 9.57$ Hz), 5.23 (dd, 1H, H-4, $J = 9.57, 9.57$ Hz).

¹³C NMR (CDCl₃): δ 20.5, 20.5, 20.6, 20.6, 61.7, 67.9, 70.6, 72.6, 74.1, 87.9, 169.2, 169.3, 170.1, 170.6.

m/z calculated: 373.32

m/z found: 396.1 (+Na)

$R_f = 0.61$ (hexanes / ethyl acetate 2:1).

Melting Point: 128-130 °C.

$[\alpha]_D$: -30.5 (c 1.0, CH_2Cl_2).

Preparation of glucosyl triazole **8** from glucosyl azide **3**.

In a 100 mL round-bottom flask equipped with a magnetic stir bar, glucosyl azide **3** (0.373 g, 1 mmol) was added to a mixture of CuSO_4 (0.01 g, 0.04 mmol, ascorbic acid (0.1 g, 0.56 mmol) and propargyl alcohol (0.177 mL, 4.0 mmol) in 1:1 $\text{H}_2\text{O}:\text{EtOH}$ (5 mL). The reaction was allowed to proceed at RT overnight. The reaction was analyzed by TLC (2:1, hexanes / ethyl acetate, $R_f = 0.18$), which showed consumption of starting material and formation of a new product. The product was filtered and washed with cold water to afford a solid. The product was subject to recrystallization from hot methanol to yield triazole **8** (0.322 g, 0.750 mmol, 75%) as a white solid.

^1H NMR (CDCl_3): δ 1.89, 2.04, 2.08, 2.09 (4s, 12H total, 4 x COCH_3), 3.49 (bs, 1H, hydroxyl signal), 4.02 (ddd, 1H, H-5, $J = 2.07, 4.95, 10.12$ Hz), 4.15 (dd, 1H, H-6, $J = 2.13, 12.59$ Hz), 4.31 (dd, 1H, H-6', $J = 5.00, 12.59$ Hz), 4.81 (s, 2H, triazole- CH_2), 5.26 (dd, 1H, H-2, $J = 9.66, 9.69$ Hz), 5.41-5.49 (m, 2H, H-3, H-4), 5.90 (d, 1H, H-1, $J = 8.93$ Hz), 7.82 (s, 1H, triazole-H).

^{13}C NMR (CDCl_3): δ 20.2, 20.5, 20.5, 20.7, 56.6, 61.5, 67.7, 70.3, 72.6, 75.1, 85.8, 120.0, 148.6, 169.2, 169.3, 170.1, 170.6.

m/z calculated: 429.14

m/z found: 452.2 (+Na)

$R_f = 0.18$ (hexanes / ethyl acetate 1:3).

Melting Point: 165-168 °C.

$[\alpha]_D^{20}$: -41 (c 1.0, CH_2Cl_2).

Preparation of aldehyde **9** from alcohol **8**.

In an oven-dried 100 mL round-bottom flask equipped with a magnetic stir bar, glucosyl triazole alcohol **8** (1.00 g, 2.32 mmol) was added to pyridinium chlorochromate (3.00 g, 13.9 mmol) with an equivalent amount of 4 Å molecular sieves (3.00 g) in CH_2Cl_2 (90 mL). The mixture was allowed to react for 48 hours at room temperature. The reaction was monitored by TLC (1:3, hexanes / ethyl acetate, $R_f = 0.52$). Upon completion, the reaction was filtered through silica gel using 1:3 hexanes / ethyl acetate. The solvent was removed from the appropriate fractions yielding a white solid. The product was subject to recrystallization in hot methanol to yield **9** (0.498 g, 1.16 mmol, 50%) as a white solid.

^1H NMR (CDCl_3): δ 1.91, 2.04, 2.08, 2.09 (4s, 12H total, 4 x COCH_3), 4.05 (ddd, 1H, H-5, $J = 2.28, 4.88, 10.02$ Hz), 4.18 (dd, 1H, H-6, $J = 1.96, 12.54$ Hz), 4.32 (dd, 1H, H-6', $J = 4.84, 12.59$ Hz), 5.27 (dd, 1H, H-2, $J = 9.28, 10.24$ Hz), 5.38-5.49 (m, 2H, H-3, H-4), 5.95 (d, 1H, H-1, $J = 8.79$ Hz), 8.39 (s, 1H, triazole-H), 10.15 (s, 1H, aldehyde-H).

^{13}C NMR (CDCl_3): δ 20.1, 20.5, 20.5, 20.6, 61.4, 67.5, 70.6, 72.2, 75.4, 86.0, 124.1, 147.9, 168.9, 169.2, 169.8, 170.4, 184.4.

m/z calculated: 427.12

m/z found: 450.2 (+Na)

$R_f = 0.52$ (hexanes / ethyl acetate 3:1).

Melting Point: 175-181 °C.

$[\alpha]_D^{20}$: -21 (c 1.0, CH_2Cl_2).

Preparation of alkyne **10** from aldehyde **9**.

To a flame-dried 50 mL round-bottom flask equipped with a magnetic stir bar potassium *tert*-butoxide (0.134 g, 1.20 mmol) was added to dry THF (1.5 mL). The solution was allowed to cool to -78 °C, then dimethyl(diazomethyl)phosphonate (**27**) (0.180 g, 1.20 mmol) in dry THF (2 mL) and glucosyl aldehyde **9** (0.429 g, 1.00 mmol), in dry THF (4 mL) were added and allowed to stir for 12 hours at -78 °C. TLC (1:3, hexanes / ethyl acetate, $R_f = 0.734$) showed complete consumption of starting material and formation of a new spot with a higher R_f value than the starting material and several new spots with a lower R_f value than the starting material. Upon completion, the reaction was washed with water (1 x 25 mL) and then extracted with methylene chloride (3 x 25 mL). The organic layer was washed with brine (1 x 25 mL) and the organic layer was dried over anhydrous MgSO_4 . After filtering, the solvent was reduced and flash column chromatography was performed to isolate **10** in analytically pure form. The solvent was reduced yielding **10** (0.013 g, 0.31 mmol, 10%) as a white solid.

^1H NMR (CDCl_3): δ 1.92, 2.06, 2.09, 2.11 (4s, 12H total, 4 x COCH_3), 3.27 (s, 1H, alkyne-H), 4.01 (ddd, 1H, H-5, $J = 2.18, 5.01, 10.01$ Hz), 4.15 (dd, 1H, H-6, $J = 2.06, 12.56$ Hz), 4.35 (dd, 1H, H-6', $J = 5.08, 12.78$ Hz), 5.24 (dd, 1H, H-4, $J = 9.57, 10.05$

Hz), 5.41-5.43 (m, 2H, H-2, H-3), 5.89 (d, 1H, H-1, $J = 5.12$ Hz), 7.92 (s, 1H, triazole-H).

^{13}C NMR (CDCl_3): δ 20.14, 20.49, 20.52, 20.66, 61.44, 67.60, 70.20, 72.34, 72.50, 75.30, 81.82, 85.83, 125.07, 130.91, 168.9, 169.3, 169.9, 170.4.

m/z calculated: 423.37

m/z found: 446.2 (+Na)

$R_f = 0.734$ (hexanes / ethyl acetate 3:1).

α,β -Unsaturated ketone 16.

In a flame-dried 50 mL round-bottom flask equipped with a magnetic stir bar under a nitrogen atmosphere, dimethyl-2-oxopropylphosphonate **11** (0.382 mL, 0.233 mmol) was added and *p*-toluenesulfonyl azide **13** (0.551 g, 2.80 mmol) to a suspension of K_2CO_3 in MeCN. TLC (ethyl acetate) showed complete consumption of starting material after 2 hours, and formation of a new spot with a lower R_f value than the starting material. Aldehyde **9** was then added and allowed to stir for sixteen hours. TLC (1:3 hexanes / ethyl acetate) showed the complete consumption of starting material and formation of a new spot with a lower R_f value than aldehyde **9** (1.00 g, 2.33 mmol). Upon completion of this reaction, flash column chromatography (1:3 hexanes / ethyl acetate) was performed to isolate the compound. The solvent was reduced yielding **16** (0.819 g, 1.75 mmol, 75%) as a white solid.

^1H NMR (CDCl_3): δ 1.43 (s, 3H, ketone COCH_3), 1.90, 2.04, 2.09, 2.38 (4s, 12H total, 4 x COCH_3), 4.05 (ddd, 1H, H-5, $J = 2.85, 4.82, 10.08$ Hz), 4.17 (dd, 1H, H-6, $J = 2.01, 12.84$ Hz), 4.33 (dd, 1H, H-6', $J = 4.97, 12.78$ Hz), 5.24-5.31 (m, 1H, H-2), 5.42-5.48 (m, 2H, H-3, H-4), 5.92 (d, 1H, H-1, $J = 9.25$ Hz), 6.97 (d, 1H, ketone α -H, $J = 16.31$ Hz), 7.49 (d, 1H, ketone β -H, $J = 16.31$ Hz), 7.99 (s, 1H, triazole-H).

^{13}C NMR (CDCl_3): δ 20.1, 20.5, 20.5, 20.7, 26.9, 27.9, 61.4, 67.6, 70.2, 72.4, 75.2, 85.8, 121.9, 129.1, 130.1, 144.3, 168.9, 169.3, 169.9, 170.4, 197.8.

m/z calculated: 467.2

m/z found: 490.2 (+Na)

$R_f = 0.245$ (hexanes / ethyl acetate 1:3).

Melting Point: 201-210 $^\circ\text{C}$.

Preparation of sulfonyl azides **13, **19**, and **21** from sulfonyl chlorides **17**, **18**, and **20**.**

In a 50 mL round-bottom flask equipped with magnetic stir bar the appropriate sulfonyl chloride (22.6 mmol) was added to ethanol (50 mL) and the reaction was purged with nitrogen gas. Sodium azide (24.9 mmol) was dissolved in a small amount of water, diluted with ethanol (11 mL) and then added to the flask dropwise *via* syringe. These reactions generally were complete in 8 hours and were monitored *via* TLC (1:1 hexanes / ethyl acetate). The reaction was diluted with water (20 mL), the aqueous layers were extracted with methylene chloride (3 x 50 mL), and the organic layer was dried over anhydrous MgSO_4 . The solvent was reduced, yielding compounds **13**, **19**, & **21** as oil or colorless crystals with yields ranging from 80-85%.

***p*-Toluenesulfonyl azide (13).**

^1H NMR (CDCl_3): δ 2.49 (s, 3H), 7.39-7.43 (m, 2H, Ar-H), 7.82-7.87 (m, 2H, Ar-H).

^{13}C NMR (CDCl_3): δ 125.4, 131.7, 132.6, 133.1, 135.8, 147.8.

m/z calculated: 197.03

m/z found: 220.0 (+Na)

R_f = 0.56 (hexanes / ethyl acetate 3:1).

***o*-Nitrobenzenesulfonyl azide (19).**

^1H NMR (CDCl_3): δ 7.81-7.95 (m, 3H, Ar-H), 8.20 (dd, 1H, J = 7.79, 9.08 Hz).

^{13}C NMR (CDCl_3): δ 125.4, 131.7, 132.6, 133.1, 135.8, 147.8.

m/z calculated: 228.00

m/z found: 251.3 (+Na)

R_f = 0.18 (hexanes / ethyl acetate 3:1).

***p*-Nitrobenzenesulfonyl azide (21).**

^1H NMR (CDCl_3): δ 8.16-8.19 (m, 2H, Ar-H), 8.44-8.18 (m, 2H, Ar-H).

^{13}C NMR (CDCl_3): δ 128.9, 124.19.

m/z calculated: 228.00

m/z found: 204.1 (+Na, $-\text{NO}_2$)

R_f = 0.23 (hexanes / ethyl acetate 3:1).

Preparation of 4-chlorophenylacetylene (25) from 4-chlorobenzaldehyde (24).

In an oven-dried 100 mL round-bottom flask equipped with a magnetic stir bar, dimethyl-2-oxopropylphosphonate (0.164 mL, 1.2 mmol) was added dropwise to a suspension of *p*-ABSA (0.351 g, 1.20 mmol) and K₂CO₃ (0.415 g, 3.00 mmol) in acetonitrile (15 mL). This mixture was allowed to react for 2 hours, and was monitored by TLC (1:1 hexanes / ethyl acetate). 4-Chlorobenzaldehyde (0.141 g, 1.00 mmol) was dissolved in MeOH (3 mL) and then added dropwise to the reaction. The mixture was allowed to react for 36 hours. The reaction was monitored by TLC (5:1, hexanes / ethyl acetate, R_f = 0.470). The reaction was filtered through silica gel using 5:1 hexanes / ethyl acetate. The solvent was removed from the relevant fractions yielding **25** (0.0274 g, 0.201 mmol, 20%) as a colorless oil.

¹H NMR (CDCl₃): δ 3.10 (s, 1H, alkyne) 7.29 (d, 2H, *J* = 9.0 Hz, Ar-H), 7.41 (d, 2H, *J* = 9.0 Hz, Ar-H).

¹³C NMR (CDCl₃): δ 78.1, 82.4, 120.6, 128.7, 133.3, 133.4.

m/z calculated: 136.01

m/z found: 124.9 (-Cl, +Na, +H)

R_f = 0.30 (ethyl acetate).

Preparation of dimethyl(diazomethyl)phosphonate (27) from dimethyl methylphosphonate (28).

To a flame-dried 250 mL round-bottom flask 40 mL of dry THF was added. Dimethyl methylphosphonate (**28**, 2.29 g, 2.00 mL, 18.4 mmol) was added and the

mixture was cooled to $-78\text{ }^{\circ}\text{C}$. *n*-Butyllithium (7.34 mL of a 2.50 M solution in hexanes, 18.4 mmol) was added over 5 minutes and the solution was allowed to stir at $-78\text{ }^{\circ}\text{C}$ for 30 minutes. 2,2,2-Trifluoroethyl trifluoroacetate (5.41 g, 3.73 mL, 27.6 mmol) was added rapidly, and the solution was allowed to stir at $-78\text{ }^{\circ}\text{C}$ for 15 minutes. The solution was warmed to room temperature, partitioned between diethyl ether (250 mL) and 3% HCl (10 mL), and then washed with saturated aqueous NaHCO_3 (1 x 10 mL) and saturated aqueous NaCl (1 x 10 mL). The organic layer was separated, dried over MgSO_4 , and concentrated to afford dimethyl (3,3,3-trifluoro-2,2-dihydroxypropyl)-phosphonate **29**. This crude sample was immediately dissolved in dry CH_3CN (40 mL). *p*-ABSA (3.97 g, 16.5 mmol) was added and the solution was cooled to $0\text{ }^{\circ}\text{C}$. Triethylamine (1.66 g, 2.29 mL, 16.5 mmol) was then added dropwise over 5 minutes. The mixture was warmed to room temperature and allowed to stir overnight. The solvent was reduced, chloroform was added, and 4-acetamidobenzenesulfonamide was filtered over a glass frit. After concentration of the filtrate, column chromatography was used to purify the crude compound (EtOAc) to yield **27** (1.33 g, 8.86 mmol, 48%) as a yellow oil.

^1H NMR (CDCl_3): δ 3.78 (d, 6H, $\text{OCH}_3 \times 2$, $J = 10.85\text{ Hz}$).

^{13}C NMR (CDCl_3): δ 28.0 (d, $J = 231.68\text{ Hz}$), 53.0 (d, $J = 5.14\text{ Hz}$).

IR (thin film/ NaCl) 3055, 2987, 2306, 2110, 1733, 1422, 1374, 1266, 1046, 896, 829, 740, 705, 634, 607 cm^{-1} .

m/z calculated: 150.02

m/z found: 173.5 (+Na)

R_f = 0.30 (ethyl acetate).

Preparation of 5'-azido-5'-deoxy-2',3'-*O*-isopropylidene uridine (40) from 2',3'-*O*-isopropylidene uridine (38).

In an oven-dried 50 mL round-bottom flask equipped with a magnetic stir bar, 2',3'-*O*-isopropylidene uridine (0.28 g, 1.00 mmol) was dissolved in dry 1,4-dioxane (2 mL) under a nitrogen atmosphere. DBU (1.5 mmol) and DPPA (1.00 mmol) were added dropwise, and this mixture was left to react overnight. The reaction was monitored by TLC (1:5 ethanol / ethyl acetate). Upon completion of this reaction, sodium azide (0.640 g, 10 mmol) and 15-crown-5 (0.1 mmol) were added and the mixture was left to react overnight at 80 °C. Reaction progress was monitored *via* TLC (1:1 hexanes / ethyl acetate). Upon completion of this reaction, flash column chromatography (1:1 hexanes / ethyl acetate) was performed to isolate the compound. The solvent was reduced yielding **40** (0.544 g, 1.76 mmol, 50%) as a colorless oil.

^1H NMR (CDCl_3): δ 1.35 (s, 3H), 1.57 (s, 3H), 3.63 (d, 2H, $J = 5.75$ Hz), 4.24 (dd, 1H, $J = 5.30, 9.34$ Hz), 4.83 (dd, 1H, $J = 4.20, 6.44$ Hz), 5.03 (dd, 1H, $J = 2.16, 6.49$ Hz), 5.67 (d, 1H, $J = 5.75$ Hz), 5.77 (dd, 1H, $J = 0.23, 7.85$ Hz), 7.34 (d, 1H, $J = 8.34$ Hz), 8.95 (bs, 1H).

^{13}C NMR (CDCl_3): δ 25.2, 27.1, 52.3, 81.5, 84.3, 85.7, 94.7, 102.8, 114.8, 142.2, 150.0, 163.1.

IR (thin film/NaCl) 2985, 2940, 2907, 2254, 2107, 1734, 1465, 1375, 1360, 1152, 1096, 1046, 909, 731, 651, 608 cm^{-1} .

m/z calculated: 309.28

m/z found: 332.2 (+Na)

R_f = 0.378 (hexanes / ethyl acetate 1:1).

Preparation of bis(1,2,3-triazole) 41 from alkyne 10 and 5'-azido-5'-deoxy-2',3'-O-isopropylidene uridine (40).

In a 100 mL round-bottom flask equipped with a magnetic stir bar, alkyne **10** (0.012 g, 0.028 mmol) was added to a mixture of CuSO_4 , ascorbic acid and 5'-azido-5'-deoxy-2',3'-O-isopropylidene uridine (**40**) (0.020 g, 0.0623 mmol) in 1:1 H_2O :EtOH (5 mL). The reaction was allowed to proceed at RT overnight. The reaction was analyzed by TLC (ethyl acetate, R_f = 0.309), which showed consumption of starting material and formation of a new product. The reaction was filtered through silica gel using ethyl acetate. Isolation of **41** from the crude mixture was unsuccessful.

m/z calculated: 733.24

m/z found: 756.9 (+Na)

R_f = 0.309 (ethyl acetate).

Typical procedure for the deprotection of acetyl-protected sugars 3, 8, 9 and 46 to yield 44, 45, 47 and 48.

In a dry test tube methanol (5 mL) was added to a sodium pellet, thus forming sodium methoxide. To a 50 mL round-bottom flask equipped with magnetic stir bar,

acetyl-protected sugar **3**, **8**, **9**, or **46** (1 mmol) was added in methanol (50 mL). Sodium methoxide was added slowly, and this mixture was left to react for 2 hours. Acidic ion-exchange resin (1.00 g) was then added to the mixture and let stir for 30 minutes. This reaction was monitored *via* TLC (ethyl acetate). The ion-exchange resin was filtered and the solvent was reduced, yielding compounds **44**, **45**, **47**, and **48** as crystals with yields ranging from 90-95%.

Deprotected triazole 44.

m/z calculated: 411.30

m/z found: 433.0 (+Na)

$R_f = 0.01$ (ethyl acetate).

Deprotected aldehyde 45.

m/z calculated: 411.30

m/z found: 433.0 (+Na)

$R_f = 0.01$ (ethyl acetate).

Deprotected phenyl triazole 47.

^1H NMR (DMSO): δ 1.24, (s, 1H, -OH), 1.66 (bs, 3H, -OH), 2.88 (dd, 1H, H-5, $J = 5.34$, 10.08), 2.97 (dd, 1H, H-6, $J = 9.16$, 18.24 Hz), 3.79 (dd, 1H, H-6', $J = 5.62$, 10.17 Hz), 4.32 (d, 1H, H-2, $J = 4.82$ Hz), 4.47 (d, 1H, H-3, $J = 4.26$ Hz), 4.58 (s, 1H, H-4), 4.72 (d,

1H, H-1, $J = 9.29$ Hz), 6.48-6.52 (m, 1H, Ar-H), 6.59-6.64 (m, 2H, Ar-H), 7.02-7.05 (m, 2H, Ar-H), 7.97 (s, 1H, triazole-H).

^{13}C NMR (DMSO): δ . 60.8, 69.6, 72.2, 76.9, 80.0, 87.7, 120.5, 125.2, 127.9, 128.9, 130.6, 146.3.

m/z calculated: 411.30

m/z found: 433.0 (+Na)

$R_f = 0.05$ (ethyl acetate).

Deprotected glucosyl azide 48.

m/z calculated: 411.30

m/z found: 433.0 (+Na)

$R_f = 0.11$ (ethyl acetate).

Preparation of acetyl-protected glucosyl phenyl triazole (46) from deprotected glucosyl phenyl triazole (47).

In a 50 mL round-bottom flask equipped with magnetic stir bar, deprotected glucosyl phenyl triazole **47** (0.05 g, 0.163 mmol) and acetic anhydride (3 mL) were added in pyridine (4 mL) at 0 °C. This reaction was allowed to stir overnight and was monitored by TLC (1:1 hexanes / ethyl acetate). The solution was washed with 5% H_2SO_4 (2 x 10 mL), water (2 x 10 mL) and brine (1 x 10 mL). The aqueous layer was extracted with methylene chloride (2 x 20 mL) and the organic layer was dried over

anhydrous MgSO₄. After filtration, the solvent was reduced to yield **46** (0.077 g, 0.161 mmol, 99%) as a white crystalline solid.

¹H NMR (CDCl₃): δ 1.66, 1.89, 2.04, 2.09 (4s, 12H total, 4 x COCH₃, 4.04 (ddd, 1H, H-5, *J* = 2.27, 7.29, 12.30 Hz), 4.17 (dd, 1H, H-6, *J* = 2.24, 12.79 Hz), 4.34 (dd, 1H, H-6', *J* = 5.27, 12.78 Hz), 5.28 (dd, 1H, H-2, *J* = 9.28, 10.05 Hz), 5.45 (dd, 1H, H-3, *J* = 9.29, 9.29 Hz), 5.53 (dd, 1H, H-4, *J* = 9.54, 9.29 Hz), 5.94 (d, 1H, H-1, *J* = 9.30 Hz), 7.26-7.85 (m, 5H, Ar-H), 8.01 (s, 1H, triazole-H).

¹³C NMR (CDCl₃): δ 20.2, 20.5, 20.5, 20.7, 61.6, 67.8, 70.2, 72.7, 75.2, 85.8, 117.7, 125.9, 128.6, 128.9, 129.9, 148.5, 169.0, 169.4, 169.9, 170.5.

m/z calculated: 411.30

m/z found: 433.0 (+Na)

R_f = 0.344 (hexanes / ethyl acetate 1:1).

References:

1. Voet, D.; Voet, J. G., “*Biochemistry 3rd Edition*” John Wiley & Sons, New York, New York, **2003**, 73, 357-358.
2. Hanessian, S., “*Preparative Carbohydrate Chemistry*” Marcel Dekker, Inc., **1997**, 207-250.
3. Bols, M., “*Carbohydrate Building Blocks*” John Wiley & Sons, Inc. **1996**, 1-2.
4. El Khadem, H. S., “*Carbohydrate Chemistry; Monosaccharides and Their Oligomers*” Academic Press, Inc. **1988**, 1-5.
5. Guthrie, R. D.; Honeyman, J., “*An Introduction to the Chemistry of Carbohydrates*” Oxford University Press, **1968**, 1-3.
6. Collins, P. M.; Ferrier, R. J., “*Monosaccharides: Their Chemistry and Their Roles in Natural Products*” John Wiley & Sons, **1995**, 1-15.
7. Boons, G.-J., “*Carbohydrate Chemistry*” Thomson Science, **1998**, 430-442.
8. Pigman, W.; Horton, D., “*The Carbohydrates: Chemistry and Biochemistry 2nd Edition*” Academic Press, **1972**, 1-7.
9. Kennedy, J., “*Carbohydrate Chemistry*” Oxford University Press, **1988**, 1-4.
10. Robertson, J., “*Protecting Group Chemistry*” Oxford University Press, **2000**, 1-27.
11. Kolb, H. C.; Finn, M. G.; Sharpless, K. B. *Angew. Chem. Int. Ed.* **2001**, 40, 2004-2021.
12. Kolb, H. C.; Sharpless, K. B. *Drug Discovery Today* **2003**, 40, 1128-1137.
13. Huisgen, R., *Proceedings of the Chemical Society of London*, **1961**, 357-369.

14. Huisgen, R., 1,3-Dipolar Cycloadditions – Introduction, Survey, Mechanism. In *1,3-Dipolar Cycloaddition Chemistry*. Padwa, A, Ed.; Wiley: New York, **1984**, 1-176.
15. Tornøe, C. E.; Christensen, C.; Meldal, M. *J. Org. Chem.* **2002**, *67*, 3057-3064.
16. Akula, R. A.; Temelkoff, N. D. A.; Norris, P., *Heterocycles*, **2004**, *63*, 2719-2725.
17. Appukkuttan, P.; Dehaen, W.; Fokin, V.V.; Van der Eycken, E. *Org. Lett.* **2004**, *6*, 4223-4225.
18. Qafsaoui, W.; Blanc, C.; Pebere, N.; Srhiri, A.; Mankowski, G., *J. Appl. Electrochem.* **2000**, *18*, 100.
19. Seyferth, D.; Marmor, R.; Hilbert, P., *J. Org. Chem.* **1971**, *36*, 1379-1385.
20. Gilbert, J.; Weerasooriya, U., *J. Org. Chem.* **1982**, *47*, 1837-1845.
21. Callant, P.; D’Haenens, L.; Vandewalle, M., *Synth. Commun.* **1984**, *14*, 155-161.
22. Roth, G. J.; Liepold, B.; Müller S. G.; Bestmann, H. J., *Synthesis*, **2004**, 59-62.
23. Muller, S.; Leipold, B.; Roth, G.; Bestmann, H. J., *Synlett*, **1996**, 521-522.
24. <http://www.cdc.gov/mmwr/preview/mmwrhtml/mm5126al.htm>
25. Lowry, F. D., *New Eng. J. Med.* **1998**, *17*, 520-532.
26. Kneidinger, B.; O’Riordan, K.; Li, J.; Brisson, J.; Lee, J. C.; Lam, J. S. *J. Bio. Chem.* **2003**, *278*, 3615-3627.
27. O’Riordan, K.; Lee, J. C., *Clin. Microbiol. Rev.* **2004**, 218-234.
28. Sau, S.; Bhasen, N.; Wann, E. R.; Lee, J. C.; Foster, T. J.; Lee, C. Y., *Microbiol.* **1997**, *143*, 2395-2405.
29. Portoles, M.; Kiser, K. B.; Bhasin, N.; Chan, K.; Lee, J. C. *Infec. and Immun.* **2001**, *69*, 917-923.

30. Christianson, S.; Golding, G. R.; Campbell, J. *J. Clin. Microbiol.* **2007**, *46*, 1904-1911.
31. Cohen, J., "*The Staphylococci*" John Wiley & Sons, Inc., **1972**.
32. <http://www.history.com/encyclopedia.do?articleId=201185>
33. Chambers, H. F., *Emerg. Infect. Dis.* **2001**, *7*, 178-182.
34. Johnson, A.P.; Aucken, H. M.; Cavendish, D.; Ganner, M.; Wale, M. C.; Warner, M.; Livermoore, D. M.; Cookson, B. D., *J. Antimicrob. Chem.* **2001**, *48*, 143-144.
35. Chang, S.; Sievert, D. M.; Hageman, J. C.; Boulton, M. L.; Tenover, F. C.; Downes, F. P.; Shah, S.; Rudrik, J. T.; Pupp, G. R.; Brown, W. J.; Cardo, D.; Fridkin, S. K. *N. Engl. J. Med.* **2003**, *14*, 1342-1347.
36. Klevens, R. M.; Morrison, M. A.; Nadle, J.; Petit, S.; Gershman, K.; Ray, S.; Harrison, L. H.; Lynfield, R.; Dumyati, G.; Townes, J. M.; Craig, A. S.; Zell, E. R.; Fosheim, G. E.; McDougal, L. K.; Carey, R. B.; Fridkin, S. K., *J. of Amer. Med. Assoc.* **2007**, 1763-1771.
37. Stein, R., *Washington Post*, **2007**, 10-17-2007.
38. Akula, R., *Approaches to Pyranose Carbohydrids*. M.S. Thesis, Youngstown State University, Youngstown, OH, December **2004**.
39. Patton, G. C., *Development and Applications of Click Chemistry*, **2004**, <http://www.scs.uiuc.edu/>.
40. Hunsen, M., *Tetrahedron Lett.* **2005**, *46*, 1651-1653.
41. Pankiewicz, K. W.; Lesiak, K.; Watanabe, K. A., *J. Am. Chem. Soc.* **1997**, *119*, 3691-3695.
42. Anzai, K.; Uzawa, J., *J. Org. Chem.* **1984**, *49*, 5076-5080.

43. Liu, F.; Austin, D. J., *J. Org. Chem.* **2001**, *66*, 8643-8645.
44. Brown, D; Velthuisen, E.; Commerford, J.; Brisbois, R; Hoye, T. R., *J. Org. Chem.* **1996**, *61*, 2540-2541.

Appendix A

NMR, IR, & Mass Spectra

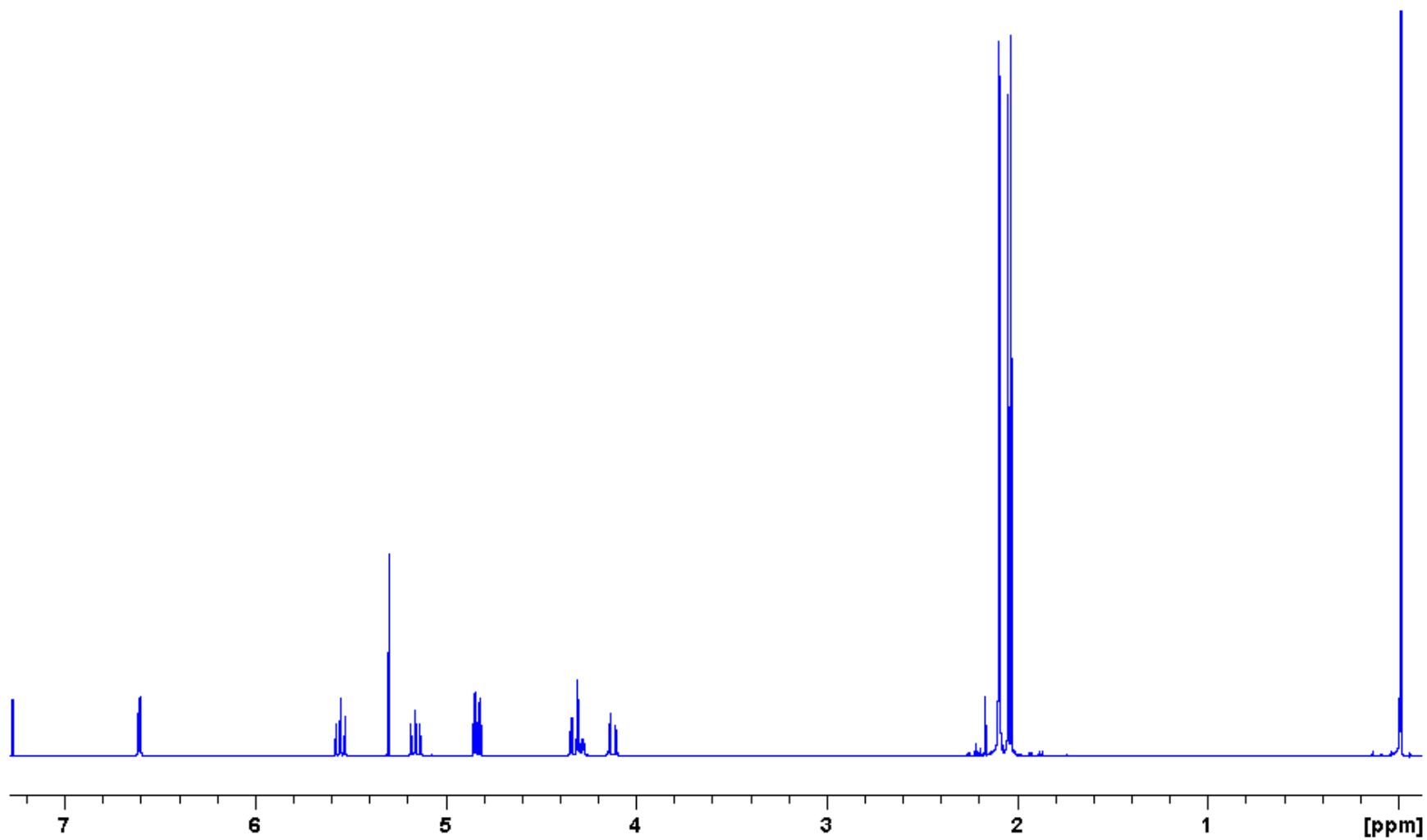


Figure 17: 400 MHz ^1H spectrum of glucosyl bromide 2.

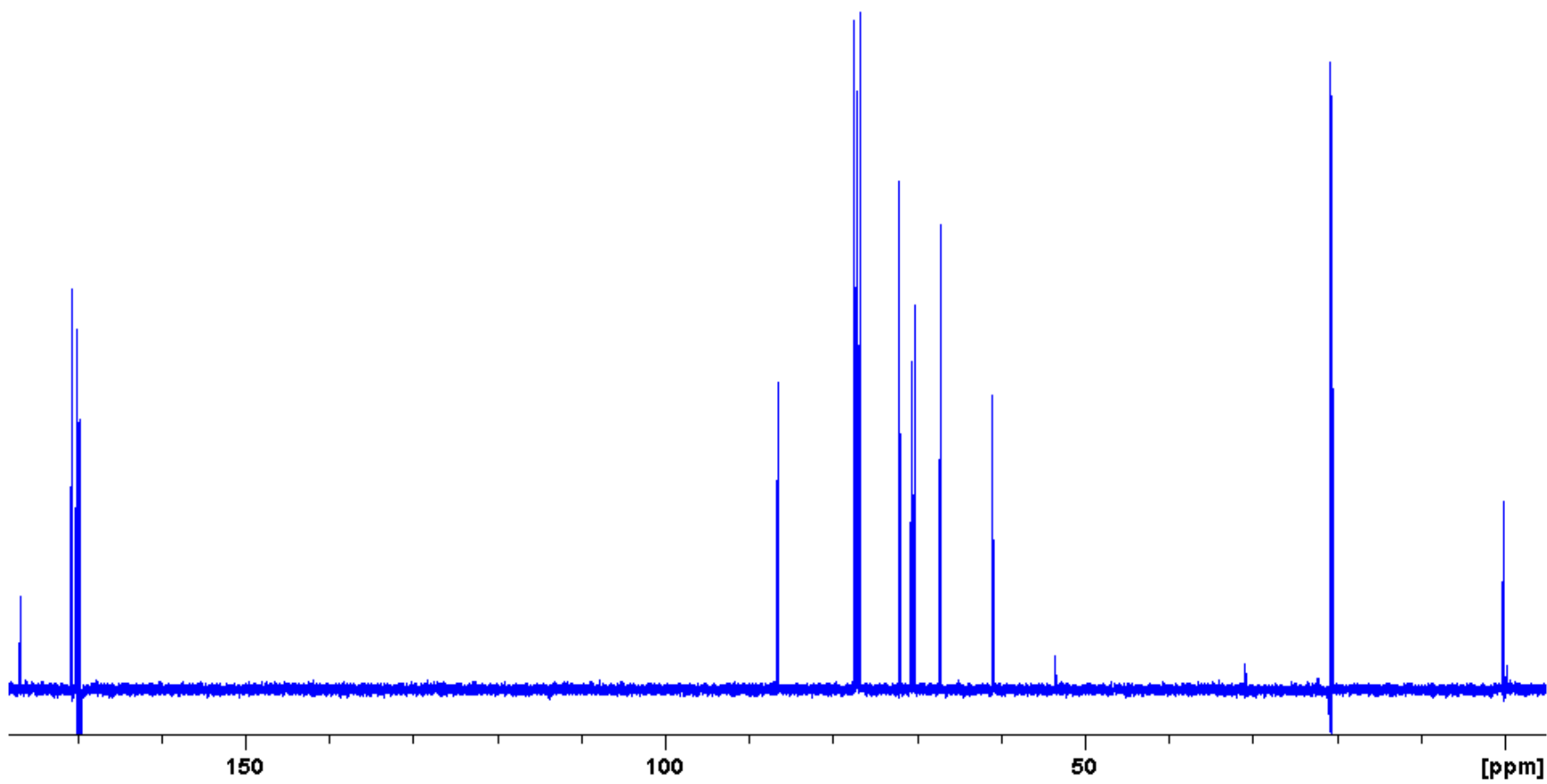


Figure 18: 100 MHz ^{13}C spectrum of glucosyl bromide 2.

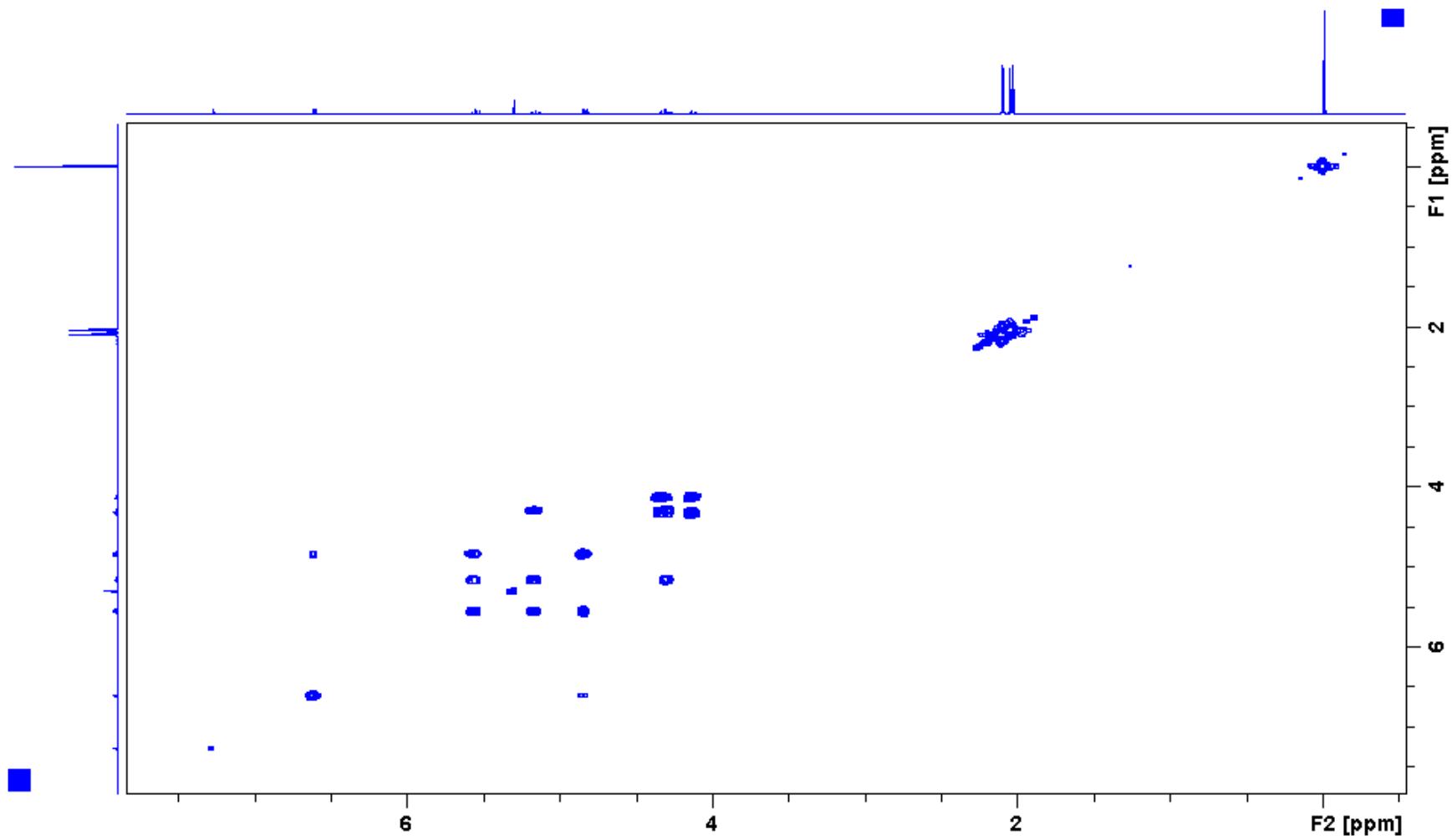


Figure 19: 400 MHz ^1H - ^1H COSY spectrum of glucosyl bromide **2**.

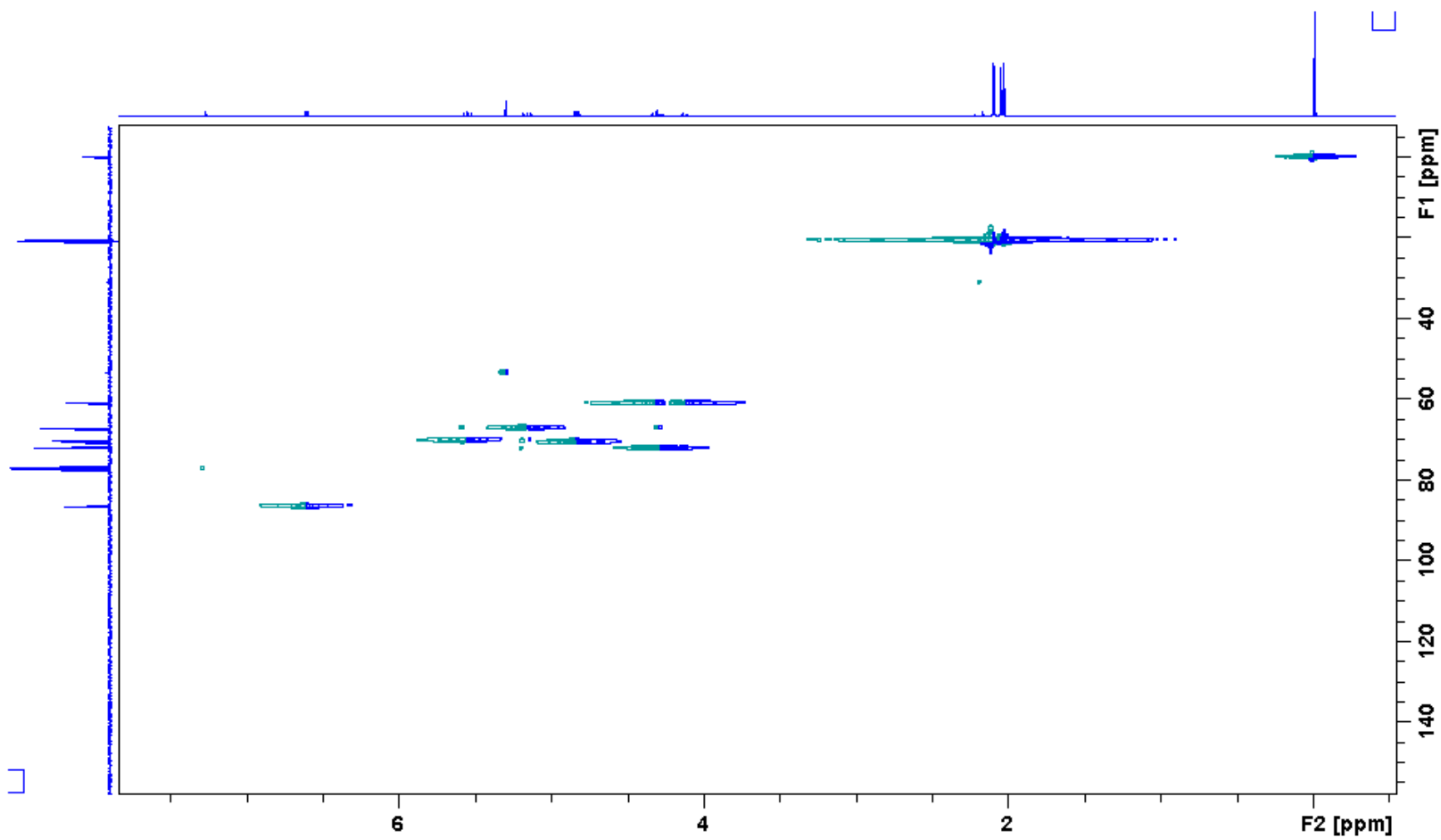


Figure 20: 400 MHz ^1H - ^{13}C HSQC spectrum of glucosyl bromide **2**.

Display Report

Analysis Info

Method XQ Default.ms Instrument Esquire-LC_00135

Acquisition Parameter

Ion Source Type	ESI	Mass Range Mode	Std/Normal	Ion Polarity	Positive	Alternating Ion Polarity	n/a
Scan Begin	100.00 m/z	Scan End	700.00 m/z	Averages	10 Spectra	Accumulation Time	20604 μ s
Capillary Exit	113.9 Volt	Skim 1	38.9 Volt	Trap Drive	50.7	Auto MS/MS	Off

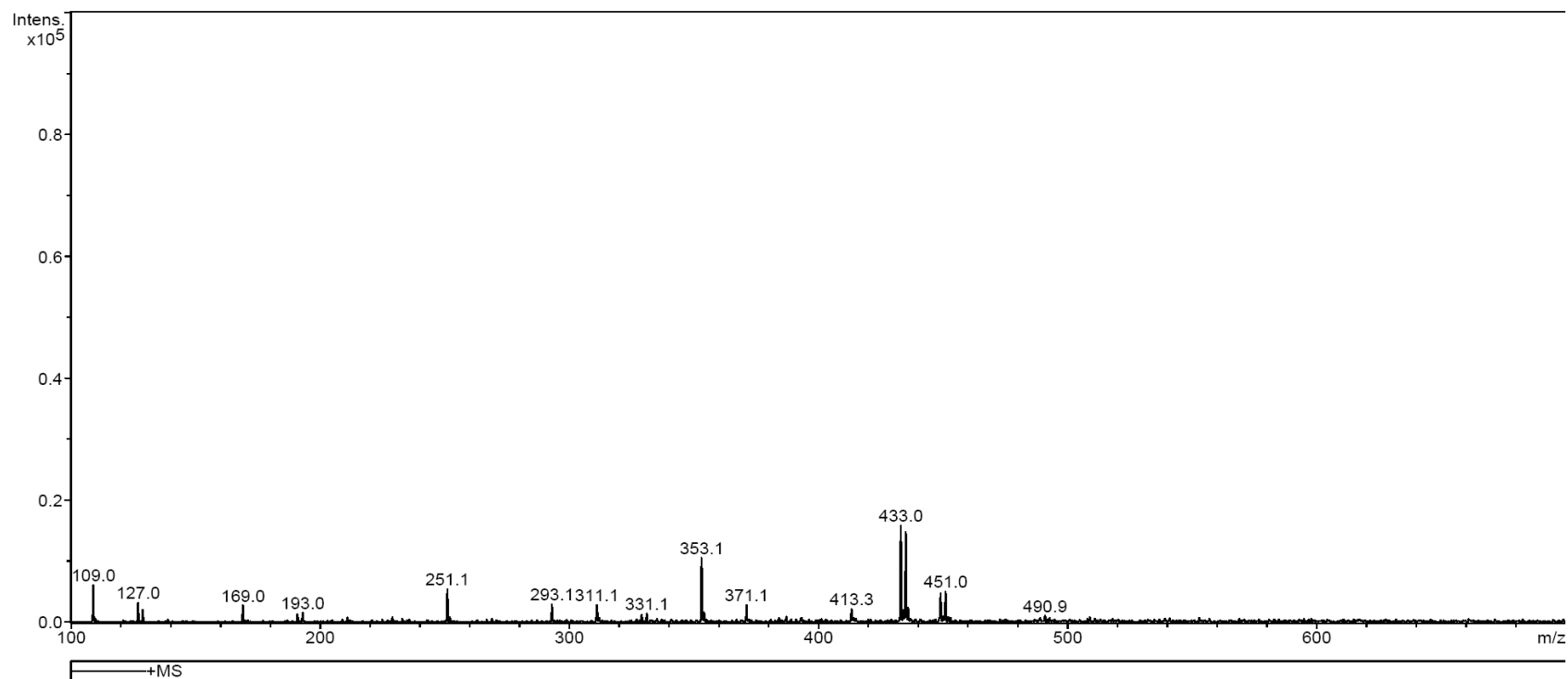


Figure 21: Mass spectrum of glucosyl bromide 2.

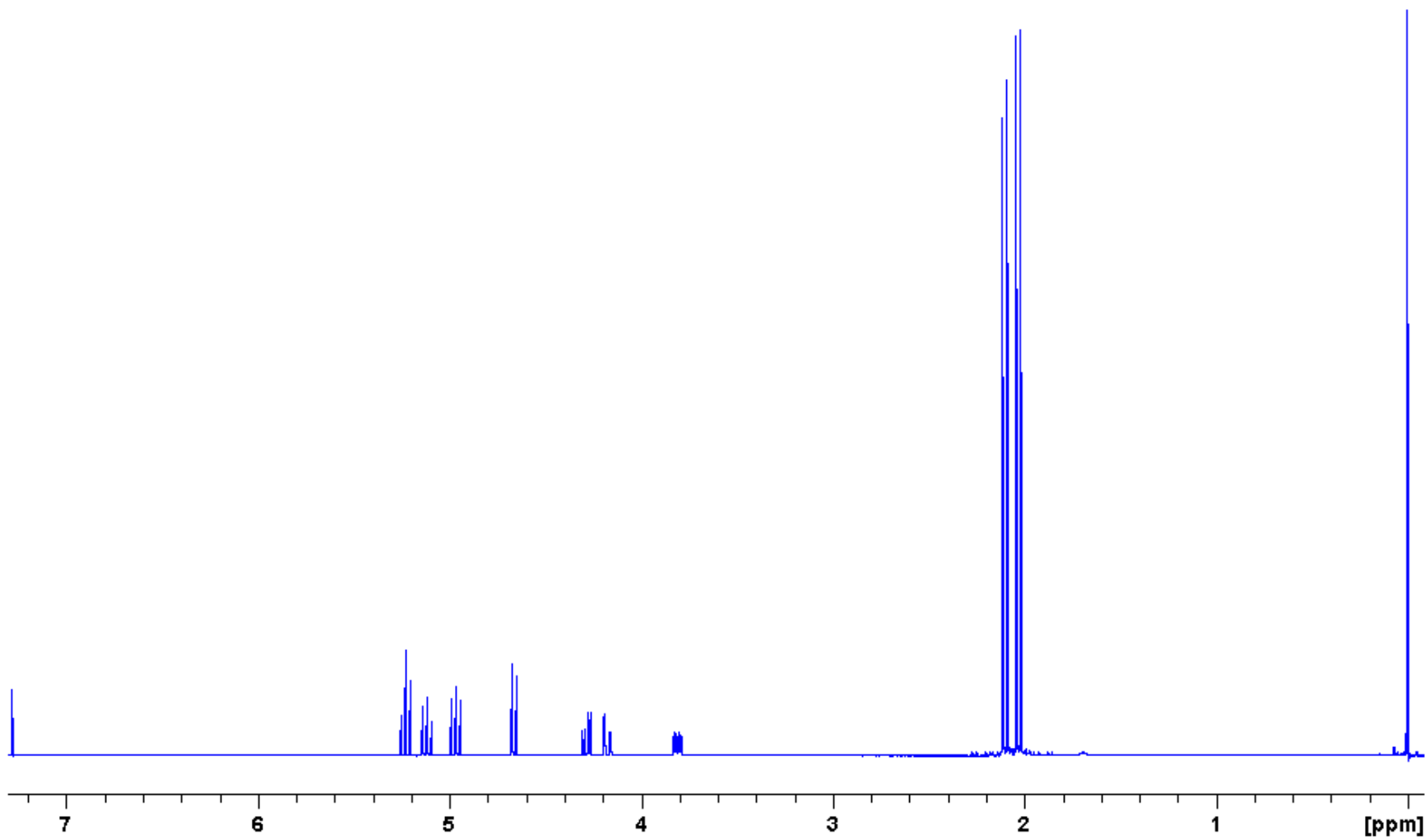


Figure 22: 400 MHz ^1H spectrum of glucosyl azide 3.

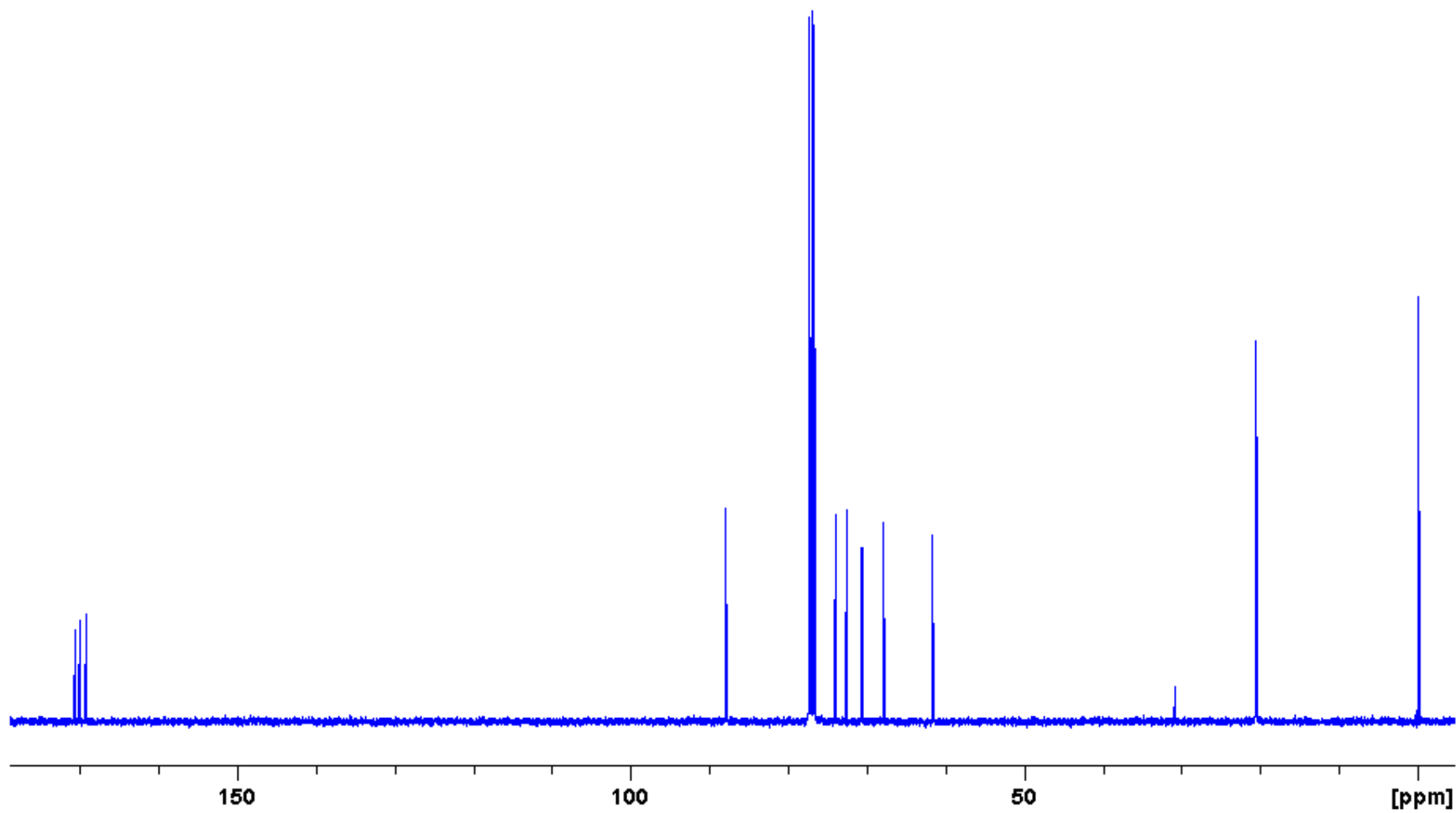


Figure 23: 100 MHz ^{13}C spectrum of glucosyl azide 3.

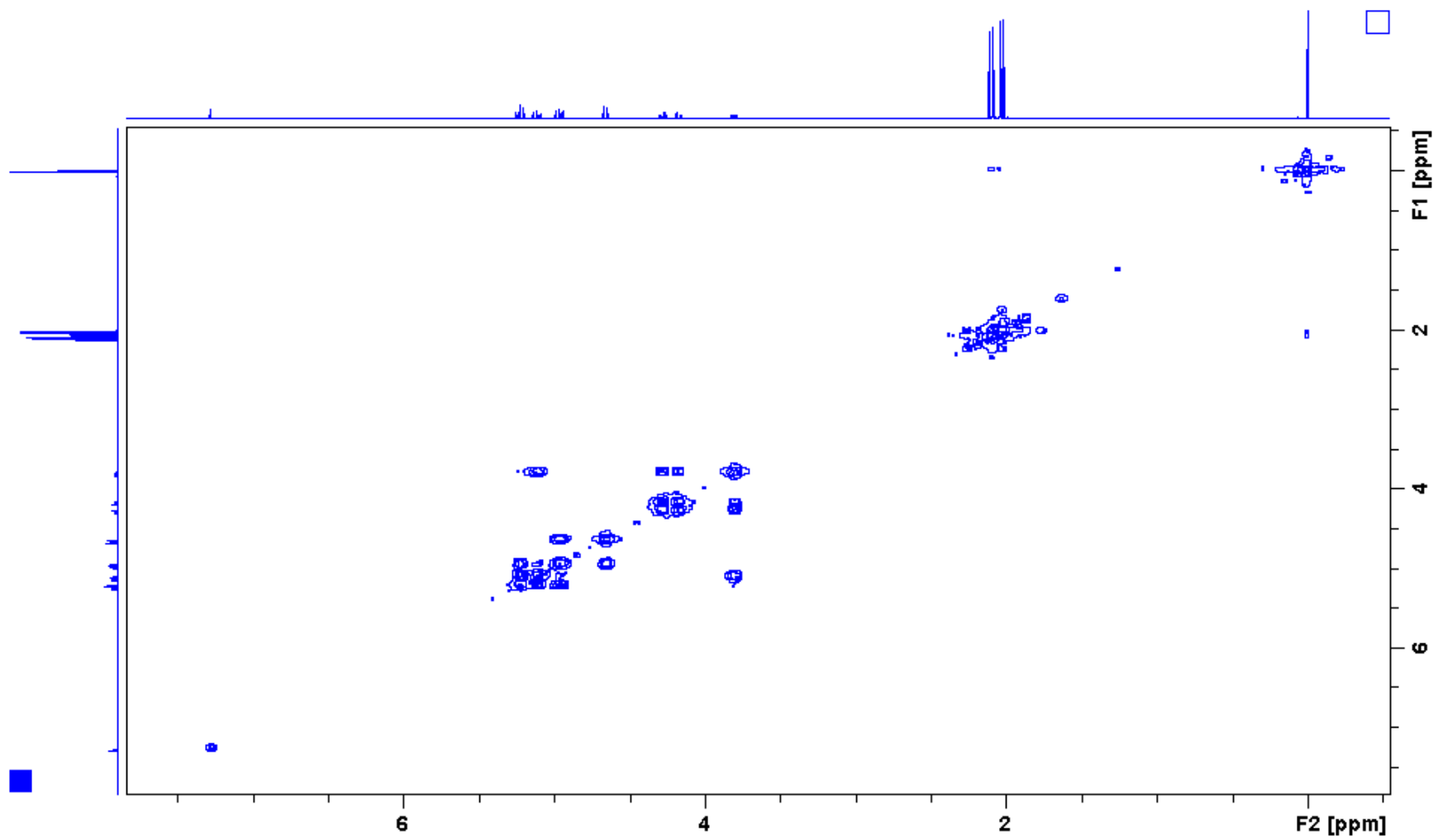


Figure 24: 400 MHz ^1H - ^1H COSY spectrum of glucosyl azide **3**.

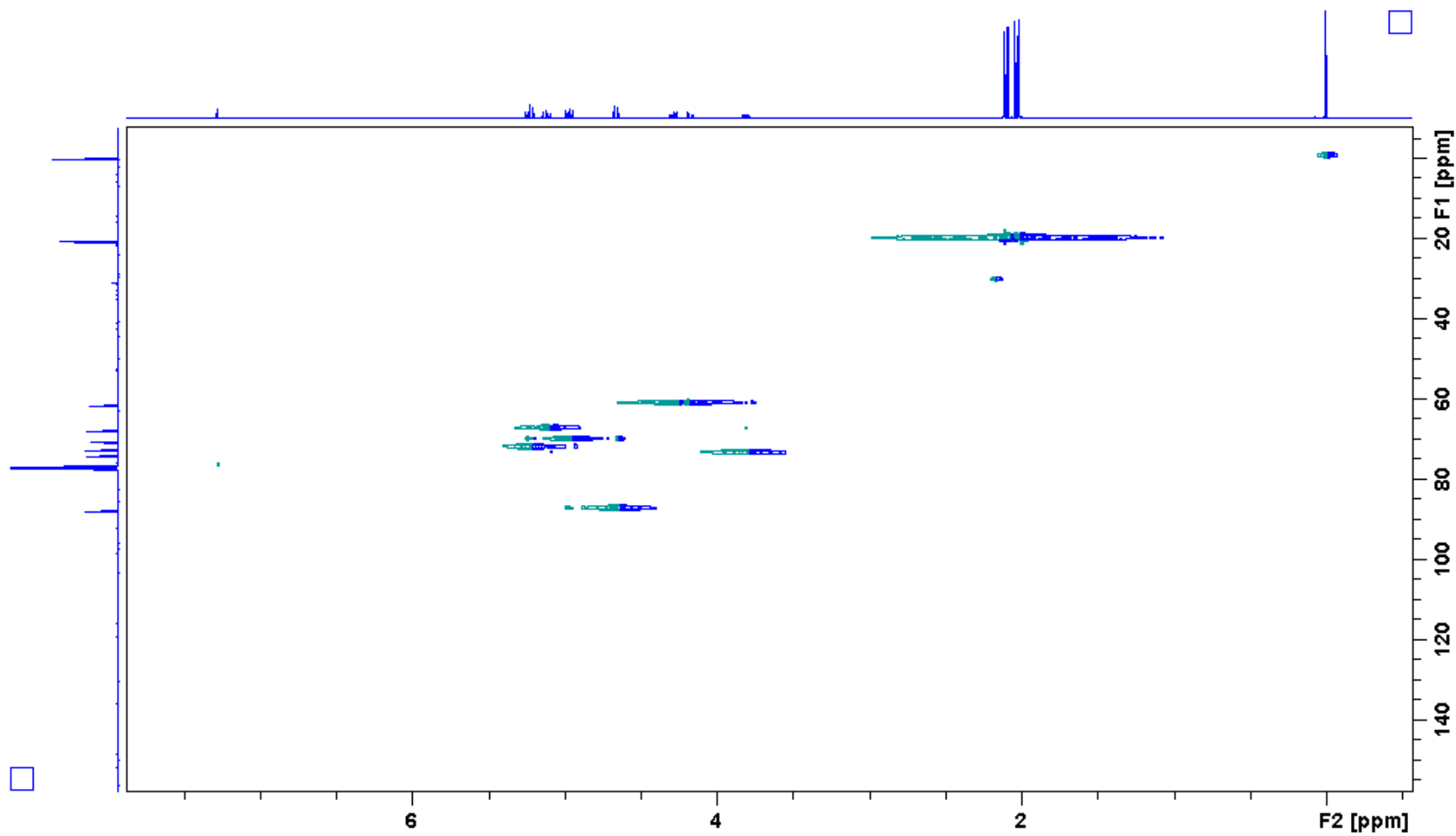


Figure 25: 400 MHz ^1H - ^{13}C HSQC spectrum of glucosyl azide **3**.

Display Report

Analysis Info

Method XQ Default.ms Instrument Esquire-LC_00135

Acquisition Parameter

Ion Source Type	ESI	Mass Range Mode	Std/Normal	Ion Polarity	Positive	Alternating Ion Polarity	n/a
Scan Begin	100.00 m/z	Scan End	600.00 m/z	Averages	10 Spectra	Accumulation Time	1072 μ s
Capillary Exit	110.9 Volt	Skim 1	36.9 Volt	Trap Drive	49.2	Auto MS/MS	Off

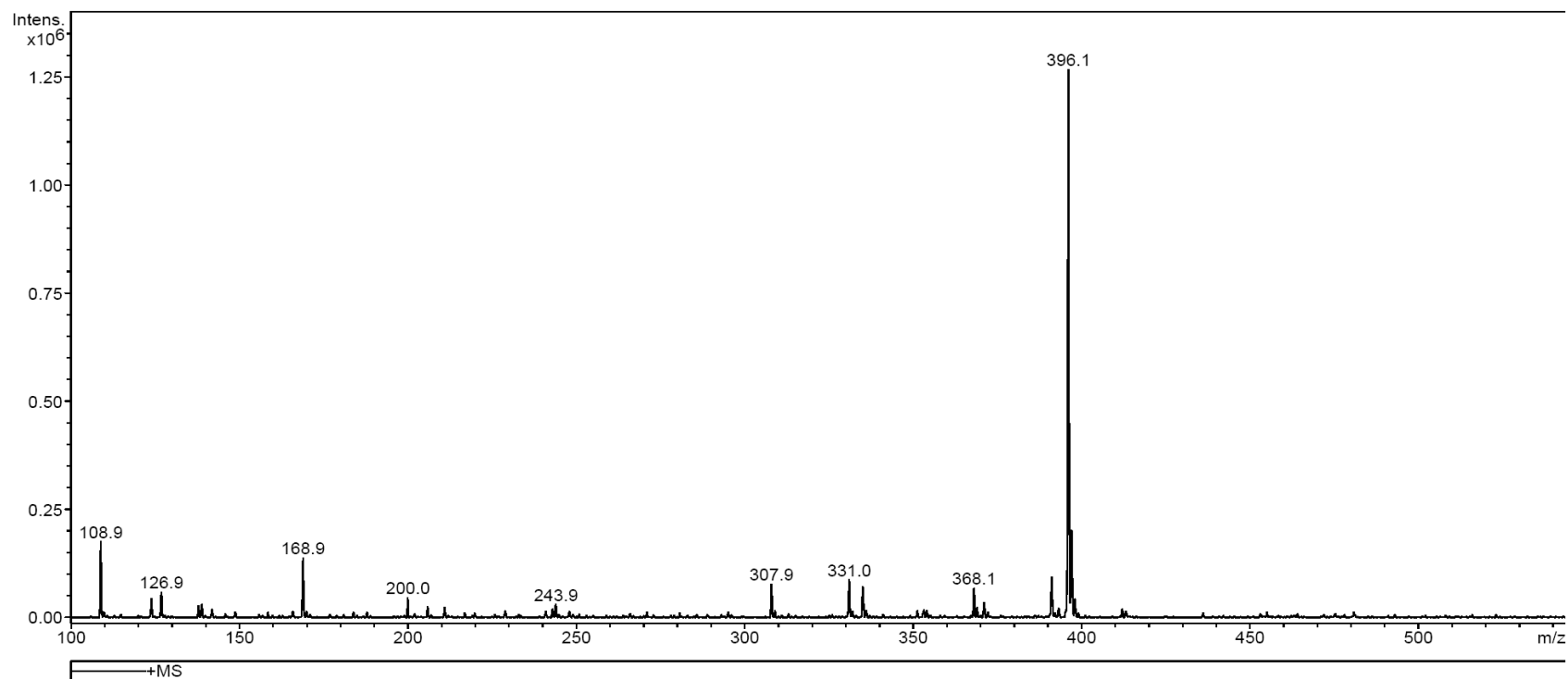


Figure 26: Mass spectrum of glucosyl azide 3.

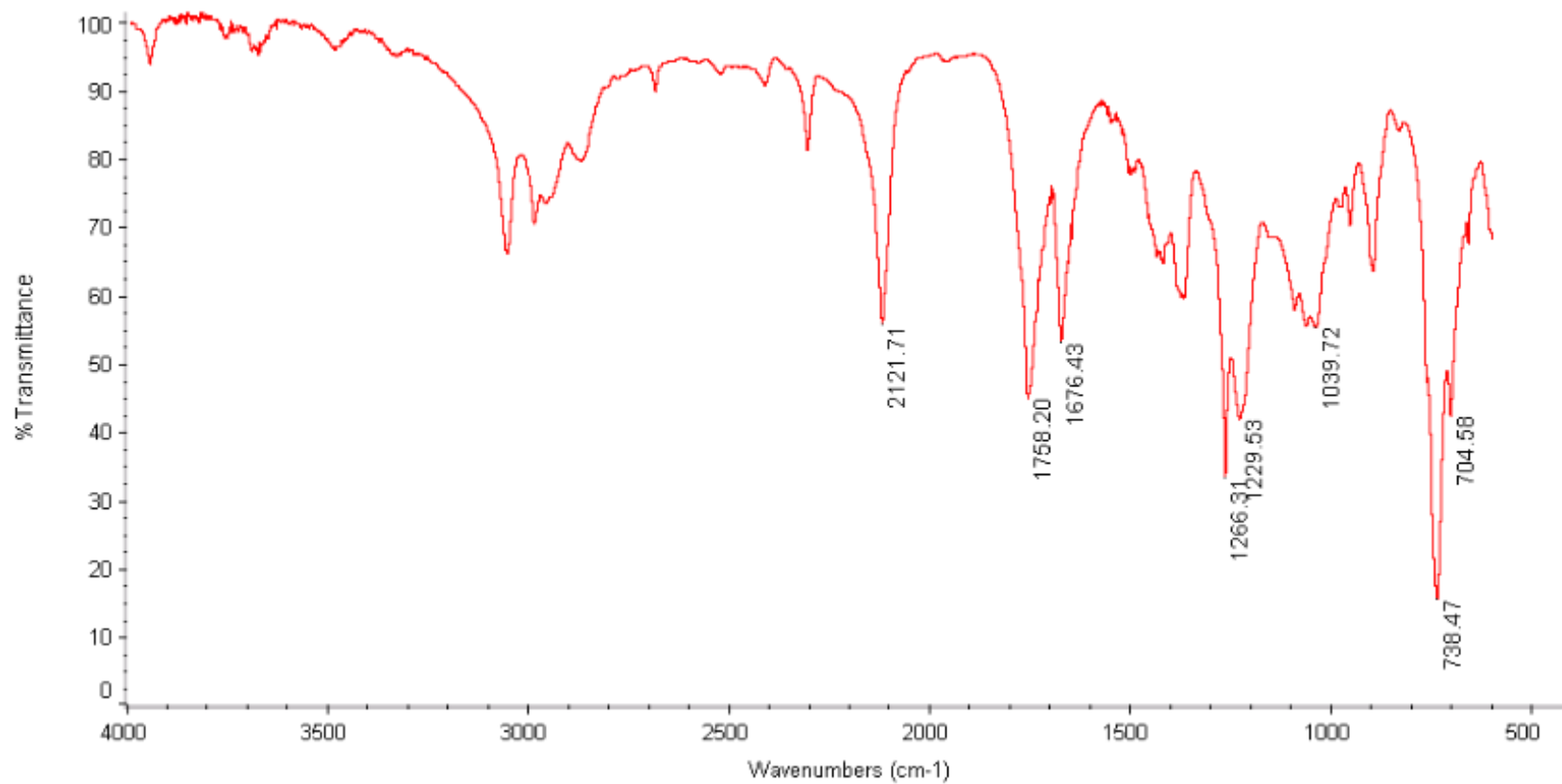


Figure 27: Infrared spectrum of glucosyl azide **3**.

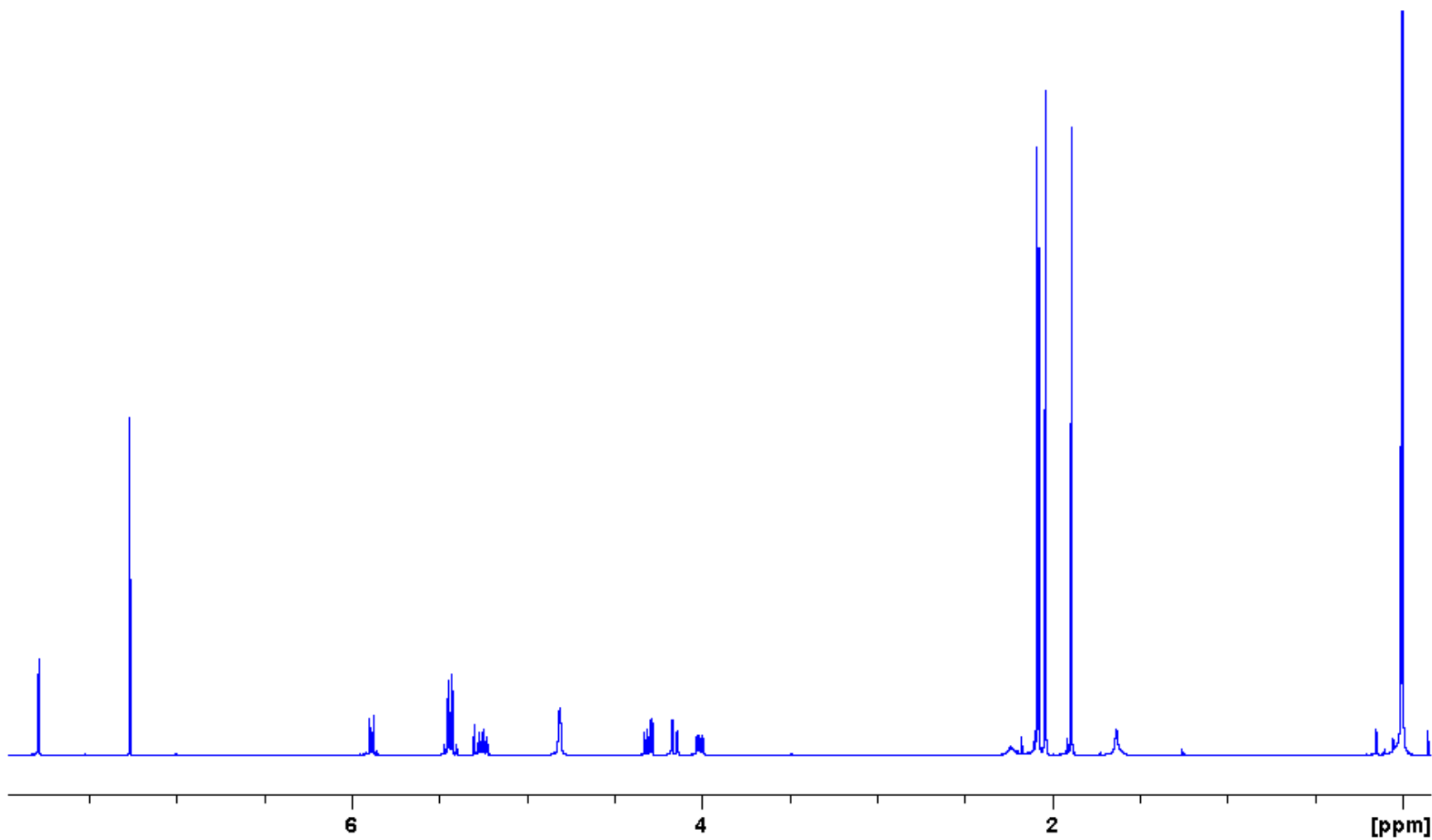


Figure 28: 400 MHz ^1H spectrum of glucosyl triazole **8**.

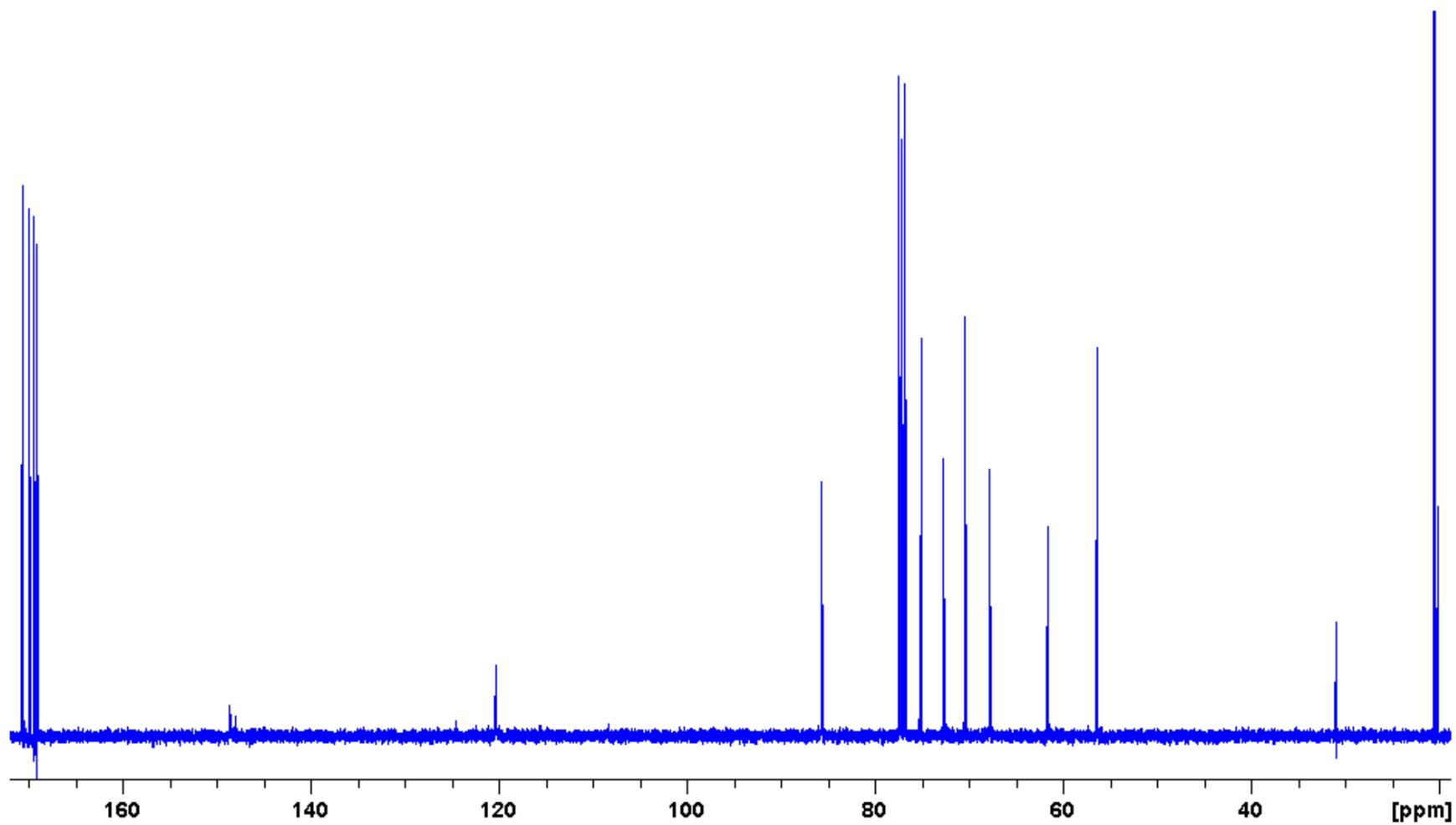


Figure 29: 100 MHz ^{13}C spectrum of glucosyl triazole 8.

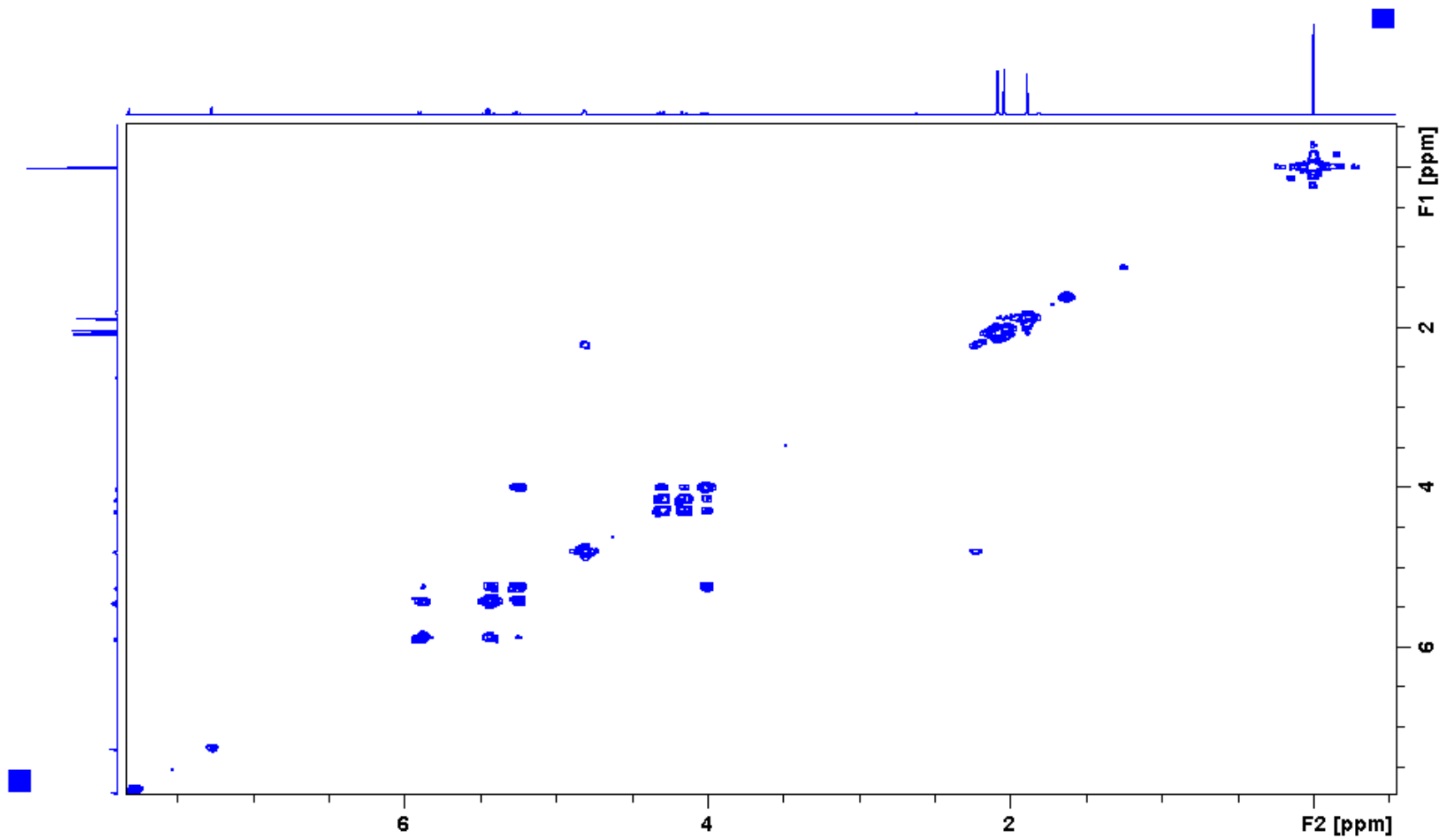


Figure 30: 400 MHz ¹H-¹H COSY spectrum of glucosyl triazole **8**.

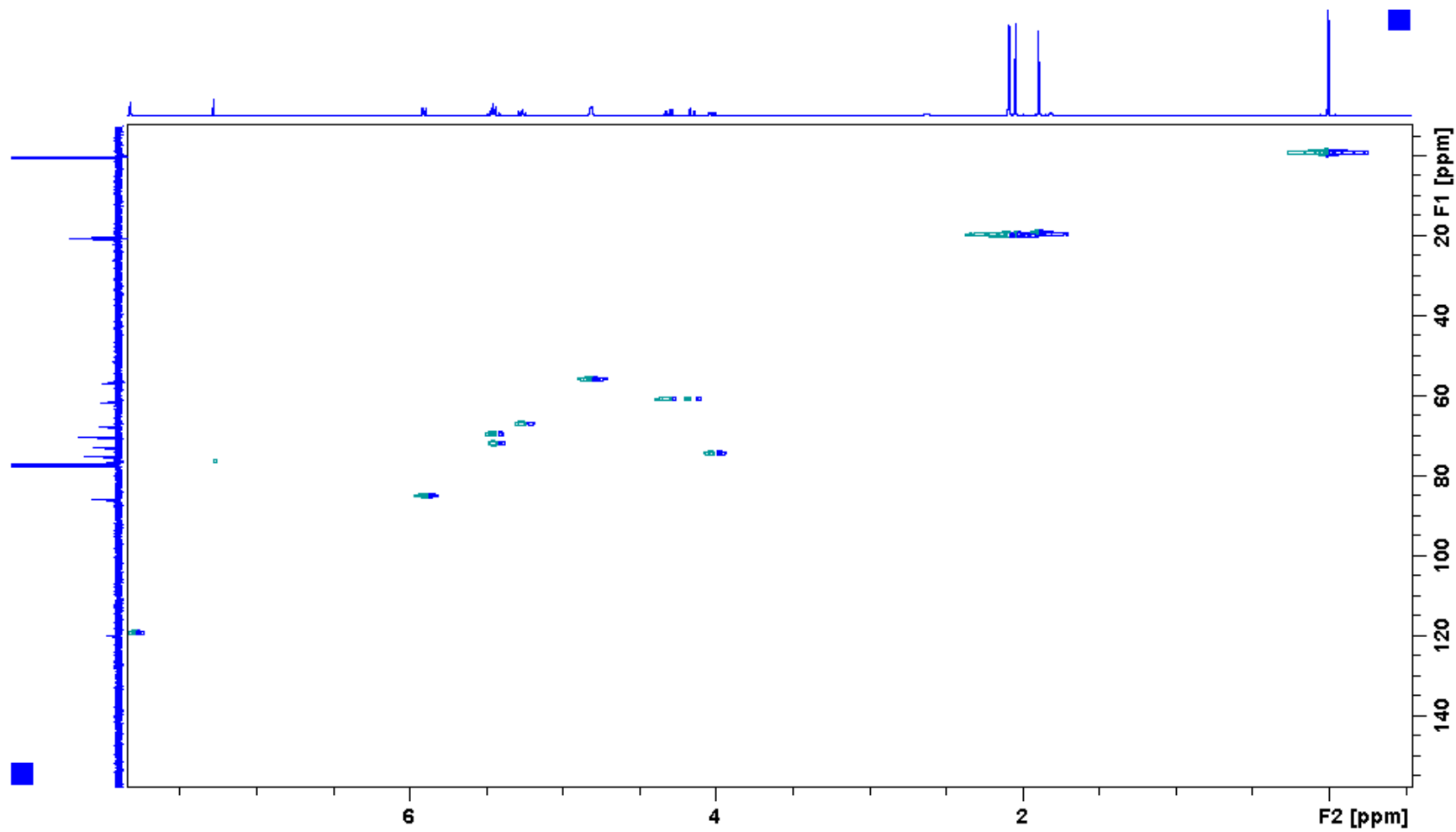


Figure 31: 400 MHz ^1H - ^{13}C HSQC spectrum of glucosyl triazole **8**.

Display Report

Analysis Info

Method XQ Default.ms Instrument Esquire-LC_00135

Acquisition Parameter

Ion Source Type	ESI	Mass Range Mode	Std/Normal	Ion Polarity	Positive	Alternating Ion Polarity	n/a
Scan Begin	100.00 m/z	Scan End	600.00 m/z	Averages	10 Spectra	Accumulation Time	3428 μ s
Capillary Exit	115.2 Volt	Skim 1	39.8 Volt	Trap Drive	51.4	Auto MS/MS	Off

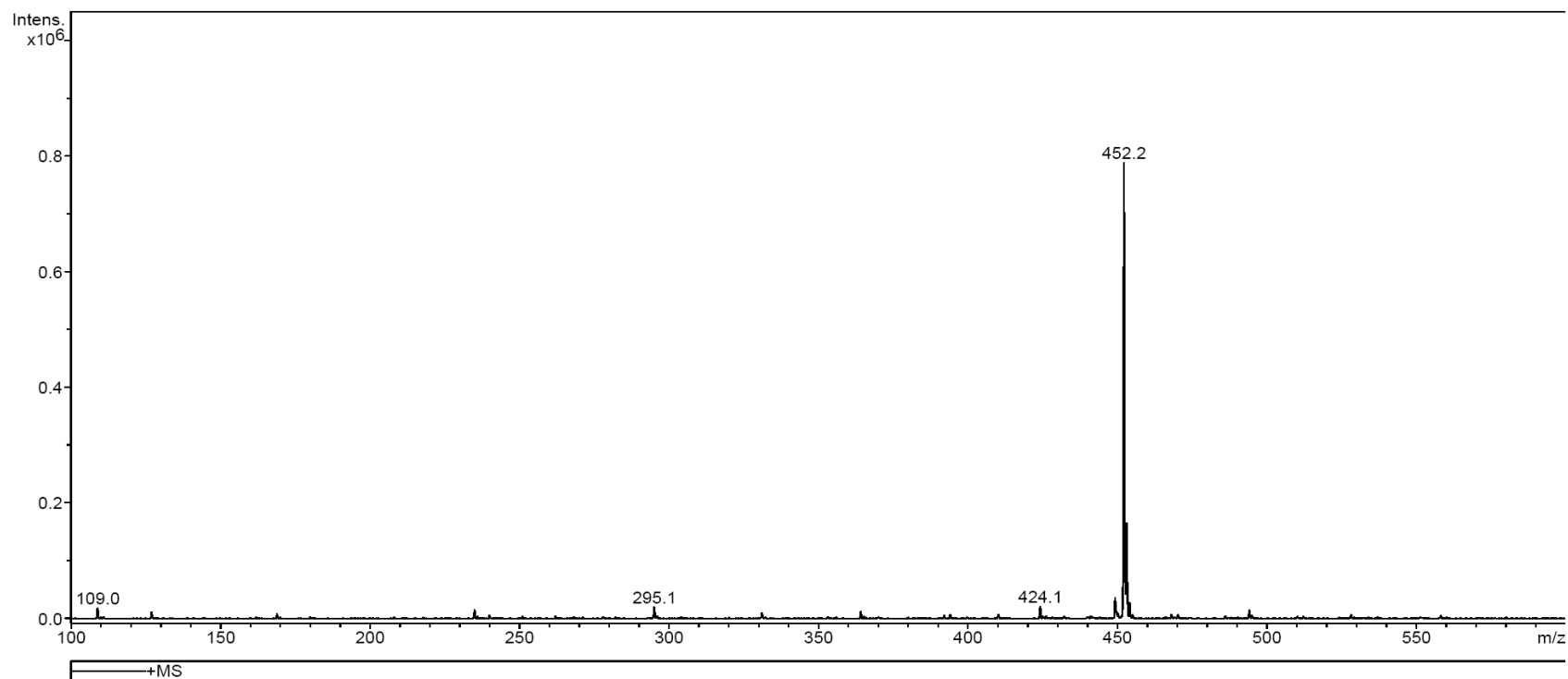


Figure 32: Mass spectrum of glucosyl triazole **8**.

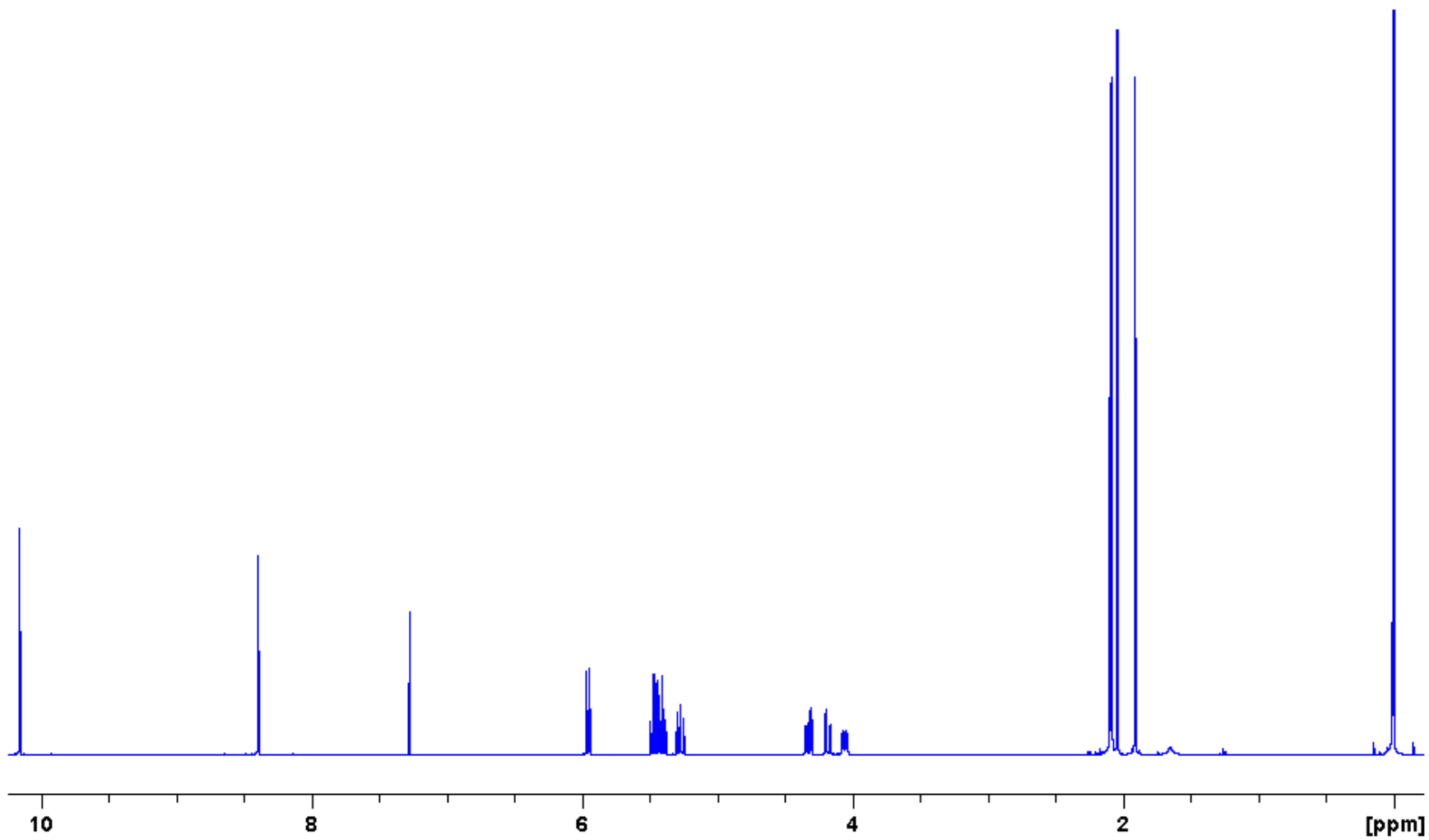


Figure 33: 400 MHz ^1H spectrum of aldehyde 9.

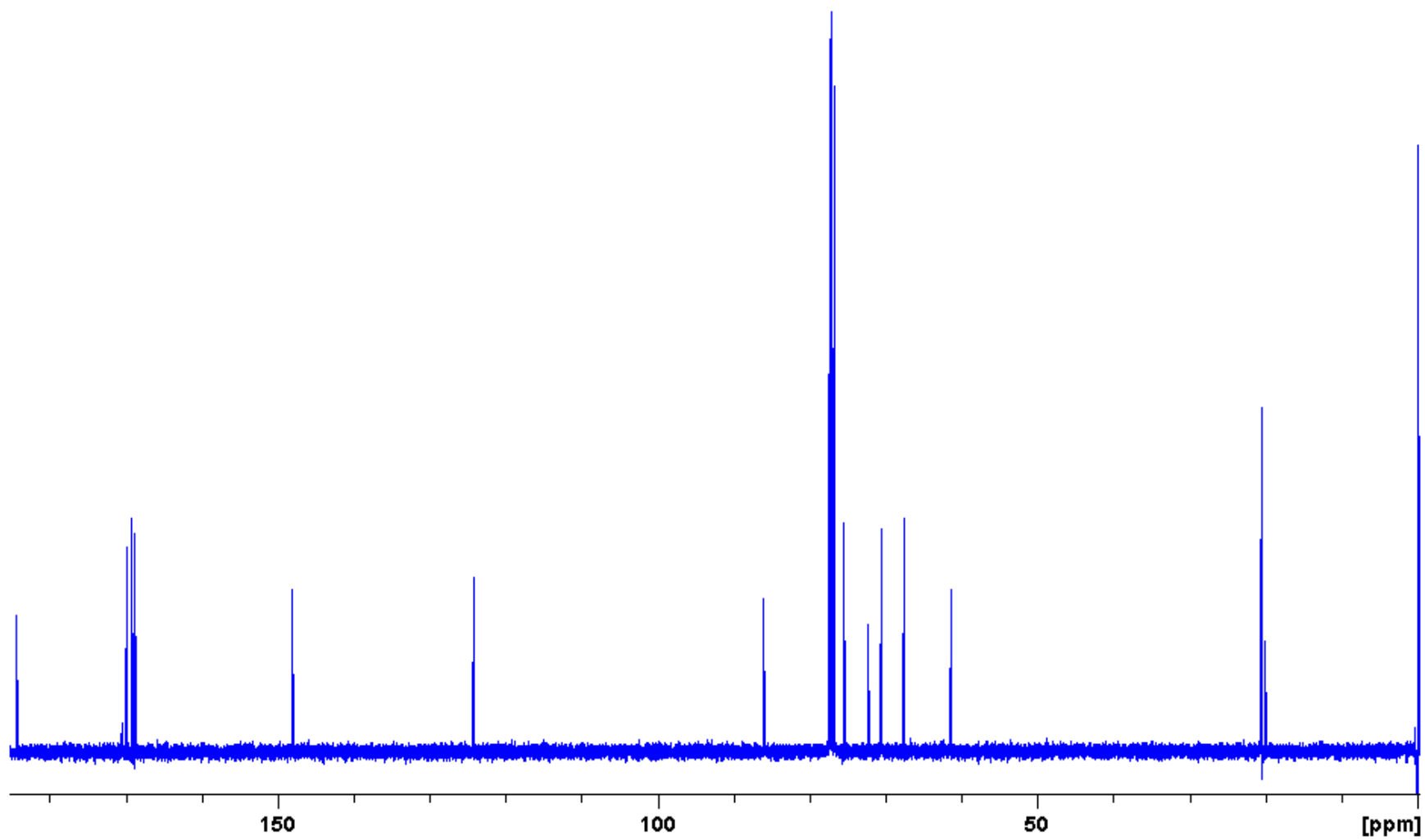


Figure 34: 100 MHz ^{13}C spectrum of aldehyde 9.

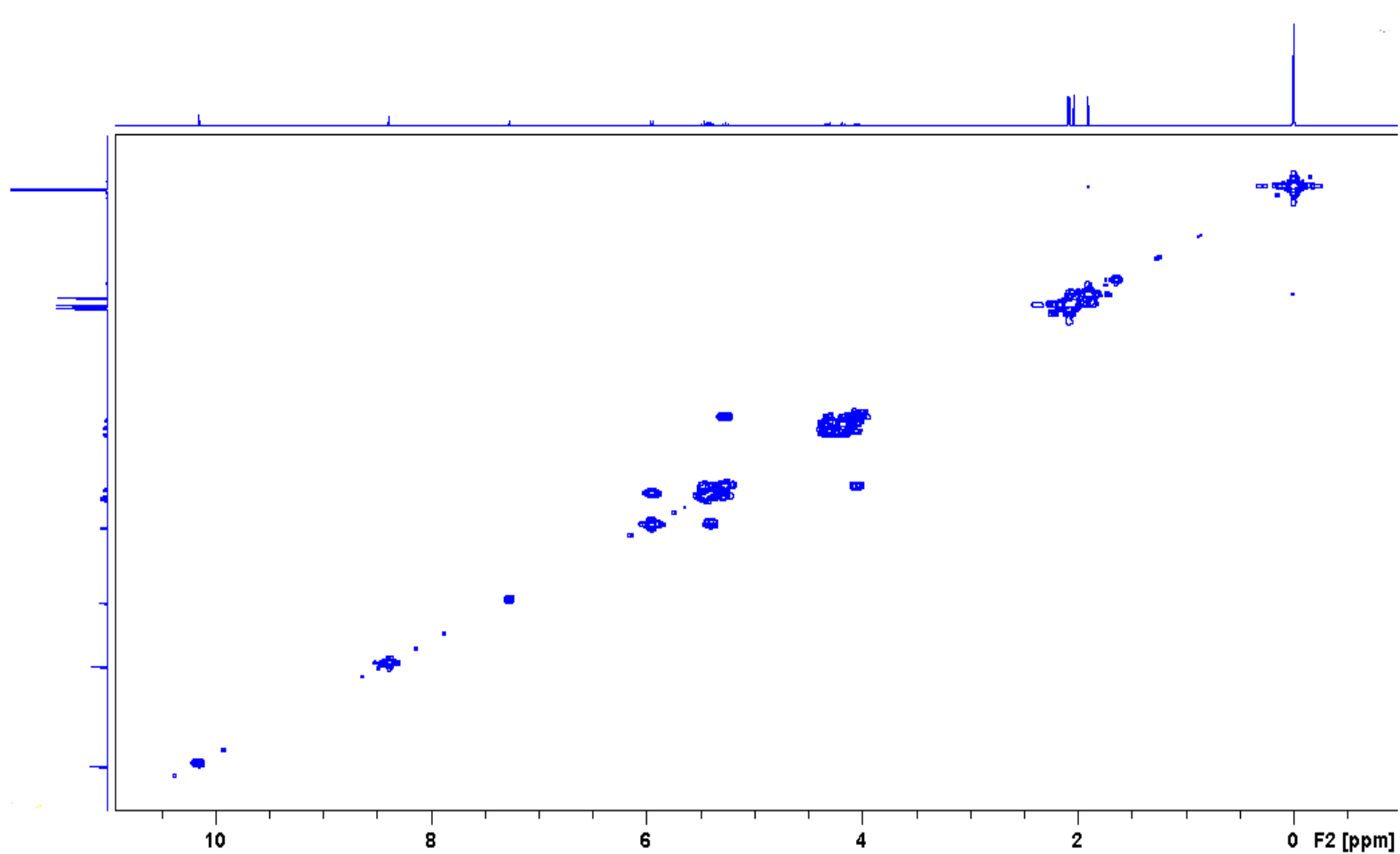


Figure 35: 400 MHz ^1H - ^1H COSY spectrum of aldehyde **9**.

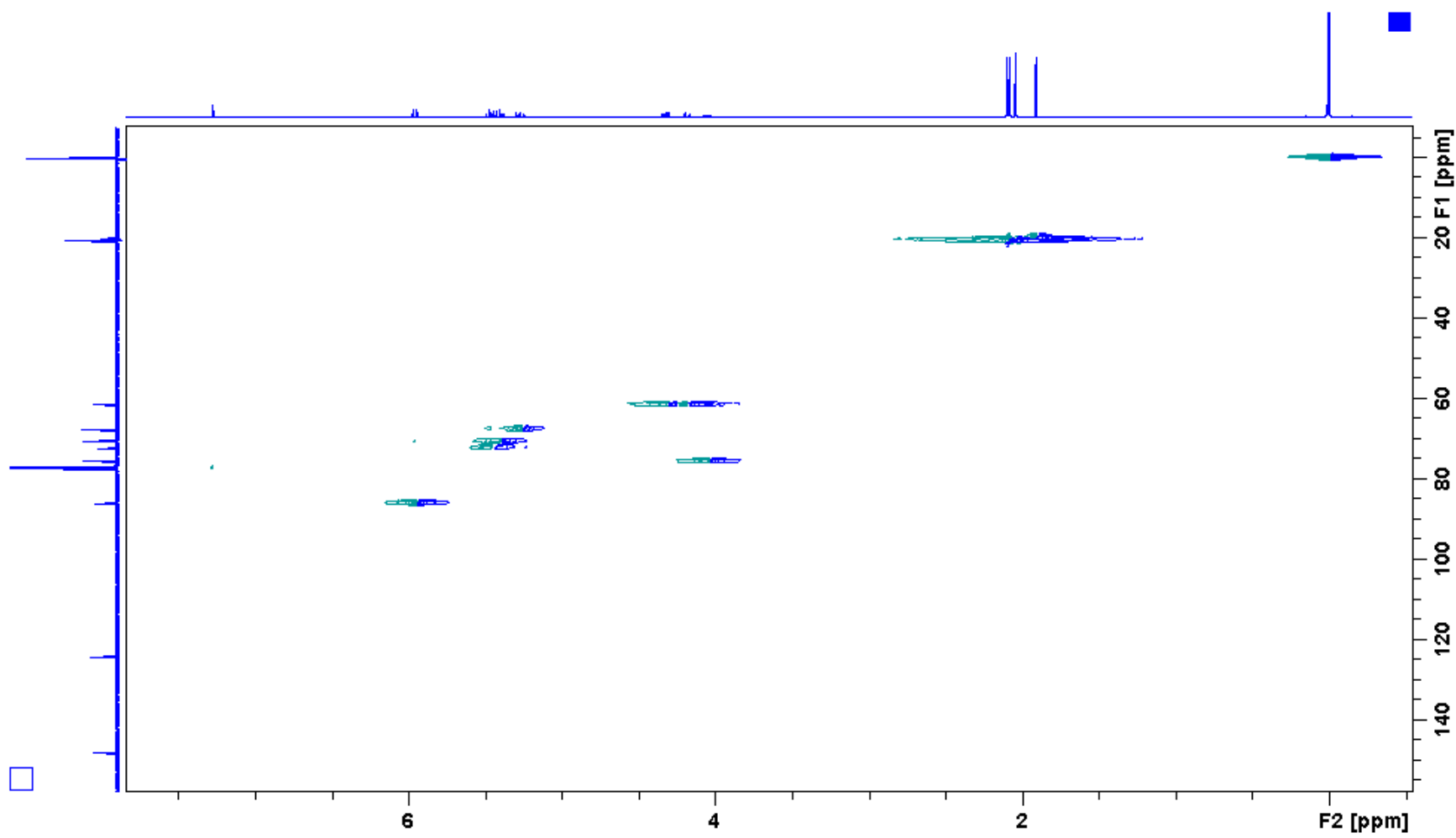


Figure 36: 400 MHz ^1H - ^{13}C HSQC spectrum of aldehyde **9**.

Display Report

Analysis Info

Method XQ Default.ms Instrument Esquire-LC_00135

Acquisition Parameter

Ion Source Type	ESI	Mass Range Mode	Std/Normal	Ion Polarity	Positive	Alternating Ion Polarity	n/a
Scan Begin	100.00 m/z	Scan End	630.00 m/z	Averages	10 Spectra	Accumulation Time	777 μ s
Capillary Exit	115.2 Volt	Skim 1	39.8 Volt	Trap Drive	51.4	Auto MS/MS	Off

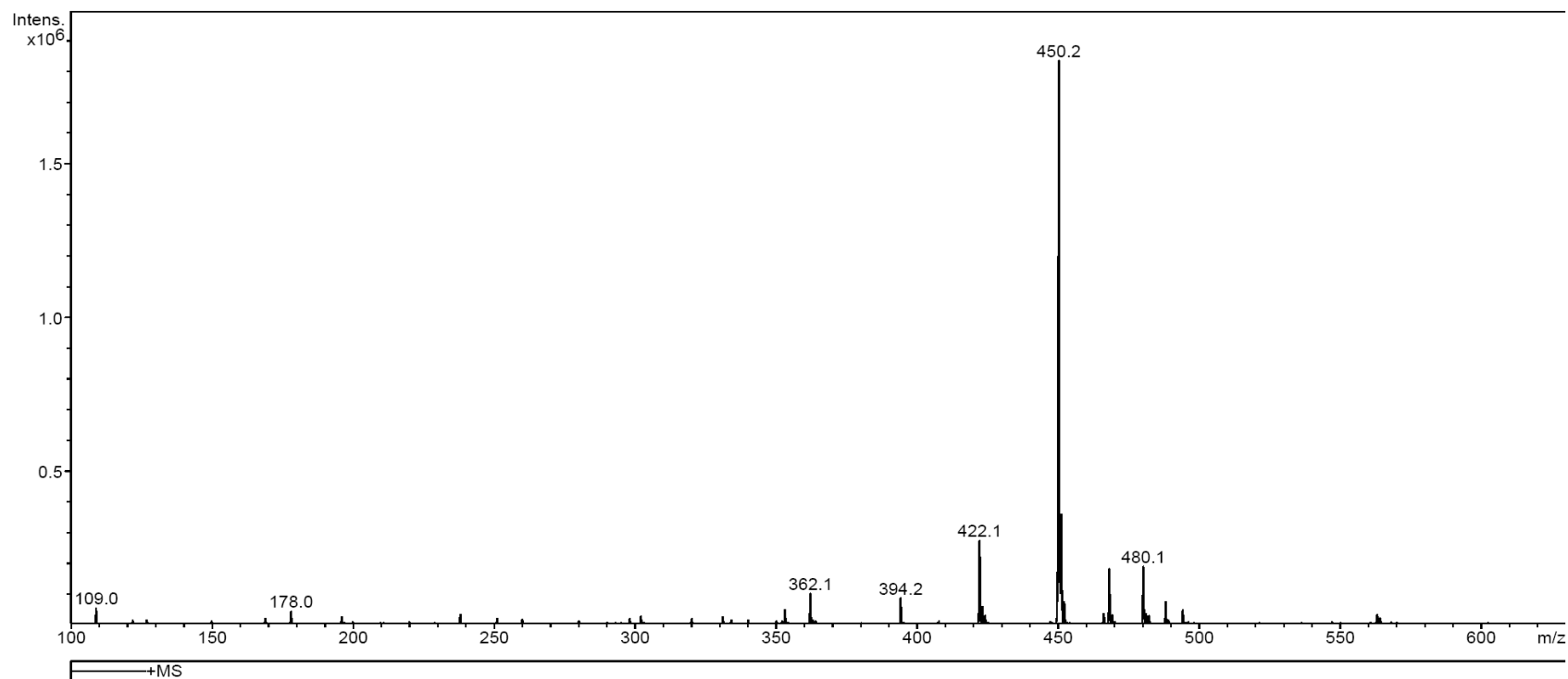


Figure 37: Mass spectrum of aldehyde 9.

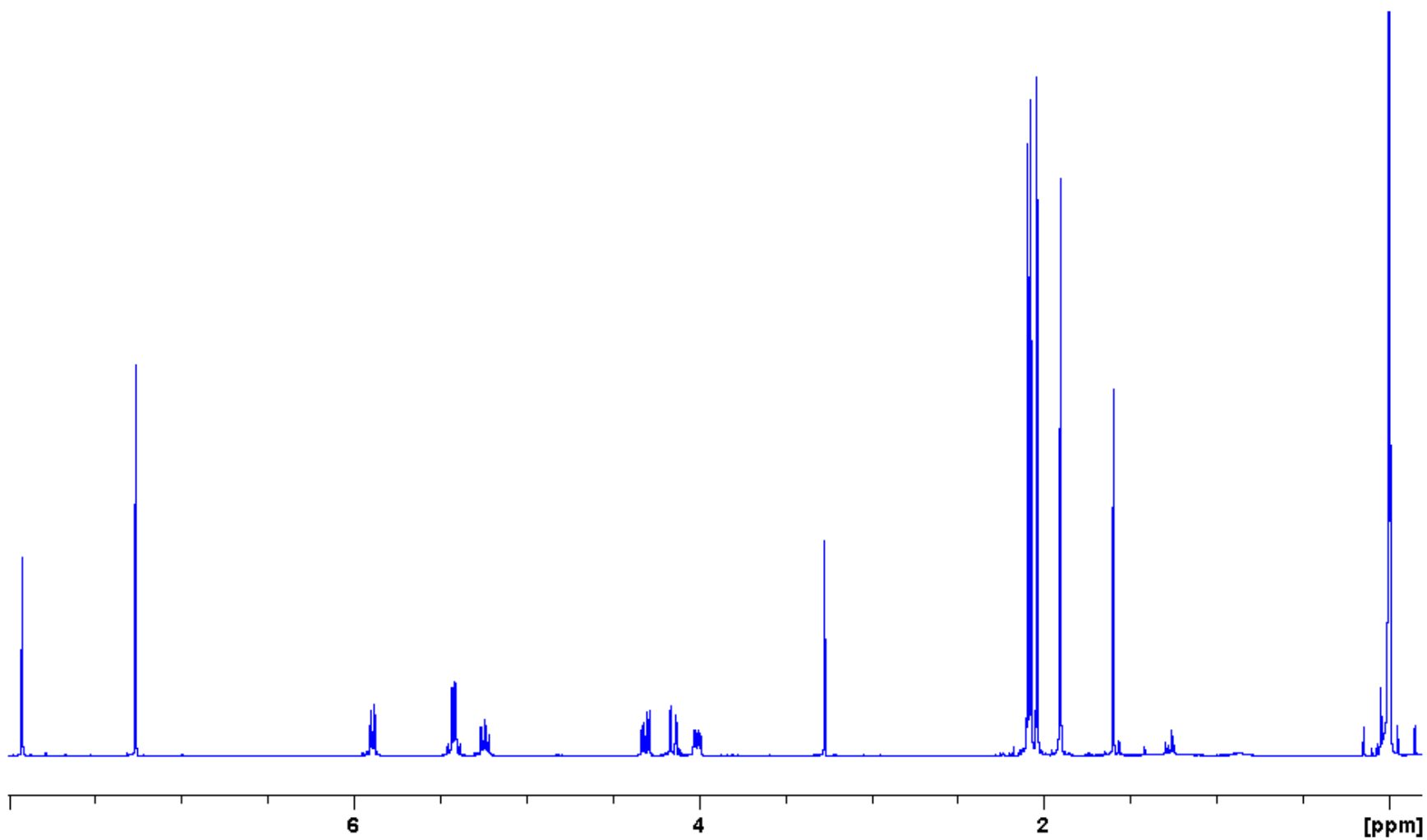


Figure 38: 400 MHz ^1H spectrum of alkyne 10.

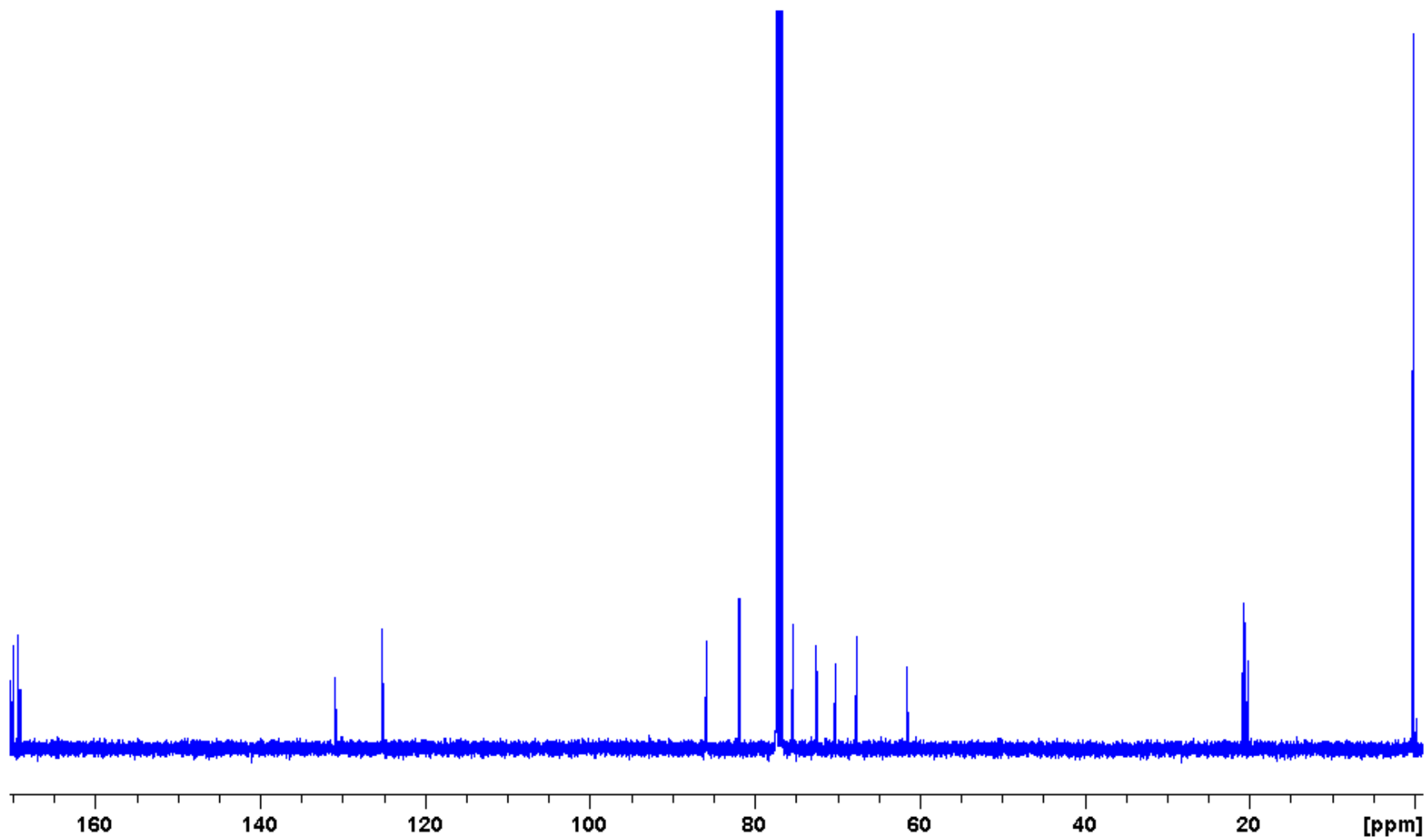


Figure 39: 100 MHz ^{13}C spectrum of alkyne **10**.

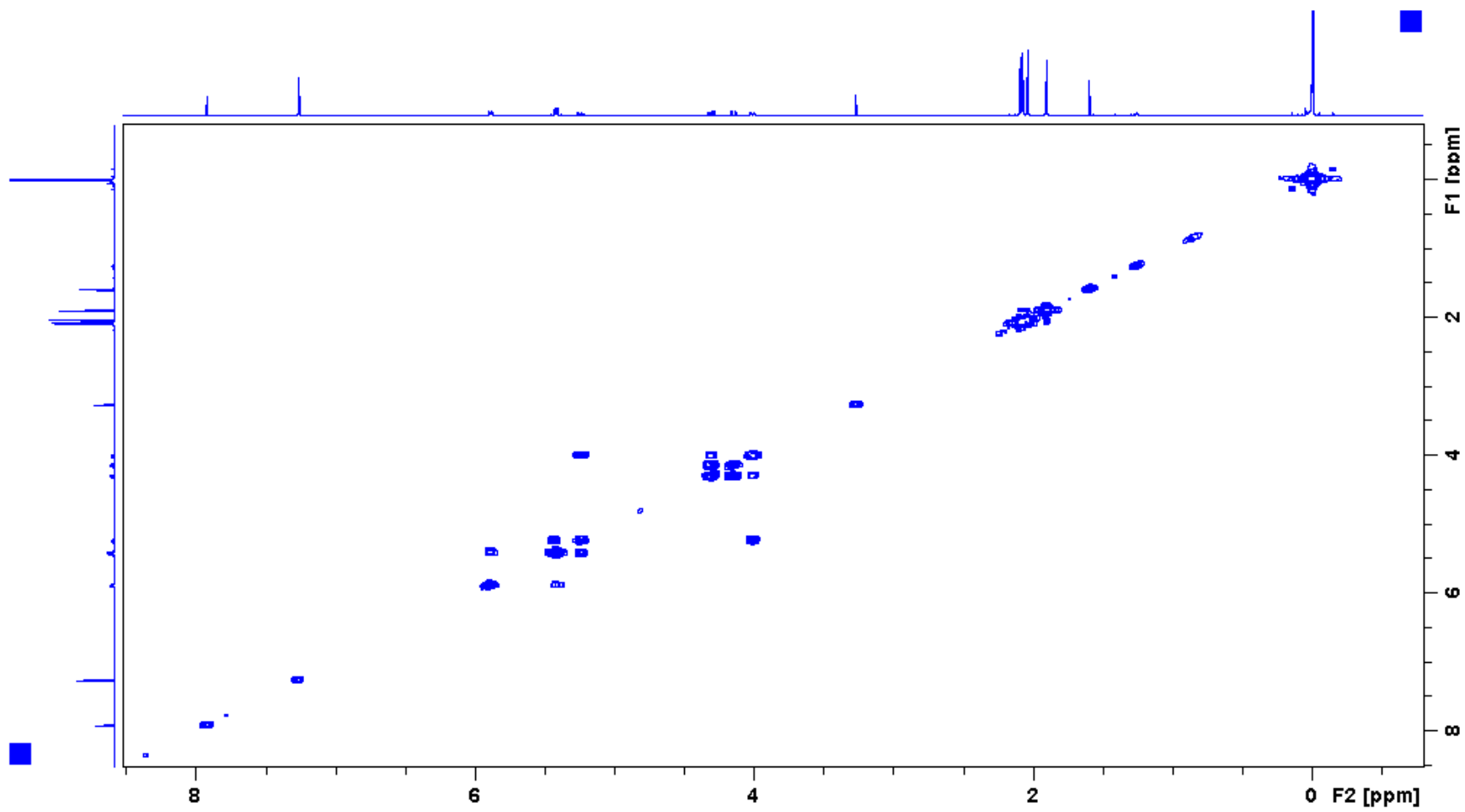


Figure 40: 400 MHz ^1H - ^1H COSY spectrum of alkyne **10**.

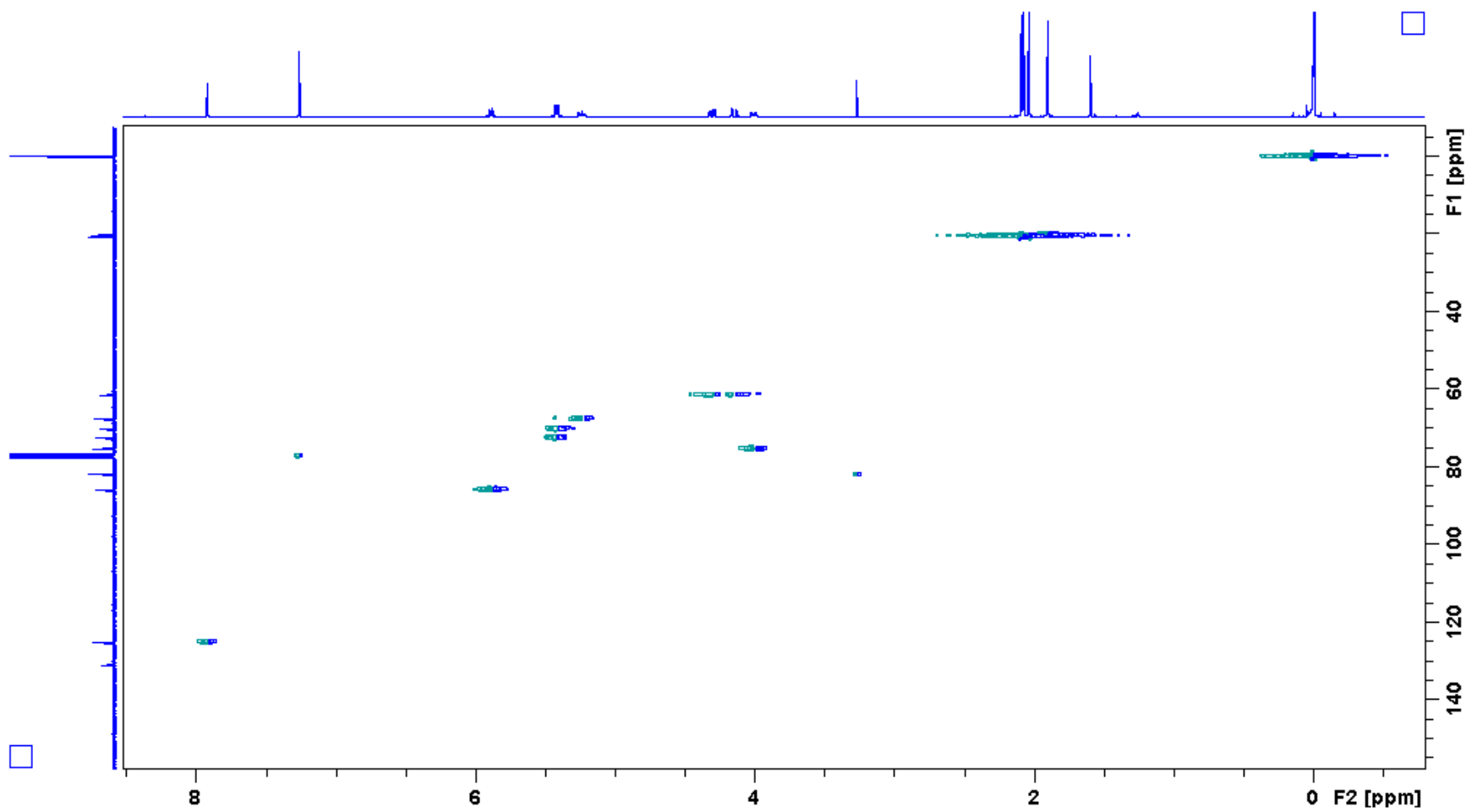


Figure 41: 400 MHz ^1H - ^{13}C HSQC spectrum of alkyne **10**.

Display Report

Analysis Info

Method XQ Default.ms Instrument Esquire-LC_00135

Acquisition Parameter

Ion Source Type	ESI	Mass Range Mode	Std/Normal	Ion Polarity	Positive	Alternating Ion Polarity	n/a
Scan Begin	300.00 m/z	Scan End	475.00 m/z	Averages	10 Spectra	Accumulation Time	50000 μ s
Capillary Exit	116.5 Volt	Skim 1	40.6 Volt	Trap Drive	52.0	Auto MS/MS	Off

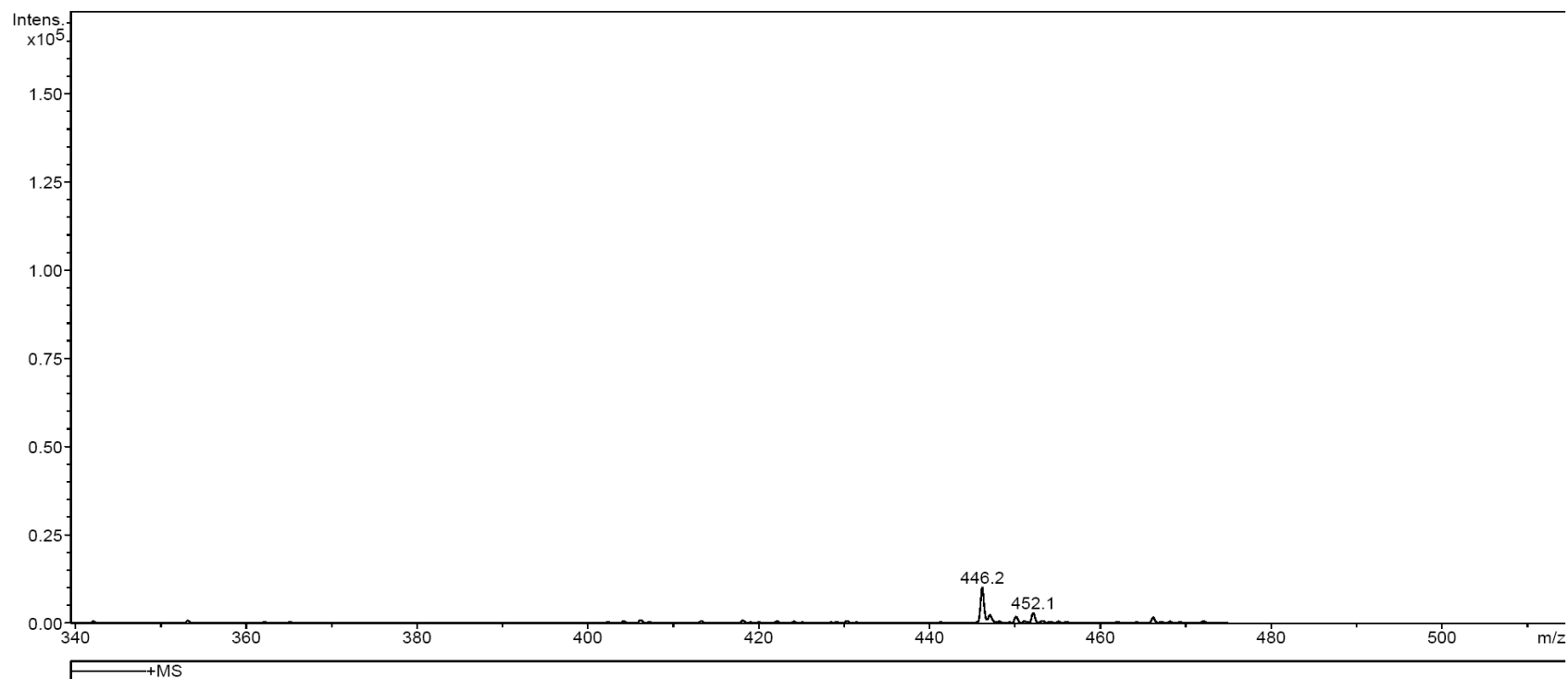


Figure 42: Mass spectrum alkyne 10.

Display Report

Analysis Info

Method XQ Default.ms Instrument Esquire-LC_00135

Acquisition Parameter

Ion Source Type	ESI	Mass Range Mode	Std/Normal	Ion Polarity	Positive	Alternating Ion Polarity	n/a
Scan Begin	100.00 m/z	Scan End	350.00 m/z	Averages	10 Spectra	Accumulation Time	4697 μ s
Capillary Exit	79.9 Volt	Skim 1	13.3 Volt	Trap Drive	43.2	Auto MS/MS	Off

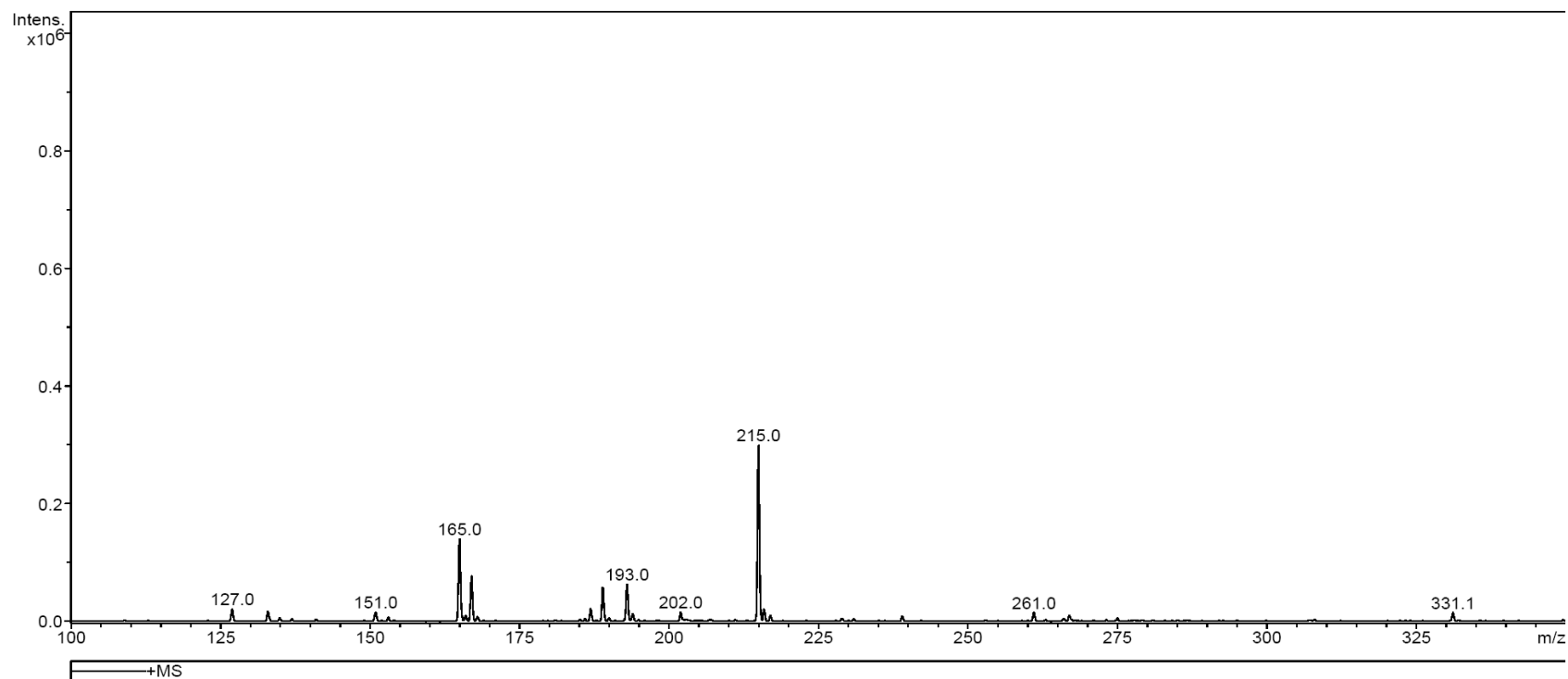


Figure 43: Mass spectrum of dimethyl-2-oxopropylphosphonate (**11**).

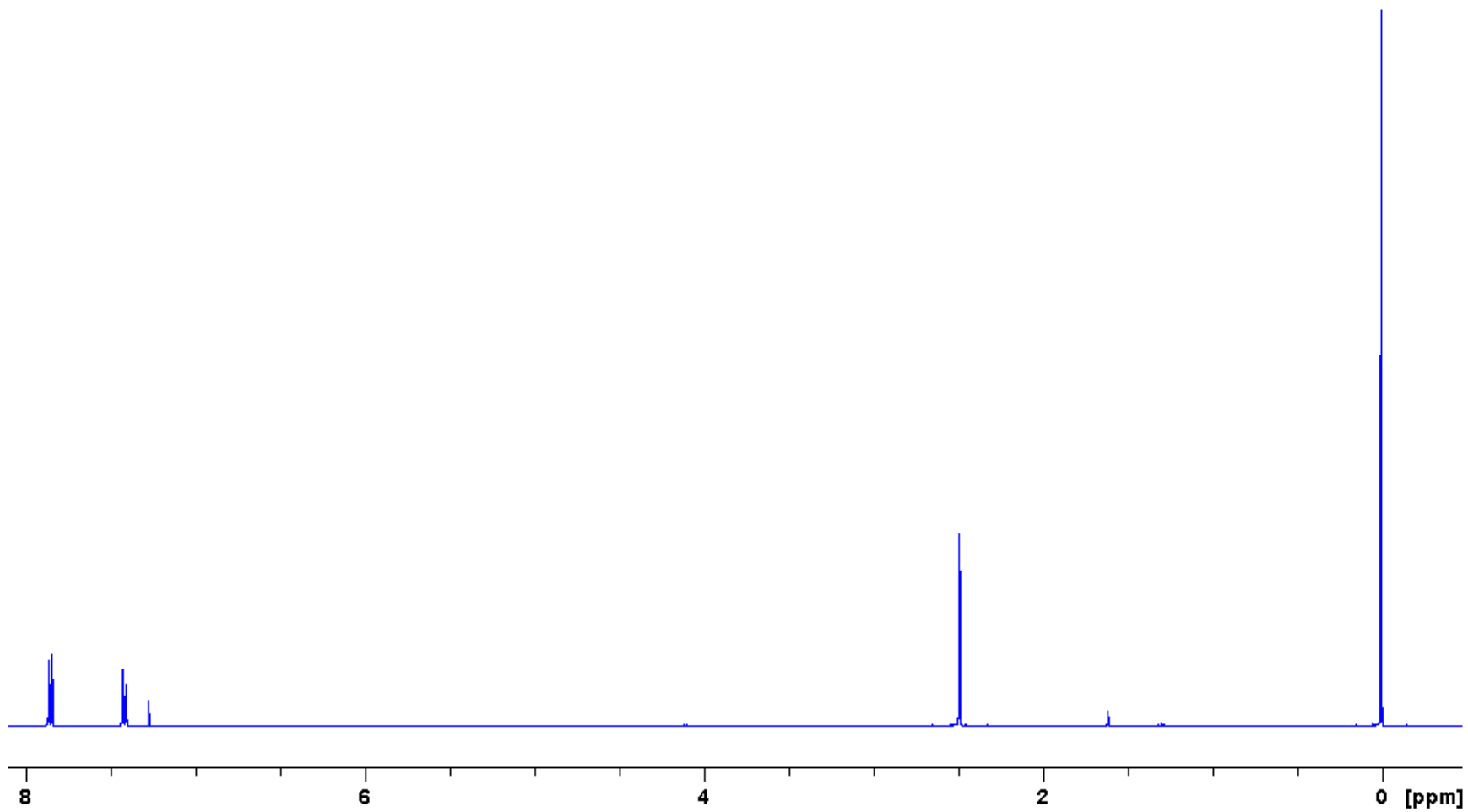


Figure 44: 400 MHz ¹H spectrum of *p*-toluenesulfonyl azide (**13**).

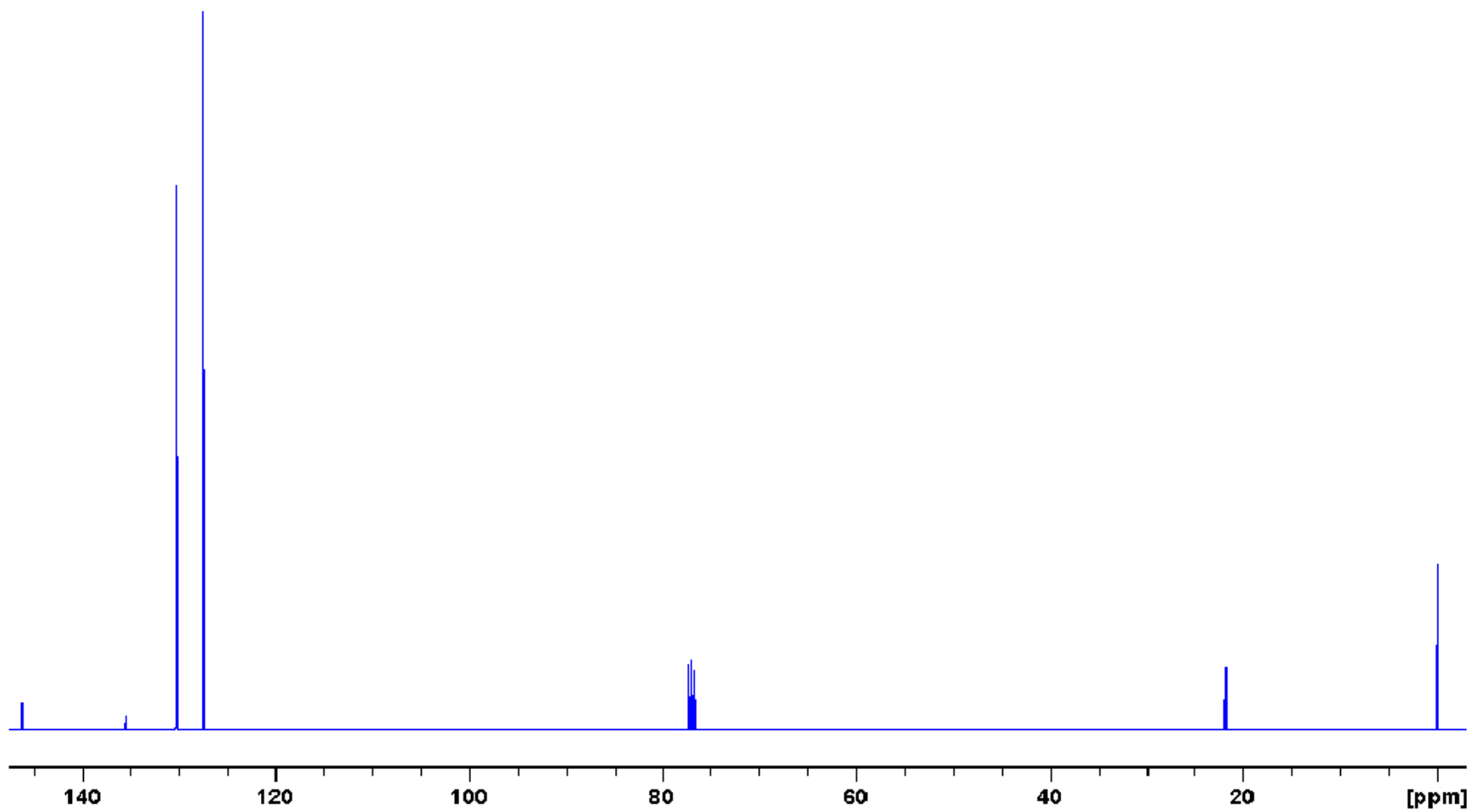


Figure 45: 100 MHz ^{13}C spectrum of *p*-toluenesulfonyl azide (13).

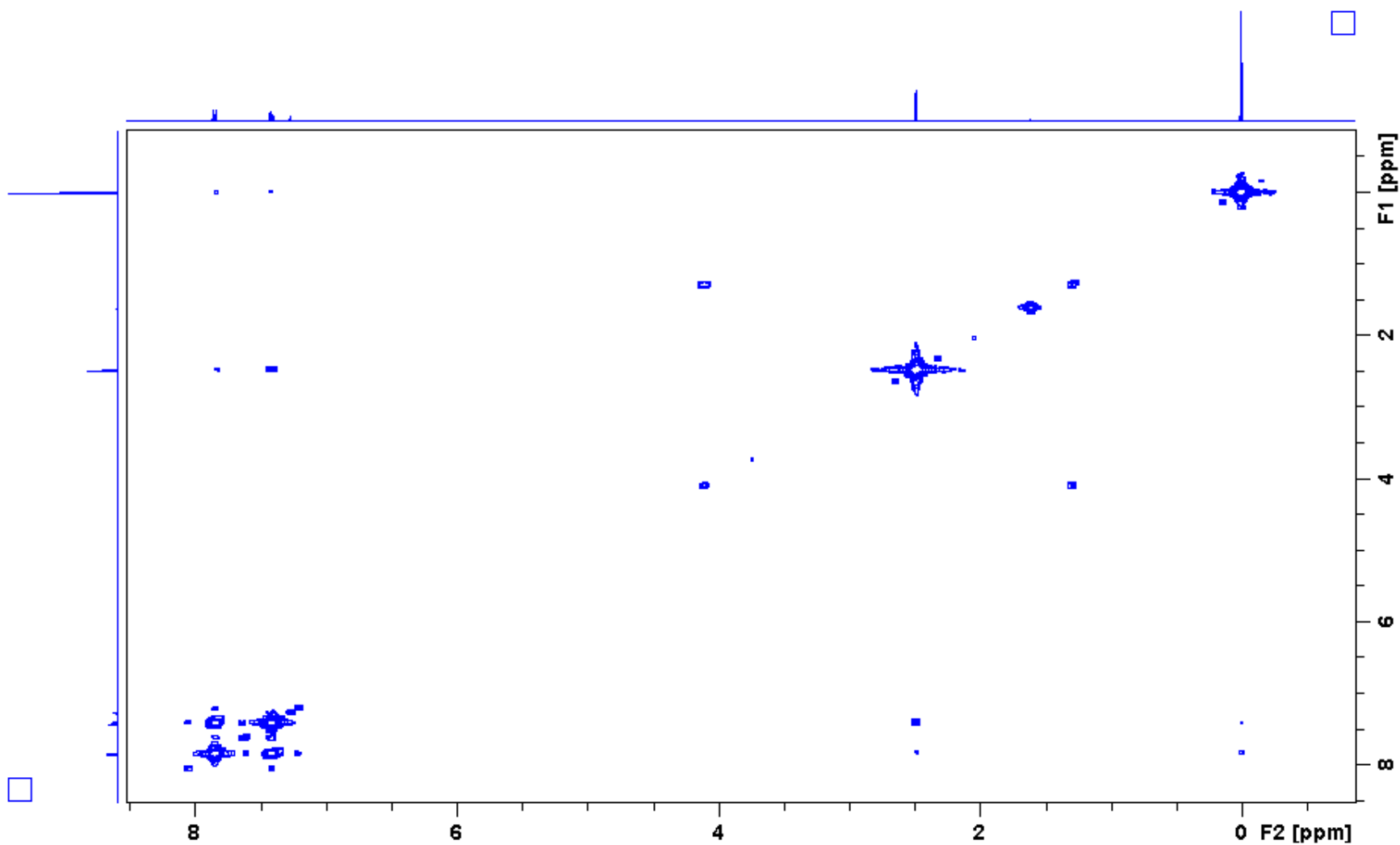


Figure 46: 400 MHz ¹H-¹H COSY spectrum of *p*-toluenesulfonyl azide (13).

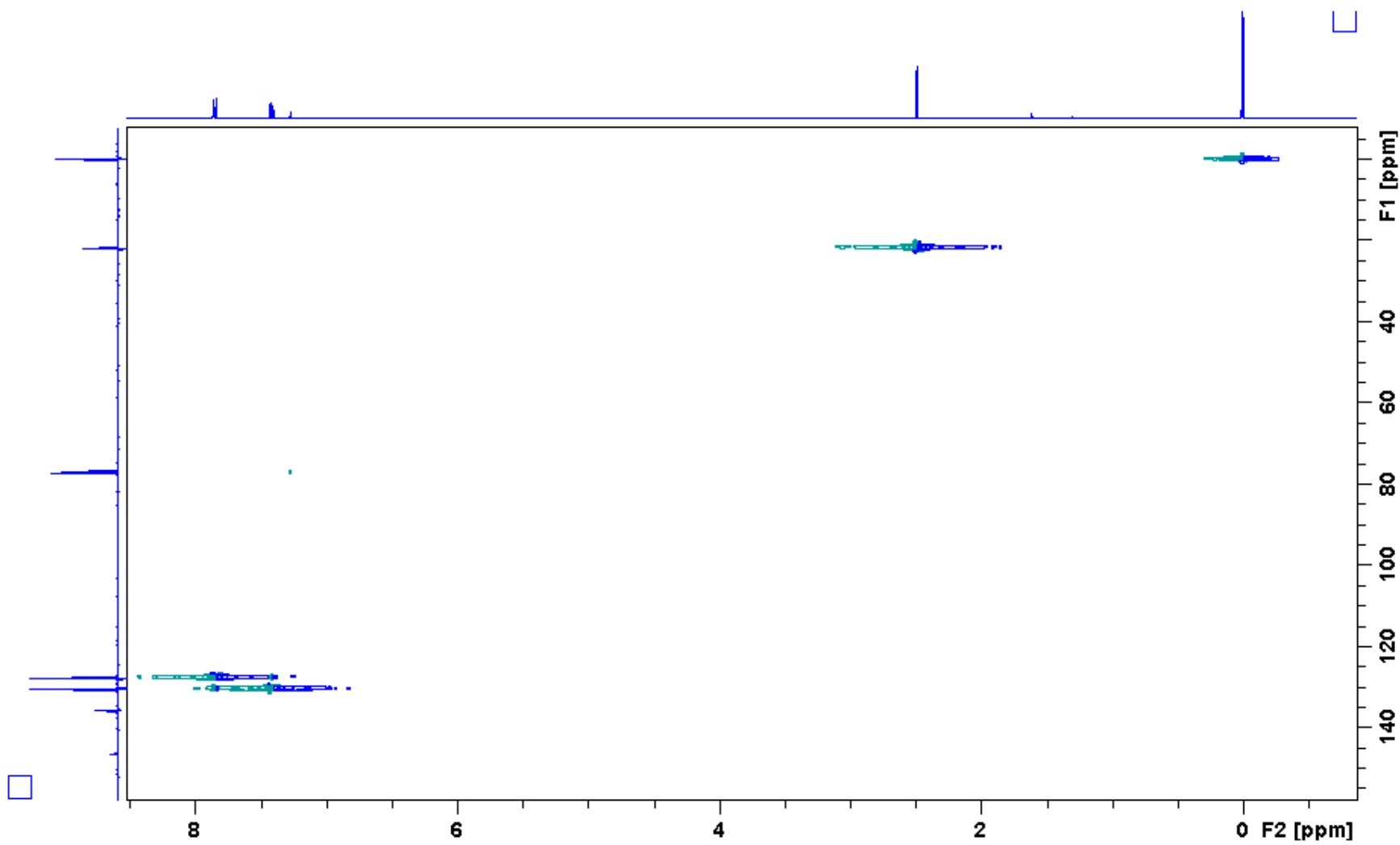


Figure 47: 400 MHz ^1H - ^{13}C HSQC spectrum of *p*-toluenesulfonyl azide (**13**).

Display Report

Analysis Info

Method XQ Default.ms Instrument Esquire-LC_00135

Acquisition Parameter

Ion Source Type	ESI	Mass Range Mode	Std/Normal	Ion Polarity	Positive	Alternating Ion Polarity	n/a
Scan Begin	50.00 m/z	Scan End	400.00 m/z	Averages	10 Spectra	Accumulation Time	6075 μ s
Capillary Exit	95.7 Volt	Skim 1	25.8 Volt	Trap Drive	42.5	Auto MS/MS	Off

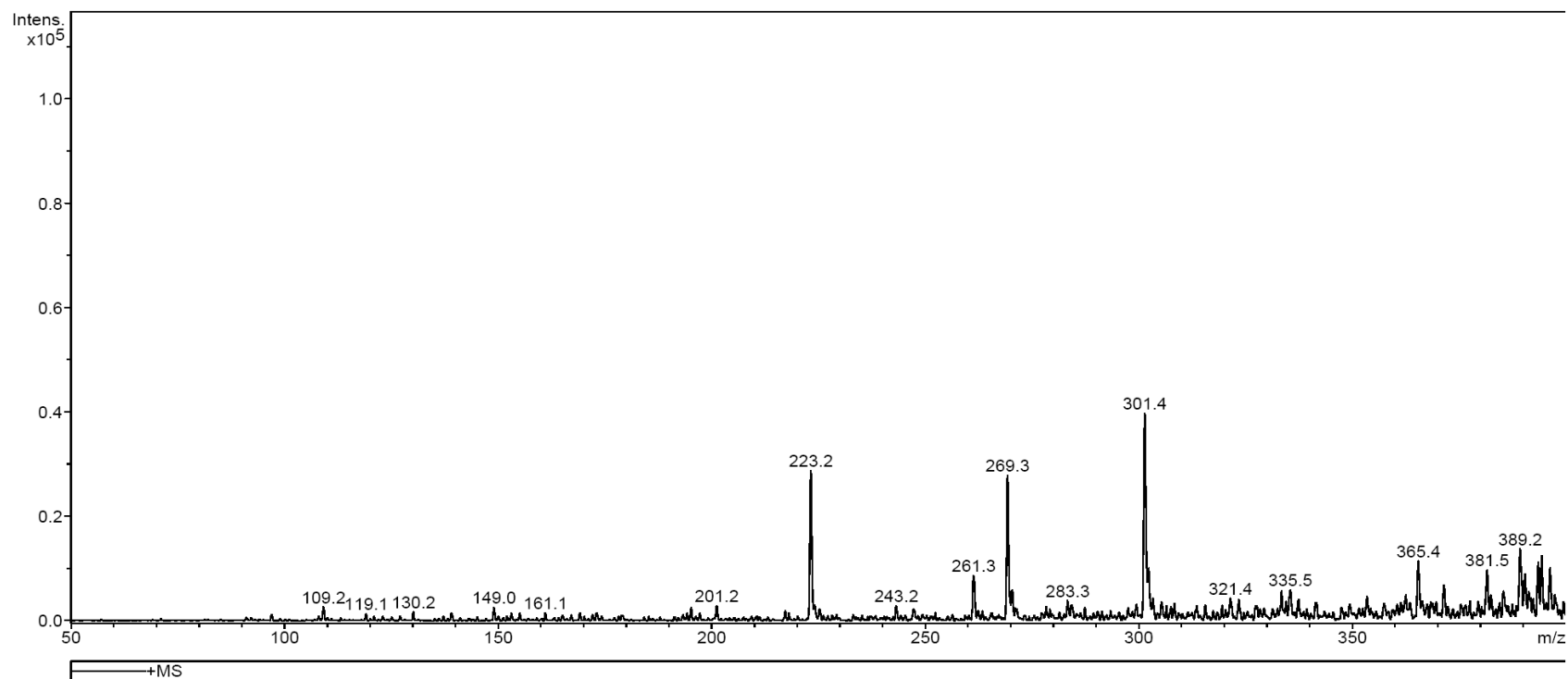


Figure 48: Mass spectrum of *p*-toluenesulfonyl azide (13).

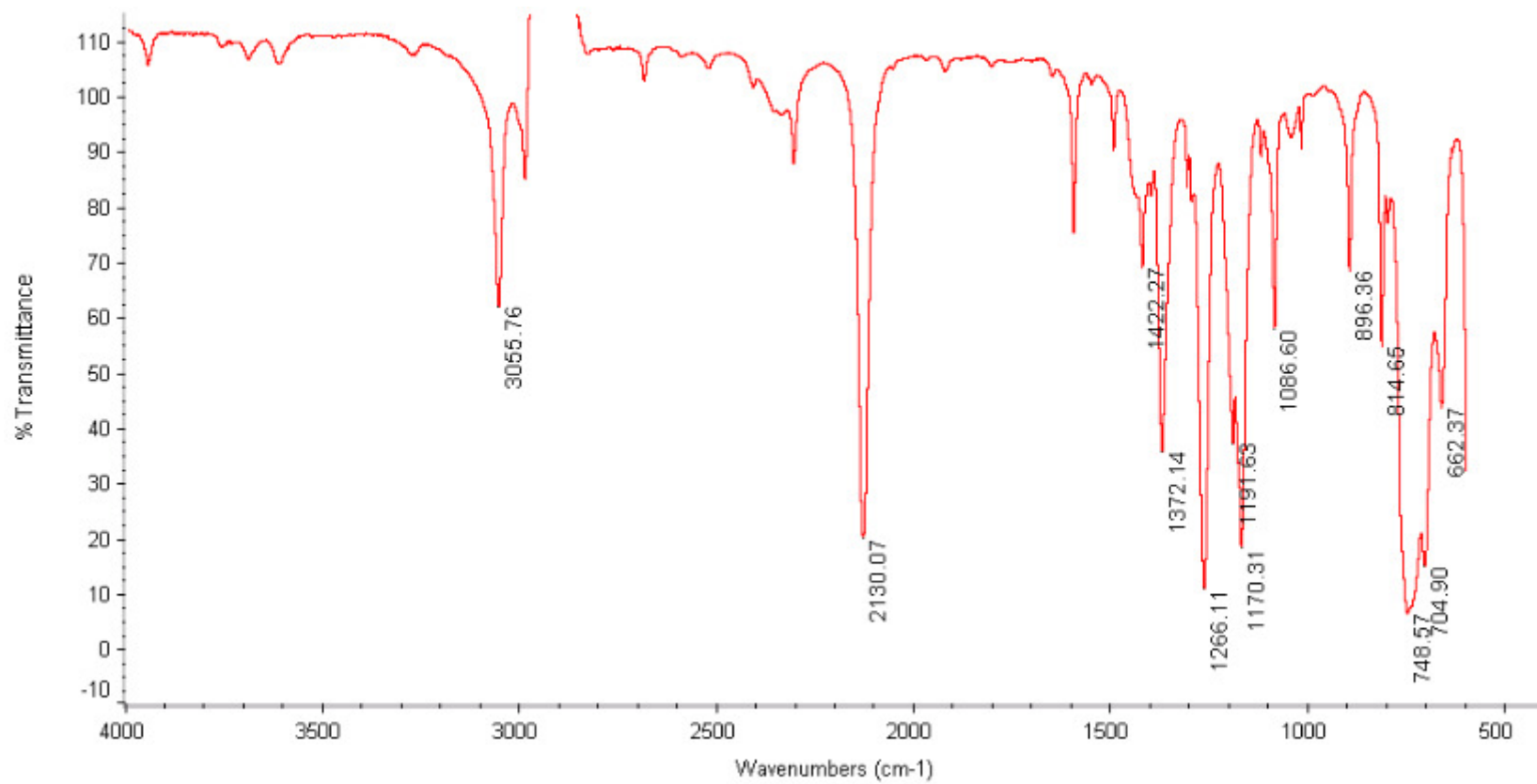


Figure 49: Infrared spectrum of *p*-toluenesulfonyl azide (13).

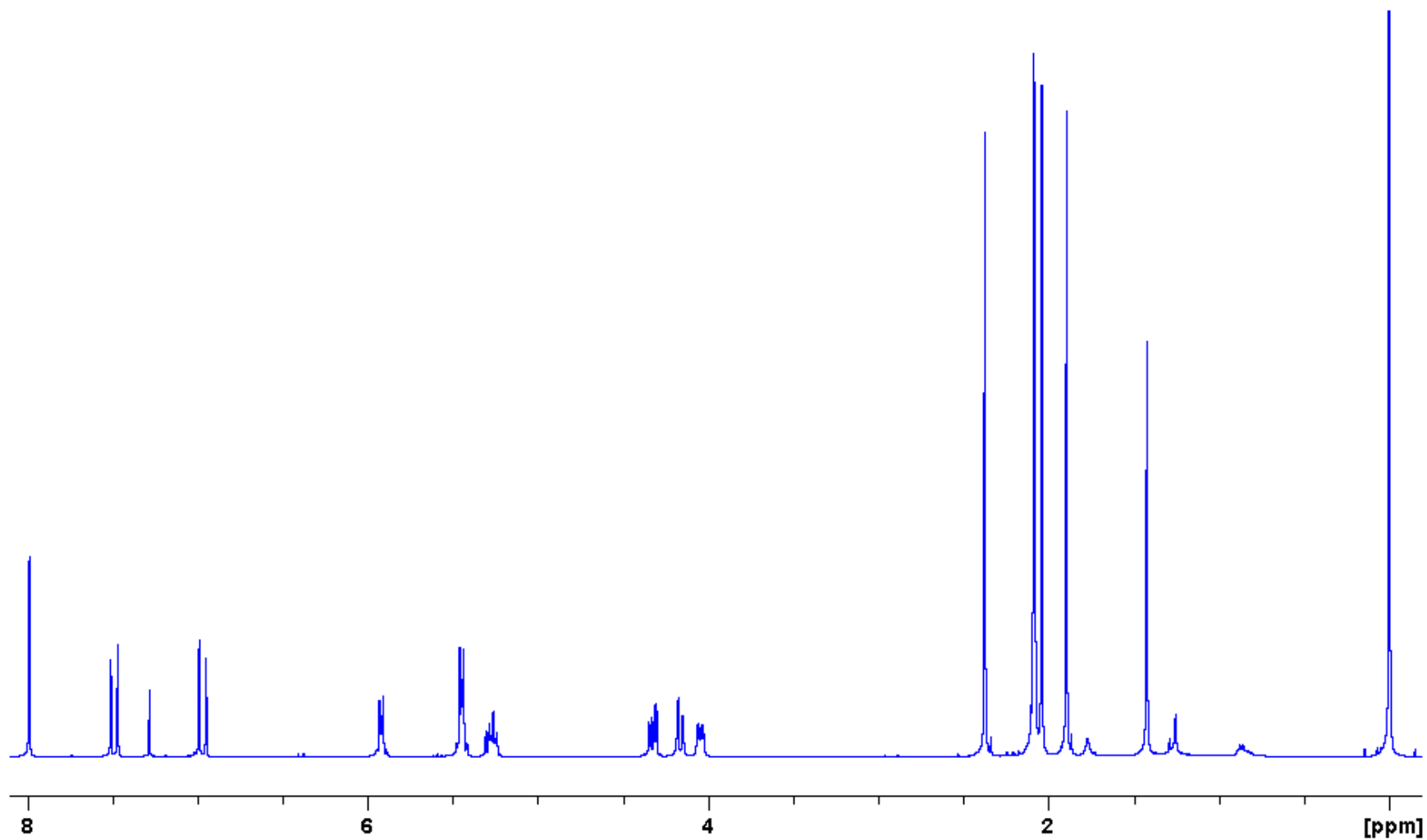


Figure 50: 400 MHz ¹H spectrum of α,β-unsaturated ketone **16**.

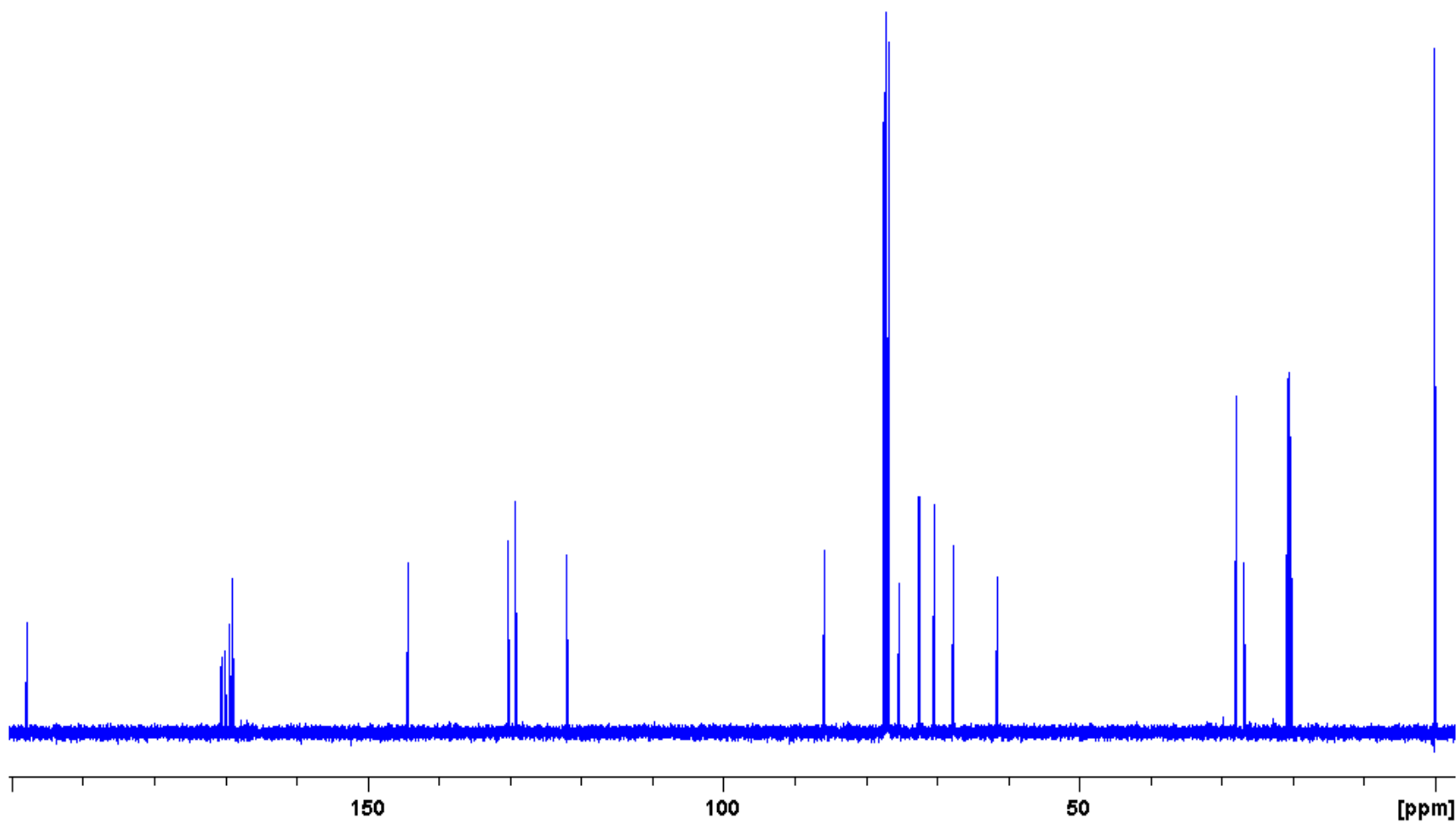


Figure 51: 100 MHz ^{13}C spectrum of α,β -unsaturated ketone **16**.

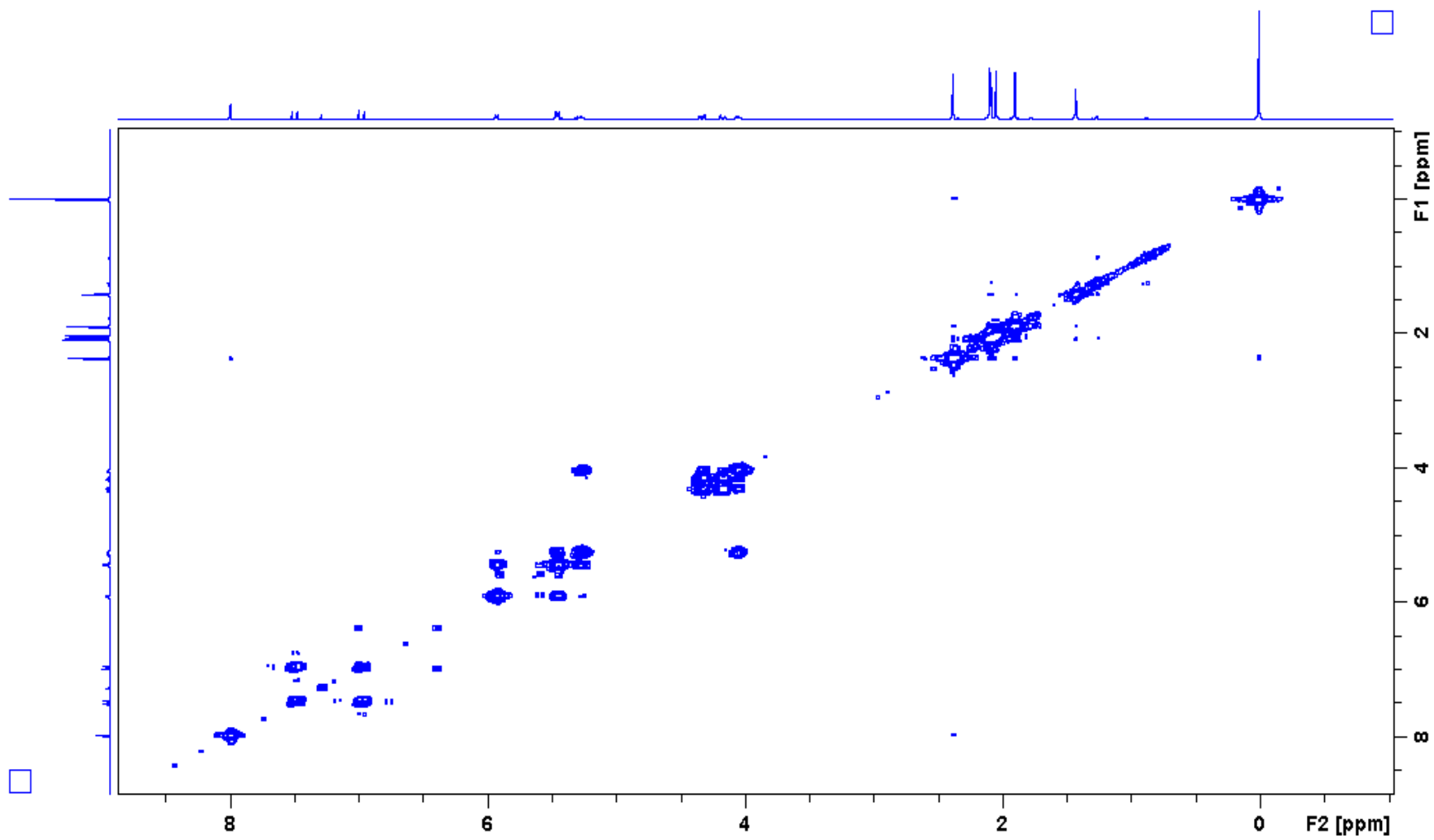


Figure 52: 400 MHz ^1H - ^1H COSY spectrum of α,β -unsaturated ketone **16**.

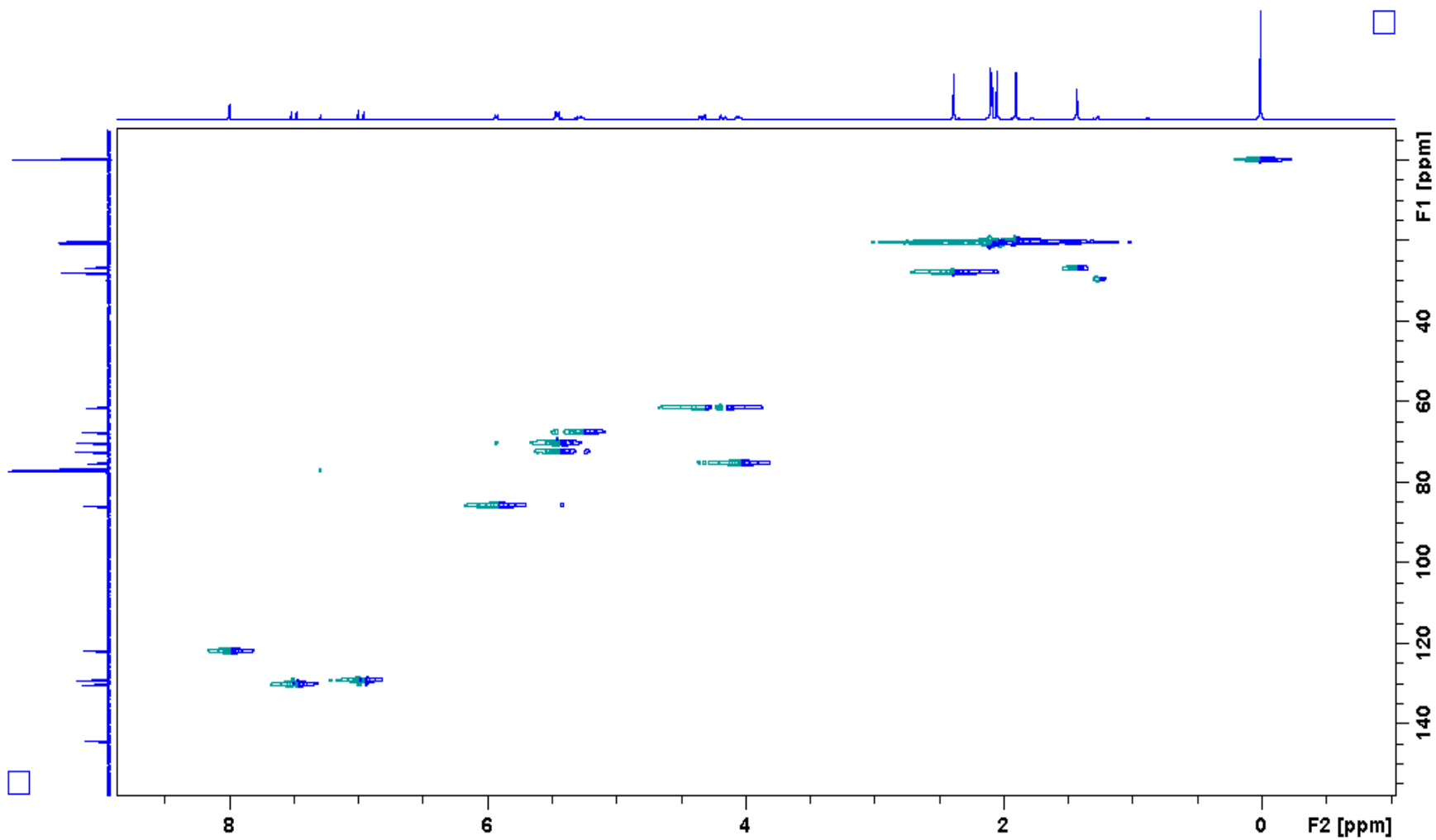


Figure 53: 400 MHz ^1H - ^{13}C HSQC spectrum of α,β -unsaturated ketone **16**.

Display Report

Analysis Info

Method XQ Default.ms Instrument Esquire-LC_00135

Acquisition Parameter

Ion Source Type	ESI	Mass Range Mode	Std/Normal	Ion Polarity	Positive	Alternating Ion Polarity	n/a
Scan Begin	100.00 m/z	Scan End	550.00 m/z	Averages	10 Spectra	Accumulation Time	838 μ s
Capillary Exit	116.6 Volt	Skim 1	40.7 Volt	Trap Drive	52.1	Auto MS/MS	Off

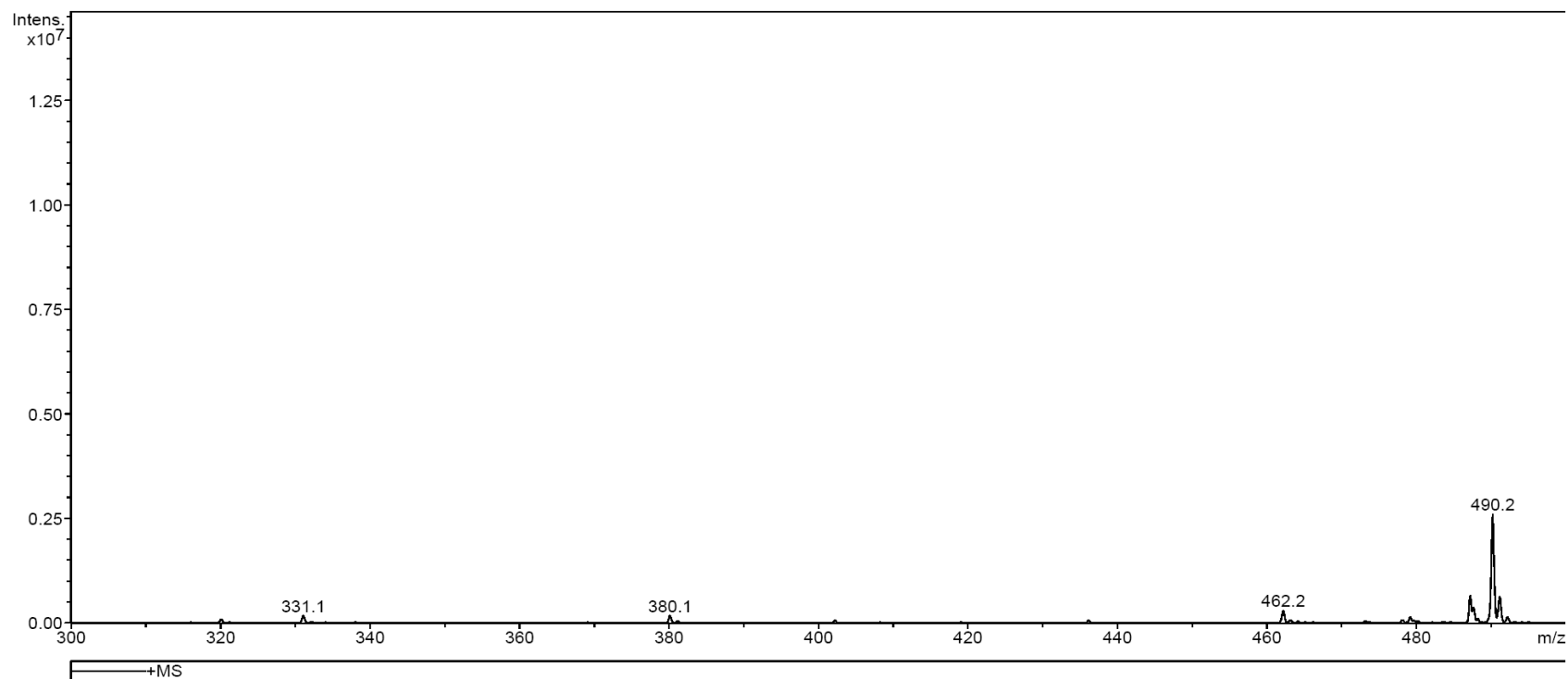


Figure 54: Mass spectrum of α,β -unsaturated ketone **16**.

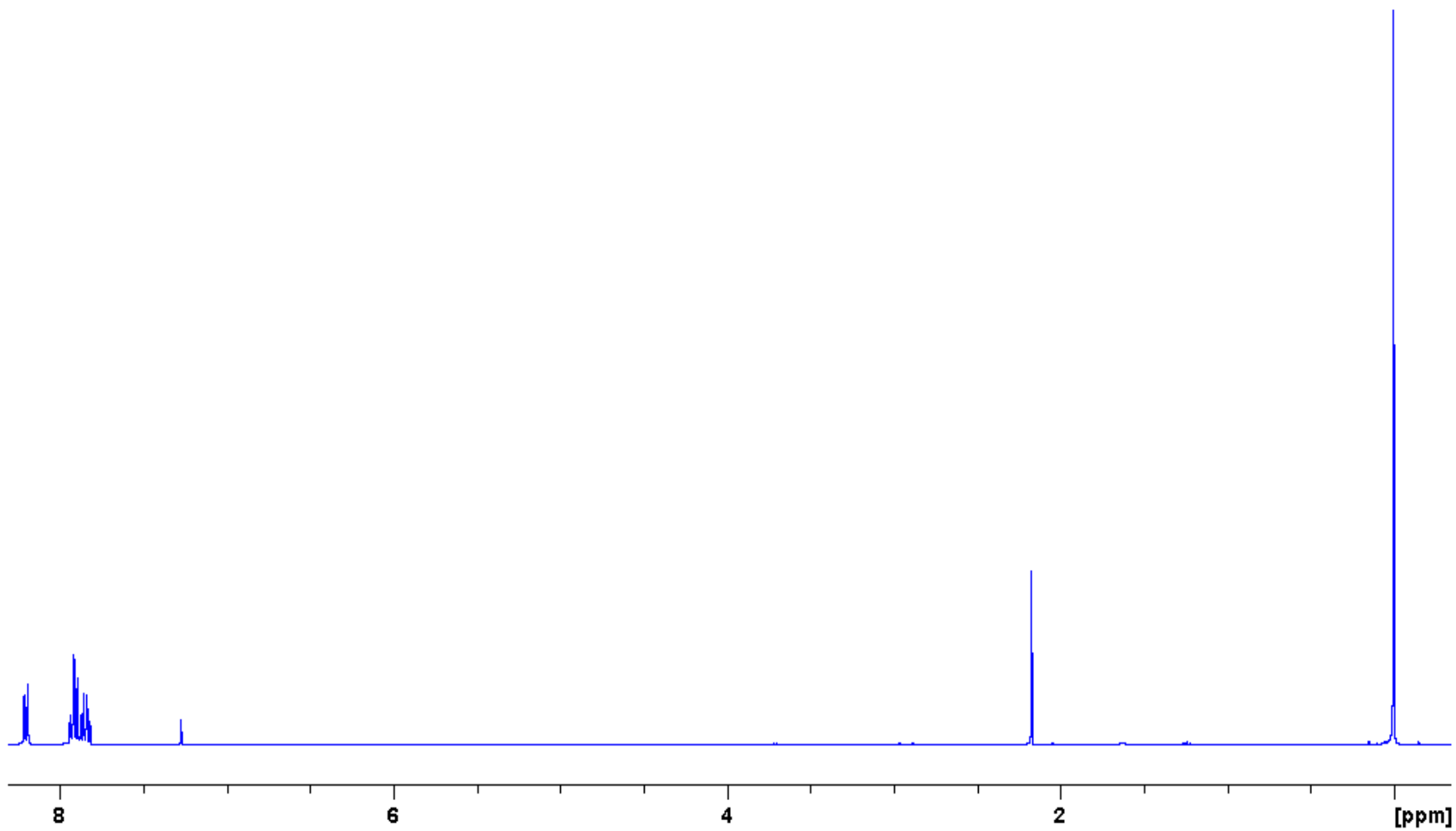


Figure 55: 400 MHz ¹H spectrum of *o*-nitrobenzenesulfonyl azide (**19**).

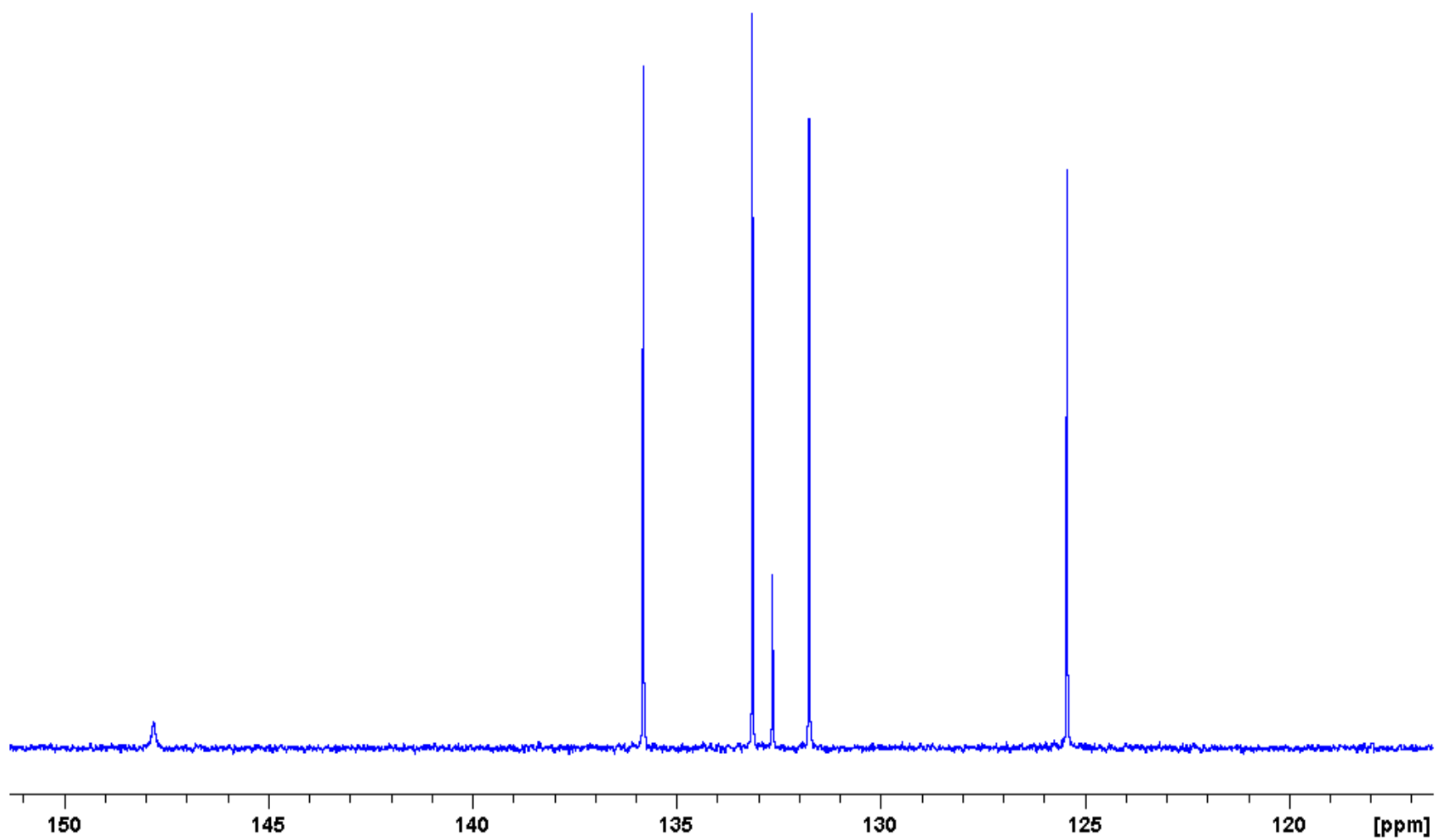


Figure 56: 100 MHz ^{13}C spectrum of *o*-nitrobenzenesulfonyl azide (19).

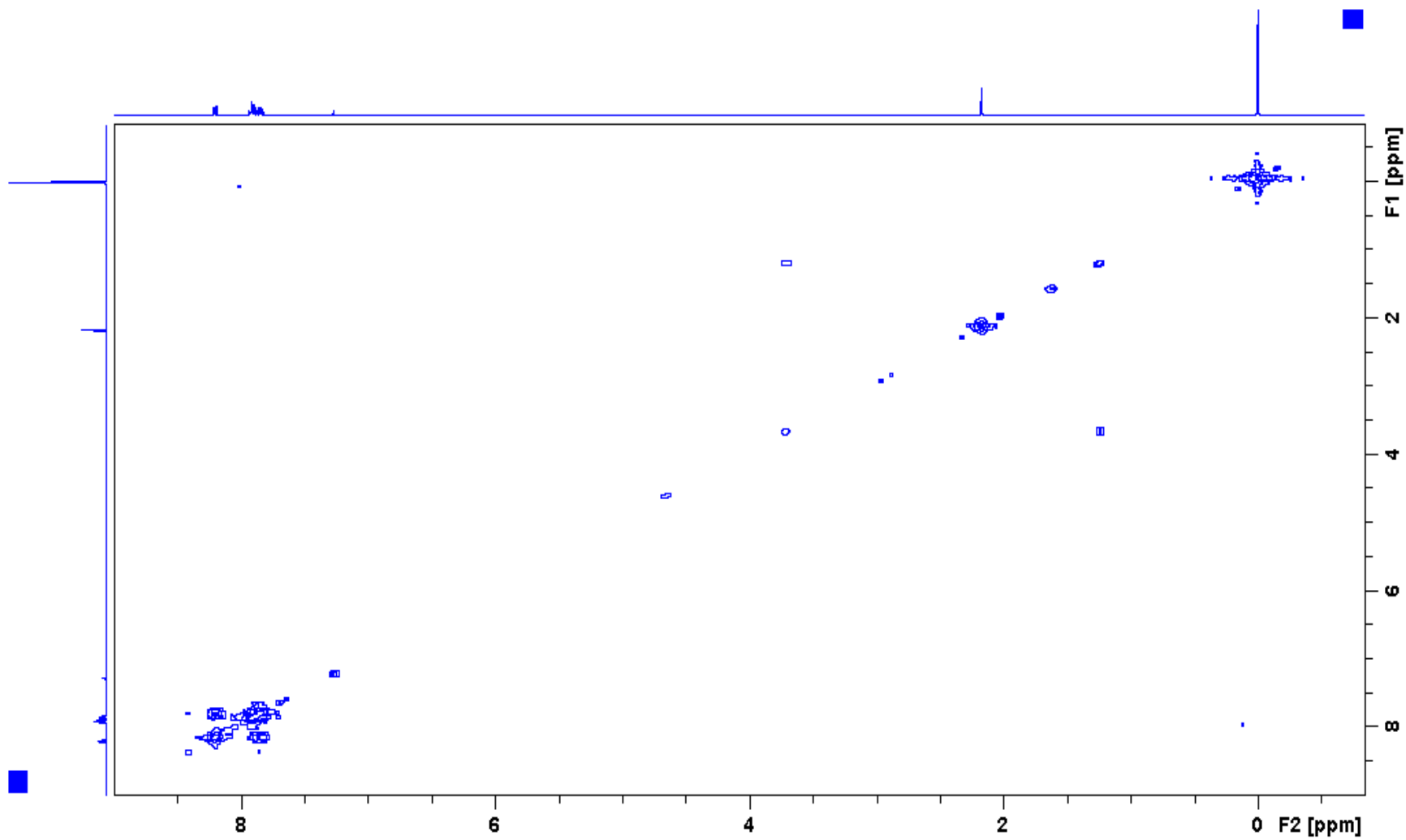


Figure 57: 400 MHz ¹H-¹H COSY spectrum of *o*-nitrobenzenesulfonyl azide (**19**).

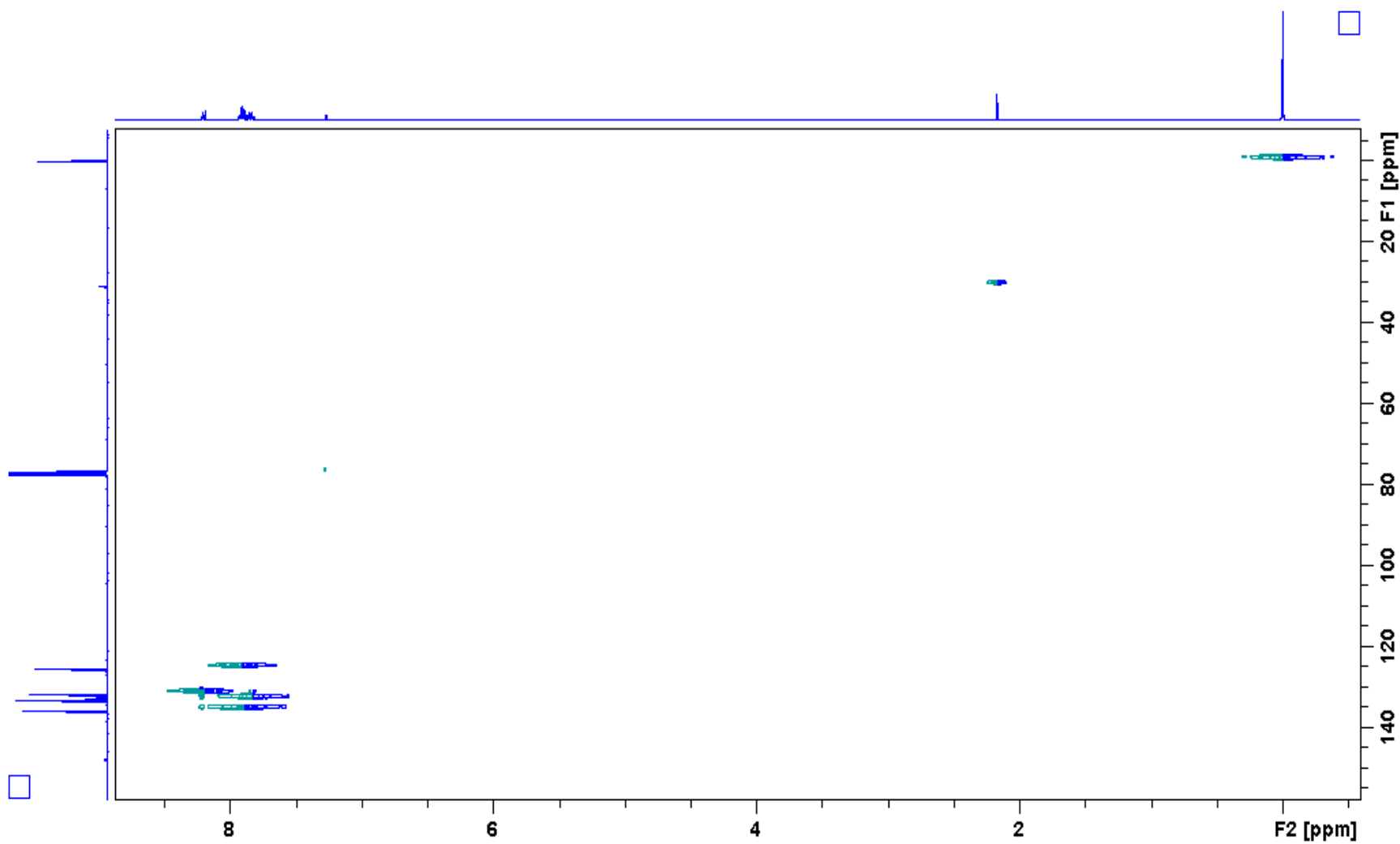


Figure 58: 400 MHz ^1H - ^{13}C HSQC spectrum of *o*-nitrobenzenesulfonyl azide (**19**).

Display Report

Analysis Info

Method XQ Default.ms Instrument Esquire-LC_00135

Acquisition Parameter

Ion Source Type	ESI	Mass Range Mode	Std/Normal	Ion Polarity	Positive	Alternating Ion Polarity	n/a
Scan Begin	100.00 m/z	Scan End	400.00 m/z	Averages	10 Spectra	Accumulation Time	1995 μ s
Capillary Exit	80.5 Volt	Skim 1	13.8 Volt	Trap Drive	43.7	Auto MS/MS	Off

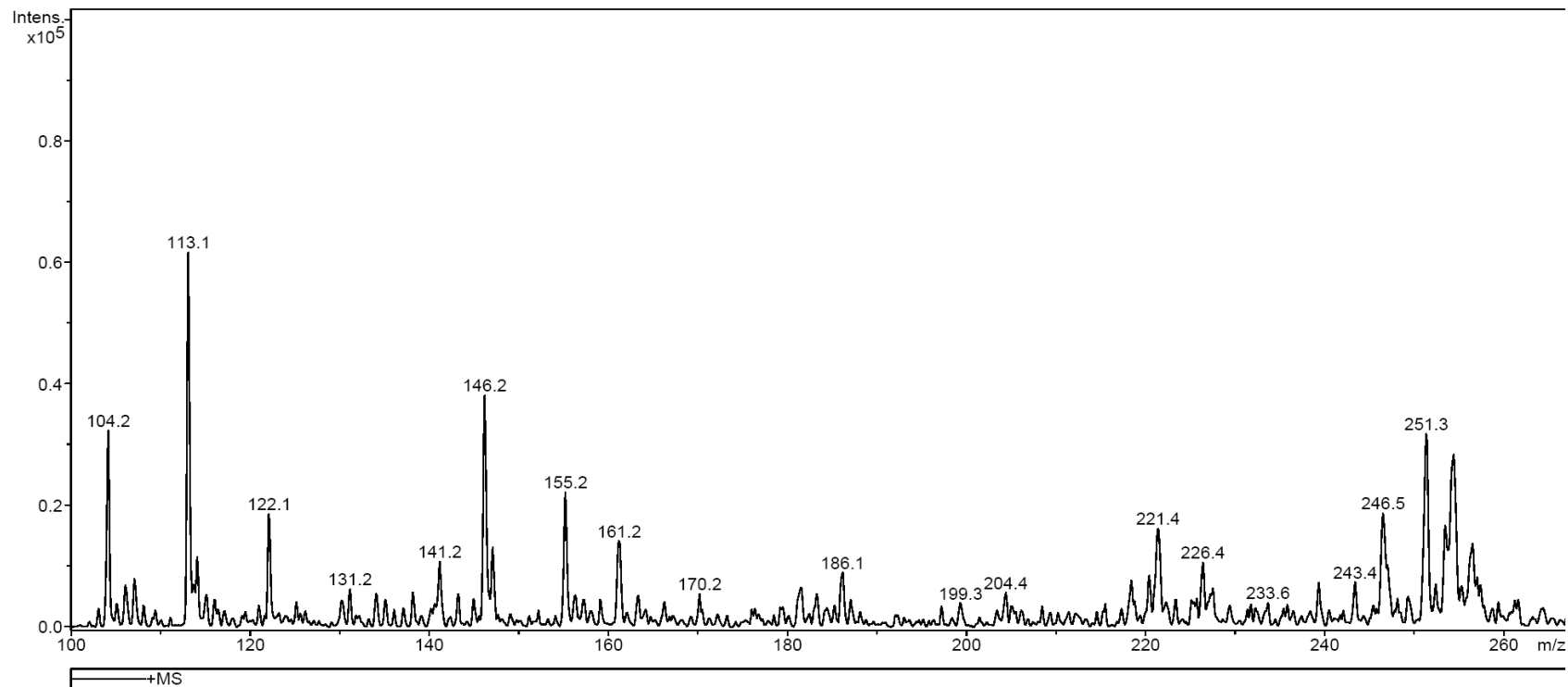


Figure 59: Mass spectrum of *o*-nitrobenzenesulfonyl azide (19).

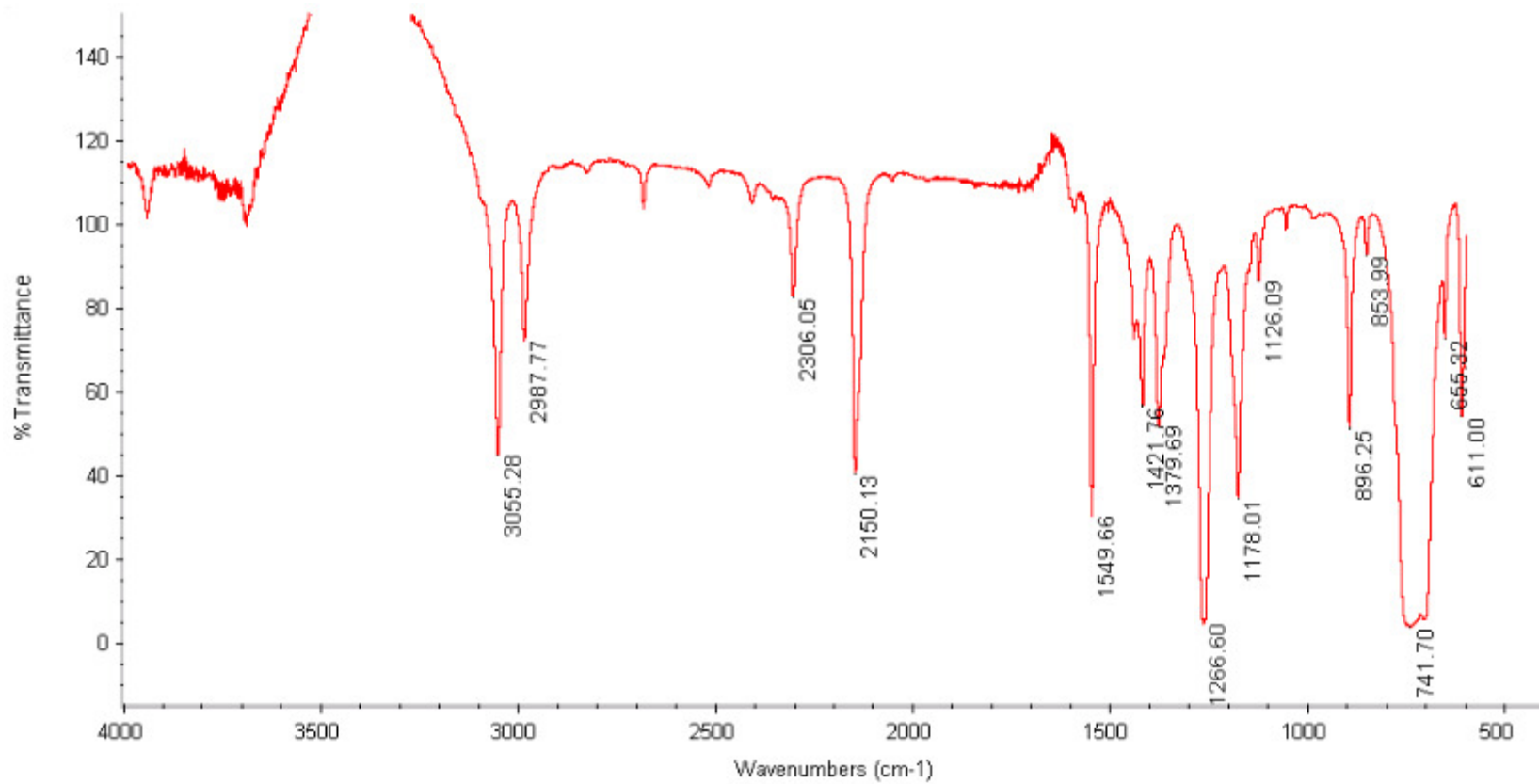


Figure 60: Infrared spectrum of *o*-nitrobenzenesulfonyl azide (**19**).

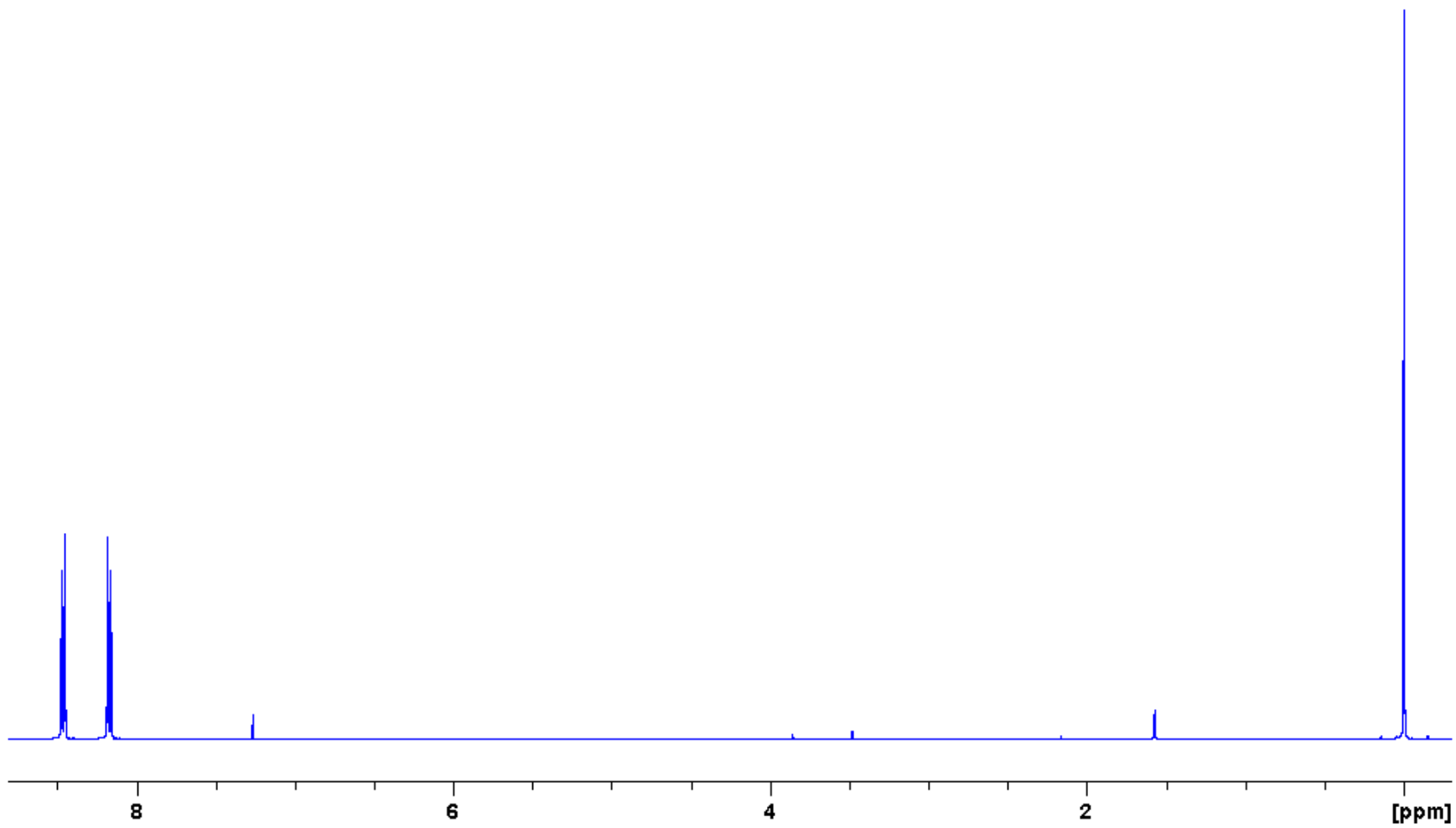


Figure 61: 400 MHz ¹H spectrum of *p*-nitrobenzenesulfonyl azide (**21**).

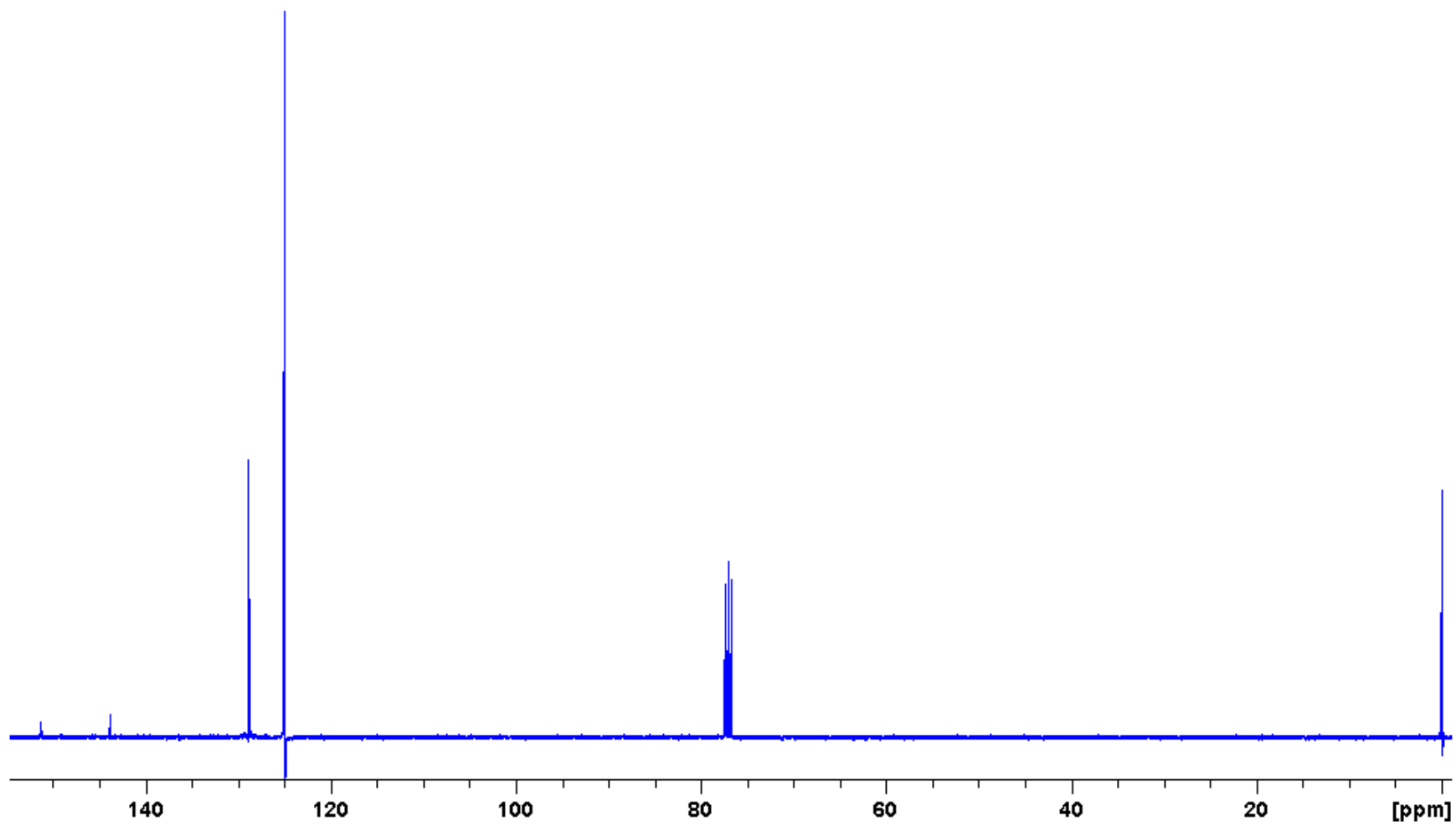


Figure 62: 100 MHz ^{13}C spectrum of *p*-nitrobenzenesulfonyl azide (**21**).

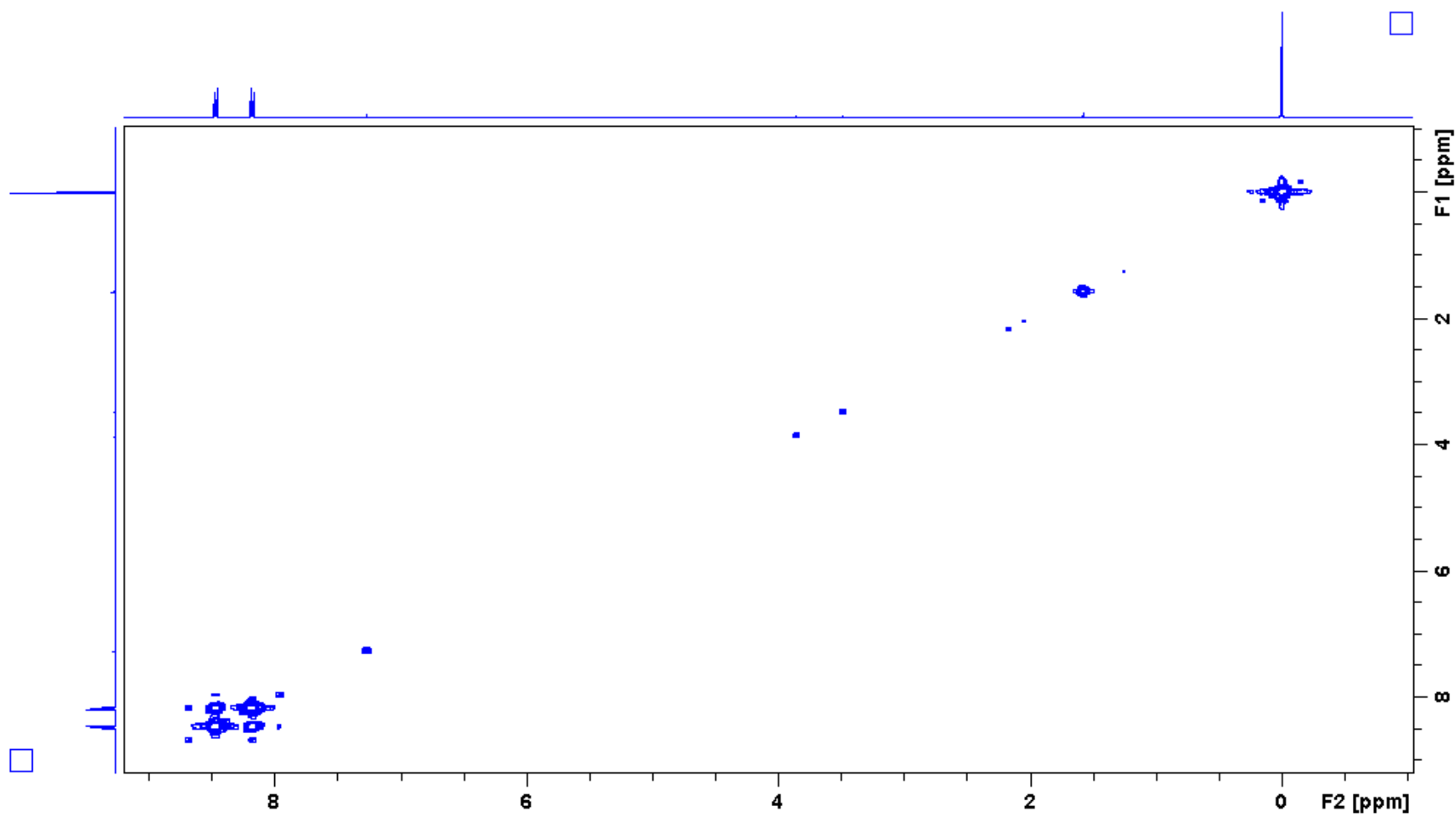


Figure 63: 400 MHz ¹H-¹H COSY spectrum of *p*-nitrobenzenesulfonyl azide (**21**).

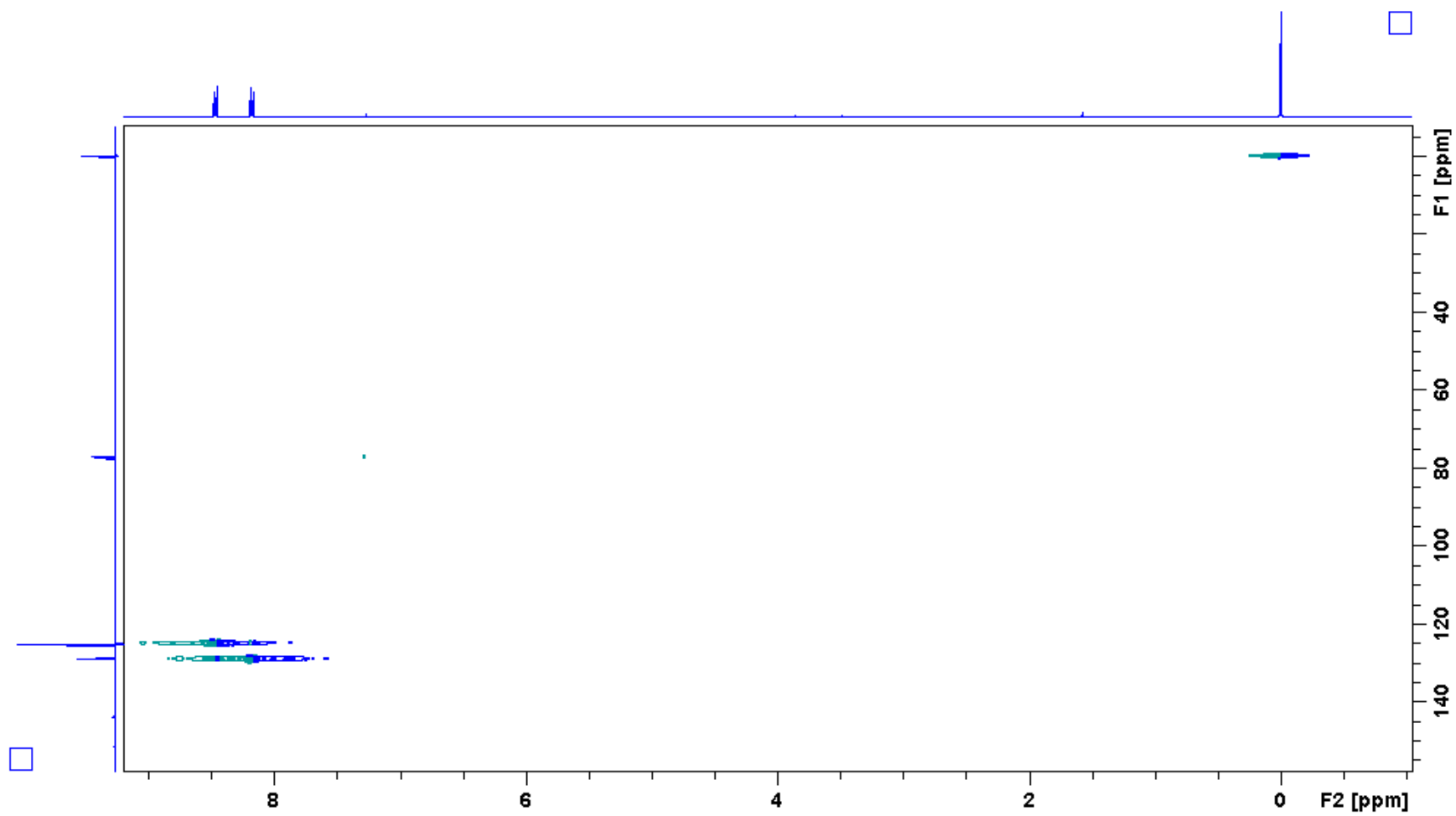


Figure 64: 400 MHz ^1H - ^{13}C HSQC spectrum of *p*-nitrobenzenesulfonyl azide (**21**).

Display Report

Analysis Info

Method XQ Default.ms Instrument Esquire-LC_00135

Acquisition Parameter

Ion Source Type	ESI	Mass Range Mode	Std/Normal	Ion Polarity	Positive	Alternating Ion Polarity	n/a
Scan Begin	100.00 m/z	Scan End	400.00 m/z	Averages	10 Spectra	Accumulation Time	35542 μ s
Capillary Exit	98.6 Volt	Skim 1	28.1 Volt	Trap Drive	43.7	Auto MS/MS	Off

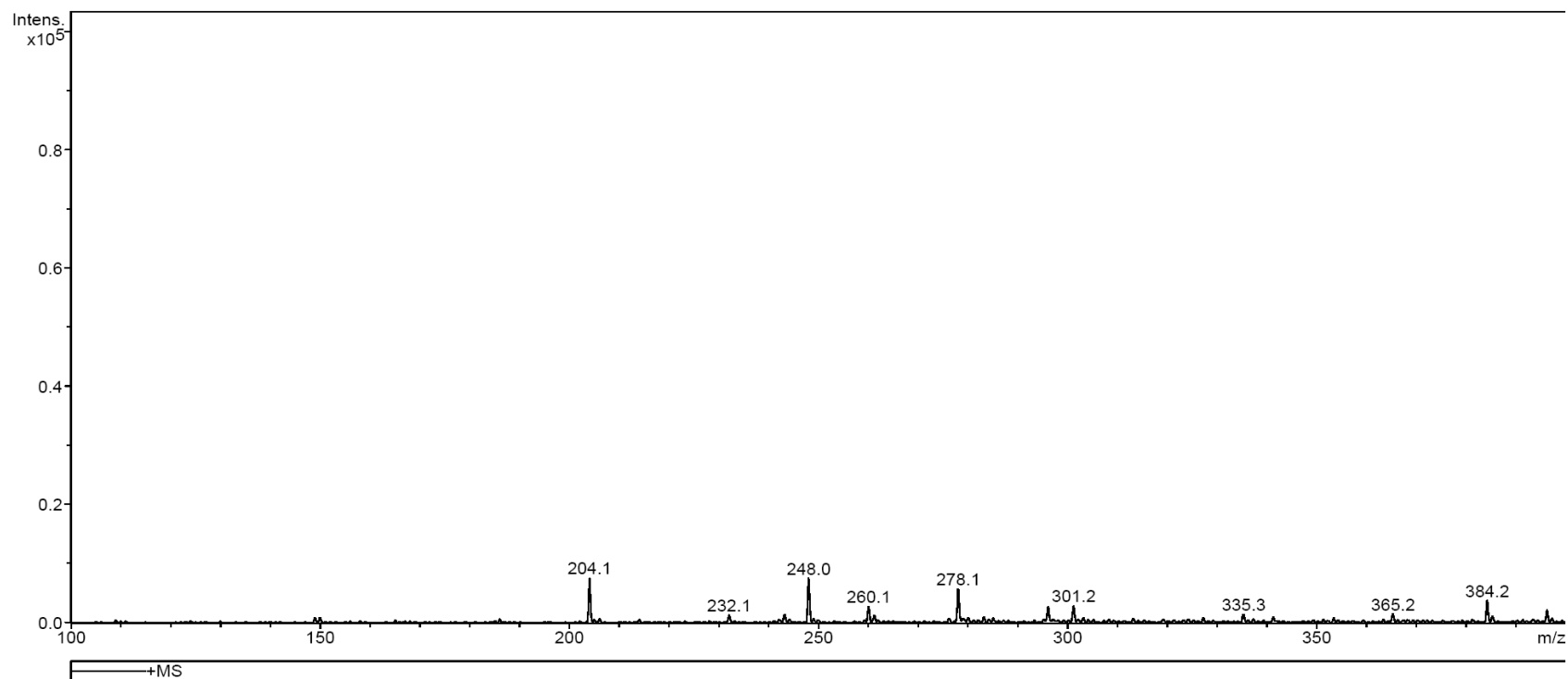


Figure 65: Mass spectrum of *p*-nitrobenzenesulfonyl azide (**21**).

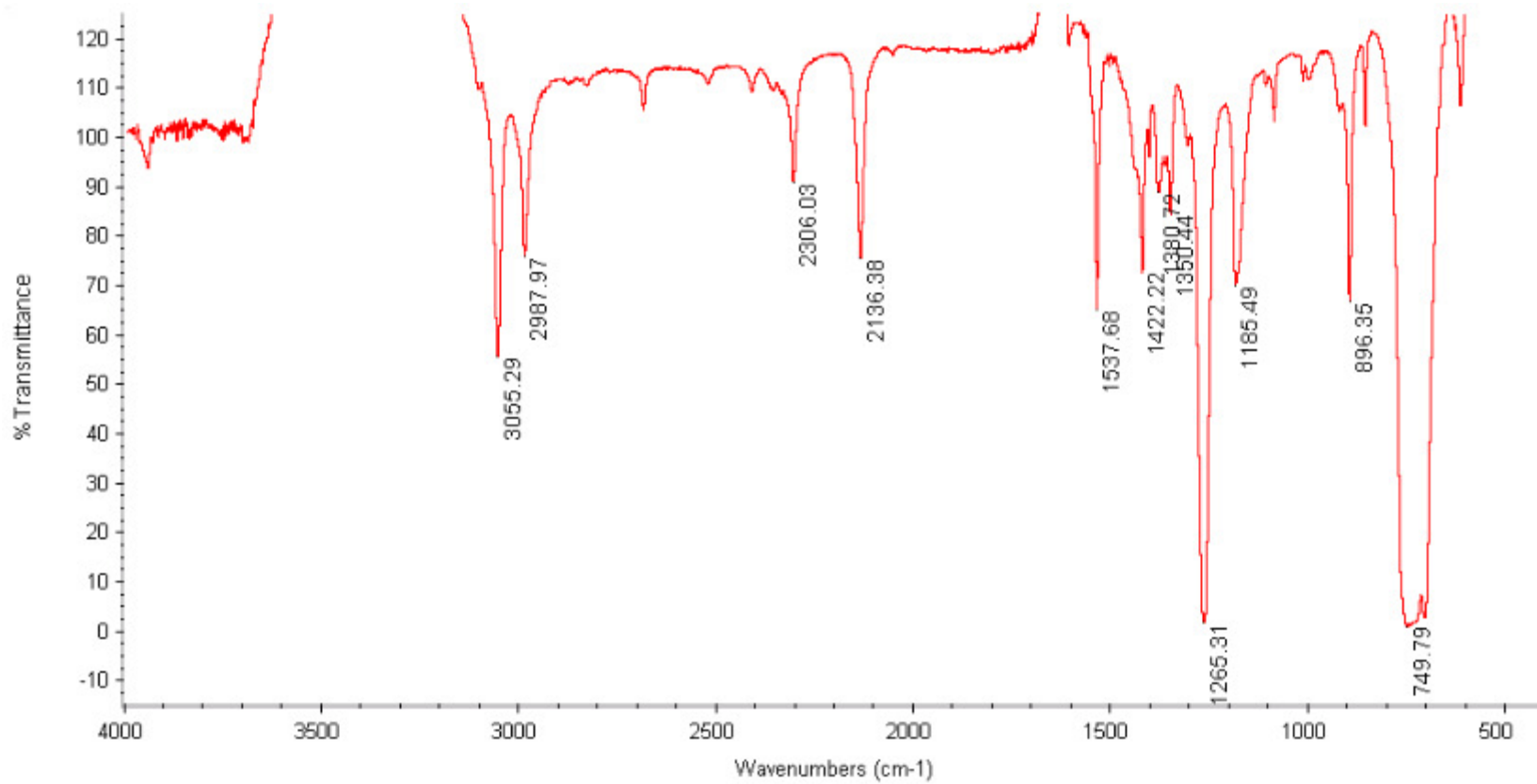


Figure 66: Infrared spectrum of *p*-nitrobenzenesulfonyl azide (**21**).

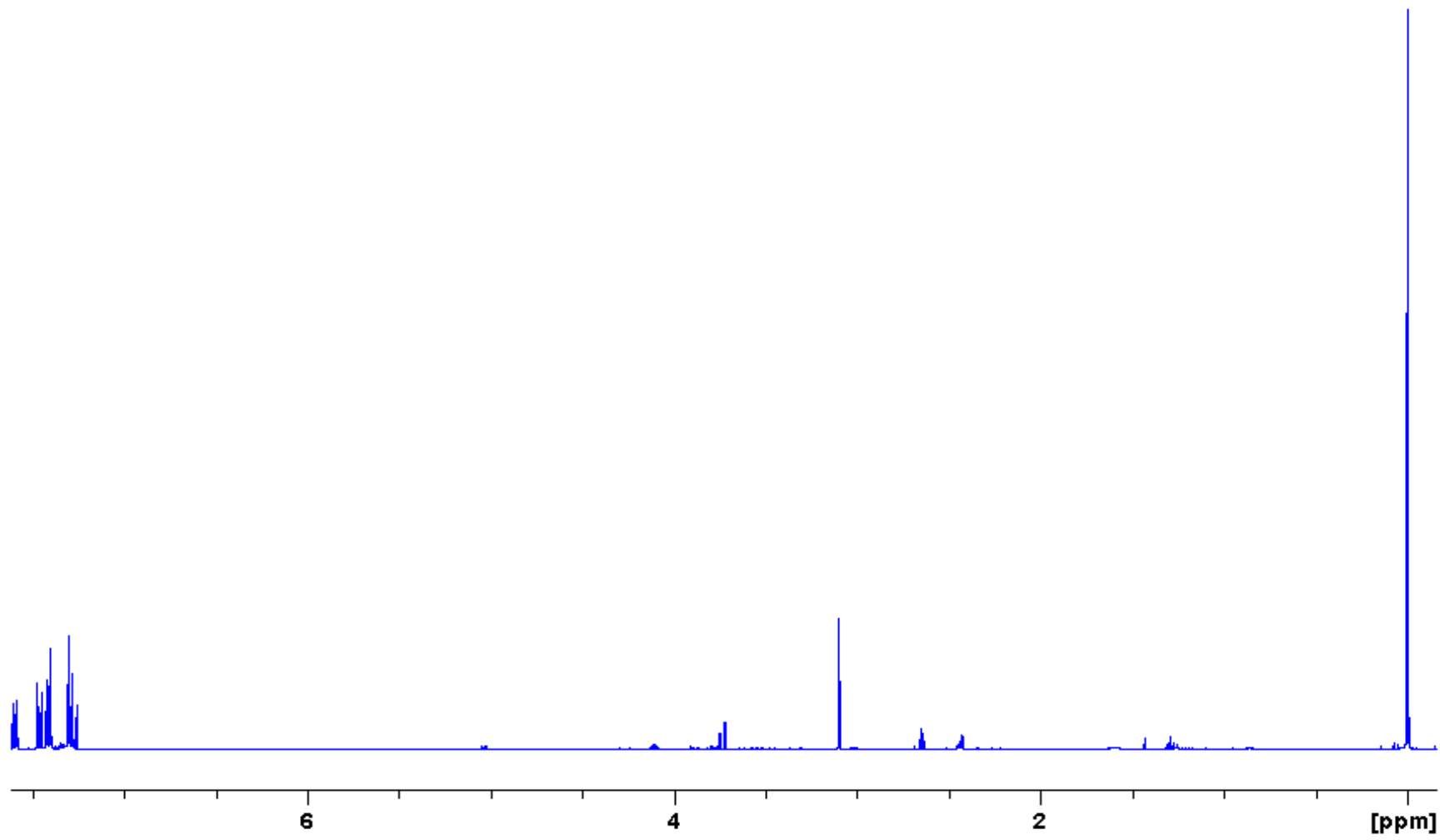


Figure 67: 400 MHz ^1H spectrum of 4-chlorophenylacetylene (25).

Display Report

Analysis Info

Method XQ Default.ms Instrument Esquire-LC_00135

Acquisition Parameter

Ion Source Type	ESI	Mass Range Mode	Std/Normal	Ion Polarity	Positive	Alternating Ion Polarity	n/a
Scan Begin	50.00 m/z	Scan End	250.00 m/z	Averages	10 Spectra	Accumulation Time	50000 μ s
Capillary Exit	91.8 Volt	Skim 1	22.9 Volt	Trap Drive	41.0	Auto MS/MS	Off

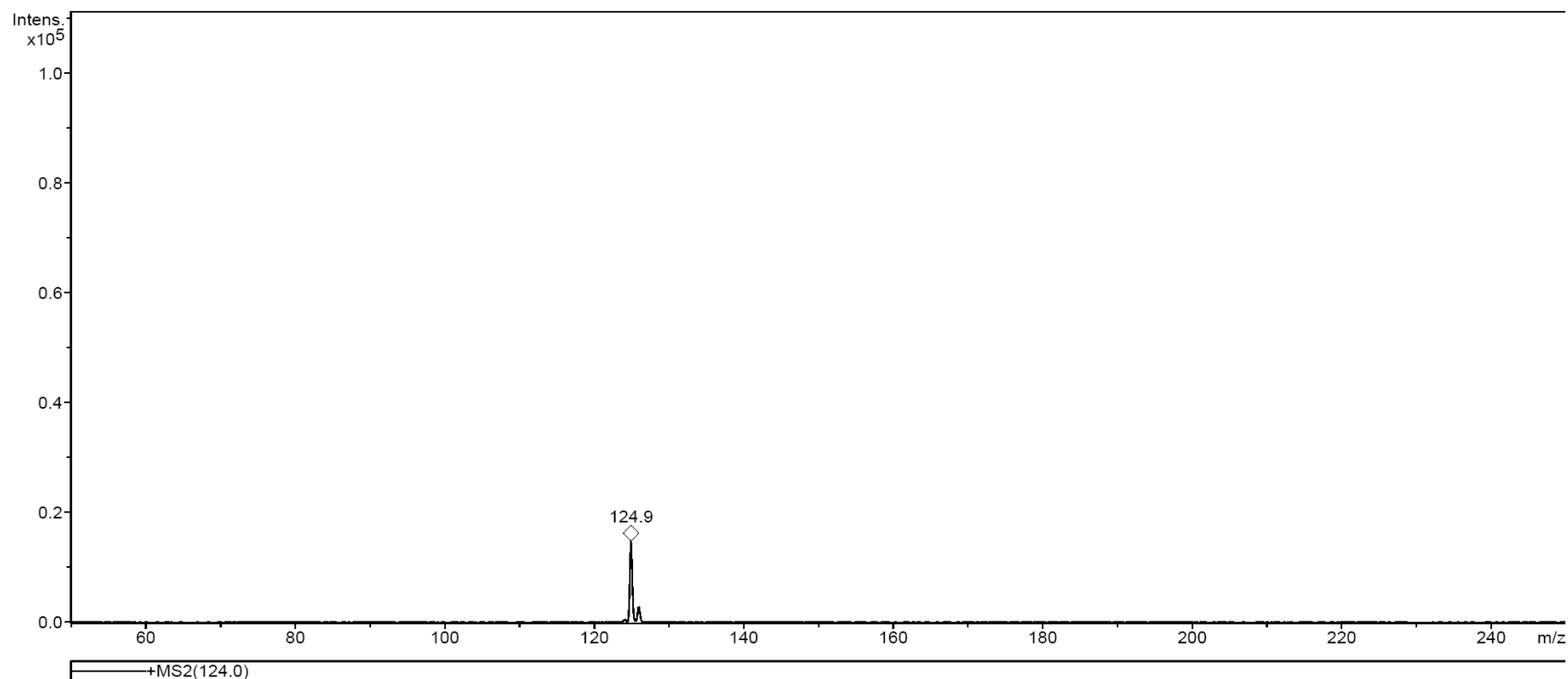


Figure 68: Mass spectrum of 4-chlorophenylacetylene (**25**).

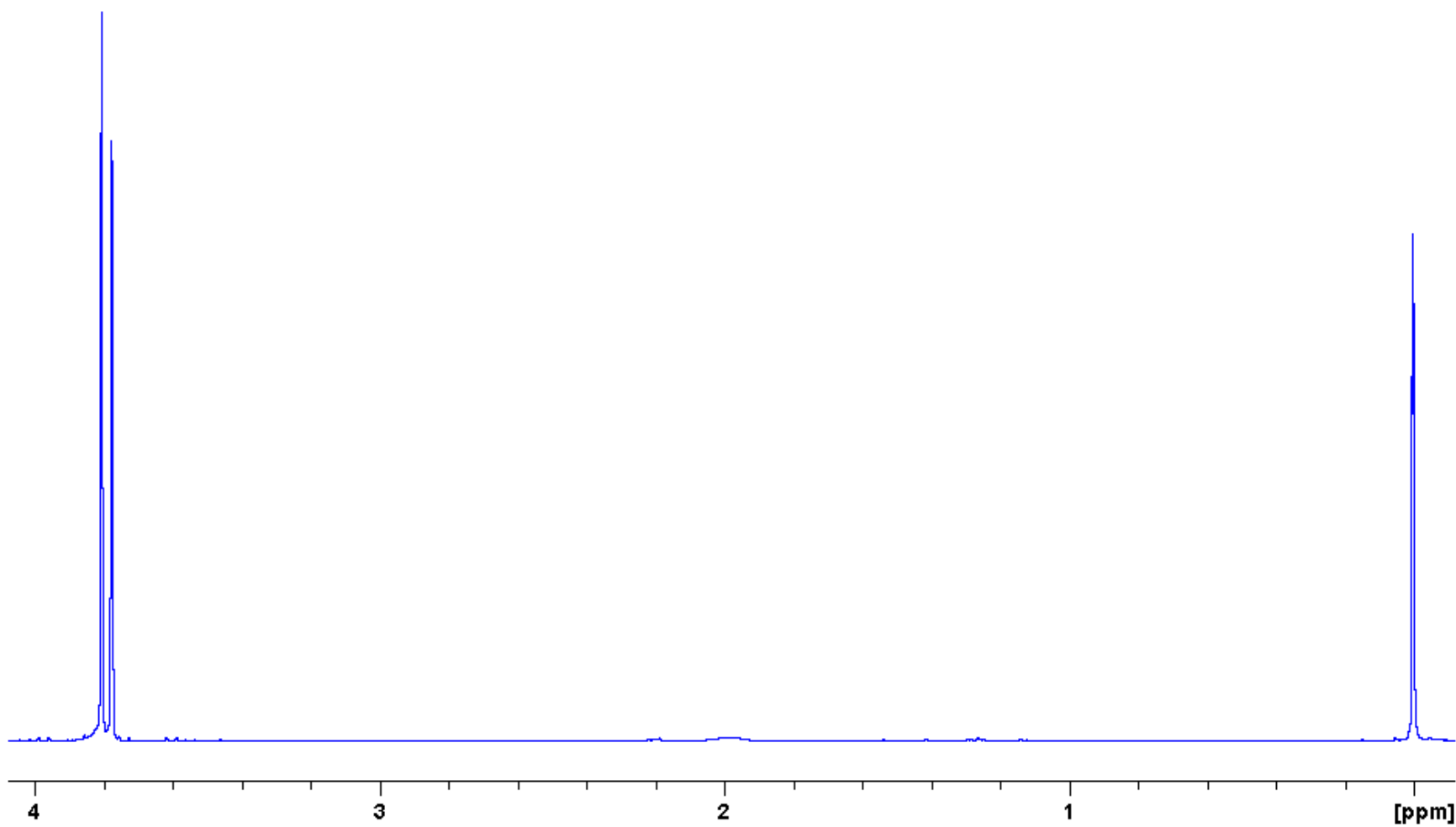


Figure 69: 400 MHz ^1H spectrum of dimethyl(diazomethyl)phosphonate (27).

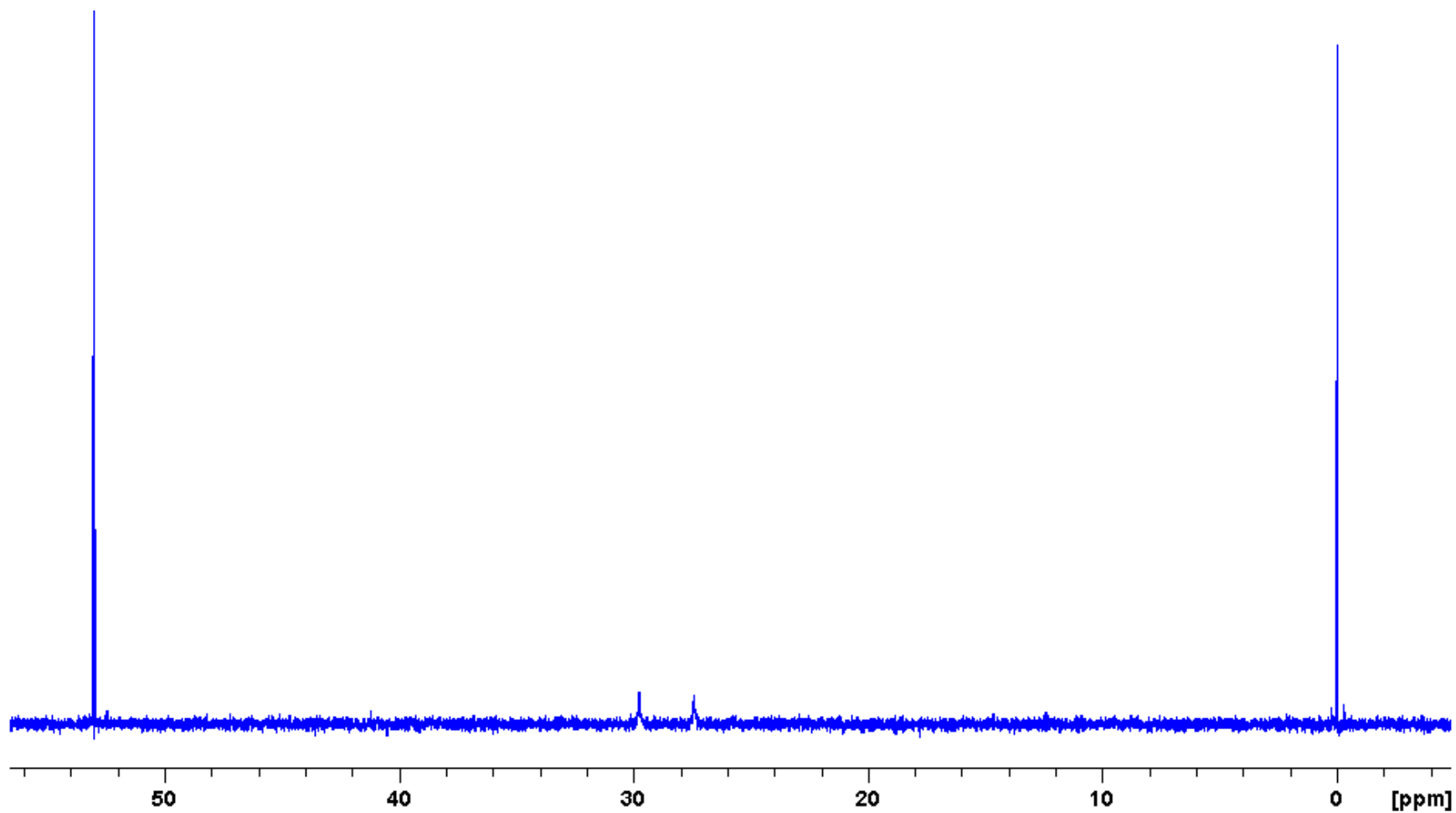


Figure 70: 100 MHz ^{13}C spectrum of dimethyl(diazomethyl)phosphonate (27).

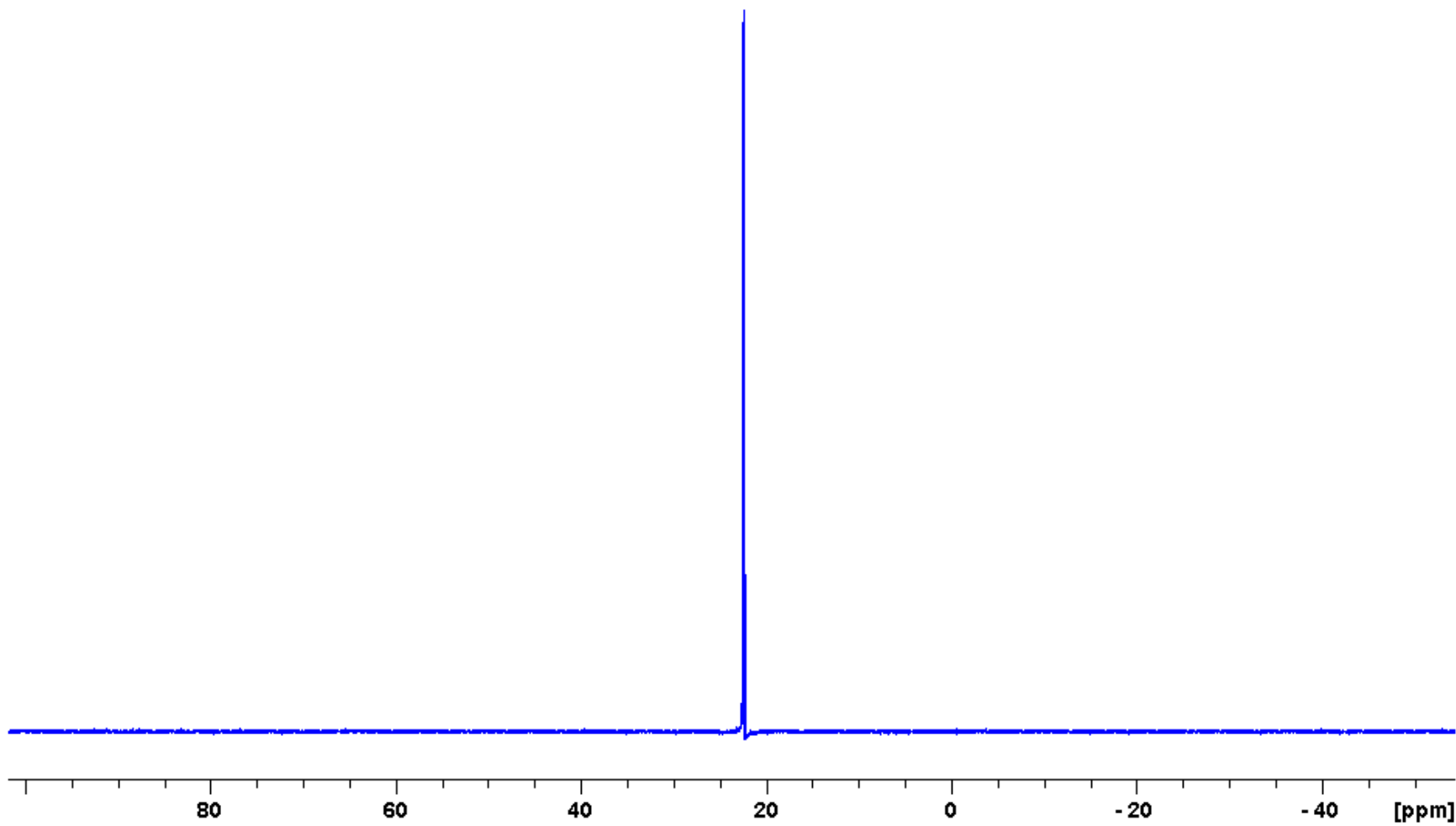


Figure 71: 161 MHz ^{31}P spectrum of dimethyl(diazomethyl)phosphonate (**27**).

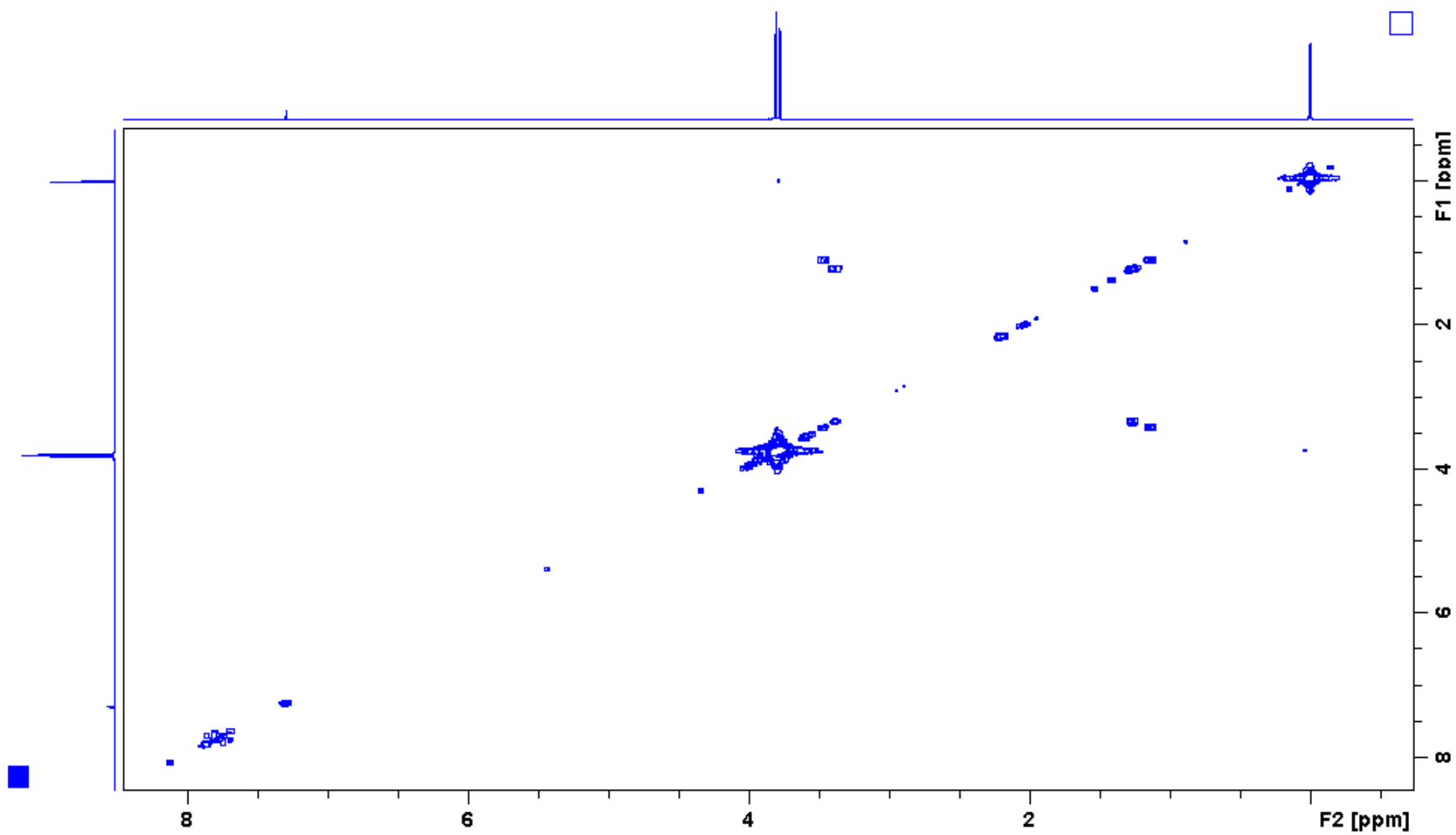


Figure 72: 400 MHz ^1H - ^1H COSY spectrum of dimethyl(diazomethyl)phosphonate (**27**).

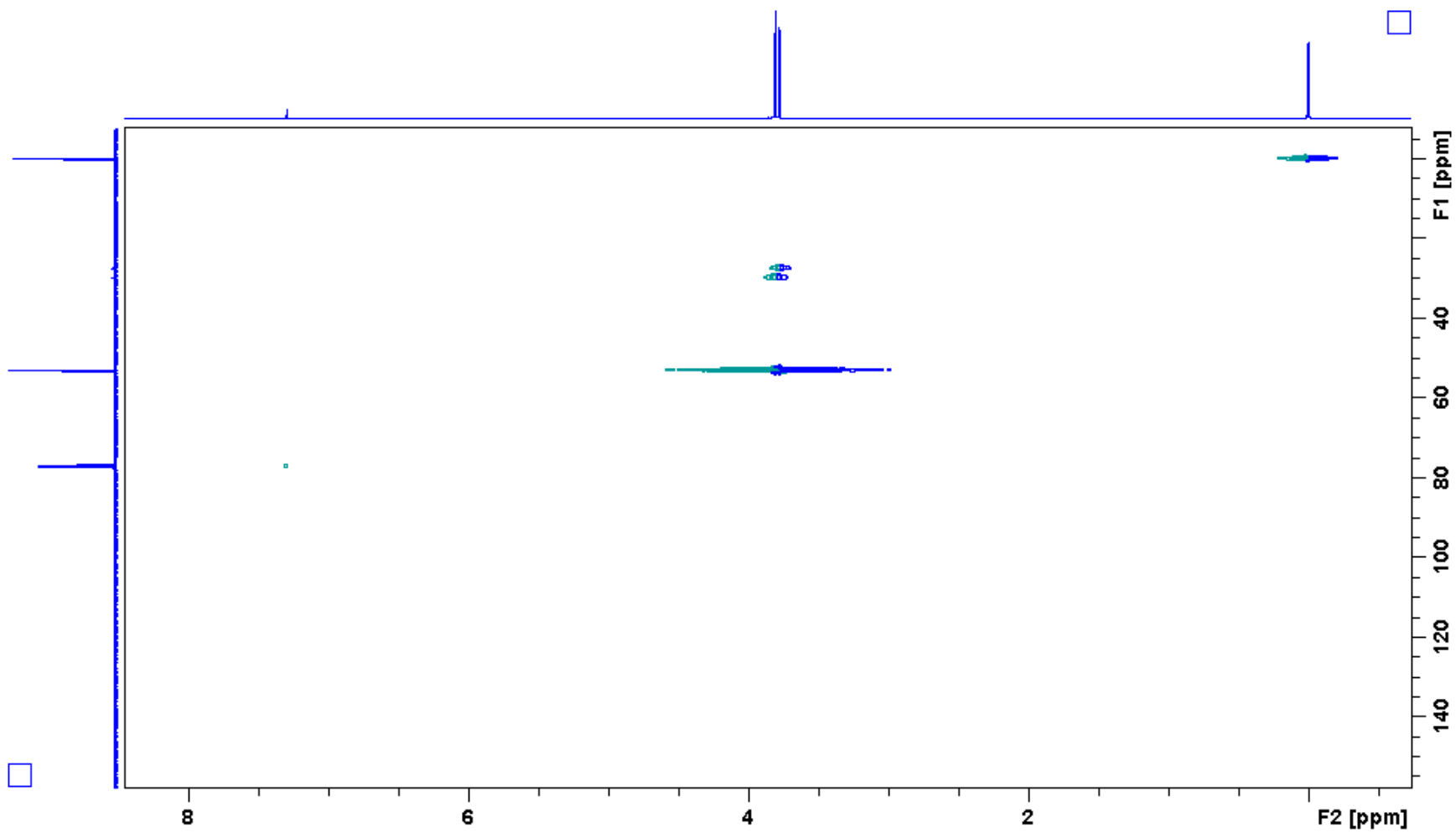


Figure 73: 400 MHz ^1H - ^{13}C HSQC spectrum of dimethyl(diazomethyl)phosphonate (**27**).

Display Report

Analysis Info

Method XQ Default.ms Instrument Esquire-LC_00135

Acquisition Parameter

Ion Source Type	ESI	Mass Range Mode	Std/Normal	Ion Polarity	Positive	Alternating Ion Polarity	n/a
Scan Begin	100.00 m/z	Scan End	200.00 m/z	Averages	10 Spectra	Accumulation Time	50000 μ s
Capillary Exit	73.2 Volt	Skim 1	7.5 Volt	Trap Drive	42.5	Auto MS/MS	Off

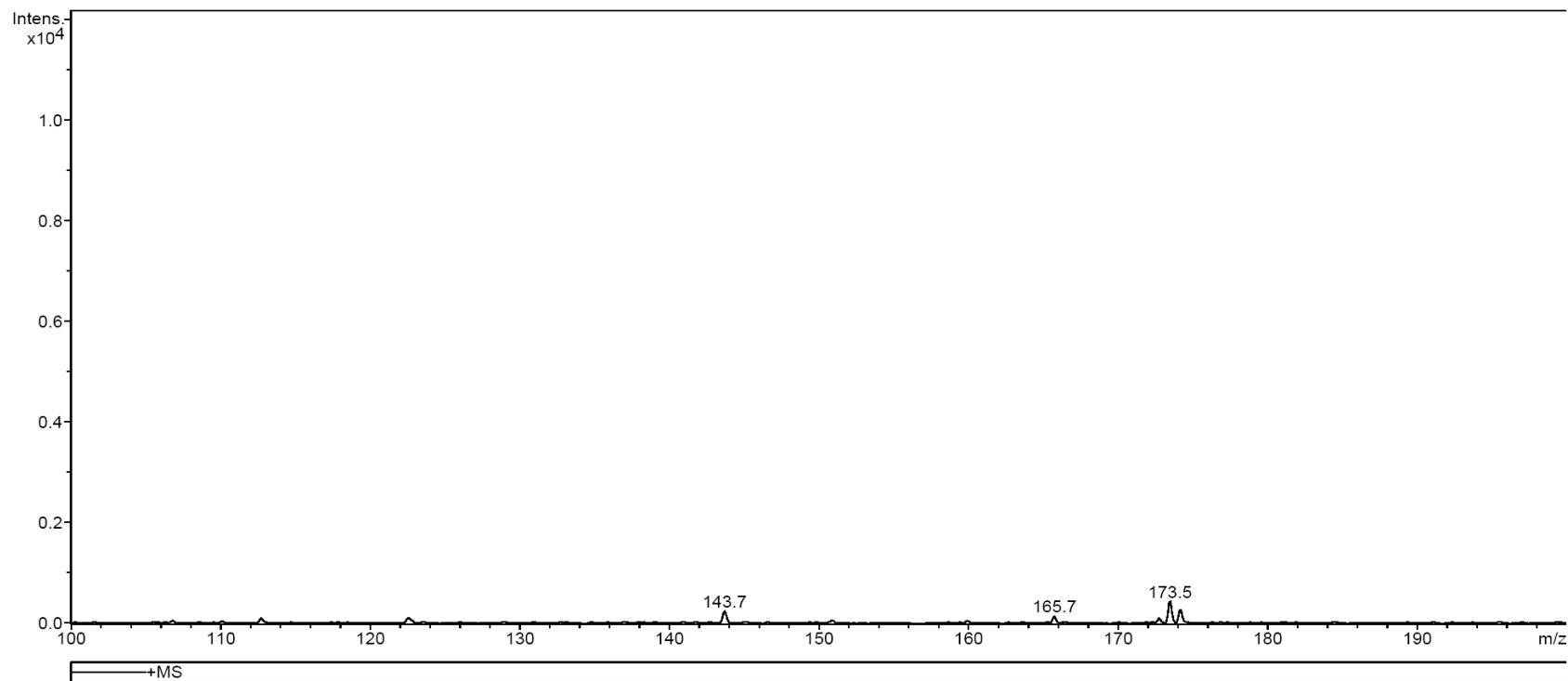


Figure 74: Mass spectrum of dimethyl(diazomethyl)phosphonate (**27**).

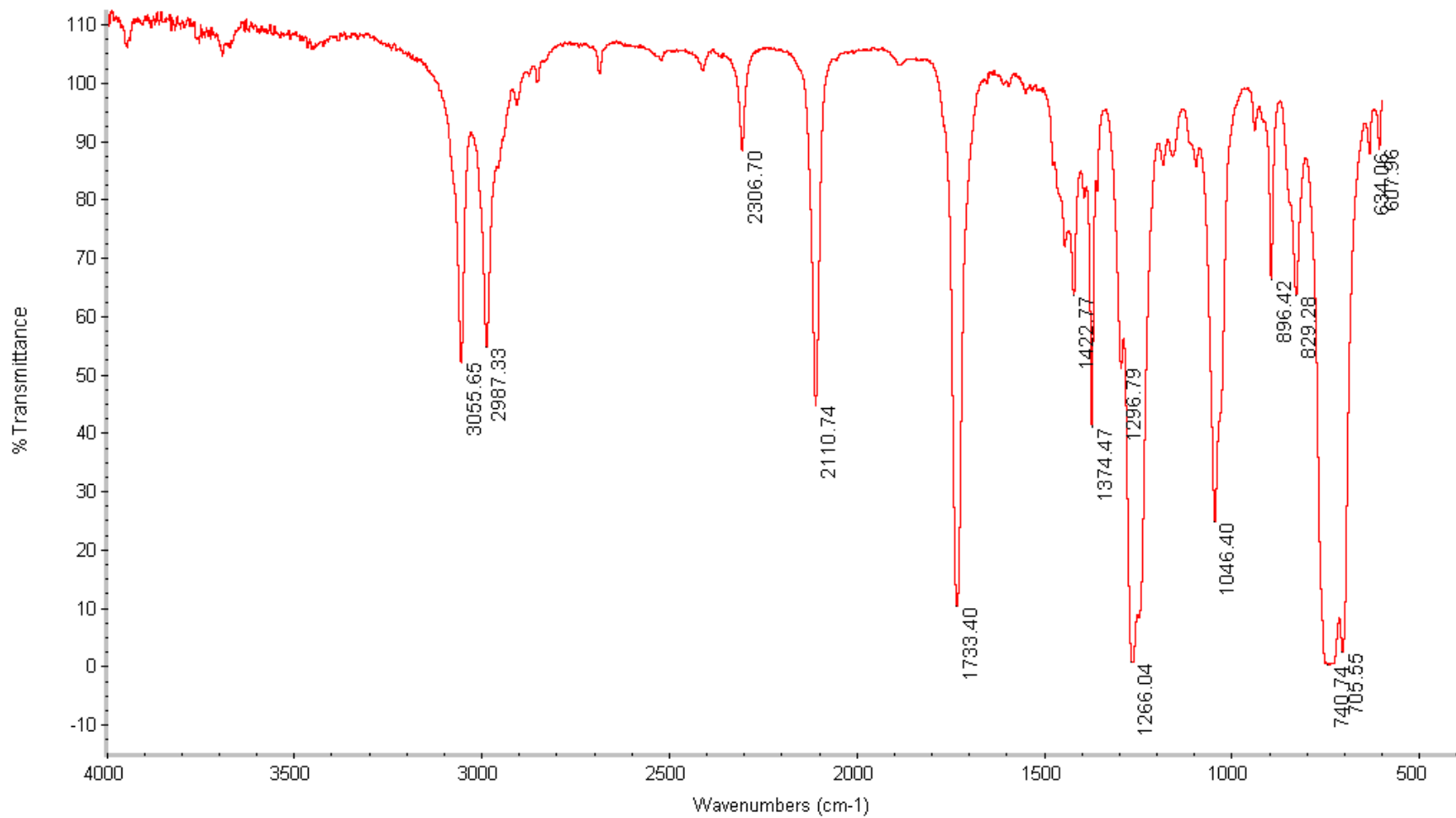


Figure 75: Infrared spectrum of dimethyl(diazomethyl)phosphonate (**27**).

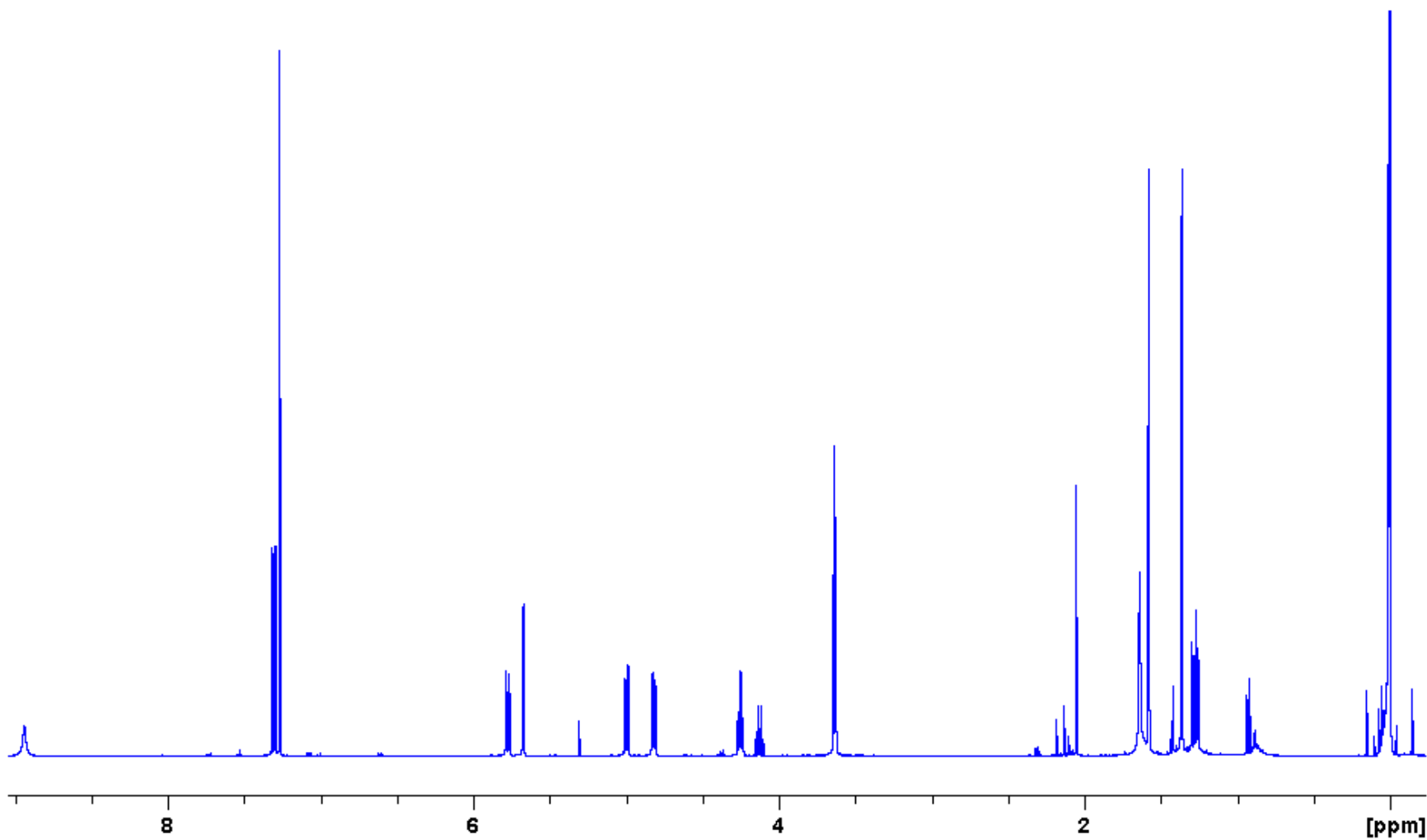


Figure 76: 400 MHz ^1H spectrum of 5'-azido-5'-deoxy-2',3'-O-isopropylidene uridine (**40**).

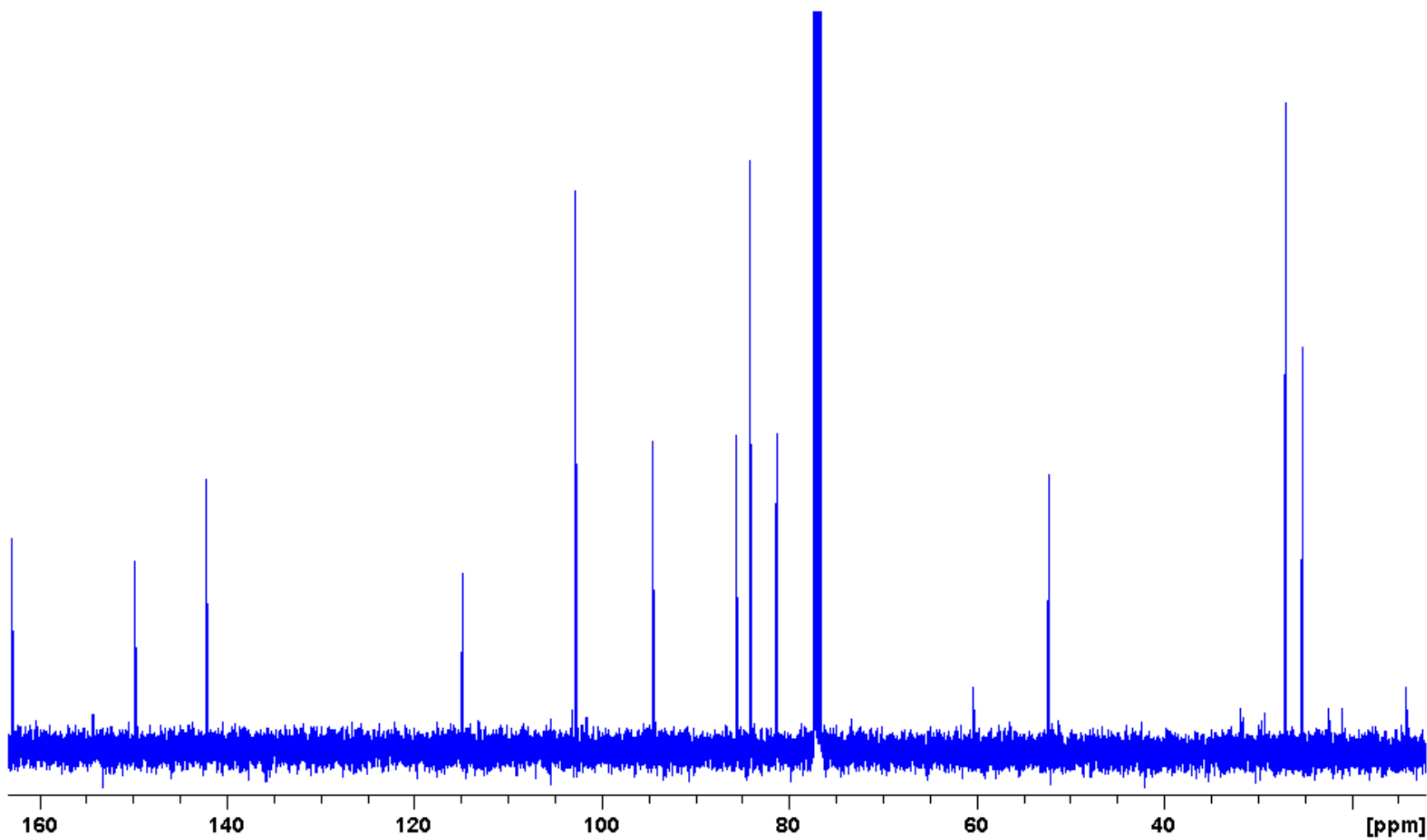


Figure 77: 100 MHz ^{13}C spectrum of 5'-azido-5'-deoxy-2',3'-*O*-isopropylidene uridine (**40**).

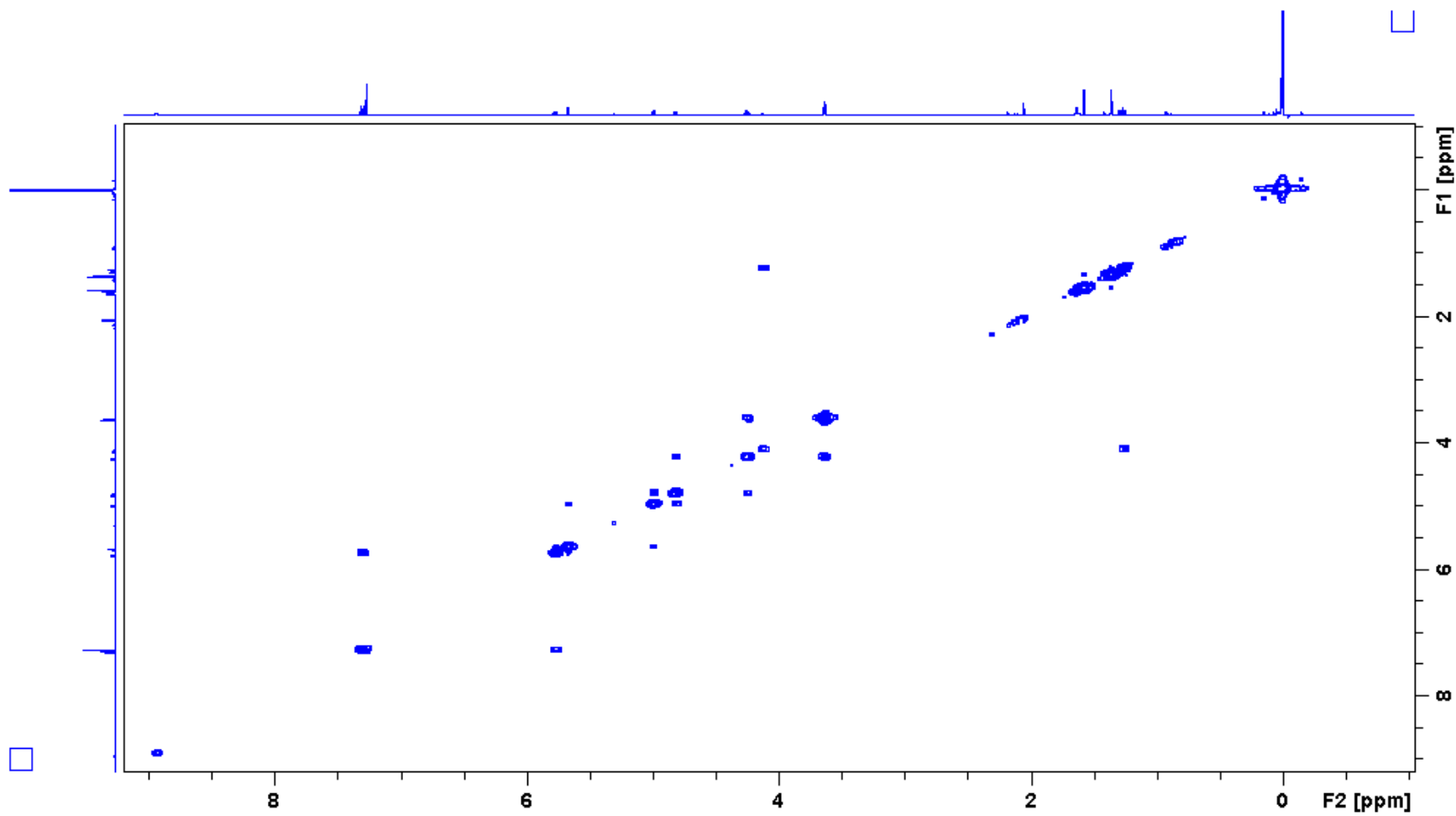


Figure 78: 400 MHz ^1H - ^1H COSY spectrum of 5'-azido-5'-deoxy-2',3'-*O*-isopropylidene uridine (**40**).

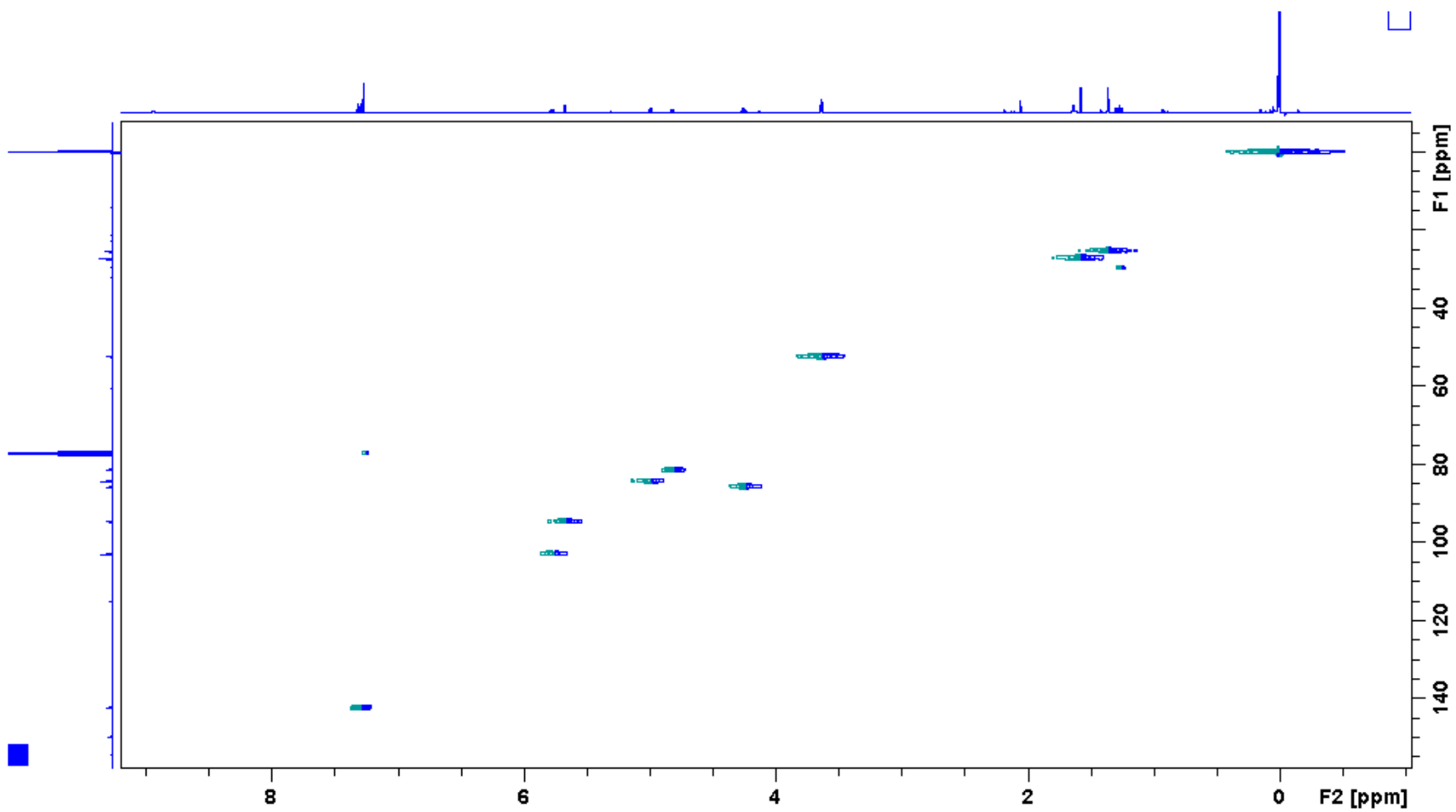


Figure 79: 400 MHz ^1H - ^{13}C HSQC spectrum of 5'-azido-5'-deoxy-2',3'-*O*-isopropylidene uridine (**40**).

Display Report

Analysis Info

Method XQ Default.ms Instrument Esquire-LC_00135

Acquisition Parameter

Ion Source Type	ESI	Mass Range Mode	Std/Normal	Ion Polarity	Positive	Alternating Ion Polarity	n/a
Scan Begin	100.00 m/z	Scan End	400.00 m/z	Averages	5 Spectra	Accumulation Time	14952 μ s
Capillary Exit	105.8 Volt	Skim 1	33.2 Volt	Trap Drive	46.8	Auto MS/MS	Off

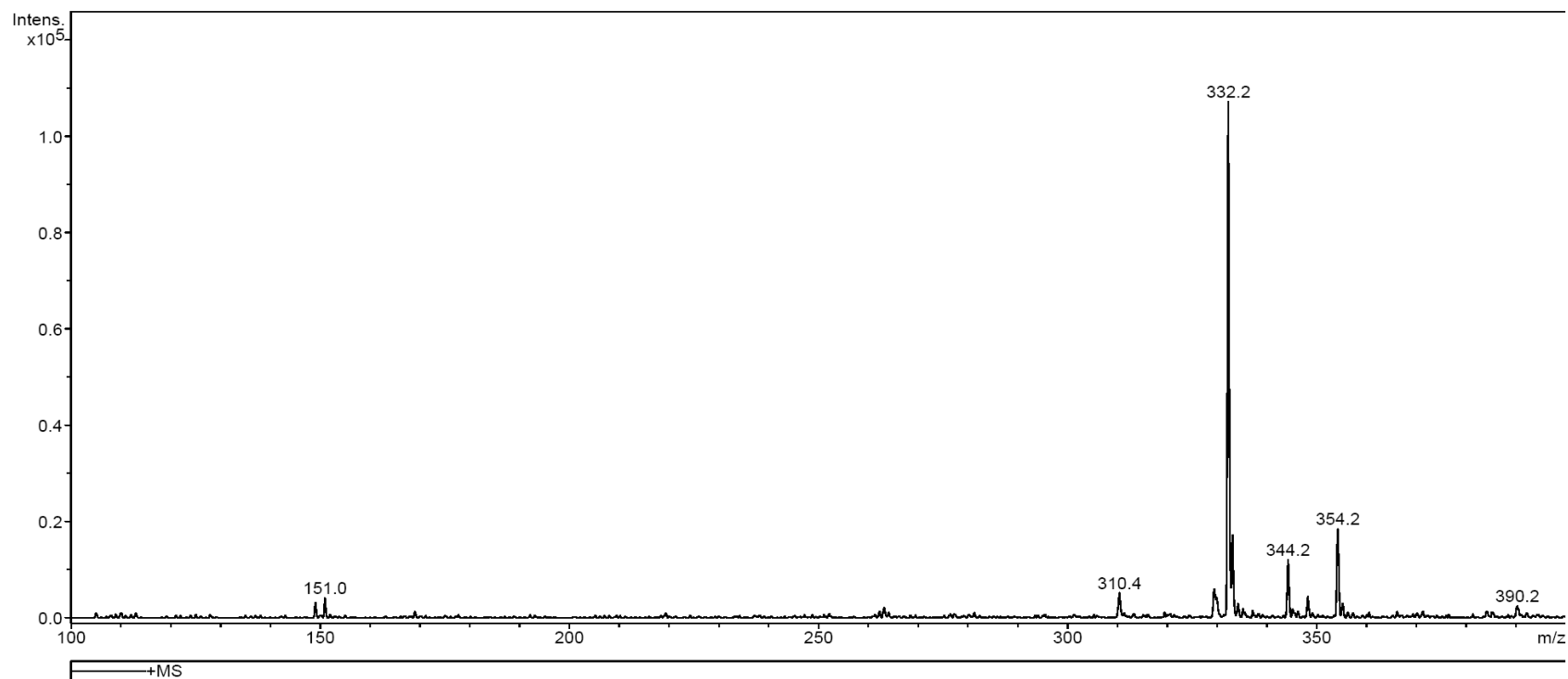


Figure 80: Mass spectrum of 5'-azido-5'-deoxy-2',3'-O-isopropylidene uridine (**40**).

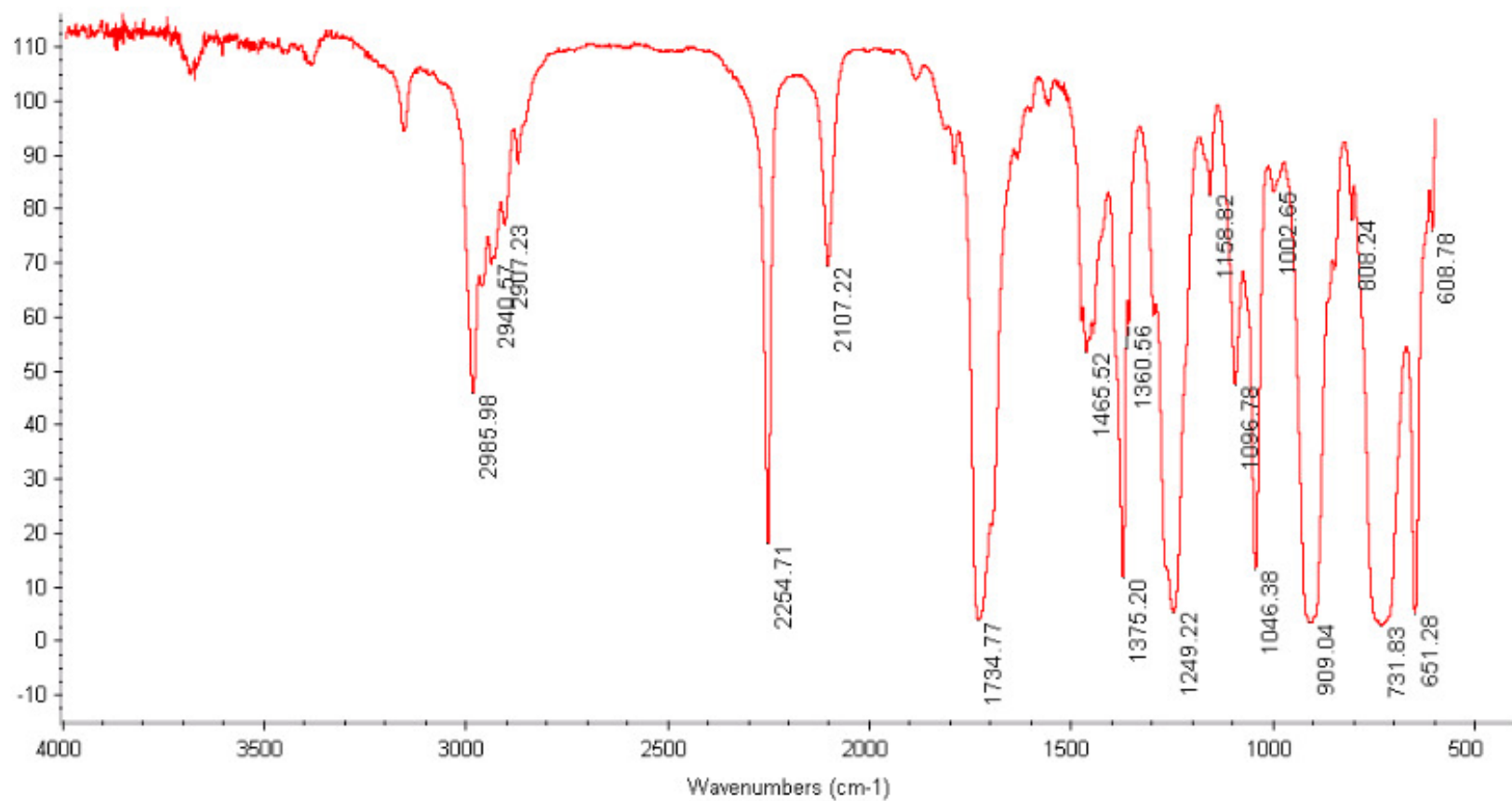


Figure 81: Infrared spectrum of 5'-azido-5'-deoxy-2',3'-*O*-isopropylidene uridine (**40**).

Display Report

Analysis Info

Method XQ Default.ms Instrument Esquire-LC_00135

Acquisition Parameter

Ion Source Type	ESI	Mass Range Mode	Std/Normal	Ion Polarity	Positive	Alternating Ion Polarity	n/a
Scan Begin	300.00 m/z	Scan End	900.00 m/z	Averages	10 Spectra	Accumulation Time	18999 μ s
Capillary Exit	128.3 Volt	Skim 1	48.3 Volt	Trap Drive	68.9	Auto MS/MS	Off

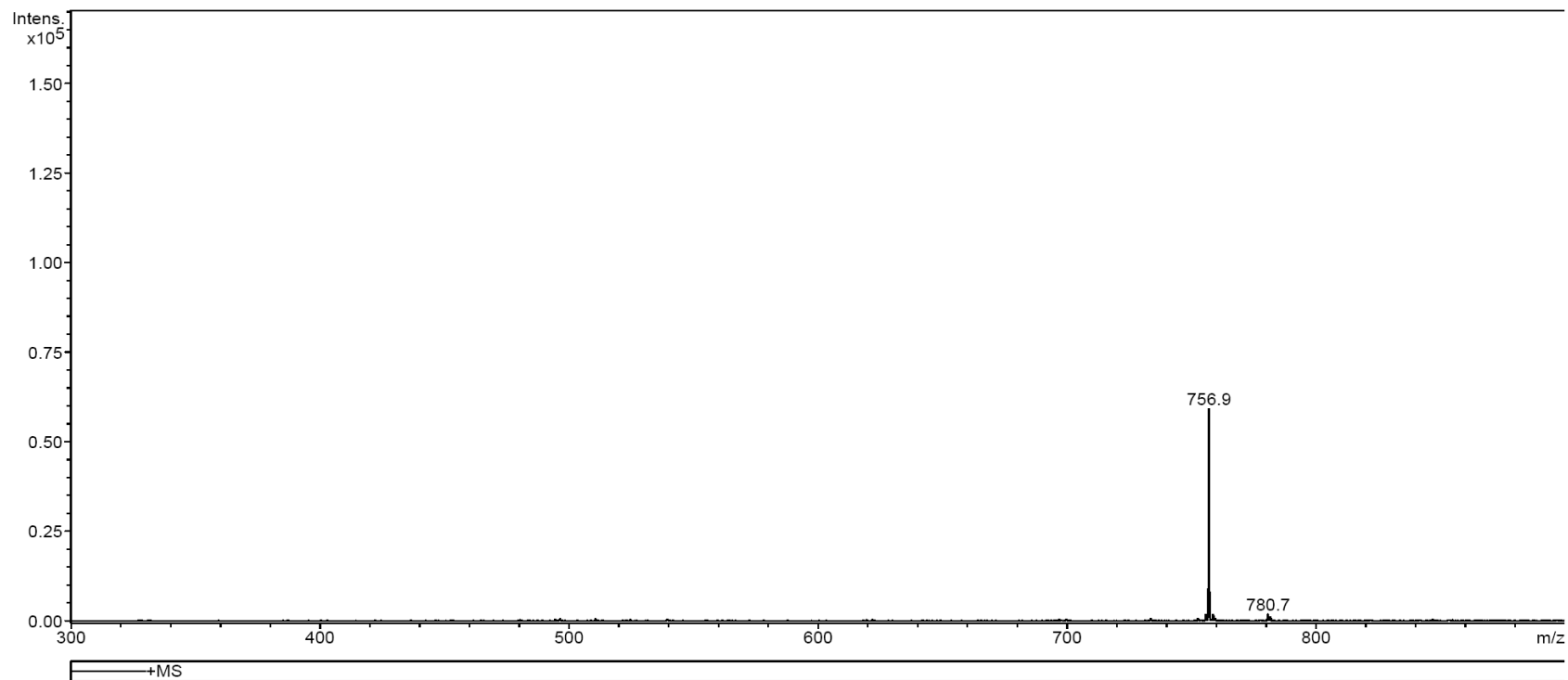


Figure 82: Mass spectrum of bis(1,2,3-triazole) **41**.

Display Report

Analysis Info

Method XQ Default.ms Instrument Esquire-LC_00135

Acquisition Parameter

Ion Source Type	ESI	Mass Range Mode	Std/Normal	Ion Polarity	Positive	Alternating Ion Polarity	n/a
Scan Begin	100.00 m/z	Scan End	400.00 m/z	Averages	10 Spectra	Accumulation Time	11180 μ s
Capillary Exit	101.6 Volt	Skim 1	30.3 Volt	Trap Drive	44.9	Auto MS/MS	Off

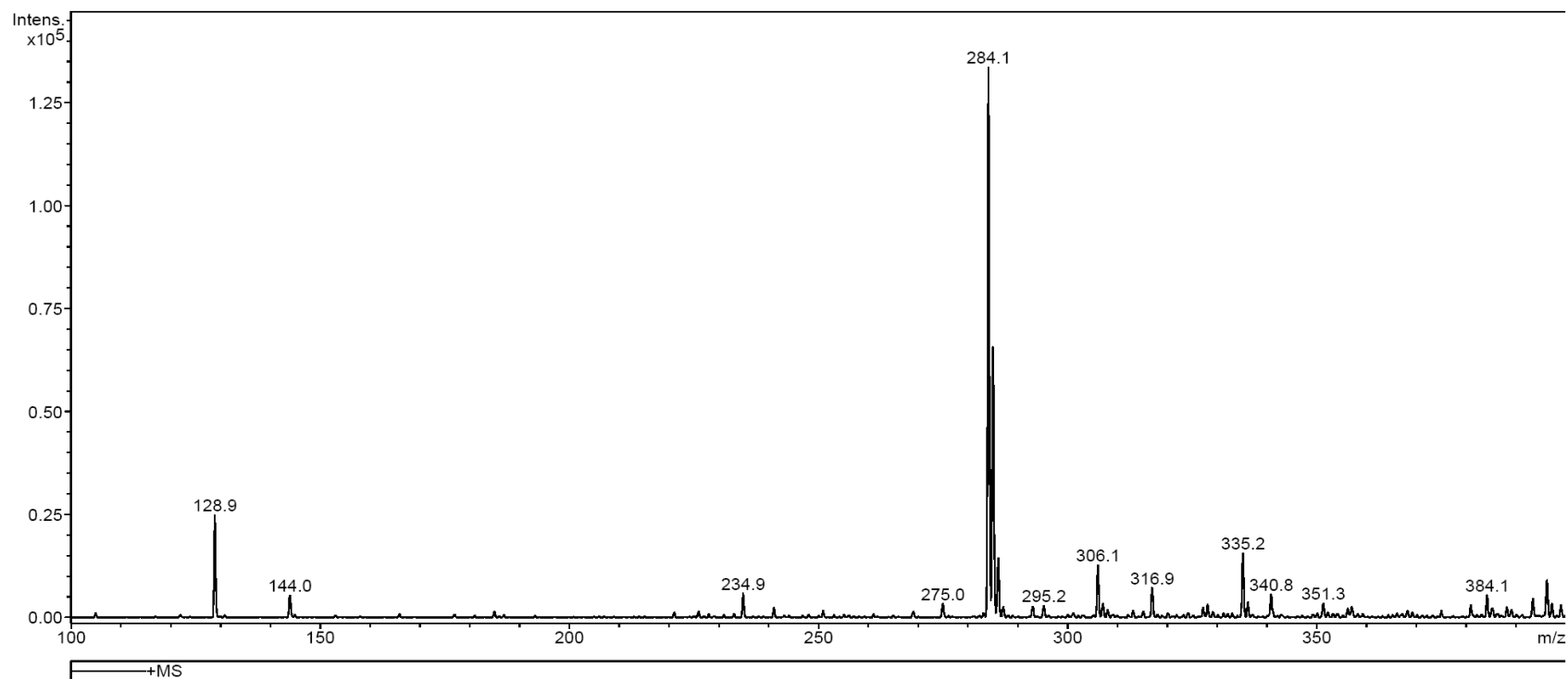


Figure 83: Mass spectrum of deprotected triazole **44**.

Display Report

Analysis Info

Method XQ Default.ms Instrument Esquire-LC_00135

Acquisition Parameter

Ion Source Type	ESI	Mass Range Mode	Std/Normal	Ion Polarity	Positive	Alternating Ion Polarity	n/a
Scan Begin	100.00 m/z	Scan End	450.00 m/z	Averages	10 Spectra	Accumulation Time	9184 μ s
Capillary Exit	101.5 Volt	Skim 1	30.1 Volt	Trap Drive	44.9	Auto MS/MS	Off

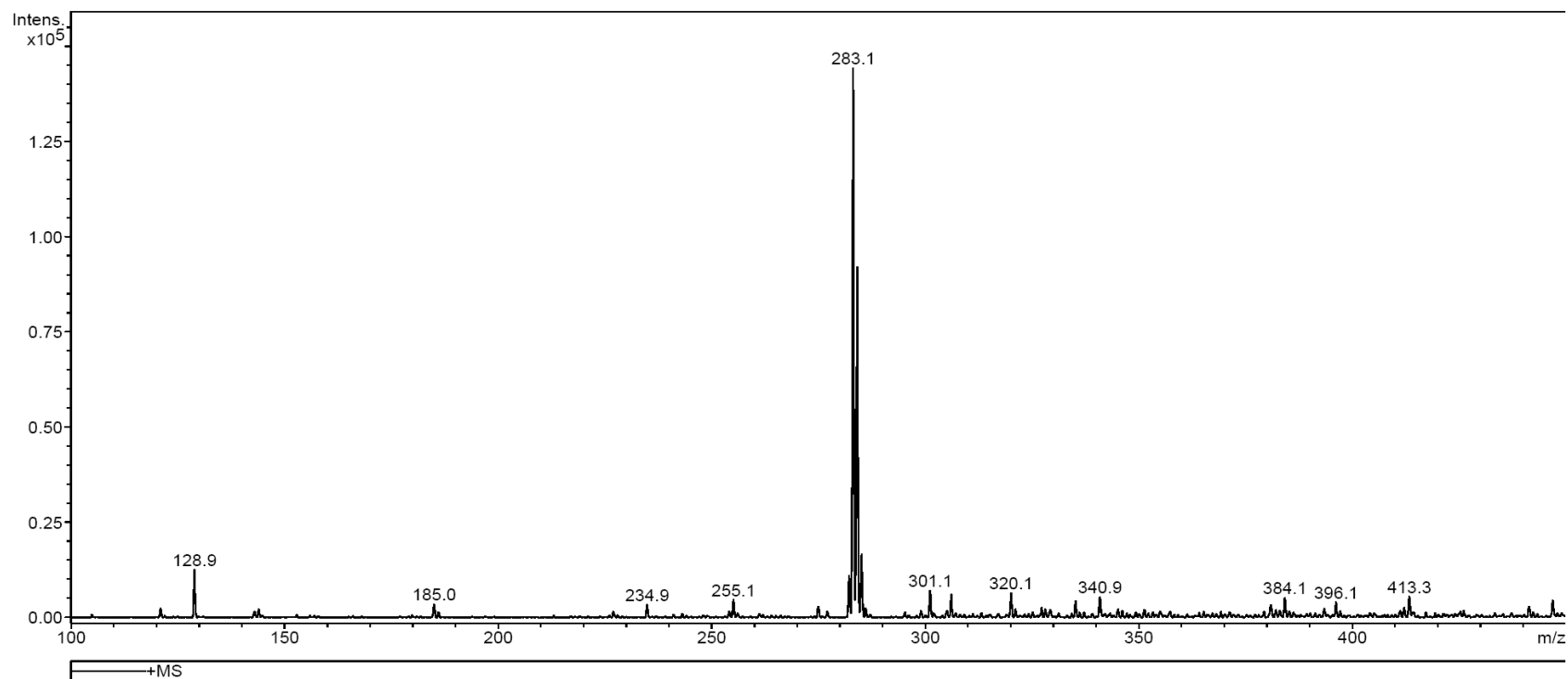


Figure 84: Mass spectrum of deprotected aldehyde **45**.

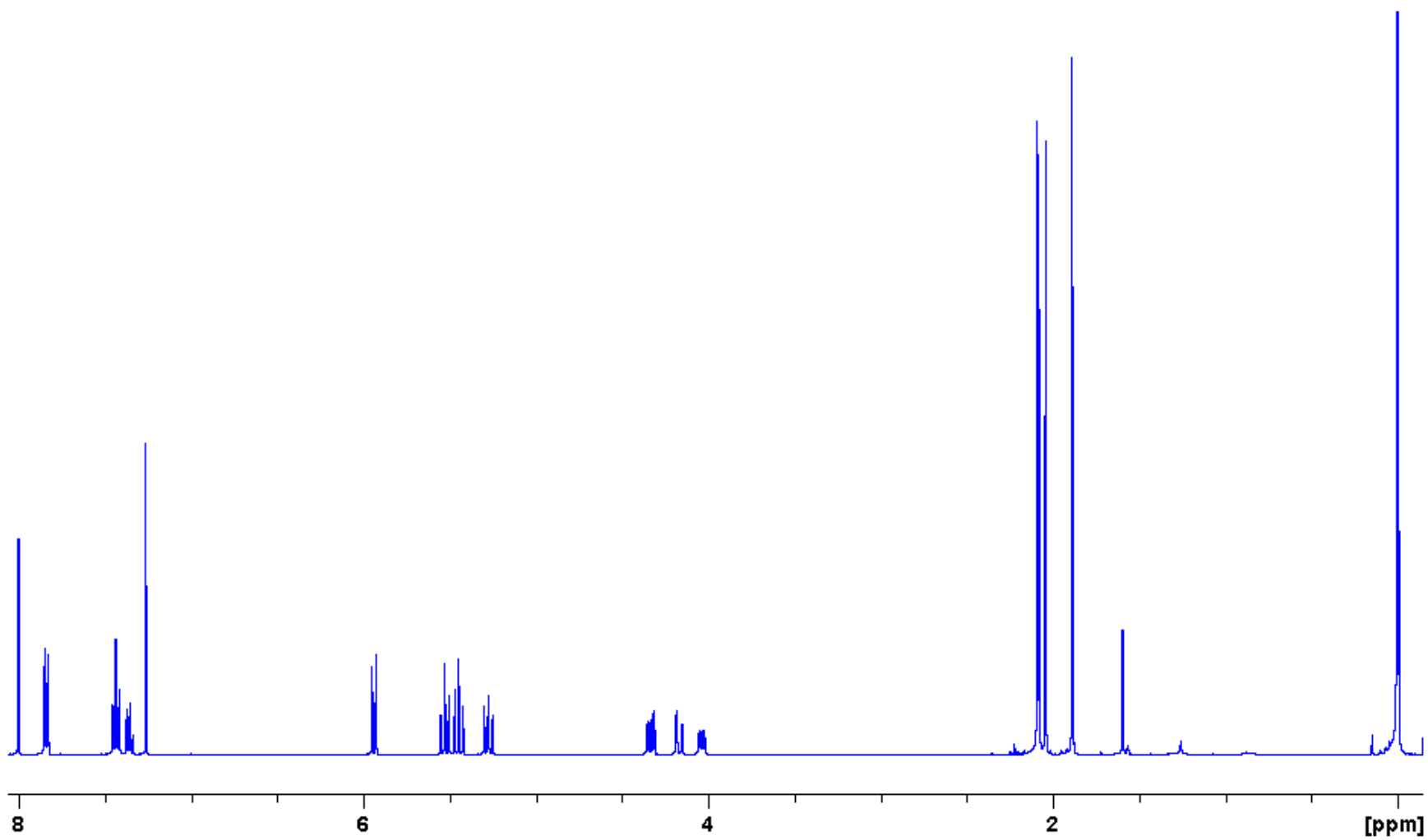


Figure 85: 400 MHz ¹H spectrum of phenyl triazole **46**.

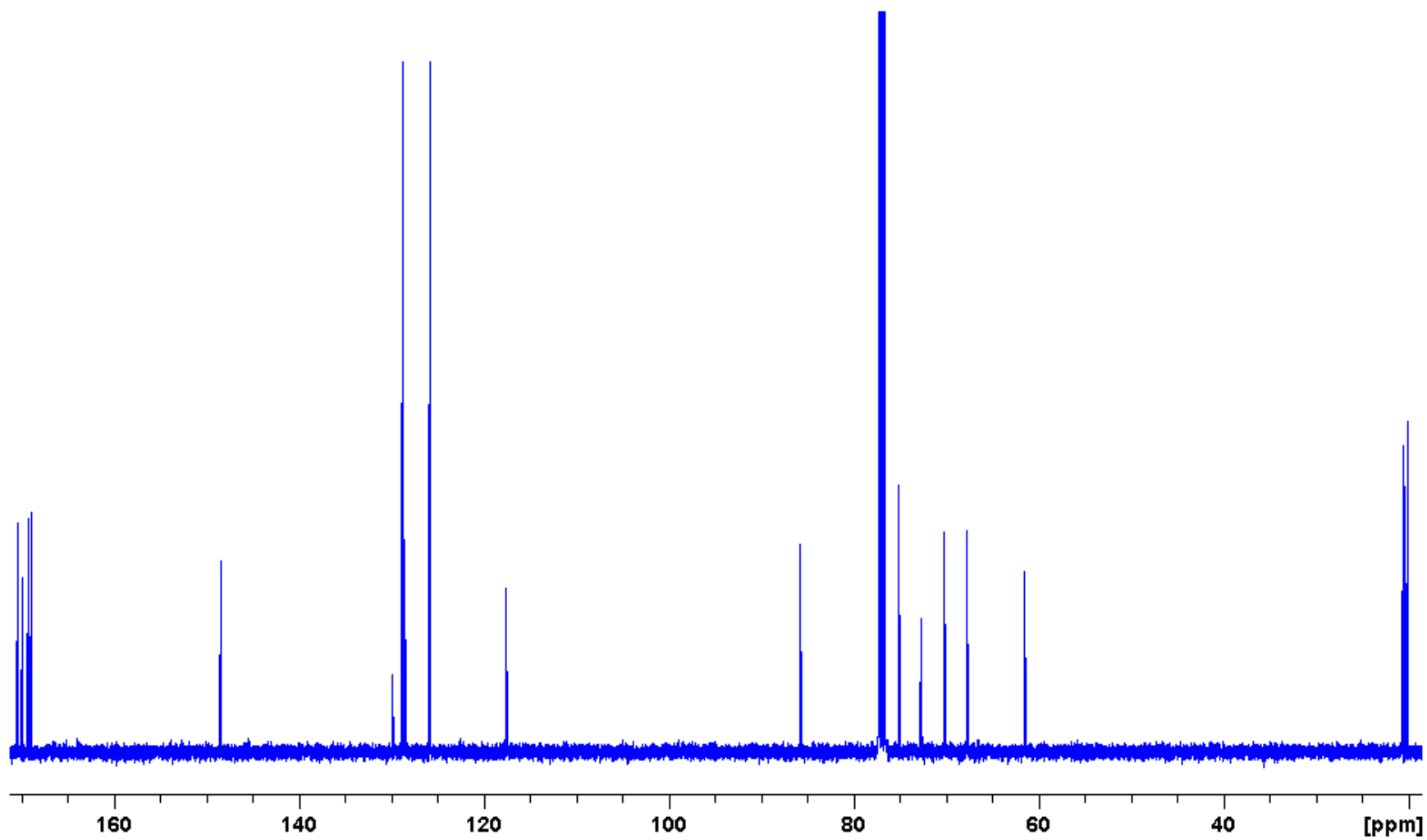


Figure 86: 100 MHz ^{13}C spectrum of phenyl triazole **46**.

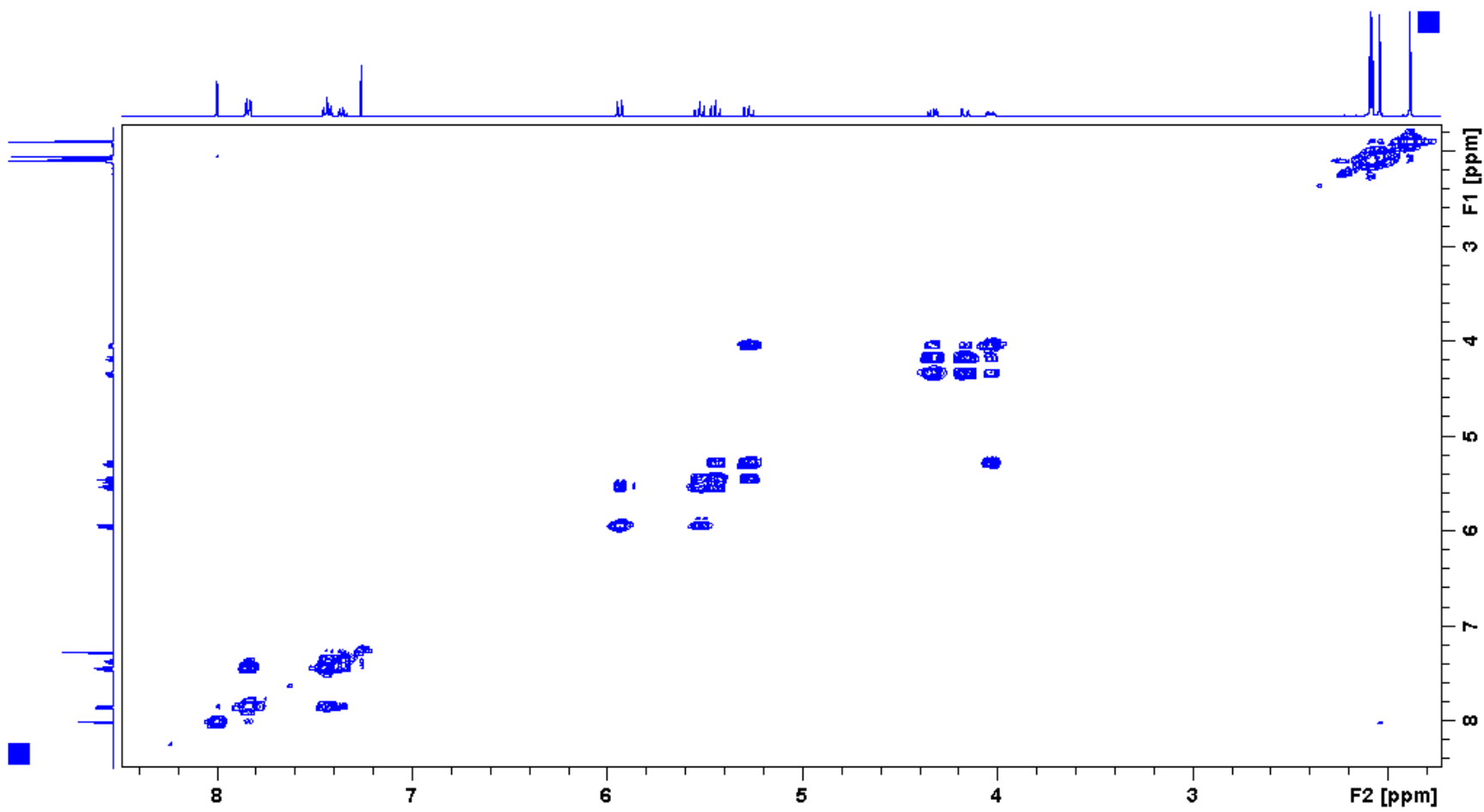


Figure 87: 400 MHz ^1H - ^{13}C HSQC spectrum of phenyl triazole 46.

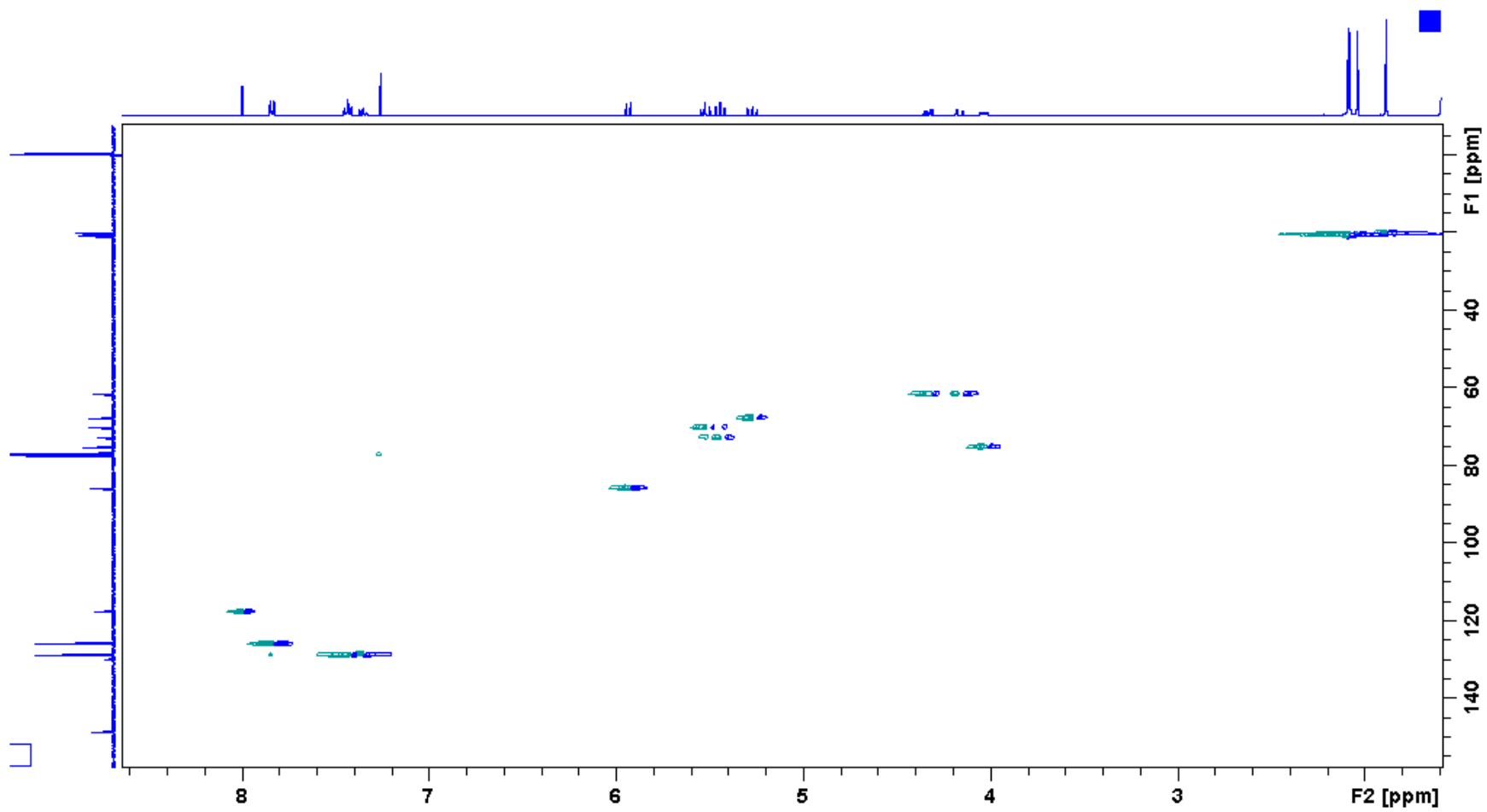


Figure 88: 400 MHz ¹H-¹H COSY spectrum of phenyl triazole **46**.

Display Report

Analysis Info

Method XQ Default.ms Instrument Esquire-LC_00135

Acquisition Parameter

Ion Source Type	ESI	Mass Range Mode	Std/Normal	Ion Polarity	Positive	Alternating Ion Polarity	n/a
Scan Begin	200.00 m/z	Scan End	600.00 m/z	Averages	5 Spectra	Accumulation Time	29004 μ s
Capillary Exit	119.7 Volt	Skim 1	42.8 Volt	Trap Drive	53.7	Auto MS/MS	Off

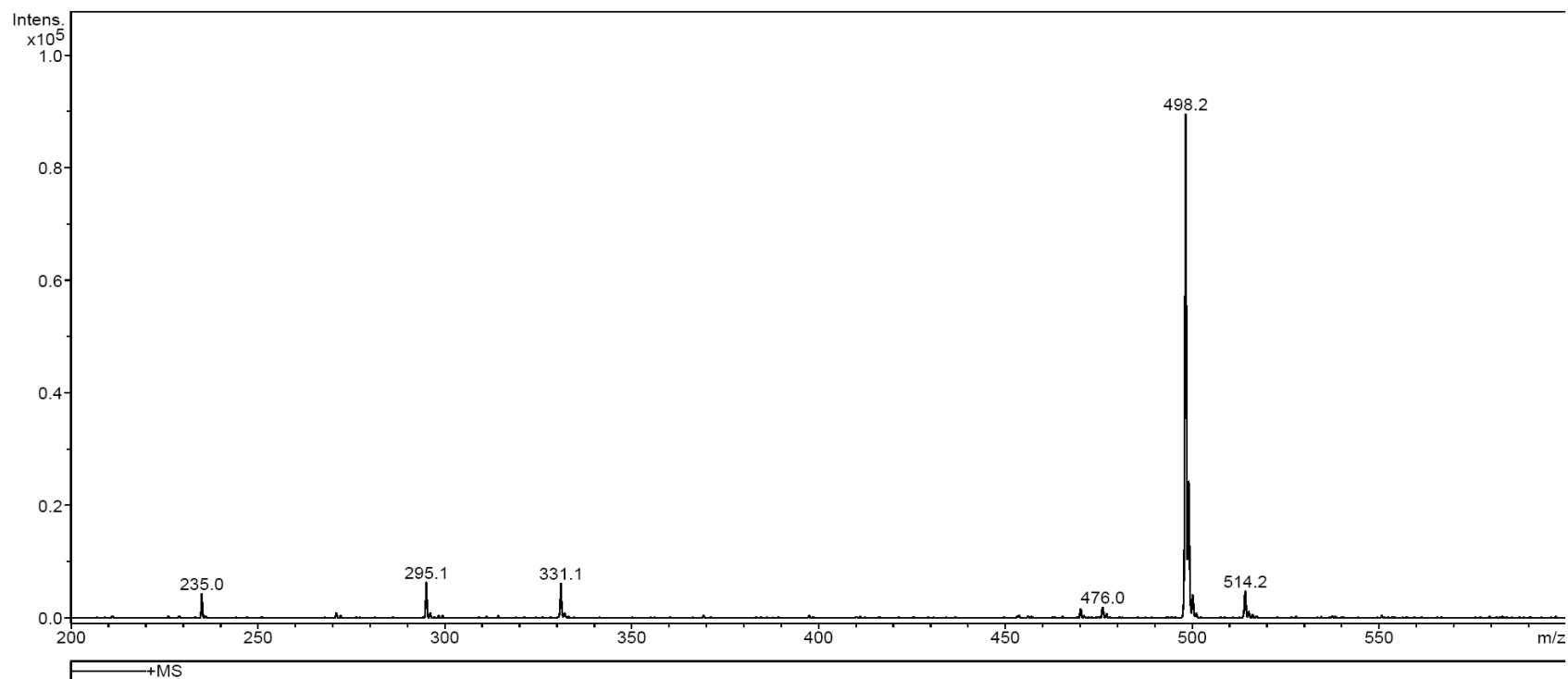


Figure 89: Mass spectrum of phenyl triazole **46**.

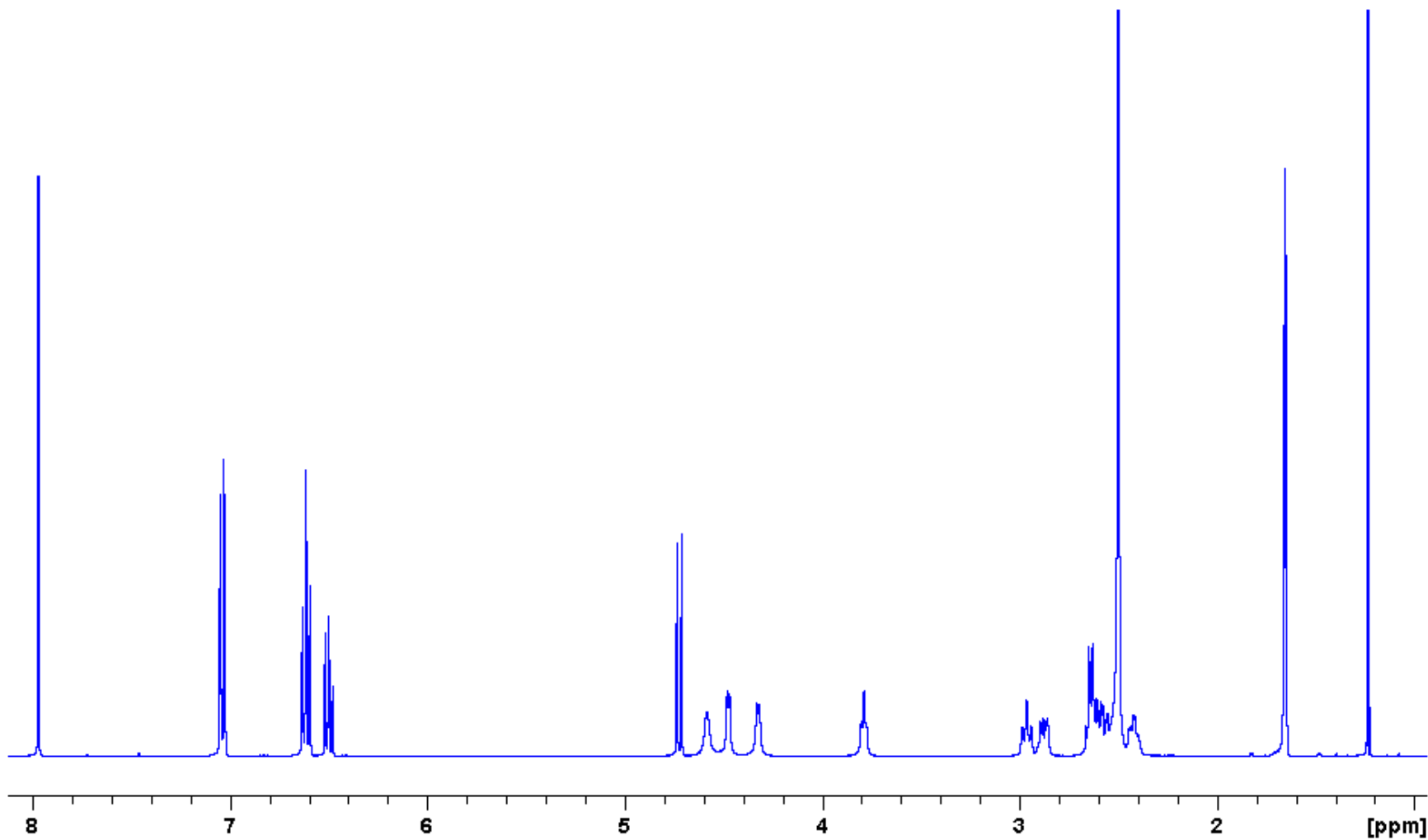


Figure 90: 400 MHz ¹H spectrum of deprotected phenyl triazole 47.

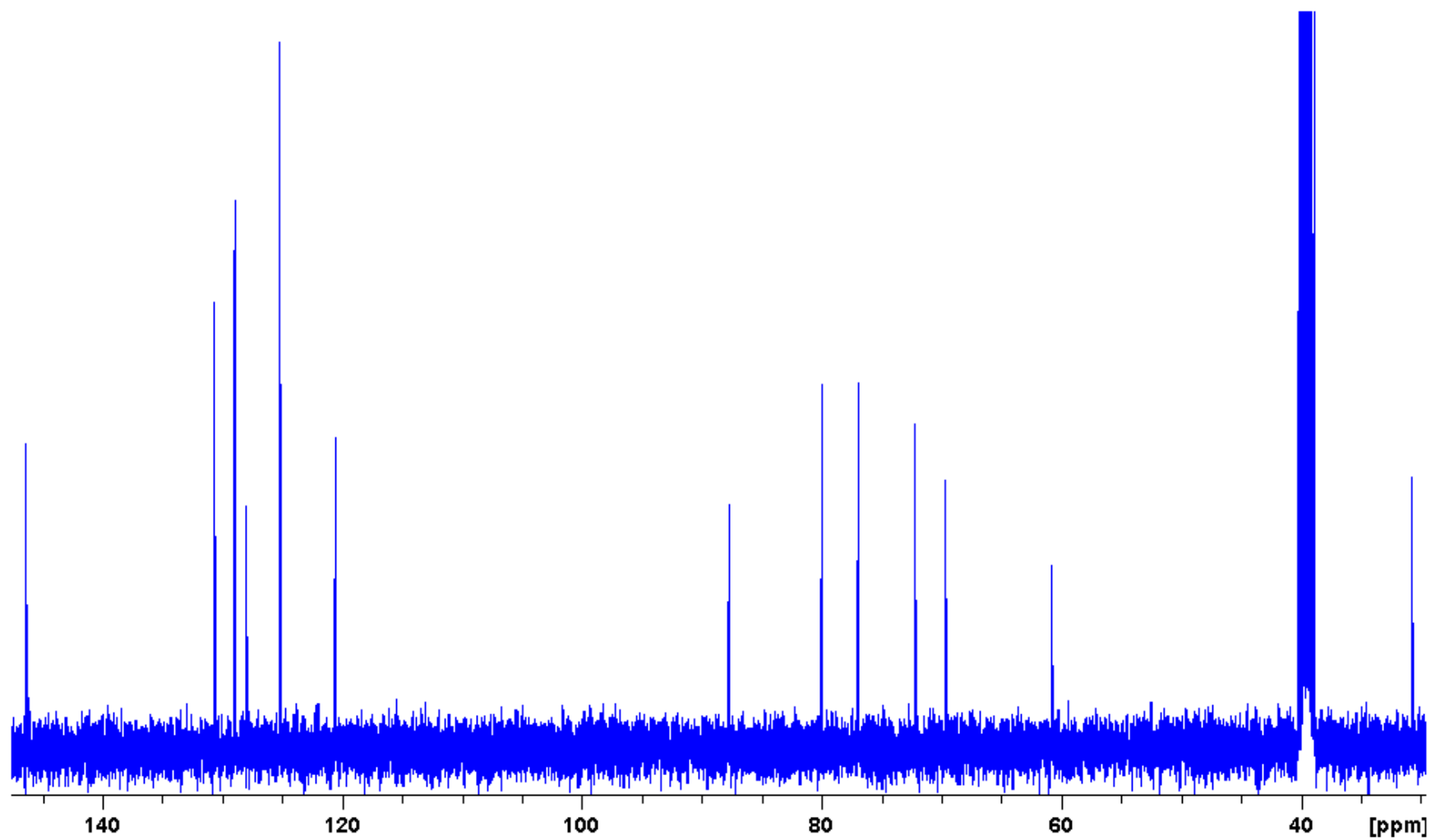


Figure 91: 100 MHz ^{13}C spectrum of deprotected phenyl triazole 47.

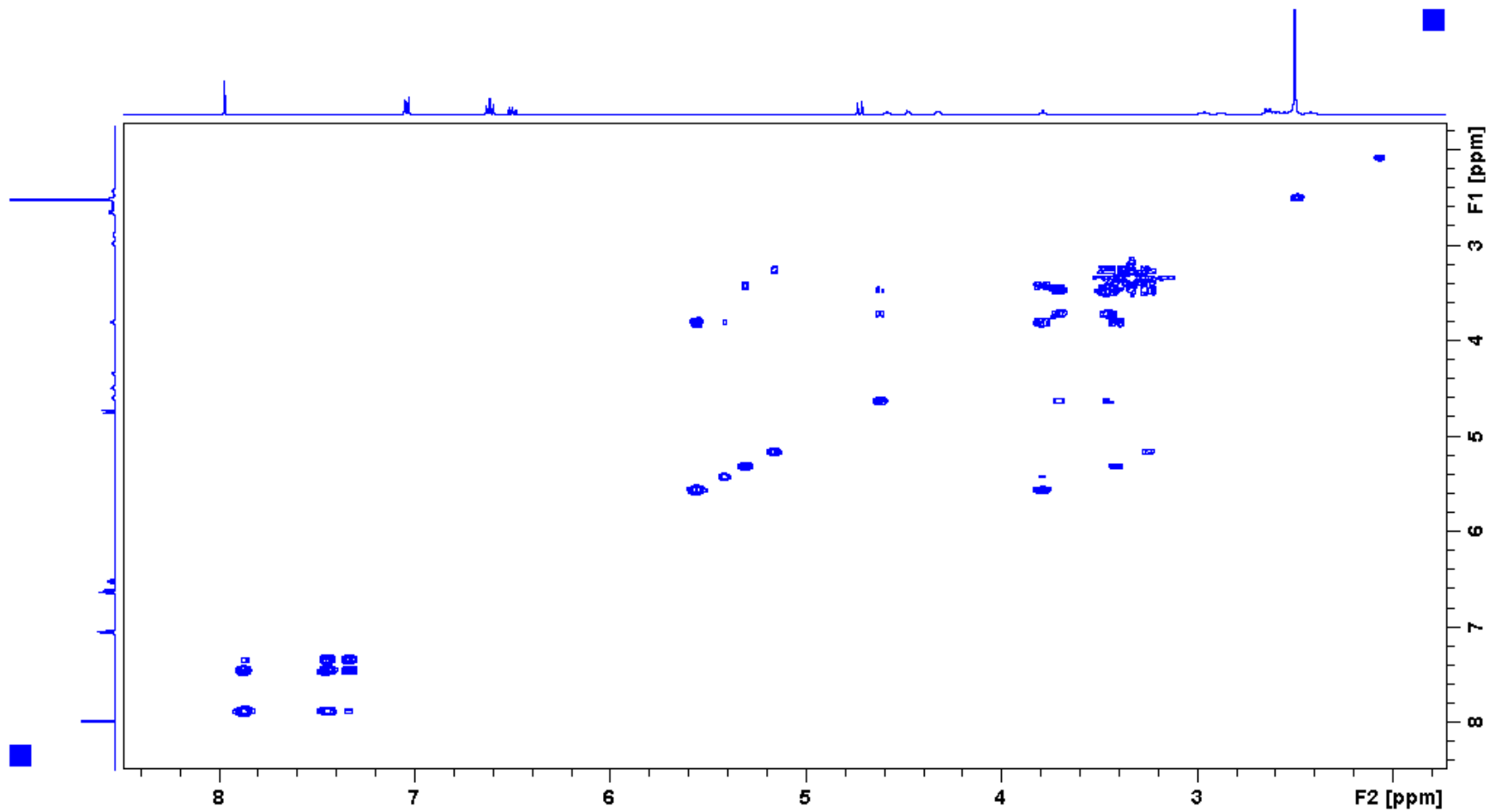


Figure 92: 400 MHz ¹H-¹H COSY spectrum of deprotected phenyl triazole 47.

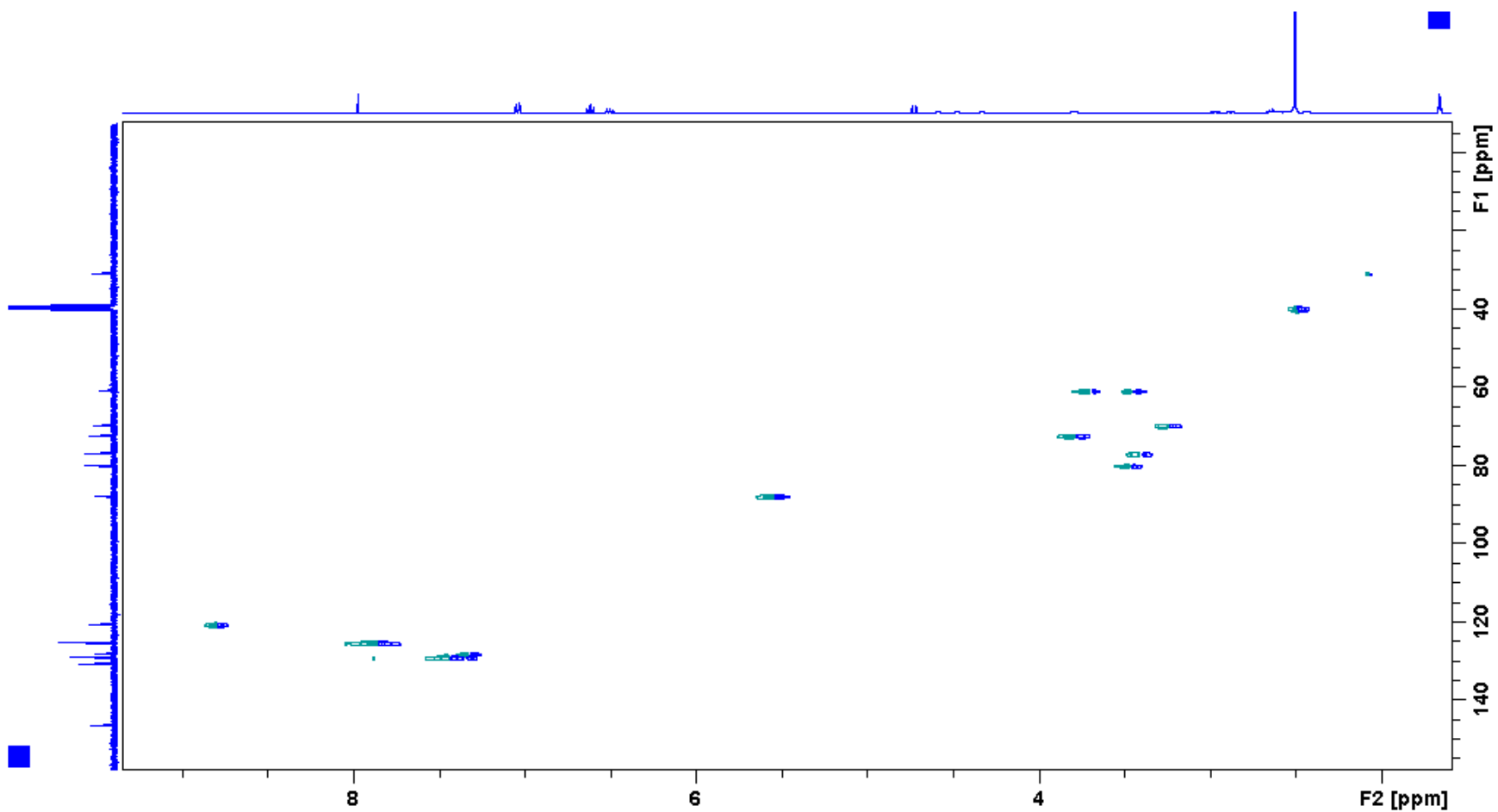


Figure 93: 400 MHz ^1H - ^{13}C HSQC spectrum of deprotected phenyl triazole **47**.

Display Report

Analysis Info

Method XQ Default.ms Instrument Esquire-LC_00135

Acquisition Parameter

Ion Source Type	ESI	Mass Range Mode	Std/Normal	Ion Polarity	Positive	Alternating Ion Polarity	n/a
Scan Begin	100.00 m/z	Scan End	600.00 m/z	Averages	10 Spectra	Accumulation Time	24066 μ s
Capillary Exit	106.8 Volt	Skim 1	33.9 Volt	Trap Drive	47.2	Auto MS/MS	Off

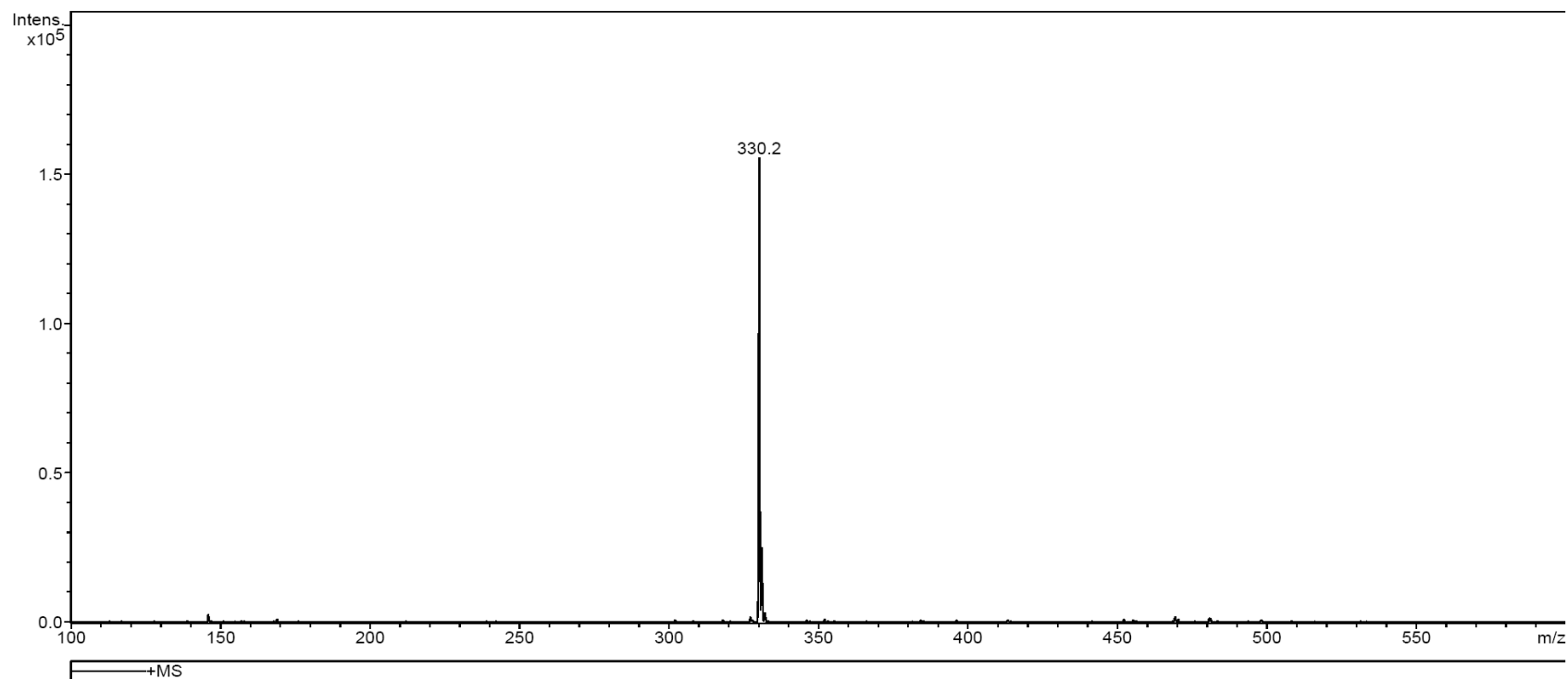


Figure 94: Mass spectrum of deprotected phenyl triazole **47**.

Display Report

Analysis Info

Method XQ Default.ms Instrument Esquire-LC_00135

Acquisition Parameter

Ion Source Type	ESI	Mass Range Mode	Std/Normal	Ion Polarity	Positive	Alternating Ion Polarity	n/a
Scan Begin	100.00 m/z	Scan End	450.00 m/z	Averages	10 Spectra	Accumulation Time	10920 μ s
Capillary Exit	96.5 Volt	Skim 1	26.4 Volt	Trap Drive	42.8	Auto MS/MS	Off

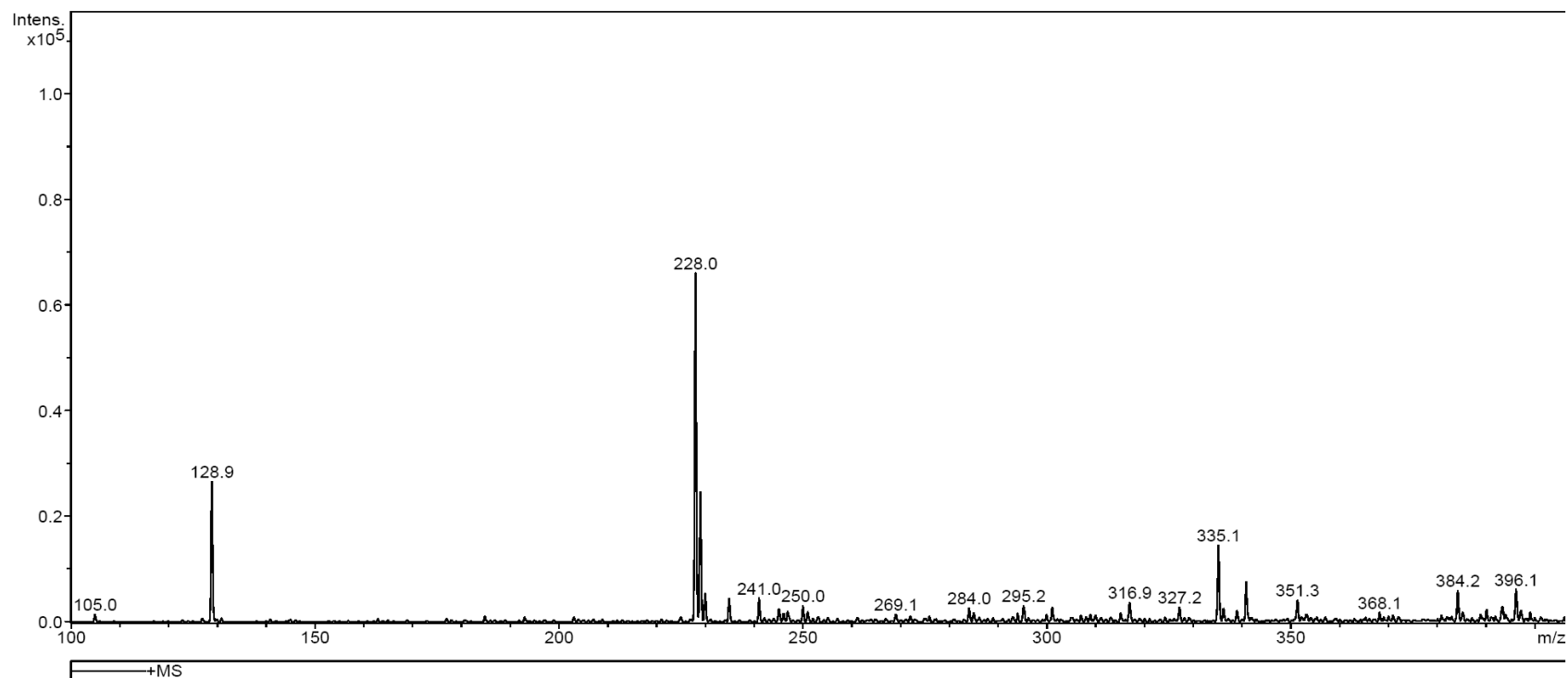


Figure 95: Mass spectrum of deprotected glucosyl azide **48**.

Appendix B

X-Ray Crystallography

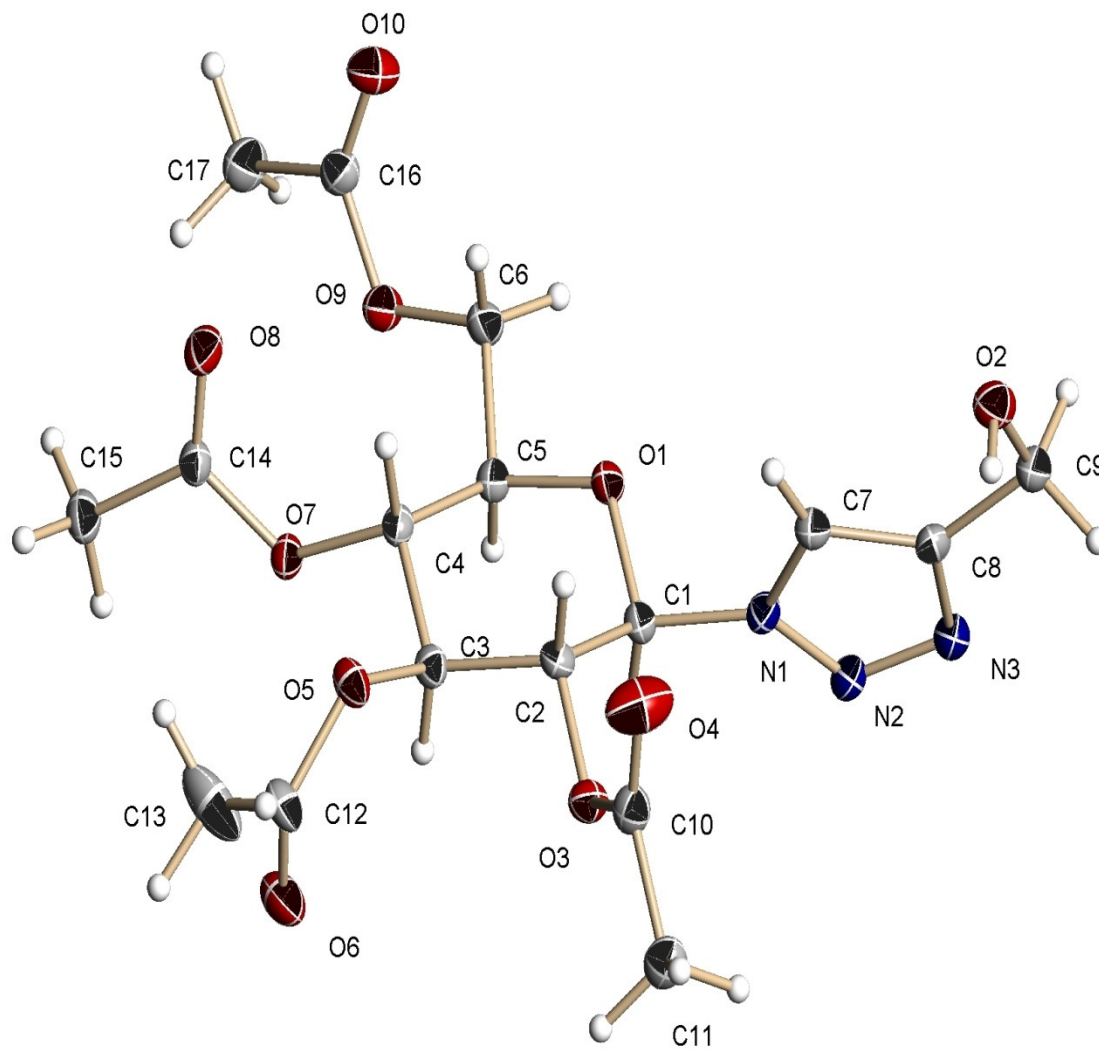


Figure 96: X-Ray crystal structure of glucosyl triazole **8**.

Table 1. Crystal data and structure refinement for 08mz001_0m:

Identification code: 08mz001_0m
 Empirical formula: C17 H23 N3 O10
 Formula weight: 429.38
 Temperature: 100(2) K
 Wavelength: 0.71073 Å
 Crystal system: Monoclinic
 Space group: P2₁
 Unit cell dimensions:
 a = 7.4933(8) Å, α = 90°
 b = 9.2787(10) Å, β = 104.261(2)°
 c = 14.7649(15) Å, γ = 90°
 Volume, Z: 994.94(18) Å³, 2
 Density (calculated): 1.433 Mg/m³
 Absorption coefficient: 0.119 mm⁻¹
 F(000): 452
 Crystal size: 0.70 × 0.22 × 0.14 mm
 Crystal shape, colour: needle, colourless
 θ range for data collection: 2.62 to 28.28°
 Limiting indices: $-9 \leq h \leq 9$, $-12 \leq k \leq 12$, $-19 \leq l \leq 19$
 Reflections collected: 10159
 Independent reflections: 2619 (R(int) = 0.0217)
 Completeness to $\theta = 28.28^\circ$: 100.0 %
 Absorption correction: multi-scan
 Max. and min. transmission: 0.983 and 0.909
 Refinement method: Full-matrix least-squares on F^2
 Data / restraints / parameters: 2619 / 1 / 276
 Goodness-of-fit on F^2 : 1.054
 Final R indices [$I > 2\sigma(I)$]: R1 = 0.0297, wR2 = 0.0752
 R indices (all data): R1 = 0.0314, wR2 = 0.0769
 Largest diff. peak and hole: 0.291 and -0.175 e × Å⁻³

Refinement of F^2 against ALL reflections. The weighted R-factor wR and goodness of fit are based on F^2 , conventional R-factors R are based on F , with F set to zero for negative F^2 . The threshold expression of $F^2 > 2\sigma(F^2)$ is used only for calculating R-factors

Treatment of hydrogen atoms:

All hydrogen atoms were placed in calculated positions and were refined

with an isotropic displacement parameter 1.5 (methyl) or 1.2 times (all others) that of the adjacent carbon atom.

Table 2. Atomic coordinates [$\times 10^4$] and equivalent isotropic displacement parameters [$\text{\AA}^2 \times 10^3$] for 08mz001_0m. U(eq) is defined as one third of the trace of the orthogonalized U_{ij} tensor.

	x	y	z	U(eq)
C(1)	6481(2)	9141(2)	932(1)	17(1)
C(2)	5068(2)	9019(2)	1517(1)	17(1)
C(3)	6129(2)	8952(2)	2538(1)	16(1)
C(4)	7517(2)	7725(2)	2705(1)	16(1)
C(5)	8733(2)	7771(2)	2004(1)	18(1)
C(6)	9785(3)	6386(2)	1946(1)	22(1)
C(7)	4452(2)	8279(2)	-593(1)	19(1)
C(8)	4334(2)	8729(2)	-1490(1)	19(1)
C(9)	3308(3)	8059(2)	-2393(1)	23(1)
C(10)	2124(2)	10142(2)	962(1)	21(1)
C(11)	1194(3)	11578(2)	831(1)	25(1)
C(12)	4592(3)	9643(2)	3720(1)	23(1)
C(13)	3128(3)	9145(3)	4177(2)	43(1)
C(14)	8926(2)	6831(2)	4242(1)	18(1)
C(15)	9978(3)	7271(2)	5207(1)	24(1)
C(16)	11883(2)	4897(2)	2986(1)	21(1)
C(17)	13553(3)	4889(2)	3787(1)	29(1)
N(1)	5644(2)	9216(2)	-58(1)	17(1)
N(2)	6247(2)	10206(2)	-590(1)	21(1)
N(3)	5429(2)	9918(2)	-1463(1)	22(1)
O(1)	7569(2)	7875(1)	1077(1)	18(1)
O(2)	1960(2)	7059(2)	-2249(1)	24(1)
O(3)	3955(2)	10298(2)	1385(1)	19(1)
O(4)	1420(2)	8991(2)	743(1)	39(1)
O(5)	4813(2)	8648(2)	3083(1)	20(1)
O(6)	5467(2)	10741(2)	3886(1)	30(1)
O(7)	8647(2)	7958(1)	3643(1)	18(1)
O(8)	8379(2)	5629(2)	4020(1)	28(1)
O(9)	11242(2)	6241(2)	2782(1)	21(1)
O(10)	11179(2)	3836(2)	2577(1)	29(1)

All esds (except the esd in the dihedral angle between two l.s. planes) are estimated using the full covariance matrix. The cell esds are taken into account individually in the estimation of esds in distances, angles and torsion angles; correlations between esds in cell parameters are only used when they are defined by crystal symmetry. An approximate (isotropic) treatment of cell esds is used for estimating esds involving l.s. planes.

Table 3. Bond lengths [\AA] and angles [deg] for 08mz001_0m.

C(1)-O(1)	1.416(2)	C(17)-H(17B)	0.9800
C(1)-N(1)	1.443(2)	C(17)-H(17C)	0.9800
C(1)-C(2)	1.526(2)	N(1)-N(2)	1.357(2)
C(1)-H(1)	1.0000	N(2)-N(3)	1.311(2)
C(2)-O(3)	1.435(2)	O(2)-H(2A)	0.8400
C(2)-C(3)	1.523(2)		
C(2)-H(2)	1.0000	O(1)-C(1)-N(1)	106.46(13)
C(3)-O(5)	1.445(2)	O(1)-C(1)-C(2)	107.84(14)
C(3)-C(4)	1.521(2)	N(1)-C(1)-C(2)	112.81(14)
C(3)-H(3)	1.0000	O(1)-C(1)-H(1)	109.9
C(4)-O(7)		N(1)-C(1)-H(1)	109.9
1.4504(19)		C(2)-C(1)-H(1)	109.9
C(4)-C(5)	1.538(2)	O(3)-C(2)-C(3)	108.18(13)
C(4)-H(4)	1.0000	O(3)-C(2)-C(1)	108.85(14)
C(5)-O(1)		C(3)-C(2)-C(1)	107.31(13)
1.4333(19)		O(3)-C(2)-H(2)	110.8
C(5)-C(6)	1.521(3)	C(3)-C(2)-H(2)	110.8
C(5)-H(5)	1.0000	C(1)-C(2)-H(2)	110.8
C(6)-O(9)	1.439(2)	O(5)-C(3)-C(4)	107.27(14)
C(6)-H(6A)	0.9900	O(5)-C(3)-C(2)	107.32(13)
C(6)-H(6B)	0.9900	C(4)-C(3)-C(2)	111.10(14)
C(7)-N(1)	1.352(2)	O(5)-C(3)-H(3)	110.4
C(7)-C(8)	1.370(2)	C(4)-C(3)-H(3)	110.4
C(7)-H(7)	0.9500	C(2)-C(3)-H(3)	110.4
C(8)-N(3)	1.369(3)	O(7)-C(4)-C(3)	104.95(14)
C(8)-C(9)	1.501(2)	O(7)-C(4)-C(5)	109.56(13)
C(9)-O(2)	1.426(2)	C(3)-C(4)-C(5)	111.42(14)
C(9)-H(9A)	0.9900	O(7)-C(4)-H(4)	110.3
C(9)-H(9B)	0.9900	C(3)-C(4)-H(4)	110.3
C(10)-O(4)	1.200(3)	C(5)-C(4)-H(4)	110.3
C(10)-O(3)	1.368(2)	O(1)-C(5)-C(6)	101.83(13)
C(10)-C(11)	1.494(3)	O(1)-C(5)-C(4)	108.78(13)
C(11)-H(11A)	0.9800	C(6)-C(5)-C(4)	114.56(15)
C(11)-H(11B)	0.9800	O(1)-C(5)-H(5)	110.4
C(11)-H(11C)	0.9800	C(6)-C(5)-H(5)	110.4
C(12)-O(6)	1.204(2)	C(4)-C(5)-H(5)	110.4
C(12)-O(5)	1.357(2)	O(9)-C(6)-C(5)	108.97(14)
C(12)-C(13)	1.496(3)	O(9)-C(6)-H(6A)	109.9
C(13)-H(13A)	0.9800	C(5)-C(6)-H(6A)	109.9
C(13)-H(13B)	0.9800	O(9)-C(6)-H(6B)	109.9
C(13)-H(13C)	0.9800	C(5)-C(6)-H(6B)	109.9
C(14)-O(8)	1.205(2)	H(6A)-C(6)-H(6B)	108.3
C(14)-O(7)	1.352(2)	N(1)-C(7)-C(8)	104.16(16)
C(14)-C(15)	1.506(2)	N(1)-C(7)-H(7)	127.9
C(15)-H(15A)	0.9800	C(8)-C(7)-H(7)	127.9
C(15)-H(15B)	0.9800	N(3)-C(8)-C(7)	108.79(16)
C(15)-H(15C)	0.9800	N(3)-C(8)-C(9)	122.10(16)
C(16)-O(10)	1.206(2)	C(7)-C(8)-C(9)	129.02(17)
C(16)-O(9)	1.344(2)	O(2)-C(9)-C(8)	111.30(15)
C(16)-C(17)	1.495(3)	O(2)-C(9)-H(9A)	109.4
C(17)-H(17A)	0.9800	C(8)-C(9)-H(9A)	109.4

O(2)-C(9)-H(9B)	H(15A)-C(15)-H(15C)	109.5
109.4	H(15B)-C(15)-H(15C)	109.5
C(8)-C(9)-H(9B)	O(10)-C(16)-O(9)	123.80(16)
109.4	O(10)-C(16)-C(17)	124.78(18)
H(9A)-C(9)-H(9B)	O(9)-C(16)-C(17)	111.42(17)
108.0	C(16)-C(17)-H(17A)	109.5
O(4)-C(10)-O(3)	C(16)-C(17)-H(17B)	109.5
122.82(18)	H(17A)-C(17)-H(17B)	109.5
O(4)-C(10)-C(11)	C(16)-C(17)-H(17C)	109.5
126.77(16)	H(17A)-C(17)-H(17C)	109.5
O(3)-C(10)-C(11)	H(17B)-C(17)-H(17C)	109.5
110.41(16)	C(7)-N(1)-N(2)	111.31(14)
C(10)-C(11)-H(11A)	C(7)-N(1)-C(1)	128.34(15)
109.5	N(2)-N(1)-C(1)	119.68(14)
C(10)-C(11)-H(11B)	N(3)-N(2)-N(1)	106.79(15)
109.5	N(2)-N(3)-C(8)	108.94(15)
H(11A)-C(11)-H(11B)	C(1)-O(1)-C(5)	113.12(13)
109.5	C(9)-O(2)-H(2A)	109.5
C(10)-C(11)-H(11C)	C(10)-O(3)-C(2)	117.31(15)
109.5	C(12)-O(5)-C(3)	117.99(14)
H(11A)-C(11)-H(11C)	C(14)-O(7)-C(4)	117.97(14)
109.5	C(16)-O(9)-C(6)	115.68(15)
H(11B)-C(11)-H(11C)		
109.5		
O(6)-C(12)-O(5)		
124.35(17)		
O(6)-C(12)-C(13)		
126.32(19)		
O(5)-C(12)-C(13)		
109.33(17)		
C(12)-C(13)-H(13A)		
109.5		
C(12)-C(13)-H(13B)		
109.5		
H(13A)-C(13)-H(13B)		
109.5		
C(12)-C(13)-H(13C)		
109.5		
H(13A)-C(13)-H(13C)		
109.5		
H(13B)-C(13)-H(13C)		
109.5		
O(8)-C(14)-O(7)		
123.39(16)		
O(8)-C(14)-C(15)		
124.91(17)		
O(7)-C(14)-C(15)		
111.70(16)		
C(14)-C(15)-H(15A)		
109.5		
C(14)-C(15)-H(15B)		
109.5		
H(15A)-C(15)-H(15B)		
109.5		
C(14)-C(15)-H(15C)		
109.5		

Table 4. Anisotropic displacement parameters [$\text{\AA}^2 \times 10^3$] for 08mz001_0m. The anisotropic displacement factor exponent takes the form: $-2 \pi^2 [(h a^*)^2 U_{11} + \dots + 2 h k a^* b^* U_{12}]$

	U11	U22	U33	U23	U13	U12
C(1)	19(1)	17(1)	14(1)	-1(1)	4(1)	0(1)
C(2)	19(1)	15(1)	16(1)	-2(1)	4(1)	0(1)
C(3)	17(1)	17(1)	15(1)	0(1)	6(1)	-2(1)
C(4)	19(1)	15(1)	13(1)	1(1)	3(1)	-2(1)
C(5)	19(1)	18(1)	16(1)	0(1)	3(1)	1(1)
C(6)	24(1)	22(1)	18(1)	-2(1)	3(1)	5(1)
C(7)	22(1)	16(1)	17(1)	0(1)	4(1)	0(1)
C(8)	24(1)	17(1)	17(1)	2(1)	5(1)	6(1)
C(9)	30(1)	20(1)	17(1)	1(1)	3(1)	3(1)
C(10)	19(1)	24(1)	20(1)	2(1)	7(1)	2(1)
C(11)	21(1)	28(1)	26(1)	4(1)	9(1)	6(1)
C(12)	24(1)	27(1)	17(1)	-6(1)	5(1)	-4(1)
C(13)	40(1)	57(2)	41(1)	-26(1)	26(1)	-21(1)
C(14)	20(1)	20(1)	14(1)	1(1)	5(1)	0(1)
C(15)	29(1)	26(1)	16(1)	0(1)	2(1)	-4(1)
C(16)	21(1)	21(1)	22(1)	1(1)	8(1)	2(1)
C(17)	28(1)	29(1)	27(1)	2(1)	0(1)	6(1)
N(1)	20(1)	15(1)	16(1)	2(1)	4(1)	-1(1)
N(2)	27(1)	18(1)	19(1)	3(1)	7(1)	0(1)
N(3)	30(1)	20(1)	18(1)	2(1)	7(1)	1(1)
O(1)	21(1)	20(1)	14(1)	-1(1)	3(1)	4(1)
O(2)	23(1)	23(1)	24(1)	-1(1)	3(1)	2(1)
O(3)	19(1)	18(1)	21(1)	-1(1)	3(1)	1(1)
O(4)	22(1)	28(1)	61(1)	-1(1)	-1(1)	-4(1)
O(5)	22(1)	22(1)	18(1)	-4(1)	9(1)	-6(1)
O(6)	41(1)	26(1)	26(1)	-7(1)	15(1)	-9(1)
O(7)	23(1)	17(1)	14(1)	1(1)	2(1)	-4(1)
O(8)	42(1)	19(1)	20(1)	2(1)	2(1)	-4(1)
O(9)	20(1)	20(1)	21(1)	-1(1)	1(1)	1(1)
O(10)	27(1)	22(1)	36(1)	-5(1)	5(1)	0(1)

Table 5. Hydrogen coordinates ($\times 10^4$) and isotropic displacement parameters ($\text{\AA}^2 \times 10^3$) for 08mz001_0m.

	x	y	z	U(eq)
H(1)	7279	10005	1132	20
H(2)	4287	8141	1339	20
H(3)	6763	9890	2736	19
H(4)	6868	6776	2667	19
H(5)	9596	8609	2139	21
H(6A)	8942	5550	1882	26
H(6B)	10307	6414	1392	26
H(7)	3838	7490	-393	23
H(9A)	2696	8824	-2827	27
H(9B)	4190	7556	-2685	27
H(11A)	1568	12107	333	37
H(11B)	1547	12127	1415	37
H(11C)	-144	11442	658	37
H(13A)	3030	9827	4670	65
H(13B)	3450	8189	4451	65
H(13C)	1947	9093	3710	65
H(15A)	9177	7189	5639	36
H(15B)	10392	8271	5195	36
H(15C)	11049	6640	5417	36
H(17A)	13947	3893	3940	44
H(17B)	13259	5345	4331	44
H(17C)	14546	5425	3614	44
H(2A)	1012	7507	-2203	36

Table 6. Torsion angles [deg] for 07mz075m.

O(1)-C(1)-C(2)-O(3)	179.63(12)
N(1)-C(1)-C(2)-O(3)	-63.09(18)
O(1)-C(1)-C(2)-C(3)	62.78(17)
N(1)-C(1)-C(2)-C(3)	-179.94(14)
O(3)-C(2)-C(3)-O(5)	70.04(16)
C(1)-C(2)-C(3)-O(5)	-172.66(14)
O(3)-C(2)-C(3)-C(4)	-172.97(13)
C(1)-C(2)-C(3)-C(4)	-55.68(18)
O(5)-C(3)-C(4)-O(7)	-73.58(15)
C(2)-C(3)-C(4)-O(7)	169.41(12)
O(5)-C(3)-C(4)-C(5)	167.94(13)
C(2)-C(3)-C(4)-C(5)	50.93(18)
O(7)-C(4)-C(5)-O(1)	-166.79(14)
C(3)-C(4)-C(5)-O(1)	-51.10(18)
O(7)-C(4)-C(5)-C(6)	80.04(17)
C(3)-C(4)-C(5)-C(6)	-164.28(14)
O(1)-C(5)-C(6)-O(9)	170.70(14)
C(4)-C(5)-C(6)-O(9)	-72.08(19)
N(1)-C(7)-C(8)-N(3)	-0.7(2)
N(1)-C(7)-C(8)-C(9)	175.92(18)

N(3)-C(8)-C(9)-O(2)	-166.79(16)
C(7)-C(8)-C(9)-O(2)	17.0(3)
C(8)-C(7)-N(1)-N(2)	0.00(19)
C(8)-C(7)-N(1)-C(1)	-170.47(16)
O(1)-C(1)-N(1)-C(7)	62.5(2)
C(2)-C(1)-N(1)-C(7)	-55.6(2)
O(1)-C(1)-N(1)-N(2)	-107.32(17)
C(2)-C(1)-N(1)-N(2)	134.59(16)
C(7)-N(1)-N(2)-N(3)	0.7(2)
C(1)-N(1)-N(2)-N(3)	172.14(15)
N(1)-N(2)-N(3)-C(8)	-1.17(19)
C(7)-C(8)-N(3)-N(2)	1.2(2)
C(9)-C(8)-N(3)-N(2)	-175.70(17)
N(1)-C(1)-O(1)-C(5)	170.23(13)
C(2)-C(1)-O(1)-C(5)	-68.45(17)
C(6)-C(5)-O(1)-C(1)	-177.20(13)
C(4)-C(5)-O(1)-C(1)	61.48(18)
O(4)-C(10)-O(3)-C(2)	3.5(3)
C(11)-C(10)-O(3)-C(2)	-176.76(14)
C(3)-C(2)-O(3)-C(10)	-128.43(15)
C(1)-C(2)-O(3)-C(10)	115.27(16)
O(6)-C(12)-O(5)-C(3)	-2.8(3)
C(13)-C(12)-O(5)-C(3)	177.92(17)
C(4)-C(3)-O(5)-C(12)	122.56(16)
C(2)-C(3)-O(5)-C(12)	-117.98(16)
O(8)-C(14)-O(7)-C(4)	4.7(3)
C(15)-C(14)-O(7)-C(4)	-174.88(15)
C(3)-C(4)-O(7)-C(14)	130.41(15)
C(5)-C(4)-O(7)-C(14)	-109.86(16)
O(10)-C(16)-O(9)-C(6)	-8.4(3)
C(17)-C(16)-O(9)-C(6)	172.19(15)
C(5)-C(6)-O(9)-C(16)	158.31(15)

Table 7. Hydrogen bonds for 08mz001_0m [\AA and deg].

D-H...A	d(D-H)	d(H...A)	d(D...A)	<(DHA)
O(2)-H(2A)...O(10)#1	0.84	2.02	2.815(2)	158.1

Symmetry transformations used to generate equivalent atoms:

#1 -x+1, y+1/2, -z

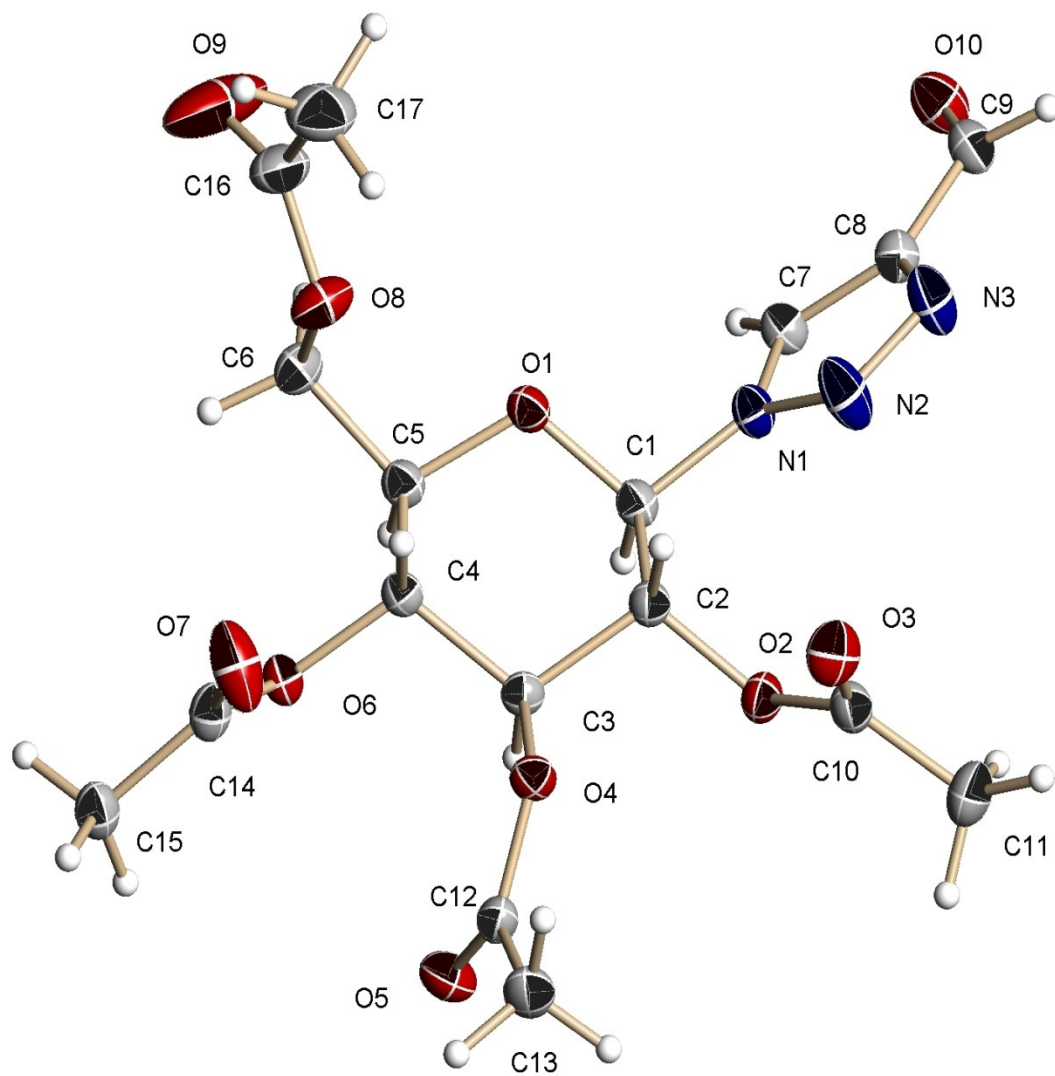


Figure 97: X-Ray crystal structure of aldehyde 9.

Table 1. Crystal data and structure refinement for 08mz018_0m:

Identification code: 08mz018_0m
 Empirical formula: C17 H21 N3 O10
 Formula weight: 427.37
 Temperature: 100(2) K
 Wavelength: 0.71073 Å
 Crystal system: Orthorhombic
 Space group: P2₁2₁2₁
 Unit cell dimensions:
 a = 7.7214(7) Å, α = 90°
 b = 15.4723(15) Å, β = 90°
 c = 16.3970(15) Å, γ = 90°
 Volume, Z: 1958.9(3) Å³, 4
 Density (calculated): 1.449 Mg/m³
 Absorption coefficient: 0.121 mm⁻¹
 F(000): 896
 Crystal size: 0.60 × 0.50 × 0.29 mm
 Crystal shape, colour: rod, colourless
 θ range for data collection: 1.81 to 28.28°
 Limiting indices: $-10 \leq h \leq 10$, $-17 \leq k \leq 20$, $-21 \leq l \leq 13$
 Reflections collected: 9563
 Independent reflections: 2766 (R(int) = 0.0274)
 Completeness to $\theta = 28.28^\circ$: 99.9 %
 Absorption correction: multi-scan
 Max. and min. transmission: 0.966 and 0.763
 Refinement method: Full-matrix least-squares on F^2
 Data / restraints / parameters: 2766 / 0 / 275
 Goodness-of-fit on F^2 : 1.035
 Final R indices [$I > 2\sigma(I)$]: R1 = 0.0362, wR2 = 0.0851
 R indices (all data): R1 = 0.0422, wR2 = 0.0890
 Largest diff. peak and hole: 0.358 and -0.279 e × Å⁻³

Refinement of F^2 against ALL reflections. The weighted R-factor wR and goodness of fit are based on F^2 , conventional R-factors R are based on F , with F set to zero for negative F^2 . The threshold expression of $F^2 > 2\sigma(F^2)$ is used only for calculating R-factors

Treatment of hydrogen atoms:

All hydrogen atoms were placed in calculated positions and were refined

with an isotropic displacement parameter 1.5 (methyl) or 1.2 times (all others) that of the adjacent carbon atom.

Table 2. Atomic coordinates [$\times 10^4$] and equivalent isotropic displacement parameters [$\text{\AA}^2 \times 10^3$] for 08mz018_0m. $U(\text{eq})$ is defined as one third of the trace of the orthogonalized U_{ij} tensor.

	x	y	z	U(eq)
C(1)	3454(3)	4643(1)	9277(1)	20(1)
C(2)	5092(3)	4348(1)	8850(1)	19(1)
C(3)	6231(3)	3904(1)	9482(1)	19(1)
C(4)	6586(3)	4520(1)	10187(1)	18(1)
C(5)	4889(3)	4877(1)	10532(1)	21(1)
C(6)	5181(3)	5593(1)	11139(1)	25(1)
C(7)	633(3)	5300(1)	8865(1)	23(1)
C(8)	124(3)	5749(1)	8188(1)	22(1)
C(9)	-1529(3)	6172(1)	8026(1)	25(1)
C(10)	5304(3)	3889(2)	7466(1)	25(1)
C(11)	4538(4)	3270(2)	6864(2)	38(1)
C(12)	8547(3)	2913(1)	9200(1)	23(1)
C(13)	10081(3)	2789(2)	8657(2)	30(1)
C(14)	9154(3)	4139(2)	10942(1)	24(1)
C(15)	9827(3)	3558(2)	11591(1)	27(1)
C(16)	6098(4)	7047(2)	10988(2)	36(1)
C(17)	7129(4)	7650(2)	10452(2)	45(1)
N(1)	2282(2)	5086(1)	8722(1)	22(1)
N(2)	2797(3)	5379(2)	7975(1)	36(1)
N(3)	1467(3)	5772(2)	7658(1)	33(1)
O(1)	3896(2)	5253(1)	9882(1)	21(1)
O(2)	4624(2)	3739(1)	8225(1)	22(1)
O(3)	6360(2)	4435(1)	7327(1)	32(1)
O(4)	7831(2)	3700(1)	9073(1)	21(1)
O(5)	7995(2)	2397(1)	9681(1)	31(1)
O(6)	7424(2)	4046(1)	10836(1)	20(1)
O(7)	10021(2)	4632(2)	10550(1)	42(1)
O(8)	6197(2)	6241(1)	10721(1)	32(1)
O(9)	5293(5)	7233(1)	11591(2)	77(1)
O(10)	-2719(2)	6182(1)	8498(1)	34(1)

All esds (except the esd in the dihedral angle between two l.s. planes)

are estimated using the full covariance matrix. The cell esds are taken

into account individually in the estimation of esds in distances, angles

and torsion angles; correlations between esds in cell parameters are only

used when they are defined by crystal symmetry. An approximate (isotropic)

treatment of cell esds is used for estimating esds involving l.s. planes.

Table 3. Bond lengths [\AA] and angles [deg] for 08mz018_0m.

C(1)-O(1)	1.411(3)
C(1)-N(1)	1.454(3)
C(1)-C(2)	1.516(3)
C(1)-H(1)	0.9800
C(2)-O(2)	1.437(2)
C(2)-C(3)	1.523(3)
C(2)-H(2)	0.9800
C(3)-O(4)	1.441(3)
C(3)-C(4)	1.523(3)
C(3)-H(3)	0.9800
C(4)-O(6)	1.446(2)
C(4)-C(5)	1.531(3)
C(4)-H(4)	0.9800
C(5)-O(1)	1.436(2)
C(5)-C(6)	1.505(3)
C(5)-H(5)	0.9800
C(6)-O(8)	1.445(3)
C(6)-H(6A)	0.9700
C(6)-H(6B)	0.9700
C(7)-N(1)	1.336(3)
C(7)-C(8)	1.366(3)
C(7)-H(7)	0.9300
C(8)-N(3)	1.354(3)
C(8)-C(9)	1.459(3)
C(9)-O(10)	1.201(3)
C(9)-H(9)	0.9300
C(10)-O(3)	1.197(3)
C(10)-O(2)	1.371(3)
C(10)-C(11)	1.497(3)
C(11)-H(11A)	0.9600
C(11)-H(11B)	0.9600
C(11)-H(11C)	0.9600
C(12)-O(5)	1.201(3)
C(12)-O(4)	1.353(3)
C(12)-C(13)	1.494(3)
C(13)-H(13A)	0.9600
C(13)-H(13B)	0.9600
C(13)-H(13C)	0.9600
C(14)-O(7)	1.201(3)
C(14)-O(6)	1.355(3)
C(14)-C(15)	1.487(3)
C(15)-H(15A)	0.9600
C(15)-H(15B)	0.9600
C(15)-H(15C)	0.9600
C(16)-O(9)	1.202(3)
C(16)-O(8)	1.323(3)
C(16)-C(17)	1.509(4)
C(17)-H(17A)	0.9600
C(17)-H(17B)	0.9600
C(17)-H(17C)	0.9600
N(1)-N(2)	1.366(3)
N(2)-N(3)	1.302(3)
O(1)-C(1)-N(1)	106.01(17)

O(1)-C(1)-C(2)	108.95(17)
N(1)-C(1)-C(2)	111.87(16)
O(1)-C(1)-H(1)	110.0
N(1)-C(1)-H(1)	110.0
C(2)-C(1)-H(1)	110.0
O(2)-C(2)-C(1)	108.49(17)
O(2)-C(2)-C(3)	109.52(16)
C(1)-C(2)-C(3)	107.68(16)
O(2)-C(2)-H(2)	110.4
C(1)-C(2)-H(2)	110.4
C(3)-C(2)-H(2)	110.4
O(4)-C(3)-C(4)	109.59(17)
O(4)-C(3)-C(2)	106.12(16)
C(4)-C(3)-C(2)	109.77(17)
O(4)-C(3)-H(3)	110.4
C(4)-C(3)-H(3)	110.4
C(2)-C(3)-H(3)	110.4
O(6)-C(4)-C(3)	108.83(16)
O(6)-C(4)-C(5)	107.08(15)
C(3)-C(4)-C(5)	110.67(17)
O(6)-C(4)-H(4)	110.1
C(3)-C(4)-H(4)	110.1
C(5)-C(4)-H(4)	110.1
O(1)-C(5)-C(6)	105.85(17)
O(1)-C(5)-C(4)	109.19(16)
C(6)-C(5)-C(4)	112.48(18)
O(1)-C(5)-H(5)	109.7
C(6)-C(5)-H(5)	109.7
C(4)-C(5)-H(5)	109.7
O(8)-C(6)-C(5)	106.18(17)
O(8)-C(6)-H(6A)	110.5
C(5)-C(6)-H(6A)	110.5
O(8)-C(6)-H(6B)	110.5
C(5)-C(6)-H(6B)	110.5
H(6A)-C(6)-H(6B)	108.7
N(1)-C(7)-C(8)	105.0(2)
N(1)-C(7)-H(7)	127.5
C(8)-C(7)-H(7)	127.5
N(3)-C(8)-C(7)	108.30(19)
N(3)-C(8)-C(9)	122.75(19)
C(7)-C(8)-C(9)	128.9(2)
O(10)-C(9)-C(8)	123.8(2)
O(10)-C(9)-H(9)	118.1
C(8)-C(9)-H(9)	118.1
O(3)-C(10)-O(2)	123.6(2)
O(3)-C(10)-C(11)	126.5(2)
O(2)-C(10)-C(11)	109.9(2)
C(10)-C(11)-H(11A)	109.5
C(10)-C(11)-H(11B)	109.5
H(11A)-C(11)-H(11B)	109.5
C(10)-C(11)-H(11C)	109.5
H(11A)-C(11)-H(11C)	109.5
H(11B)-C(11)-H(11C)	109.5
O(5)-C(12)-O(4)	123.7(2)
O(5)-C(12)-C(13)	125.9(2)
O(4)-C(12)-C(13)	110.37(19)
C(12)-C(13)-H(13A)	109.5

C(12)-C(13)-H(13B)	109.5
H(13A)-C(13)-H(13B)	109.5
C(12)-C(13)-H(13C)	109.5
H(13A)-C(13)-H(13C)	109.5
H(13B)-C(13)-H(13C)	109.5
O(7)-C(14)-O(6)	123.3(2)
O(7)-C(14)-C(15)	124.9(2)
O(6)-C(14)-C(15)	111.8(2)
C(14)-C(15)-H(15A)	109.5
C(14)-C(15)-H(15B)	109.5
H(15A)-C(15)-H(15B)	109.5
C(14)-C(15)-H(15C)	109.5
H(15A)-C(15)-H(15C)	109.5
H(15B)-C(15)-H(15C)	109.5
O(9)-C(16)-O(8)	121.8(3)
O(9)-C(16)-C(17)	127.1(3)
O(8)-C(16)-C(17)	111.1(2)
C(16)-C(17)-H(17A)	109.5
C(16)-C(17)-H(17B)	109.5
H(17A)-C(17)-H(17B)	109.5
C(16)-C(17)-H(17C)	109.5
H(17A)-C(17)-H(17C)	109.5
H(17B)-C(17)-H(17C)	109.5
C(7)-N(1)-N(2)	110.59(19)
C(7)-N(1)-C(1)	126.92(19)
N(2)-N(1)-C(1)	122.43(18)
N(3)-N(2)-N(1)	106.48(18)
N(2)-N(3)-C(8)	109.62(18)
C(1)-O(1)-C(5)	112.42(15)
C(10)-O(2)-C(2)	116.12(17)
C(12)-O(4)-C(3)	118.41(17)
C(14)-O(6)-C(4)	118.79(18)
C(16)-O(8)-C(6)	117.76(19)

Table 4. Anisotropic displacement parameters [$\text{\AA}^2 \times 10^3$] for 08mz018_0m.

The anisotropic displacement factor exponent takes the form: $-2 \pi^2 [(h a^*)^2 U_{11} + \dots + 2 h k a^* b^* U_{12}]$

	U11	U22	U33	U23	U13	U12
C(1)	19(1)	23(1)	19(1)	2(1)	0(1)	1(1)
C(2)	19(1)	21(1)	18(1)	-1(1)	0(1)	1(1)
C(3)	17(1)	20(1)	19(1)	-1(1)	2(1)	1(1)
C(4)	17(1)	19(1)	19(1)	1(1)	1(1)	1(1)
C(5)	20(1)	23(1)	20(1)	1(1)	0(1)	1(1)
C(6)	26(1)	27(1)	21(1)	-3(1)	4(1)	1(1)
C(7)	19(1)	25(1)	24(1)	2(1)	1(1)	0(1)
C(8)	22(1)	24(1)	21(1)	2(1)	0(1)	-3(1)

C(9)	23(1)	25(1)	27(1)	5(1)	-4(1)	-2(1)
C(10)	27(1)	30(1)	19(1)	-1(1)	-2(1)	7(1)
C(11)	50(2)	40(1)	23(1)	-7(1)	-5(1)	1(1)
C(12)	23(1)	24(1)	21(1)	-4(1)	-4(1)	5(1)
C(13)	28(1)	33(1)	28(1)	-4(1)	1(1)	11(1)
C(14)	20(1)	35(1)	18(1)	-3(1)	1(1)	1(1)
C(15)	23(1)	36(1)	21(1)	-2(1)	0(1)	5(1)
C(16)	50(2)	24(1)	35(1)	-5(1)	3(1)	6(1)
C(17)	58(2)	26(1)	49(2)	3(1)	3(2)	-1(1)
N(1)	20(1)	26(1)	19(1)	4(1)	1(1)	0(1)
N(2)	27(1)	55(1)	25(1)	16(1)	5(1)	9(1)
N(3)	24(1)	50(1)	24(1)	11(1)	1(1)	6(1)
O(1)	20(1)	23(1)	20(1)	0(1)	0(1)	4(1)
O(2)	25(1)	24(1)	18(1)	-1(1)	-1(1)	-1(1)
O(3)	32(1)	41(1)	24(1)	0(1)	8(1)	-2(1)
O(4)	19(1)	22(1)	21(1)	0(1)	3(1)	4(1)
O(5)	33(1)	25(1)	34(1)	6(1)	1(1)	5(1)
O(6)	19(1)	24(1)	18(1)	3(1)	-1(1)	0(1)
O(7)	24(1)	72(1)	31(1)	21(1)	-2(1)	-10(1)
O(8)	37(1)	24(1)	34(1)	-7(1)	10(1)	-4(1)
O(9)	129(3)	31(1)	73(2)	-12(1)	48(2)	-2(1)
O(10)	27(1)	38(1)	36(1)	7(1)	3(1)	5(1)

Table 5. Hydrogen coordinates ($\times 10^4$) and isotropic displacement parameters ($\text{\AA}^2 \times 10^3$) for 08mz018_0m.

	x	y	z	U(eq)
H(1)	2868	4147	9526	24
H(2)	5699	4843	8611	23
H(3)	5673	3375	9681	22
H(4)	7330	4995	10004	22
H(5)	4228	4410	10788	25
H(6A)	4085	5834	11317	30
H(6B)	5799	5378	11612	30
H(7)	-24	5171	9324	27
H(9)	-1671	6450	7527	30
H(11A)	5052	2710	6936	57
H(11B)	4761	3472	6320	57
H(11C)	3311	3231	6950	57
H(13A)	9768	2423	8207	44
H(13B)	11002	2524	8960	44
H(13C)	10458	3340	8454	44
H(15A)	9594	3806	12116	40
H(15B)	11054	3486	11524	40

H(15C)	9268	3005	11551	40
H(17A)	8025	7919	10769	67
H(17B)	6376	8086	10234	67
H(17C)	7640	7329	10013	67

Table 6. Torsion angles [deg] for 07mz075m.

O(1)-C(1)-C(2)-O(2)	-179.02(15)
N(1)-C(1)-C(2)-O(2)	-62.1(2)
O(1)-C(1)-C(2)-C(3)	62.5(2)
N(1)-C(1)-C(2)-C(3)	179.41(17)
O(2)-C(2)-C(3)-O(4)	67.1(2)
C(1)-C(2)-C(3)-O(4)	-175.10(16)
O(2)-C(2)-C(3)-C(4)	-174.54(16)
C(1)-C(2)-C(3)-C(4)	-56.8(2)
O(4)-C(3)-C(4)-O(6)	-73.0(2)
C(2)-C(3)-C(4)-O(6)	170.81(16)
O(4)-C(3)-C(4)-C(5)	169.57(16)
C(2)-C(3)-C(4)-C(5)	53.4(2)
O(6)-C(4)-C(5)-O(1)	-172.21(16)
C(3)-C(4)-C(5)-O(1)	-53.7(2)
O(6)-C(4)-C(5)-C(6)	70.6(2)
C(3)-C(4)-C(5)-C(6)	-170.92(17)
O(1)-C(5)-C(6)-O(8)	-63.1(2)
C(4)-C(5)-C(6)-O(8)	56.1(2)
N(1)-C(7)-C(8)-N(3)	1.4(3)
N(1)-C(7)-C(8)-C(9)	-176.9(2)
N(3)-C(8)-C(9)-O(10)	-177.7(2)
C(7)-C(8)-C(9)-O(10)	0.4(4)
C(8)-C(7)-N(1)-N(2)	-0.8(3)
C(8)-C(7)-N(1)-C(1)	176.2(2)
O(1)-C(1)-N(1)-C(7)	-73.1(3)
C(2)-C(1)-N(1)-C(7)	168.3(2)
O(1)-C(1)-N(1)-N(2)	103.6(2)
C(2)-C(1)-N(1)-N(2)	-15.0(3)
C(7)-N(1)-N(2)-N(3)	0.0(3)
C(1)-N(1)-N(2)-N(3)	-177.2(2)
N(1)-N(2)-N(3)-C(8)	0.9(3)
C(7)-C(8)-N(3)-N(2)	-1.5(3)
C(9)-C(8)-N(3)-N(2)	177.0(2)
N(1)-C(1)-O(1)-C(5)	172.96(16)
C(2)-C(1)-O(1)-C(5)	-66.5(2)
C(6)-C(5)-O(1)-C(1)	-177.49(17)
C(4)-C(5)-O(1)-C(1)	61.2(2)
O(3)-C(10)-O(2)-C(2)	7.2(3)
C(11)-C(10)-O(2)-C(2)	-173.23(19)
C(1)-C(2)-O(2)-C(10)	130.05(18)
C(3)-C(2)-O(2)-C(10)	-112.67(19)
O(5)-C(12)-O(4)-C(3)	-5.8(3)
C(13)-C(12)-O(4)-C(3)	173.76(18)
C(4)-C(3)-O(4)-C(12)	105.0(2)
C(2)-C(3)-O(4)-C(12)	-136.59(18)
O(7)-C(14)-O(6)-C(4)	4.1(3)

C(15)-C(14)-O(6)-C(4)	-175.52(17)
C(3)-C(4)-O(6)-C(14)	102.9(2)
C(5)-C(4)-O(6)-C(14)	-137.39(19)
O(9)-C(16)-O(8)-C(6)	5.1(4)
C(17)-C(16)-O(8)-C(6)	-175.9(2)
C(5)-C(6)-O(8)-C(16)	155.4(2)

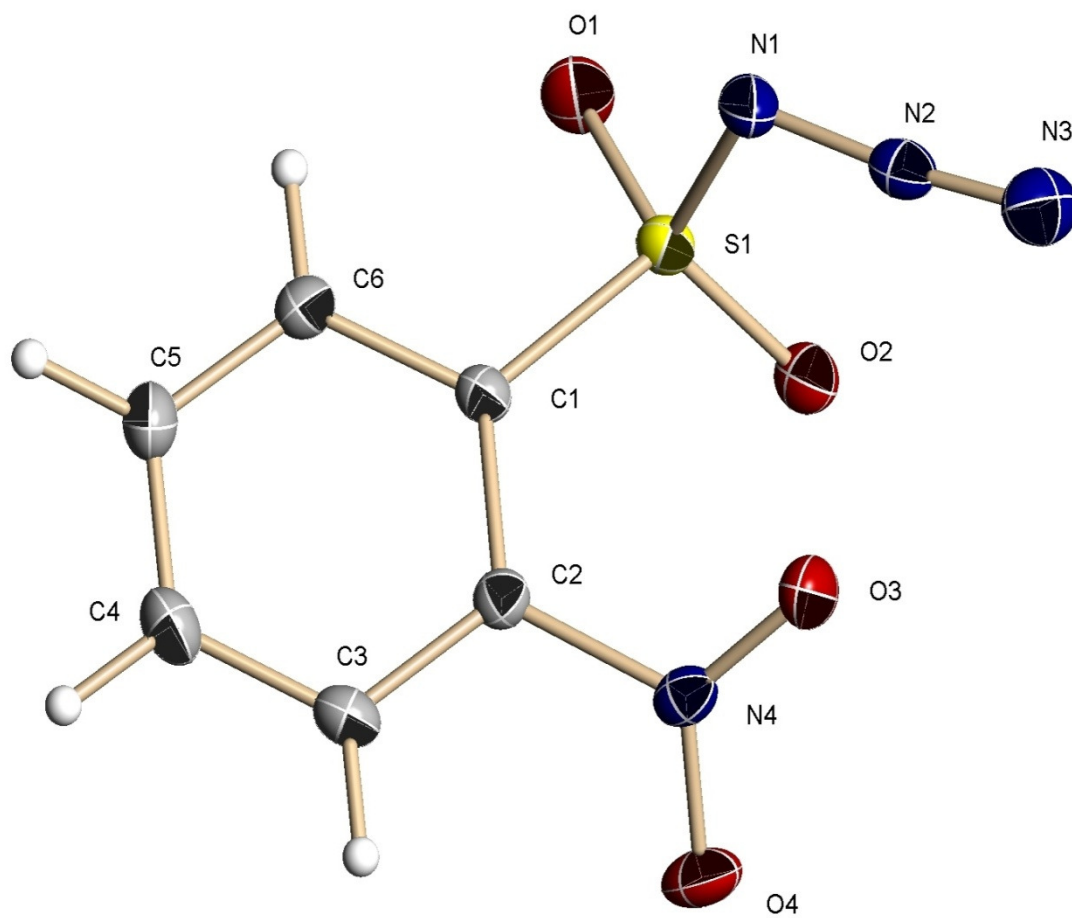


Figure 98: X-Ray crystal structure of *o*-nitrobenzylsulfonyl azide (**19**).

Table 1. Crystal data and structure refinement for 08mz259_0m:

Identification code: 08mz259_0m
 Empirical formula: C6 H4 N4 O4 S
 Formula weight: 228.19
 Temperature: 140(2) K
 Wavelength: 0.71073 Å
 Crystal system: Monoclinic
 Space group: P2₁/c
 Unit cell dimensions:
 a = 8.2153(7) Å, α = 90°
 b = 14.4507(11) Å, β = 106.5530(10)°
 c = 7.7489(6) Å, γ = 90°
 Volume, Z: 881.80(12) Å³, 4
 Density (calculated): 1.719 Mg/m³
 Absorption coefficient: 0.368 mm⁻¹
 F(000): 464
 Crystal size: 0.25 × 0.25 × 0.15 mm
 Crystal shape, colour: block, colourless
 θ range for data collection: 2.59 to 29.57°
 Limiting indices: $-11 \leq h \leq 11$, $-20 \leq k \leq 20$, $-10 \leq l \leq 10$
 Reflections collected: 9595
 Independent reflections: 2469 (R(int) = 0.0274)
 Completeness to $\theta = 29.57^\circ$: 99.8 %
 Absorption correction: multi-scan
 Max. and min. transmission: 0.946 and 0.819
 Refinement method: Full-matrix least-squares on F^2
 Data / restraints / parameters: 2469 / 0 / 136
 Goodness-of-fit on F^2 : 1.036
 Final R indices [$I > 2\sigma(I)$]: R1 = 0.0329, wR2 = 0.0808
 R indices (all data): R1 = 0.0401, wR2 = 0.0859
 Largest diff. peak and hole: 1.119 and -0.606 e × Å⁻³

Refinement of F^2 against ALL reflections. The weighted R-factor wR and goodness of fit are based on F^2 , conventional R-factors R are based on F , with F set to zero for negative F^2 . The threshold expression of $F^2 > 2\sigma(F^2)$ is used only for calculating R-factors

Treatment of hydrogen atoms:
 All hydrogen atoms were placed in calculated positions and were refined

with an isotropic displacement parameter 1.5 (methyl, hydroxyl) or 1.2 times (all others) that of the adjacent carbon or oxygen atom.

Table 2. Atomic coordinates [$\times 10^4$] and equivalent isotropic displacement parameters [$\text{\AA}^2 \times 10^3$] for 08mz259_0m. U(eq) is defined as one third of the trace of the orthogonalized U_{ij} tensor.

	x	y	z	U(eq)
C(1)	8636(2)	1492(1)	8064(2)	17(1)
C(2)	8172(2)	2429(1)	7977(2)	17(1)
C(3)	9334(2)	3106(1)	8752(2)	22(1)
C(4)	10968(2)	2850(1)	9716(2)	26(1)
C(5)	11431(2)	1925(1)	9889(2)	26(1)
C(6)	10283(2)	1251(1)	9031(2)	22(1)
N(1)	6380(2)	139(1)	8218(2)	23(1)
N(2)	4844(2)	363(1)	7885(2)	21(1)
N(3)	3469(2)	495(1)	7709(2)	29(1)
N(4)	6419(2)	2735(1)	7130(2)	19(1)
O(1)	8516(1)	-117(1)	6633(2)	30(1)
O(2)	6185(1)	968(1)	5240(1)	23(1)
O(3)	5274(1)	2277(1)	7418(2)	26(1)
O(4)	6220(2)	3450(1)	6249(2)	28(1)
S(1)	7373(1)	594(1)	6805(1)	18(1)

All esds (except the esd in the dihedral angle between two l.s. planes) are estimated using the full covariance matrix. The cell esds are taken into account individually in the estimation of esds in distances, angles and torsion angles; correlations between esds in cell parameters are only used when they are defined by crystal symmetry. An approximate (isotropic) treatment of cell esds is used for estimating esds involving l.s. planes.

Table 3. Bond lengths [\AA] and angles [deg] for 08mz259_0m.

C(1)-C(6)	1.3910(18)
C(1)-C(2)	1.4034(18)
C(1)-S(1)	1.7703(13)
C(2)-C(3)	1.3795(19)
C(2)-N(4)	1.4701(17)
C(3)-C(4)	1.388(2)
C(3)-H(3)	0.9500
C(4)-C(5)	1.386(2)
C(4)-H(4)	0.9500
C(5)-C(6)	1.387(2)
C(5)-H(5)	0.9500
C(6)-H(6)	0.9500
N(1)-N(2)	1.2566(17)
N(1)-S(1)	1.6756(13)
N(2)-N(3)	1.1147(18)
N(4)-O(3)	1.2223(16)
N(4)-O(4)	1.2232(15)
O(1)-S(1)	1.4232(11)
O(2)-S(1)	1.4285(11)
C(6)-C(1)-C(2)	118.42(12)
C(6)-C(1)-S(1)	116.18(10)
C(2)-C(1)-S(1)	124.90(10)
C(3)-C(2)-C(1)	121.28(13)
C(3)-C(2)-N(4)	116.66(12)
C(1)-C(2)-N(4)	122.01(12)
C(2)-C(3)-C(4)	119.24(13)
C(2)-C(3)-H(3)	120.4
C(4)-C(3)-H(3)	120.4
C(5)-C(4)-C(3)	120.39(13)
C(5)-C(4)-H(4)	119.8
C(3)-C(4)-H(4)	119.8
C(4)-C(5)-C(6)	120.03(14)
C(4)-C(5)-H(5)	120.0
C(6)-C(5)-H(5)	120.0
C(5)-C(6)-C(1)	120.49(13)
C(5)-C(6)-H(6)	119.8
C(1)-C(6)-H(6)	119.8
N(2)-N(1)-S(1)	114.32(10)
N(3)-N(2)-N(1)	172.99(15)
O(3)-N(4)-O(4)	124.90(13)
O(3)-N(4)-C(2)	117.54(11)
O(4)-N(4)-C(2)	117.49(12)
O(1)-S(1)-O(2)	120.22(7)
O(1)-S(1)-N(1)	103.55(7)
O(2)-S(1)-N(1)	111.17(6)
O(1)-S(1)-C(1)	106.38(6)
O(2)-S(1)-C(1)	110.00(6)
N(1)-S(1)-C(1)	104.20(6)

Table 4. Anisotropic displacement parameters [$\text{\AA}^2 \times 10^3$] for 08mz259_0m. The anisotropic displacement factor exponent takes the form: $-2 \pi^2 [(h a^*)^2 U_{11} + \dots + 2 h k a^* b^* U_{12}]$

	U11	U22	U33	U23	U13	U12
C(1)	18(1)	15(1)	18(1)	-1(1)	5(1)	-1(1)
C(2)	18(1)	17(1)	17(1)	0(1)	5(1)	1(1)
C(3)	26(1)	16(1)	24(1)	-1(1)	8(1)	-3(1)
C(4)	23(1)	25(1)	29(1)	-4(1)	5(1)	-8(1)
C(5)	17(1)	28(1)	29(1)	1(1)	2(1)	-2(1)
C(6)	19(1)	19(1)	26(1)	3(1)	5(1)	2(1)
N(1)	21(1)	21(1)	24(1)	5(1)	3(1)	-3(1)
N(2)	27(1)	17(1)	18(1)	1(1)	7(1)	-3(1)
N(3)	29(1)	28(1)	33(1)	3(1)	14(1)	1(1)
N(4)	23(1)	17(1)	17(1)	-1(1)	4(1)	4(1)
O(1)	28(1)	20(1)	41(1)	-9(1)	10(1)	3(1)
O(2)	26(1)	23(1)	17(1)	-1(1)	3(1)	-3(1)
O(3)	18(1)	25(1)	34(1)	2(1)	6(1)	1(1)
O(4)	37(1)	19(1)	27(1)	7(1)	4(1)	6(1)
S(1)	20(1)	15(1)	20(1)	-3(1)	5(1)	0(1)

Table 5. Hydrogen coordinates ($\times 10^4$) and isotropic displacement parameters ($\text{\AA}^2 \times 10^3$) for 08mz259_0m.

	x	y	z	U(eq)
H(3)	9018	3740	8629	26
H(4)	11774	3312	10259	31
H(5)	12536	1753	10595	31
H(6)	10623	621	9104	26

Table 6. Torsion angles [deg] for 08mz259_0m.

C(6)-C(1)-C(2)-C(3)	3.1(2)
S(1)-C(1)-C(2)-C(3)	-168.54(11)
C(6)-C(1)-C(2)-N(4)	-174.18(12)
S(1)-C(1)-C(2)-N(4)	14.19(19)

C(1)-C(2)-C(3)-C(4)	-3.3(2)
N(4)-C(2)-C(3)-C(4)	174.08(13)
C(2)-C(3)-C(4)-C(5)	0.3(2)
C(3)-C(4)-C(5)-C(6)	2.9(2)
C(4)-C(5)-C(6)-C(1)	-3.1(2)
C(2)-C(1)-C(6)-C(5)	0.2(2)
S(1)-C(1)-C(6)-C(5)	172.51(12)
C(3)-C(2)-N(4)-O(3)	-136.06(13)
C(1)-C(2)-N(4)-O(3)	41.34(18)
C(3)-C(2)-N(4)-O(4)	41.15(17)
C(1)-C(2)-N(4)-O(4)	-141.46(13)
N(2)-N(1)-S(1)-O(1)	-144.52(11)
N(2)-N(1)-S(1)-O(2)	-14.08(13)
N(2)-N(1)-S(1)-C(1)	104.37(11)
C(6)-C(1)-S(1)-O(1)	-17.63(13)
C(2)-C(1)-S(1)-O(1)	154.17(12)
C(6)-C(1)-S(1)-O(2)	-149.33(11)
C(2)-C(1)-S(1)-O(2)	22.46(14)
C(6)-C(1)-S(1)-N(1)	91.42(12)
C(2)-C(1)-S(1)-N(1)	-96.79(12)

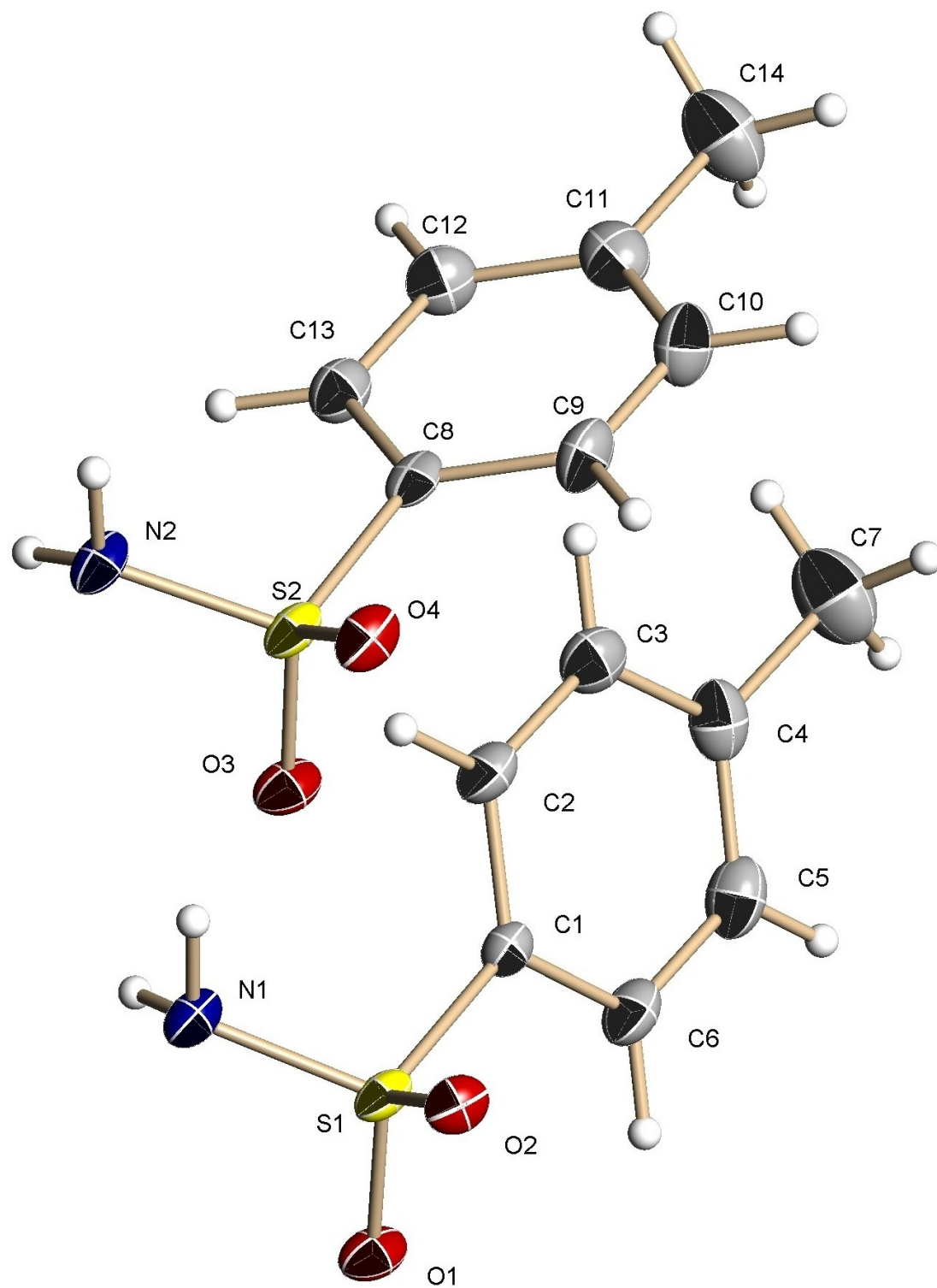


Figure 99: X-Ray crystal structure of *p*-toluenesulfonamide (**22**).

Table 1. Crystal data and structure refinement for 08mz243_0m:

Identification code: 08mz243_0m
Empirical formula: C7 H9 N O2 S
Formula weight: 171.22
Temperature: 140(2) K
Wavelength: 0.71073 Å
Crystal system: Triclinic
Space group: P1
Unit cell dimensions:
a = 5.086(2) Å, α = 101.523(5)°
b = 8.234(3) Å, β = 101.964(5)°
c = 9.771(4) Å, γ = 90.270(6)°
Volume, Z: 391.8(3) Å³, 2
Density (calculated): 1.451 Mg/m³
Absorption coefficient: 0.359 mm⁻¹
F(000): 180
Crystal size: 0.58 × 0.58 × 0.03 mm
Crystal shape, colour: plate, colourless
 θ range for data collection: 2.18 to 28.28°
Limiting indices: $-6 \leq h \leq 6$, $-10 \leq k \leq 10$, $-13 \leq l \leq 12$
Reflections collected: 3399
Independent reflections: 3197 ($R(\text{int}) = 0.0247$)
Completeness to $\theta = 28.28^\circ$: 95.7 %
Absorption correction: multi-scan
Max. and min. transmission: 0.989 and 0.735
Refinement method: Full-matrix least-squares on F^2
Data / restraints / parameters: 3197 / 7 / 213
Goodness-of-fit on F^2 : 1.037
Final R indices [$I > 2\sigma(I)$]: $R1 = 0.0408$, $wR2 = 0.1062$
 R indices (all data): $R1 = 0.0474$, $wR2 = 0.1127$
Absolute structure parameter: 0.04(7)
Largest diff. peak and hole: 1.210 and -0.545 e × Å⁻³

Refinement of F^2 against ALL reflections. The weighted R-factor wR and goodness of fit are based on F^2 , conventional R-factors R are based on F , with F set to zero for negative F^2 . The threshold expression of $F^2 > 2\sigma(F^2)$ is used only for calculating R-factors

Treatment of hydrogen atoms:

Amine H atoms were tentatively located in difference electron density Fourier maps and refined with an N-H distance of 0.91(2) Å. All other hydrogen atoms were placed geometrically and all were refined with an isotropic displacement parameter 1.5 (methyl) or 1.2 times (all others) that of the neighboring carbon or nitrogen atom. Methyl H atoms were allowed to rotate to best fit the experimental electron density.

Table 2. Atomic coordinates [$\times 10^4$] and equivalent isotropic displacement parameters [$\text{\AA}^2 \times 10^3$] for 08mz243_0m. $U(\text{eq})$ is defined as one third of the trace of the orthogonalized U_{ij} tensor.

	x	y	z	U(eq)
C(1)	1248(6)	9645(3)	10332(3)	19(1)
C(2)	3025(6)	8684(4)	9644(3)	24(1)
C(3)	2712(7)	8470(4)	8181(3)	28(1)
C(4)	668(7)	9223(4)	7373(3)	30(1)
C(5)	-1076(7)	10179(4)	8083(4)	31(1)
C(6)	-799(6)	10404(4)	9549(3)	25(1)
C(7)	335(11)	8963(6)	5773(4)	49(1)
C(8)	6147(6)	4478(3)	9959(3)	19(1)
C(9)	4098(6)	3500(4)	8998(4)	29(1)
C(10)	3872(7)	3395(4)	7545(4)	33(1)
C(11)	5673(8)	4255(4)	7025(3)	31(1)
C(12)	7736(8)	5218(4)	8007(4)	30(1)
C(13)	8008(6)	5344(4)	9465(3)	25(1)
C(14)	5405(10)	4143(6)	5443(4)	47(1)
N(1)	4596(5)	9932(3)	12947(3)	21(1)
N(2)	9367(5)	4868(3)	12634(3)	21(1)
O(1)	338(4)	11377(2)	12686(2)	23(1)
O(2)	279(4)	8348(2)	12379(2)	20(1)
O(3)	5101(4)	6247(2)	12268(2)	24(1)
O(4)	5090(4)	3206(2)	11993(2)	23(1)
S(1)	1478(1)	9838(1)	12176(1)	18(1)
S(2)	6291(1)	4704(1)	11802(1)	19(1)

All esds (except the esd in the dihedral angle between two l.s. planes) are estimated using the full covariance matrix. The cell esds are taken into account individually in the estimation of esds in distances, angles

and torsion angles; correlations between esds in cell parameters are only used when they are defined by crystal symmetry. An approximate (isotropic) treatment of cell esds is used for estimating esds involving l.s. planes.

Table 3. Bond lengths [\AA] and angles [deg] for 08mz243_0m.

C(1)-C(6)	1.388(4)
C(1)-C(2)	1.393(4)
C(1)-S(1)	1.756(3)
C(2)-C(3)	1.381(4)
C(2)-H(2)	0.9500
C(3)-C(4)	1.397(5)
C(3)-H(3)	0.9500
C(4)-C(5)	1.390(5)
C(4)-C(7)	1.508(5)
C(5)-C(6)	1.384(4)
C(5)-H(5)	0.9500
C(6)-H(6)	0.9500
C(7)-H(7A)	0.9800
C(7)-H(7B)	0.9800
C(7)-H(7C)	0.9800
C(8)-C(9)	1.378(4)
C(8)-C(13)	1.400(4)
C(8)-S(2)	1.759(3)
C(9)-C(10)	1.386(5)
C(9)-H(9)	0.9500
C(10)-C(11)	1.389(5)
C(10)-H(10)	0.9500
C(11)-C(12)	1.386(5)
C(11)-C(14)	1.507(5)
C(12)-C(13)	1.384(5)
C(12)-H(12)	0.9500
C(13)-H(13)	0.9500
C(14)-H(14A)	0.9800
C(14)-H(14B)	0.9800
C(14)-H(14C)	0.9800
N(1)-S(1)	1.603(3)
N(1)-H(1A)	0.910(19)
N(1)-H(1B)	0.901(18)
N(2)-S(2)	1.598(3)
N(2)-H(2A)	0.895(18)
N(2)-H(2B)	0.905(19)
O(1)-S(1)	1.437(2)
O(2)-S(1)	1.4343(19)
O(3)-S(2)	1.442(2)
O(4)-S(2)	1.436(2)
C(6)-C(1)-C(2)	120.0(3)

C(6)-C(1)-S(1)	119.3(2)
C(2)-C(1)-S(1)	120.6(2)
C(3)-C(2)-C(1)	119.7(3)
C(3)-C(2)-H(2)	120.2
C(1)-C(2)-H(2)	120.2
C(2)-C(3)-C(4)	121.2(3)
C(2)-C(3)-H(3)	119.4
C(4)-C(3)-H(3)	119.4
C(5)-C(4)-C(3)	118.0(3)
C(5)-C(4)-C(7)	121.4(3)
C(3)-C(4)-C(7)	120.6(3)
C(6)-C(5)-C(4)	121.6(3)
C(6)-C(5)-H(5)	119.2
C(4)-C(5)-H(5)	119.2
C(5)-C(6)-C(1)	119.5(3)
C(5)-C(6)-H(6)	120.3
C(1)-C(6)-H(6)	120.3
C(4)-C(7)-H(7A)	109.5
C(4)-C(7)-H(7B)	109.5
H(7A)-C(7)-H(7B)	109.5
C(4)-C(7)-H(7C)	109.5
H(7A)-C(7)-H(7C)	109.5
H(7B)-C(7)-H(7C)	109.5
C(9)-C(8)-C(13)	120.0(3)
C(9)-C(8)-S(2)	119.3(2)
C(13)-C(8)-S(2)	120.6(2)
C(8)-C(9)-C(10)	119.7(3)
C(8)-C(9)-H(9)	120.1
C(10)-C(9)-H(9)	120.1
C(9)-C(10)-C(11)	121.5(3)
C(9)-C(10)-H(10)	119.3
C(11)-C(10)-H(10)	119.3
C(12)-C(11)-C(10)	117.9(3)
C(12)-C(11)-C(14)	120.9(4)
C(10)-C(11)-C(14)	121.2(3)
C(13)-C(12)-C(11)	121.8(3)
C(13)-C(12)-H(12)	119.1
C(11)-C(12)-H(12)	119.1
C(12)-C(13)-C(8)	119.1(3)
C(12)-C(13)-H(13)	120.5
C(8)-C(13)-H(13)	120.5
C(11)-C(14)-H(14A)	109.5
C(11)-C(14)-H(14B)	109.5
H(14A)-C(14)-H(14B)	109.5
C(11)-C(14)-H(14C)	109.5
H(14A)-C(14)-H(14C)	109.5
H(14B)-C(14)-H(14C)	109.5
S(1)-N(1)-H(1A)	117(3)
S(1)-N(1)-H(1B)	111(3)
H(1A)-N(1)-H(1B)	107(3)
S(2)-N(2)-H(2A)	111(3)
S(2)-N(2)-H(2B)	122(3)
H(2A)-N(2)-H(2B)	113(4)
O(2)-S(1)-O(1)	117.22(13)
O(2)-S(1)-N(1)	107.49(13)
O(1)-S(1)-N(1)	108.41(14)
O(2)-S(1)-C(1)	107.34(13)

O(1)-S(1)-C(1)	107.62(13)
N(1)-S(1)-C(1)	108.49(13)
O(4)-S(2)-O(3)	117.81(13)
O(4)-S(2)-N(2)	108.37(13)
O(3)-S(2)-N(2)	107.10(13)
O(4)-S(2)-C(8)	106.71(13)
O(3)-S(2)-C(8)	107.38(12)
N(2)-S(2)-C(8)	109.27(13)

Table 4. Anisotropic displacement parameters [$\text{\AA}^2 \times 10^3$] for 08mz243_0m. The anisotropic displacement factor exponent takes the form: $-2 \pi^2 [(h a^*)^2 U_{11} + \dots + 2 h k a^* b^* U_{12}]$

	U11	U22	U33	U23	U13	U12
C(1)	15(1)	19(1)	23(1)	5(1)	3(1)	1(1)
C(2)	18(1)	24(2)	32(2)	8(1)	5(1)	4(1)
C(3)	24(2)	29(2)	34(2)	8(1)	9(1)	-2(1)
C(4)	31(2)	31(2)	27(2)	11(1)	0(1)	-10(1)
C(5)	27(2)	30(2)	36(2)	14(1)	-2(1)	-1(1)
C(6)	18(1)	23(2)	35(2)	8(1)	2(1)	3(1)
C(7)	65(3)	50(3)	30(2)	12(2)	4(2)	-4(2)
C(8)	14(1)	13(1)	31(2)	7(1)	3(1)	6(1)
C(9)	18(2)	31(2)	37(2)	10(1)	2(1)	-4(1)
C(10)	26(2)	34(2)	36(2)	9(1)	0(1)	-8(1)
C(11)	35(2)	28(2)	30(2)	7(1)	4(1)	6(1)
C(12)	31(2)	29(2)	32(2)	10(1)	10(1)	-2(1)
C(13)	22(2)	23(2)	32(2)	6(1)	6(1)	-1(1)
C(14)	63(3)	47(2)	29(2)	8(1)	4(2)	-4(2)
N(1)	16(1)	17(1)	31(1)	8(1)	6(1)	2(1)
N(2)	15(1)	15(1)	34(1)	10(1)	3(1)	4(1)
O(1)	21(1)	14(1)	36(1)	5(1)	11(1)	5(1)
O(2)	22(1)	14(1)	28(1)	10(1)	9(1)	-1(1)
O(3)	22(1)	17(1)	35(1)	7(1)	10(1)	6(1)
O(4)	21(1)	15(1)	35(1)	13(1)	7(1)	-1(1)
S(1)	13(1)	14(1)	29(1)	7(1)	7(1)	2(1)
S(2)	13(1)	15(1)	31(1)	9(1)	6(1)	3(1)

Table 5. Hydrogen coordinates ($\times 10^4$) and isotropic displacement parameters ($\text{\AA}^2 \times 10^3$) for 08mz243_0m.

	x	y	z	U(eq)
H(2)	4446	8178	10180	29
H(3)	3910	7797	7715	34
H(5)	-2491	10691	7550	37

H(6)	-2000	11072	10016	31
H(7A)	2110	8987	5532	73
H(7B)	-719	9848	5426	73
H(7C)	-601	7886	5322	73
H(9)	2845	2901	9332	35
H(10)	2453	2719	6889	39
H(12)	8998	5807	7672	36
H(13)	9438	6010	10120	31
H(14A)	4682	5168	5186	71
H(14B)	4182	3199	4913	71
H(14C)	7176	3989	5202	71
H(1A)	5660(70)	10750(40)	12810(40)	31
H(1B)	5370(80)	8970(30)	12690(40)	31
H(2A)	10150(80)	3900(30)	12470(40)	31
H(2B)	10460(70)	5750(40)	12670(40)	31

Table 6. Torsion angles [deg] for 08mz243_0m.

C(6)-C(1)-C(2)-C(3)	-1.0(5)
S(1)-C(1)-C(2)-C(3)	176.3(2)
C(1)-C(2)-C(3)-C(4)	1.1(5)
C(2)-C(3)-C(4)-C(5)	-0.9(5)
C(2)-C(3)-C(4)-C(7)	-179.4(3)
C(3)-C(4)-C(5)-C(6)	0.7(5)
C(7)-C(4)-C(5)-C(6)	179.2(3)
C(4)-C(5)-C(6)-C(1)	-0.7(5)
C(2)-C(1)-C(6)-C(5)	0.8(5)
S(1)-C(1)-C(6)-C(5)	-176.5(2)
C(13)-C(8)-C(9)-C(10)	-0.7(5)
S(2)-C(8)-C(9)-C(10)	176.1(3)
C(8)-C(9)-C(10)-C(11)	0.0(5)
C(9)-C(10)-C(11)-C(12)	0.6(5)
C(9)-C(10)-C(11)-C(14)	-179.6(4)
C(10)-C(11)-C(12)-C(13)	-0.6(5)
C(14)-C(11)-C(12)-C(13)	179.6(3)
C(11)-C(12)-C(13)-C(8)	-0.1(5)
C(9)-C(8)-C(13)-C(12)	0.8(4)
S(2)-C(8)-C(13)-C(12)	-176.0(2)
C(6)-C(1)-S(1)-O(2)	99.2(3)
C(2)-C(1)-S(1)-O(2)	-78.2(3)
C(6)-C(1)-S(1)-O(1)	-27.8(3)
C(2)-C(1)-S(1)-O(1)	154.8(2)
C(6)-C(1)-S(1)-N(1)	-145.0(2)
C(2)-C(1)-S(1)-N(1)	37.7(3)
C(9)-C(8)-S(2)-O(4)	29.1(3)
C(13)-C(8)-S(2)-O(4)	-154.1(2)
C(9)-C(8)-S(2)-O(3)	-98.1(2)
C(13)-C(8)-S(2)-O(3)	78.7(3)
C(9)-C(8)-S(2)-N(2)	146.0(2)
C(13)-C(8)-S(2)-N(2)	-37.1(3)

Table 7. Hydrogen bonds for 08mz243_0m [\AA and deg].

D-H...A	d(D-H)	d(H...A)	d(D...A)	<(DHA)
N(1)-H(1A)...O(4)#1	0.910(19)	2.32(3)	3.049(3)	137(3)
N(1)-H(1A)...O(1)#2	0.910(19)	2.46(3)	3.226(3)	141(3)
N(1)-H(1B)...O(3)	0.901(18)	2.20(3)	2.998(3)	148(4)
N(1)-H(1B)...O(2)#2	0.901(18)	2.62(3)	3.282(3)	131(3)
N(2)-H(2A)...O(1)#3	0.895(18)	2.13(3)	2.927(3)	148(4)
N(2)-H(2B)...O(2)#2	0.905(19)	2.21(3)	2.968(3)	141(3)
N(2)-H(2B)...O(3)#2	0.905(19)	2.52(3)	3.239(3)	137(3)

Symmetry transformations used to generate equivalent atoms:

#1 $x, y+1, z$ #2 $x+1, y, z$ #3 $x+1, y-1, z$

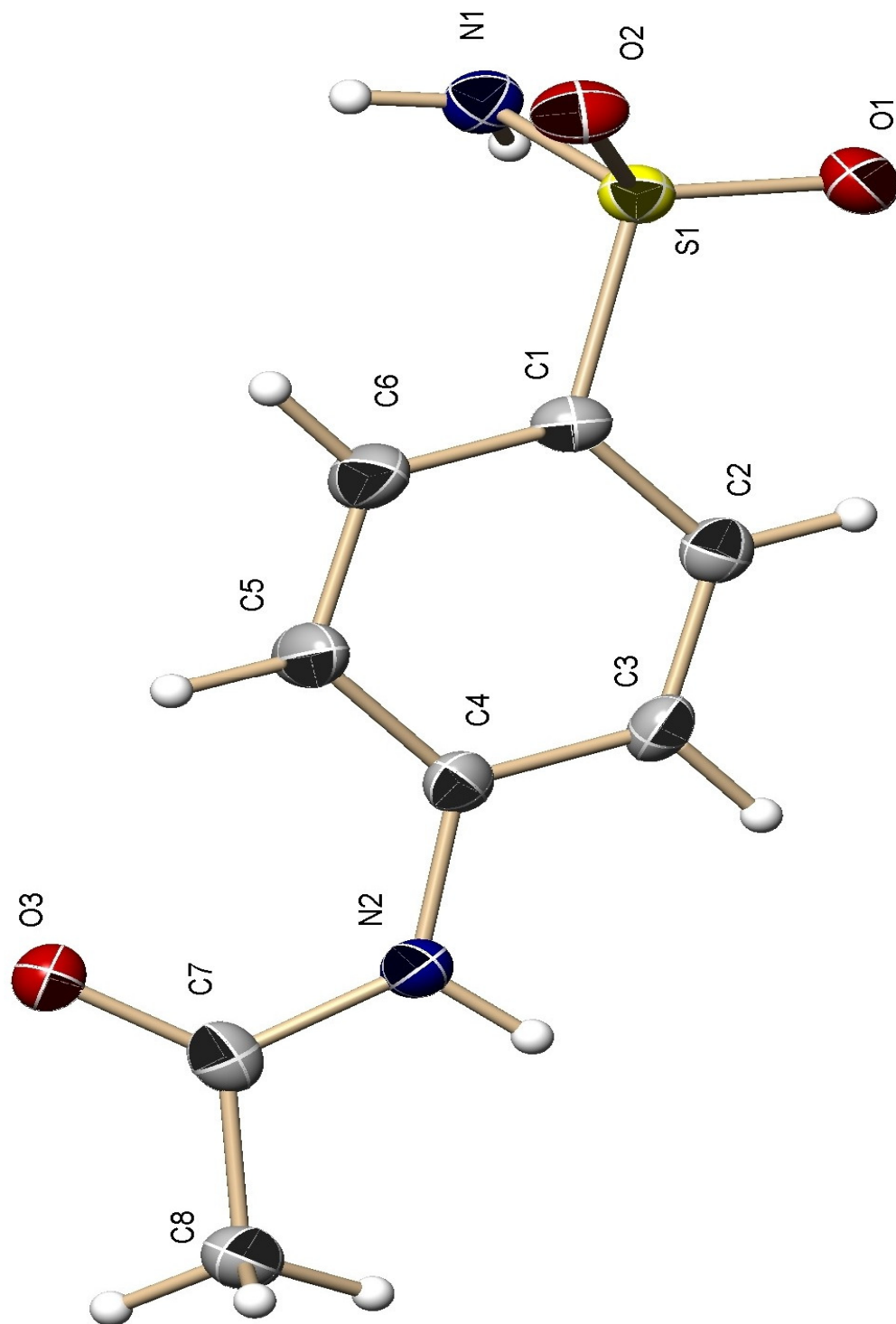


Figure 100: X-Ray crystal structure of *p*-acetamidobenzenesulfonamide (**23**).

Table 1. Crystal data and structure refinement for 08mz288_0m:

Identification code: 08mz288_0m
Empirical formula: C₈ H₁₀ N₂ O₃ S
Formula weight: 214.24
Temperature: 100(2) K
Wavelength: 0.71073 Å
Crystal system: Tetragonal
Space group: P-42₁c
Unit cell dimensions:
a = 15.2841(16) Å, $\alpha = 90^\circ$
b = 15.2841(16) Å, $\beta = 90^\circ$
c = 8.0660(17) Å, $\gamma = 90^\circ$
Volume, Z: 1884.2(5) Å³, 8
Density (calculated): 1.510 Mg/m³
Absorption coefficient: 0.326 mm⁻¹
F(000): 896
Crystal size: 0.33 × 0.11 × 0.10 mm
Crystal shape, colour: block, colourless
 θ range for data collection: 2.67 to 28.26°
Limiting indices: $-17 \leq h \leq 16$, $-3 \leq k \leq 20$, $-10 \leq l \leq 10$
Reflections collected: 4734
Independent reflections: 2188 ($R(\text{int}) = 0.0502$)
Completeness to $\theta = 28.26^\circ$: 98.0 %
Absorption correction: multi-scan
Max. and min. transmission: 0.968 and 0.699
Refinement method: Full-matrix least-squares on F^2
Data / restraints / parameters: 2188 / 0 / 135
Goodness-of-fit on F^2 : 1.085
Final R indices [$I > 2\sigma(I)$]: $R_1 = 0.0479$, $wR_2 = 0.0931$
 R indices (all data): $R_1 = 0.0686$, $wR_2 = 0.1039$
Absolute structure parameter: 0.55(12)
Largest diff. peak and hole: 0.271 and -0.292 e × Å⁻³

Refinement of F^2 against ALL reflections. The weighted R-factor wR and goodness of fit are based on F^2 , conventional R-factors R are based on F , with F set to zero for negative F^2 . The threshold expression of $F^2 > 2\sigma(F^2)$ is used only for calculating R-factors

Treatment of hydrogen atoms:

Amine H atoms were located in difference density Fourier maps and refined freely. All other hydrogen atoms were placed geometrically and all were refined with an isotropic displacement parameter 1.5 (methyl, amine) or 1.2 times (all others) that of the neighboring carbon or nitrogen atom. Methyl H atoms were allowed to rotate to best fit the experimental electron density.

Table 2. Atomic coordinates [$\times 10^4$] and equivalent isotropic displacement parameters [$\text{\AA}^2 \times 10^3$] for 08mz288_0m. $U(\text{eq})$ is defined as one third of the trace of the orthogonalized U_{ij} tensor.

	x	y	z	U(eq)
C(1)	5188(2)	2139(2)	2011(4)	23(1)
C(2)	5908(2)	2448(2)	1169(4)	23(1)
C(3)	6663(2)	1957(2)	1129(4)	24(1)
C(4)	6706(2)	1155(2)	1914(4)	22(1)
C(5)	5982(2)	840(2)	2778(4)	31(1)
C(6)	5227(2)	1340(2)	2824(4)	30(1)
C(7)	7703(2)	-137(2)	2183(4)	24(1)
C(8)	8647(2)	-388(2)	1995(4)	27(1)
N(2)	7515(2)	705(2)	1814(3)	24(1)
O(1)	4377(2)	3558(1)	1221(3)	29(1)
O(2)	3869(1)	2755(2)	3702(3)	29(1)
N(1)	3497(2)	2221(2)	933(3)	24(1)
O(3)	7137(1)	-657(1)	2663(2)	25(1)
S(1)	4206(1)	2740(1)	2030(1)	22(1)

All esds (except the esd in the dihedral angle between two l.s. planes) are estimated using the full covariance matrix. The cell esds are taken into account individually in the estimation of esds in distances, angles and torsion angles; correlations between esds in cell parameters are only used when they are defined by crystal symmetry. An approximate (isotropic) treatment of cell esds is used for estimating esds involving l.s. planes.

Table 3. Bond lengths [Å] and angles [deg] for 08mz288_0m.

C(1)-C(2)	1.376(4)	C(4)-C(5)-H(5)	120.5
C(1)-C(6)	1.388(4)	C(5)-C(6)-C(1)	120.6(3)
C(1)-S(1)	1.760(3)	C(5)-C(6)-H(6)	119.7
C(2)-C(3)	1.377(5)	C(1)-C(6)-H(6)	119.7
C(2)-H(2)	0.9500	O(3)-C(7)-N(2)	122.1(3)
C(3)-C(4)	1.380(4)	O(3)-C(7)-C(8)	122.6(3)
C(3)-H(3)	0.9500	N(2)-C(7)-C(8)	115.3(3)
C(4)-C(5)	1.394(4)	C(7)-C(8)-H(8A)	109.5
C(4)-N(2)	1.416(4)	C(7)-C(8)-H(8B)	109.5
C(5)-C(6)	1.384(5)	H(8A)-C(8)-H(8B)	109.5
C(5)-H(5)	0.9500	C(7)-C(8)-H(8C)	109.5
C(6)-H(6)	0.9500	H(8A)-C(8)-H(8C)	109.5
C(7)-O(3)	1.237(4)	H(8B)-C(8)-H(8C)	109.5
C(7)-N(2)	1.352(4)	C(7)-N(2)-C(4)	129.5(3)
C(7)-C(8)	1.501(4)	C(7)-N(2)-H(2A)	115.3
C(8)-H(8A)	0.9800	C(4)-N(2)-H(2A)	115.3
C(8)-H(8B)	0.9800	S(1)-N(1)-H(1A)	113(2)
C(8)-H(8C)	0.9800	S(1)-N(1)-H(1B)	114(3)
N(2)-H(2A)	0.8800	H(1A)-N(1)-H(1B)	115(4)
O(1)-S(1)	1.434(2)	O(1)-S(1)-O(2)	118.46(14)
O(2)-S(1)	1.443(2)	O(1)-S(1)-N(1)	107.57(14)
N(1)-S(1)	1.608(3)	O(2)-S(1)-N(1)	106.34(14)
N(1)-H(1A)	0.92(4)	O(1)-S(1)-C(1)	107.18(14)
N(1)-H(1B)	0.83(4)	O(2)-S(1)-C(1)	108.71(14)
		N(1)-S(1)-C(1)	108.22(15)
C(2)-C(1)-C(6)			
120.1(3)			
C(2)-C(1)-S(1)			
120.5(2)			
C(6)-C(1)-S(1)			
119.4(2)			
C(1)-C(2)-C(3)			
119.6(3)			
C(1)-C(2)-H(2)			
120.2			
C(3)-C(2)-H(2)			
120.2			
C(2)-C(3)-C(4)			
120.9(3)			
C(2)-C(3)-H(3)			
119.5			
C(4)-C(3)-H(3)			
119.5			
C(3)-C(4)-C(5)			
119.8(3)			
C(3)-C(4)-N(2)			
116.6(3)			
C(5)-C(4)-N(2)			
123.6(3)			
C(6)-C(5)-C(4)			
119.0(3)			
C(6)-C(5)-H(5)			
120.5			

Table 4. Anisotropic displacement parameters [$\text{\AA}^2 \times 10^3$] for 08mz288_0m. The anisotropic displacement factor exponent takes the form: $-2 \pi^2 [(h a^*)^2 U_{11} + \dots + 2 h k a^* b^* U_{12}]$

	U11	U22	U33	U23	U13	U12
C(1)	19(2)	26(2)	23(1)	-1(2)	0(1)	2(1)
C(2)	24(2)	24(2)	22(1)	0(1)	-1(1)	-2(1)
C(3)	22(2)	25(2)	27(2)	4(1)	-2(1)	-7(1)
C(4)	21(2)	21(2)	25(2)	-2(1)	-3(1)	-3(1)
C(5)	25(2)	28(2)	40(2)	13(2)	2(2)	1(1)
C(6)	24(2)	32(2)	35(2)	10(2)	4(2)	-1(1)
C(7)	30(2)	21(2)	20(1)	-2(1)	-4(2)	1(1)
C(8)	26(2)	26(2)	30(2)	-1(2)	0(2)	3(1)
N(2)	20(1)	23(1)	29(1)	5(1)	0(1)	0(1)
O(1)	28(1)	23(1)	35(1)	0(1)	-1(1)	2(1)
O(2)	25(1)	37(1)	24(1)	-4(1)	2(1)	3(1)
N(1)	22(1)	27(2)	23(1)	2(1)	-3(1)	-1(1)
O(3)	25(1)	24(1)	26(1)	0(1)	1(1)	-3(1)
S(1)	21(1)	23(1)	23(1)	0(1)	-2(1)	1(1)

Table 5. Hydrogen coordinates ($\times 10^4$) and isotropic displacement parameters ($\text{\AA}^2 \times 10^3$) for 08mz288_0m.

	x	y	z	U(eq)
H(2)	5883	2996	617	28
H(3)	7160	2173	554	29
H(5)	6006	291	3328	37
H(6)	4731	1134	3418	37
H(8A)	8942	-338	3070	41
H(8B)	8929	2	1194	41
H(8C)	8686	-993	1600	41
H(2A)	7959	1020	1460	29
H(1A)	3650(20)	2190(20)	-160(50)	37
H(1B)	3330(20)	1750(30)	1350(50)	37

Table 6. Torsion angles [deg] for 08mz288_0m.

C(6)-C(1)-C(2)-C(3)	0.4(5)
S(1)-C(1)-C(2)-C(3)	-178.2(2)
C(1)-C(2)-C(3)-C(4)	0.5(5)
C(2)-C(3)-C(4)-C(5)	-0.9(5)
C(2)-C(3)-C(4)-N(2)	-179.4(3)
C(3)-C(4)-C(5)-C(6)	0.3(5)
N(2)-C(4)-C(5)-C(6)	178.8(3)
C(4)-C(5)-C(6)-C(1)	0.6(5)
C(2)-C(1)-C(6)-C(5)	-0.9(5)
S(1)-C(1)-C(6)-C(5)	177.7(3)
O(3)-C(7)-N(2)-C(4)	1.5(5)
C(8)-C(7)-N(2)-C(4)	-177.6(3)
C(3)-C(4)-N(2)-C(7)	-166.6(3)
C(5)-C(4)-N(2)-C(7)	14.9(5)
C(2)-C(1)-S(1)-O(1)	-6.0(3)
C(6)-C(1)-S(1)-O(1)	175.4(3)
C(2)-C(1)-S(1)-O(2)	-135.1(2)
C(6)-C(1)-S(1)-O(2)	46.2(3)
C(2)-C(1)-S(1)-N(1)	109.8(3)
C(6)-C(1)-S(1)-N(1)	-68.9(3)

Table 7. Hydrogen bonds for 08mz288_0m [\AA and deg].

D-H...A	d(D-H)	d(H...A)	d(D...A)	<(DHA)
N(2)-H(2A)...O(2)#1	0.88	2.34	3.162(4)	156.3
N(1)-H(1A)...O(3)#2	0.92(4)	2.05(4)	2.941(4)	164(3)
N(1)-H(1B)...O(3)#3	0.83(4)	2.10(4)	2.933(4)	173(4)

Symmetry transformations used to generate equivalent atoms:

#1 $x+1/2, -y+1/2, -z+1/2$ #2 $y+1/2, x-1/2, z-1/2$
 #3 $-x+1, -y, z$

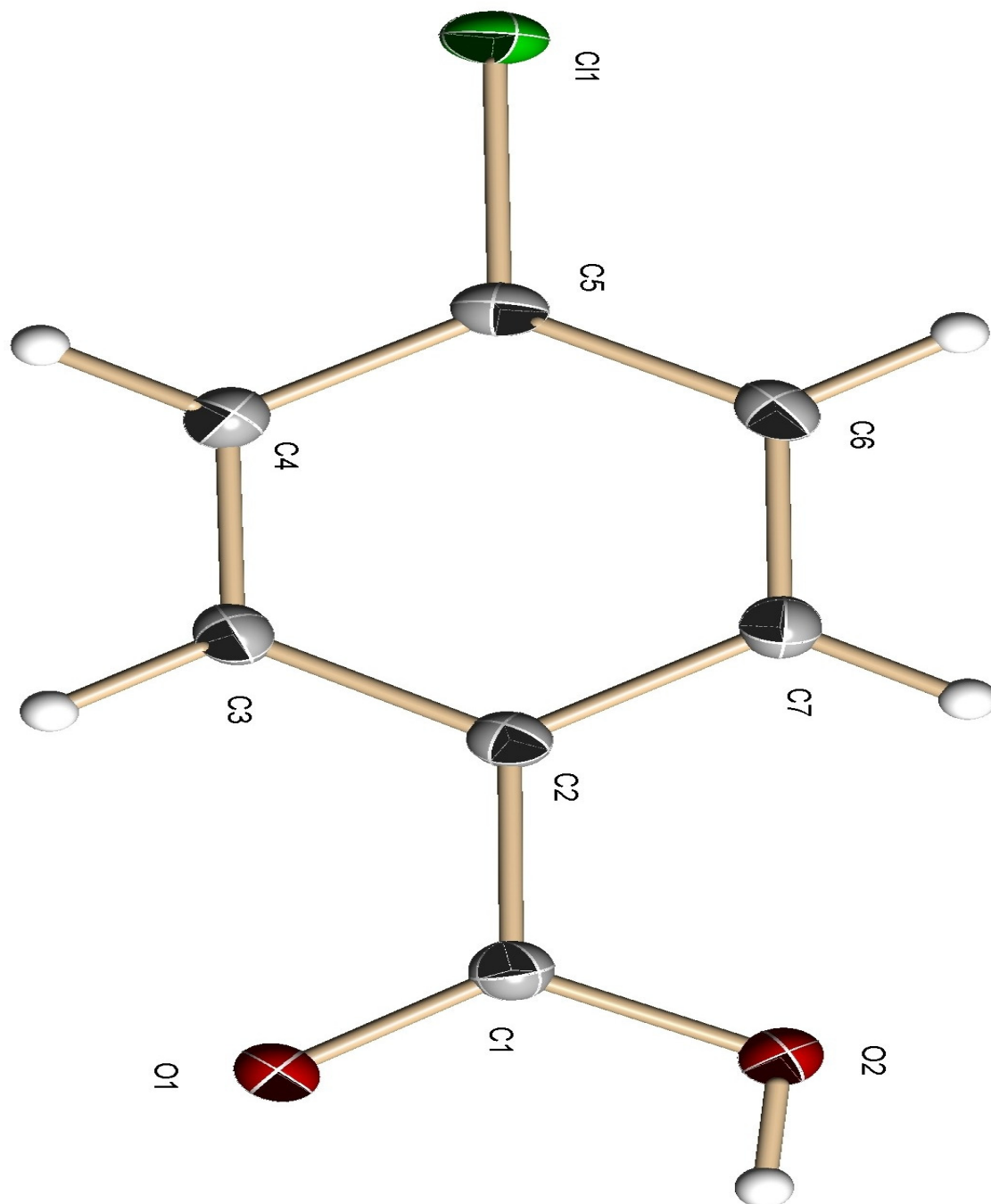


Figure 101: X-Ray crystal structure of 4-chlorobenzoic acid (26).

Table 1. Crystal data and structure refinement for 08mz367_0m:

Identification code: 08mz367_0m
 Empirical formula: C₁₇ H₂₄ Cu O₅
 Formula weight: 485.90
 Temperature: 100(2) K
 Wavelength: 0.71073 Å
 Crystal system: Triclinic
 Space group: P-1
 Unit cell dimensions:
 a = 3.7724(5) Å, α = 92.229(2)°
 b = 6.1254(9) Å, β = 94.655(2)°
 c = 14.181(2) Å, γ = 92.559(2)°
 Volume, Z: 325.98(8) Å³, 2
 Density (calculated): 1.595 Mg/m³
 Absorption coefficient: 0.507 mm⁻¹
 F(000): 160
 Crystal size: 0.55 × 0.50 × 0.17 mm
 Crystal shape, colour: block, colourless
 θ range for data collection: 1.44 to 28.28°
 Limiting indices: $-5 \leq h \leq 5$, $-8 \leq k \leq 84$, $-18 \leq l \leq 18$
 Reflections collected: 3300
 Independent reflections: 1591 ($R(\text{int}) = 0.0103$)
 Completeness to $\theta = 28.28^\circ$: 99.0 %
 Absorption correction: multi-scan
 Max. and min. transmission: 0.917 and 0.828
 Refinement method: Full-matrix least-squares on F^2
 Data / restraints / parameters: 1591 / 0 / 92
 Goodness-of-fit on F^2 : 1.043
 Final R indices [$I > 2\sigma(I)$]: $R_1 = 0.0262$, $wR_2 = 0.0728$
 R indices (all data): $R_1 = 0.0268$, $wR_2 = 0.0732$
 Largest diff. peak and hole: 0.442 and -0.219 e × Å⁻³

Refinement of F^2 against ALL reflections. The weighted R -factor wR and goodness of fit are based on F^2 , conventional R -factors R are based on F , with F set to zero for negative F^2 . The threshold expression of $F^2 > 2\sigma(F^2)$ is used only for calculating R -factors

Treatment of hydrogen atoms:

All hydrogen atoms were placed in calculated positions and were refined with an isotropic displacement parameter 1.5 (hydroxyl) or 1.2 times

(all others) that of the adjacent carbon or oxygen atom.

Table 2. Atomic coordinates [$\times 10^4$] and equivalent isotropic displacement parameters [$\text{\AA}^2 \times 10^3$] for 06rk001m. $U(\text{eq})$ is defined as one third of the trace of the orthogonalized U_{ij} tensor.

	x	y	z	U(eq)
C(1)	3985(3)	6857(2)	1050(1)	15(1)
C(2)	3192(3)	8343(2)	1847(1)	14(1)
C(3)	4031(3)	7742(2)	2777(1)	16(1)
C(4)	3351(3)	9128(2)	3531(1)	17(1)
C(5)	1852(3)	11116(2)	3342(1)	16(1)
C(6)	989(3)	11746(2)	2425(1)	16(1)
C(7)	1661(3)	10340(2)	1674(1)	16(1)
Cl(1)	1008(1)	12872(1)	4283(1)	22(1)
O(1)	5644(2)	5187(1)	1176(1)	19(1)
O(2)	2798(3)	7460(2)	208(1)	23(1)

All esds (except the esd in the dihedral angle between two l.s. planes) are estimated using the full covariance matrix. The cell esds are taken into account individually in the estimation of esds in distances, angles and torsion angles; correlations between esds in cell parameters are only used when they are defined by crystal symmetry. An approximate (isotropic) treatment of cell esds is used for estimating esds involving l.s. planes.

Table 3. Bond lengths [\AA] and angles [deg] for 08mz367_0m.

C(1)-O(1)	1.2342(14)
C(1)-O(2)	1.3136(14)
C(1)-C(2)	1.4807(15)
C(2)-C(7)	1.3979(15)
C(2)-C(3)	1.3982(15)
C(3)-C(4)	1.3875(15)
C(3)-H(3)	0.9500
C(4)-C(5)	1.3920(16)
C(4)-H(4)	0.9500
C(5)-C(6)	1.3881(16)
C(5)-Cl(1)	1.7405(11)
C(6)-C(7)	1.3893(16)
C(6)-H(6)	0.9500

C(7)-H(7)	0.9500
O(2)-H(2)	0.8400
O(1)-C(1)-O(2)	123.09(10)
O(1)-C(1)-C(2)	122.06(10)
O(2)-C(1)-C(2)	114.85(10)
C(7)-C(2)-C(3)	120.09(10)
C(7)-C(2)-C(1)	120.55(10)
C(3)-C(2)-C(1)	119.36(10)
C(4)-C(3)-C(2)	120.14(10)
C(4)-C(3)-H(3)	119.9
C(2)-C(3)-H(3)	119.9
C(3)-C(4)-C(5)	118.70(10)
C(3)-C(4)-H(4)	120.7
C(5)-C(4)-H(4)	120.7
C(6)-C(5)-C(4)	122.22(10)
C(6)-C(5)-Cl(1)	118.70(9)
C(4)-C(5)-Cl(1)	119.08(9)
C(5)-C(6)-C(7)	118.60(10)
C(5)-C(6)-H(6)	120.7
C(7)-C(6)-H(6)	120.7
C(6)-C(7)-C(2)	120.25(10)
C(6)-C(7)-H(7)	119.9
C(2)-C(7)-H(7)	119.9
C(1)-O(2)-H(2)	109.5

Table 4. Anisotropic displacement parameters [$\text{\AA}^2 \times 10^3$] for 08mz367_0m. The anisotropic displacement factor exponent takes the form: $-2 \pi^2 [(h a^*)^2 U_{11} + \dots + 2 h k a^* b^* U_{12}]$

	U11	U22	U33	U23	U13	U12
C(1)	16(1)	15(1)	15(1)	1(1)	2(1)	0(1)
C(2)	14(1)	14(1)	16(1)	-1(1)	1(1)	1(1)
C(3)	16(1)	14(1)	17(1)	2(1)	1(1)	2(1)
C(4)	19(1)	18(1)	15(1)	1(1)	1(1)	2(1)
C(5)	15(1)	16(1)	17(1)	-3(1)	3(1)	1(1)
C(6)	16(1)	14(1)	20(1)	1(1)	1(1)	3(1)
C(7)	17(1)	16(1)	16(1)	2(1)	0(1)	2(1)
Cl(1)	26(1)	21(1)	19(1)	-5(1)	4(1)	6(1)
O(1)	25(1)	16(1)	17(1)	0(1)	1(1)	7(1)
O(2)	33(1)	23(1)	14(1)	-1(1)	0(1)	12(1)

Table 5. Hydrogen coordinates ($\times 10^4$) and isotropic displacement parameters ($\text{\AA}^2 \times 10^3$) for 08mz367_0m.

	x	y	z	U(eq)
H(3)	5070	6383	2892	19
H(4)	3898	8727	4165	21
H(6)	-39	13110	2313	20
H(7)	1077	10738	1042	19
H(2)	3358	6550	-206	34

Table6. Torsion angles [deg] for 08mz367_0m.

O(1)-C(1)-C(2)-C(7)	172.85(10)
O(2)-C(1)-C(2)-C(7)	-7.00(15)
O(1)-C(1)-C(2)-C(3)	-6.33(16)
O(2)-C(1)-C(2)-C(3)	173.82(10)
C(7)-C(2)-C(3)-C(4)	-0.06(17)
C(1)-C(2)-C(3)-C(4)	179.12(10)
C(2)-C(3)-C(4)-C(5)	-0.46(17)
C(3)-C(4)-C(5)-C(6)	0.60(18)
C(3)-C(4)-C(5)-Cl(1)	-179.69(8)
C(4)-C(5)-C(6)-C(7)	-0.19(17)
Cl(1)-C(5)-C(6)-C(7)	-179.91(8)
C(5)-C(6)-C(7)-C(2)	-0.35(17)
C(3)-C(2)-C(7)-C(6)	0.47(17)
C(1)-C(2)-C(7)-C(6)	-178.70(10)

Table 7. Hydrogen bonds for 08mz367_0m [\AA and deg].

D-H...A	d(D-H)	d(H...A)	d(D...A)	<(DHA)
O(2)-H(2)...O(1)#1	0.84	1.78	2.6174(12)	173.9

Symmetry transformations used to generate equivalent atoms:

#1 -x+1, -y+1, -z

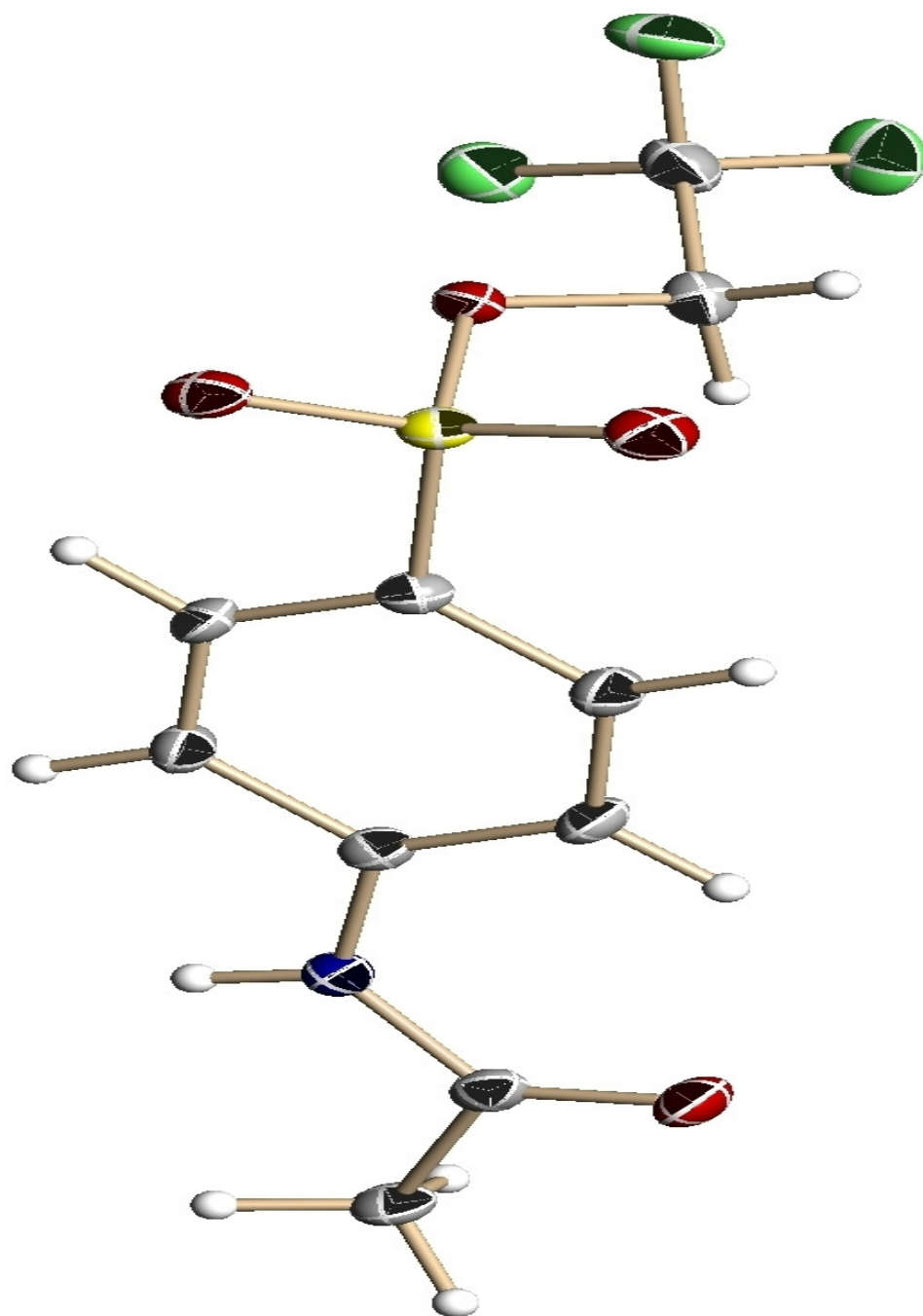


Figure 102: X-Ray crystal structure of 2,2,2-trifluoroethyl acedamidobenzenesulfonate (37).

Table 1. Crystal data and structure refinement for 08mz450_0m:

Identification code: 08mz450_0m
 Empirical formula: C10 H10 F3 N O4 S
 Formula weight: 297.26
 Temperature: 100(2) K
 Wavelength: 0.71073 Å
 Crystal system: Orthorhombic
 Space group: Pca2₁
 Unit cell dimensions:
 a = 18.2745(14) Å, $\alpha = 90^\circ$
 b = 5.2083(4) Å, $\beta = 90^\circ$
 c = 25.469(2) Å, $\gamma = 90^\circ$
 Volume, Z: 2424.1(3) Å³, 8
 Density (calculated): 1.629 Mg/m³
 Absorption coefficient: 0.316 mm⁻¹
 F(000): 1216
 Crystal size: 0.55 × 0.20 × 0.10 mm
 Crystal shape, colour: block, colourless
 θ range for data collection: 1.60 to 28.28°
 Limiting indices: $-23 \leq h \leq 17$, $-6 \leq k \leq 6$, $13 \leq l \leq 33$
 Reflections collected: 7614
 Independent reflections: 3963 ($R(\text{int}) = 0.0254$)
 Completeness to $\theta = 28.28^\circ$: 99.3 %
 Absorption correction: multi-scan
 Max. and min. transmission: 0.969 and 0.856
 Refinement method: Full-matrix least-squares on F^2
 Data / restraints / parameters: 3963 / 1 / 346
 Goodness-of-fit on F^2 : 1.040
 Final R indices [$I > 2\sigma(I)$]: R1 = 0.0414, wR2 = 0.1016
 R indices (all data): R1 = 0.0463, wR2 = 0.1062
 Absolute structure parameter: 0.49(10)
 Largest diff. peak and hole: 0.556 and -0.463 e × Å⁻³

Refinement of F^2 against ALL reflections. The weighted R-factor wR and goodness of fit are based on F^2 , conventional R-factors R are based on F , with F set to zero for negative F^2 . The threshold expression of

$F^2 > 2\sigma(F^2)$ is used only for calculating R-factors

Treatment of hydrogen atoms:

All H atoms were initially located in the difference density Fourier map, but ultimately they were placed geometrically and were refined with an isotropic displacement parameter 1.5 (methyl) or 1.2 times (all others) that of the adjacent oxygen or carbon atom

Table 2. Atomic coordinates [$\times 10^4$] and equivalent isotropic displacement parameters [$\text{\AA}^2 \times 10^3$] for 08mz450_0m. U(eq) is defined as one third of the trace of the orthogonalized U_{ij} tensor.

	x	y	z	U(eq)
C(1)	-303(2)	7365(6)	1947(1)	19(1)
C(2)	-264(2)	9554(7)	2332(1)	23(1)
C(3)	478(2)	4878(6)	1326(1)	17(1)
C(4)	1207(2)	4679(7)	1163(1)	20(1)
C(5)	1399(2)	2958(6)	779(1)	19(1)
C(6)	878(2)	1347(6)	564(1)	18(1)
C(7)	156(2)	1519(6)	723(1)	23(1)
C(8)	-53(2)	3300(6)	1102(1)	22(1)
C(9)	635(2)	2077(6)	-671(1)	22(1)
C(10)	924(2)	3523(7)	-1137(2)	26(1)
C(11)	2339(2)	341(6)	1820(1)	19(1)
C(12)	2846(2)	-907(7)	1429(1)	24(1)
C(13)	2313(2)	3941(6)	2466(1)	18(1)
C(14)	1567(2)	3818(7)	2593(1)	20(1)
C(15)	1293(2)	5498(6)	2969(1)	20(1)
C(16)	1745(2)	7250(6)	3213(1)	19(1)
C(17)	2491(2)	7385(6)	3086(1)	21(1)
C(18)	2769(2)	5730(6)	2713(1)	19(1)
C(19)	1828(2)	6354(8)	4432(2)	30(1)
C(20)	1569(2)	5082(10)	4895(2)	47(1)
F(1)	384(1)	4817(4)	-1373(1)	39(1)
F(2)	1438(1)	5239(4)	-1008(1)	33(1)
F(3)	1222(1)	1968(5)	-1499(1)	36(1)
F(4)	1358(2)	6793(9)	5270(1)	81(1)
F(5)	2065(2)	3594(6)	5113(2)	67(1)
F(6)	977(2)	3624(7)	4797(2)	79(1)
N(1)	339(1)	6740(5)	1710(1)	19(1)
N(2)	2640(1)	2371(5)	2082(1)	18(1)
O(1)	-881(1)	6231(5)	1851(1)	25(1)
O(2)	1849(1)	-1771(4)	185(1)	23(1)
O(3)	548(1)	-2494(4)	-34(1)	26(1)
O(4)	1274(1)	964(4)	-424(1)	20(1)
O(5)	1716(1)	-429(4)	1891(1)	22(1)
O(6)	683(1)	10196(5)	3538(1)	25(1)
O(7)	1946(1)	11090(5)	3839(1)	34(1)

O(8)	1215(1)	7497(5)	4172(1)	30(1)
S(1)	1391(1)	9317(2)	3691(1)	23(1)
S(2)	1141(1)	-802(1)	73(1)	19(1)

All esds (except the esd in the dihedral angle between two l.s. planes)

are estimated using the full covariance matrix. The cell esds are taken

into account individually in the estimation of esds in distances, angles

and torsion angles; correlations between esds in cell parameters are only

used when they are defined by crystal symmetry. An approximate (isotropic)

treatment of cell esds is used for estimating esds involving l.s. planes.

Table 3. Bond lengths [\AA] and angles [deg] for 08mz450_0m.

C(1)-O(1)	1.233(4)	C(11)-O(5)	1.222(4)
C(1)-N(1)	1.359(4)	C(11)-N(2)	1.365(4)
C(1)-C(2)	1.505(4)	C(11)-C(12)	1.507(4)
C(2)-H(2A)	0.9800	C(12)-H(12A)	0.9800
C(2)-H(2B)	0.9800	C(12)-H(12B)	0.9800
C(2)-H(2C)	0.9800	C(12)-H(12C)	0.9800
C(3)-C(8)	1.394(4)	C(13)-C(18)	1.398(4)
C(3)-C(4)	1.398(4)	C(13)-C(14)	1.403(4)
C(3)-N(1)	1.402(4)	C(13)-N(2)	1.409(4)
C(4)-C(5)	1.373(5)	C(14)-C(15)	1.391(4)
C(4)-H(4)	0.9500	C(14)-H(14)	0.9500
C(5)-C(6)	1.382(4)	C(15)-C(16)	1.379(5)
C(5)-H(5)	0.9500	C(15)-H(15)	0.9500
C(6)-C(7)	1.384(4)	C(16)-C(17)	1.403(5)
C(6)-S(2)	1.747(3)	C(16)-S(1)	1.748(3)
C(7)-C(8)	1.391(5)	C(17)-C(18)	1.380(5)
C(7)-H(7)	0.9500	C(17)-H(17)	0.9500
C(8)-H(8)	0.9500	C(18)-H(18)	0.9500
C(9)-O(4)	1.449(4)	C(19)-O(8)	1.431(4)
C(9)-C(10)	1.502(5)	C(19)-C(20)	1.433(6)
C(9)-H(9A)	0.9900	C(19)-H(19A)	0.9900
C(9)-H(9B)	0.9900	C(19)-H(19B)	0.9900
C(10)-F(1)	1.337(4)	C(20)-F(5)	1.314(5)
C(10)-F(2)	1.338(4)	C(20)-F(6)	1.346(5)
C(10)-F(3)	1.342(4)	C(20)-F(4)	1.363(6)

N(1)-H(1)	0.8800	C(7)-C(8)-C(3)	119.0(3)
N(2)-H(2)	0.8800	C(7)-C(8)-H(8)	120.5
O(2)-S(2)	1.418(2)	C(3)-C(8)-H(8)	120.5
O(3)-S(2)	1.424(2)	O(4)-C(9)-C(10)	105.1(3)
O(4)-S(2)	1.584(2)	O(4)-C(9)-H(9A)	110.7
O(6)-S(1)	1.427(2)	C(10)-C(9)-H(9A)	110.7
O(7)-S(1)	1.422(3)	O(4)-C(9)-H(9B)	110.7
O(8)-S(1)	1.581(3)	C(10)-C(9)-H(9B)	110.7
		H(9A)-C(9)-H(9B)	108.8
O(1)-C(1)-N(1)		F(1)-C(10)-F(2)	107.0(3)
122.5(3)		F(1)-C(10)-F(3)	107.2(3)
O(1)-C(1)-C(2)		F(2)-C(10)-F(3)	106.7(3)
122.2(3)		F(1)-C(10)-C(9)	110.4(3)
N(1)-C(1)-C(2)		F(2)-C(10)-C(9)	112.8(3)
115.4(3)		F(3)-C(10)-C(9)	112.5(3)
C(1)-C(2)-H(2A)		O(5)-C(11)-N(2)	123.9(3)
109.5		O(5)-C(11)-C(12)	121.9(3)
C(1)-C(2)-H(2B)		N(2)-C(11)-C(12)	114.2(3)
109.5		C(11)-C(12)-H(12A)	109.5
H(2A)-C(2)-H(2B)		C(11)-C(12)-H(12B)	109.5
109.5		H(12A)-C(12)-H(12B)	109.5
C(1)-C(2)-H(2C)		C(11)-C(12)-H(12C)	109.5
109.5		H(12A)-C(12)-H(12C)	109.5
H(2A)-C(2)-H(2C)		H(12B)-C(12)-H(12C)	109.5
109.5		C(18)-C(13)-C(14)	120.4(3)
H(2B)-C(2)-H(2C)		C(18)-C(13)-N(2)	116.5(3)
109.5		C(14)-C(13)-N(2)	123.0(3)
C(8)-C(3)-C(4)		C(15)-C(14)-C(13)	118.6(3)
119.9(3)		C(15)-C(14)-H(14)	120.7
C(8)-C(3)-N(1)		C(13)-C(14)-H(14)	120.7
124.5(3)		C(16)-C(15)-C(14)	120.8(3)
C(4)-C(3)-N(1)		C(16)-C(15)-H(15)	119.6
115.6(3)		C(14)-C(15)-H(15)	119.6
C(5)-C(4)-C(3)		C(15)-C(16)-C(17)	120.7(3)
120.2(3)		C(15)-C(16)-S(1)	120.0(2)
C(5)-C(4)-H(4)		C(17)-C(16)-S(1)	119.3(2)
119.9		C(18)-C(17)-C(16)	119.1(3)
C(3)-C(4)-H(4)		C(18)-C(17)-H(17)	120.5
119.9		C(16)-C(17)-H(17)	120.5
C(4)-C(5)-C(6)		C(17)-C(18)-C(13)	120.4(3)
120.1(3)		C(17)-C(18)-H(18)	119.8
C(4)-C(5)-H(5)		C(13)-C(18)-H(18)	119.8
119.9		O(8)-C(19)-C(20)	108.4(3)
C(6)-C(5)-H(5)		O(8)-C(19)-H(19A)	110.0
119.9		C(20)-C(19)-H(19A)	110.0
C(5)-C(6)-C(7)		O(8)-C(19)-H(19B)	110.0
120.2(3)		C(20)-C(19)-H(19B)	110.0
C(5)-C(6)-S(2)		H(19A)-C(19)-H(19B)	108.4
118.9(2)		F(5)-C(20)-F(6)	107.4(4)
C(7)-C(6)-S(2)		F(5)-C(20)-F(4)	106.6(4)
120.9(2)		F(6)-C(20)-F(4)	105.7(4)
C(6)-C(7)-C(8)		F(5)-C(20)-C(19)	113.1(4)
120.5(3)		F(6)-C(20)-C(19)	112.0(4)
C(6)-C(7)-H(7)		F(4)-C(20)-C(19)	111.6(4)
119.7		C(1)-N(1)-C(3)	129.2(3)
C(8)-C(7)-H(7)		C(1)-N(1)-H(1)	115.4
119.7		C(3)-N(1)-H(1)	115.4

C(11)-N(2)-C(13)
128.2(3)
C(11)-N(2)-H(2)
115.9
C(13)-N(2)-H(2)
115.9
C(9)-O(4)-S(2)
117.09(19)
C(19)-O(8)-S(1)
116.7(2)
O(7)-S(1)-O(6)
120.70(16)
O(7)-S(1)-O(8)
109.21(17)
O(6)-S(1)-O(8)
102.69(14)
O(7)-S(1)-C(16)
108.70(16)
O(6)-S(1)-C(16)
110.03(16)
O(8)-S(1)-C(16)
104.16(14)
O(2)-S(2)-O(3)
120.88(15)
O(2)-S(2)-O(4)
103.19(13)
O(3)-S(2)-O(4)
108.92(14)
O(2)-S(2)-C(6)
109.50(15)
O(3)-S(2)-C(6)
108.91(14)
O(4)-S(2)-C(6)
104.07(14)

Table 4. Anisotropic displacement parameters [$\text{\AA}^2 \times 10^3$] for 08mz450_0m. The anisotropic displacement factor exponent takes the form: $-2 \pi^2 [(h a^*)^2 U_{11} + \dots + 2 h k a^* b^* U_{12}]$

	U11	U22	U33	U23	U13	U12
C(1)	19(2)	23(2)	17(2)	4(1)	2(1)	1(1)
C(2)	20(2)	27(2)	22(2)	-7(1)	5(1)	4(1)
C(3)	19(1)	16(1)	17(1)	3(1)	2(1)	-1(1)
C(4)	14(1)	21(2)	24(2)	-2(1)	-1(1)	-1(1)
C(5)	12(1)	23(2)	22(2)	0(1)	2(1)	2(1)
C(6)	19(1)	18(2)	17(1)	-1(1)	2(1)	1(1)
C(7)	18(2)	26(2)	24(2)	-6(1)	1(1)	-4(1)
C(8)	14(1)	27(2)	25(2)	-3(1)	5(1)	0(1)
C(9)	21(2)	21(2)	23(2)	-1(1)	-4(1)	1(1)
C(10)	27(2)	30(2)	21(2)	-1(1)	-7(1)	2(1)
C(11)	22(2)	19(2)	16(1)	2(1)	2(1)	3(1)
C(12)	26(2)	25(2)	20(2)	-3(1)	6(1)	2(1)
C(13)	18(2)	18(2)	17(2)	3(1)	1(1)	-2(1)
C(14)	14(1)	25(2)	22(2)	-6(1)	-1(1)	-1(1)
C(15)	17(2)	22(2)	20(2)	-2(1)	3(1)	0(1)
C(16)	18(2)	19(2)	19(2)	-2(1)	2(1)	2(1)
C(17)	21(2)	21(2)	20(2)	-2(1)	-4(1)	-3(1)
C(18)	14(1)	22(2)	21(2)	3(1)	1(1)	-3(1)
C(19)	30(2)	35(2)	25(2)	-9(2)	-6(2)	13(2)
C(20)	40(2)	56(3)	45(3)	14(2)	-9(2)	-3(2)
F(1)	35(1)	39(1)	42(1)	13(1)	-9(1)	7(1)
F(2)	34(1)	35(1)	29(1)	4(1)	-1(1)	-8(1)
F(3)	48(1)	43(1)	19(1)	-4(1)	3(1)	7(1)
F(4)	70(2)	140(3)	31(2)	4(2)	15(2)	24(2)
F(5)	40(1)	82(2)	79(2)	42(2)	-21(2)	-3(1)
F(6)	40(2)	99(3)	99(3)	57(2)	-19(2)	-25(2)
N(1)	17(1)	22(1)	18(1)	-4(1)	1(1)	-2(1)
N(2)	14(1)	20(1)	19(1)	-1(1)	3(1)	-2(1)
O(1)	15(1)	31(1)	30(1)	-7(1)	5(1)	0(1)
O(2)	24(1)	23(1)	22(1)	0(1)	3(1)	7(1)
O(3)	29(1)	22(1)	27(1)	-7(1)	2(1)	-2(1)
O(4)	18(1)	26(1)	16(1)	0(1)	0(1)	2(1)
O(5)	19(1)	23(1)	24(1)	-2(1)	-1(1)	-3(1)
O(6)	22(1)	26(1)	28(1)	-1(1)	1(1)	3(1)
O(7)	27(1)	34(1)	40(2)	-16(1)	-2(1)	-4(1)
O(8)	24(1)	42(2)	23(1)	-6(1)	0(1)	9(1)
S(1)	21(1)	24(1)	25(1)	-7(1)	1(1)	2(1)
S(2)	21(1)	19(1)	18(1)	-2(1)	3(1)	1(1)

Table 5. Hydrogen coordinates ($\times 10^4$) and isotropic displacement parameters ($\text{\AA}^2 \times 10^3$) for 08mz450_0m.

	x	y	z	U(eq)
H(2A)	-365	11172	2149	35
H(2B)	227	9621	2486	35
H(2C)	-627	9294	2610	35
H(4)	1570	5739	1319	23
H(5)	1891	2876	660	23
H(7)	-200	413	573	28
H(8)	-551	3439	1206	26
H(9A)	379	3251	-426	26
H(9B)	289	720	-784	26
H(12A)	2992	-2602	1559	36
H(12B)	3281	167	1382	36
H(12C)	2593	-1099	1092	36
H(14)	1255	2612	2425	24
H(15)	789	5438	3058	24
H(17)	2800	8598	3254	25
H(18)	3273	5807	2623	23
H(19A)	2189	7692	4528	36
H(19B)	2070	5104	4196	36
H(1)	722	7630	1814	23
H(2)	3096	2746	2000	21

Table 6. Torsion angles [deg] for 07mz242m.

C(8)-C(3)-C(4)-C(5)	0.9(5)
N(1)-C(3)-C(4)-C(5)	-178.4(3)
C(3)-C(4)-C(5)-C(6)	-2.4(5)
C(4)-C(5)-C(6)-C(7)	2.2(5)
C(4)-C(5)-C(6)-S(2)	179.5(3)
C(5)-C(6)-C(7)-C(8)	-0.4(5)
S(2)-C(6)-C(7)-C(8)	-177.7(3)
C(6)-C(7)-C(8)-C(3)	-1.1(5)
C(4)-C(3)-C(8)-C(7)	0.9(5)
N(1)-C(3)-C(8)-C(7)	-179.9(3)
O(4)-C(9)-C(10)-F(1)	-174.9(3)
O(4)-C(9)-C(10)-F(2)	-55.3(4)
O(4)-C(9)-C(10)-F(3)	65.5(3)
C(18)-C(13)-C(14)-C(15)	-0.3(5)
N(2)-C(13)-C(14)-C(15)	-178.3(3)
C(13)-C(14)-C(15)-C(16)	0.0(5)
C(14)-C(15)-C(16)-C(17)	0.3(5)
C(14)-C(15)-C(16)-S(1)	-179.2(3)
C(15)-C(16)-C(17)-C(18)	-0.2(5)
S(1)-C(16)-C(17)-C(18)	179.3(3)
C(16)-C(17)-C(18)-C(13)	-0.1(5)
C(14)-C(13)-C(18)-C(17)	0.4(5)
N(2)-C(13)-C(18)-C(17)	178.5(3)

O(8)-C(19)-C(20)-F(5)	168.7(4)
O(8)-C(19)-C(20)-F(6)	47.1(5)
O(8)-C(19)-C(20)-F(4)	-71.1(4)
O(1)-C(1)-N(1)-C(3)	2.0(5)
C(2)-C(1)-N(1)-C(3)	-177.6(3)
C(8)-C(3)-N(1)-C(1)	1.3(5)
C(4)-C(3)-N(1)-C(1)	-179.4(3)
O(5)-C(11)-N(2)-C(13)	-0.4(5)
C(12)-C(11)-N(2)-C(13)	179.6(3)
C(18)-C(13)-N(2)-C(11)	173.5(3)
C(14)-C(13)-N(2)-C(11)	-8.5(5)
C(10)-C(9)-O(4)-S(2)	-177.5(2)
C(20)-C(19)-O(8)-S(1)	172.1(3)
C(19)-O(8)-S(1)-O(7)	-48.6(3)
C(19)-O(8)-S(1)-O(6)	-177.8(2)
C(19)-O(8)-S(1)-C(16)	67.4(3)
C(15)-C(16)-S(1)-O(7)	-174.0(3)
C(17)-C(16)-S(1)-O(7)	6.5(3)
C(15)-C(16)-S(1)-O(6)	-39.8(3)
C(17)-C(16)-S(1)-O(6)	140.7(3)
C(15)-C(16)-S(1)-O(8)	69.7(3)
C(17)-C(16)-S(1)-O(8)	-109.8(3)
C(9)-O(4)-S(2)-O(2)	174.4(2)
C(9)-O(4)-S(2)-O(3)	44.8(2)
C(9)-O(4)-S(2)-C(6)	-71.2(2)
C(5)-C(6)-S(2)-O(2)	37.6(3)
C(7)-C(6)-S(2)-O(2)	-145.0(3)
C(5)-C(6)-S(2)-O(3)	171.8(3)
C(7)-C(6)-S(2)-O(3)	-10.9(3)
C(5)-C(6)-S(2)-O(4)	-72.1(3)
C(7)-C(6)-S(2)-O(4)	105.2(3)

Symmetry transformations used to generate equivalent atoms:

#1 -x+1, -y, -z+1

Table 7. Hydrogen bonds for 08mz450_0m [\AA and deg].

D-H...A	d(D-H)	d(H...A)	d(D...A)	<(DHA)
N(1)-H(1)...O(5)#1	0.88	2.09	2.952(3)	167.3
N(2)-H(2)...O(1)#2	0.88	1.98	2.860(3)	176.2

Symmetry transformations used to generate equivalent atoms:

#1 x, y+1, z #2 x+1/2, -y+1, z

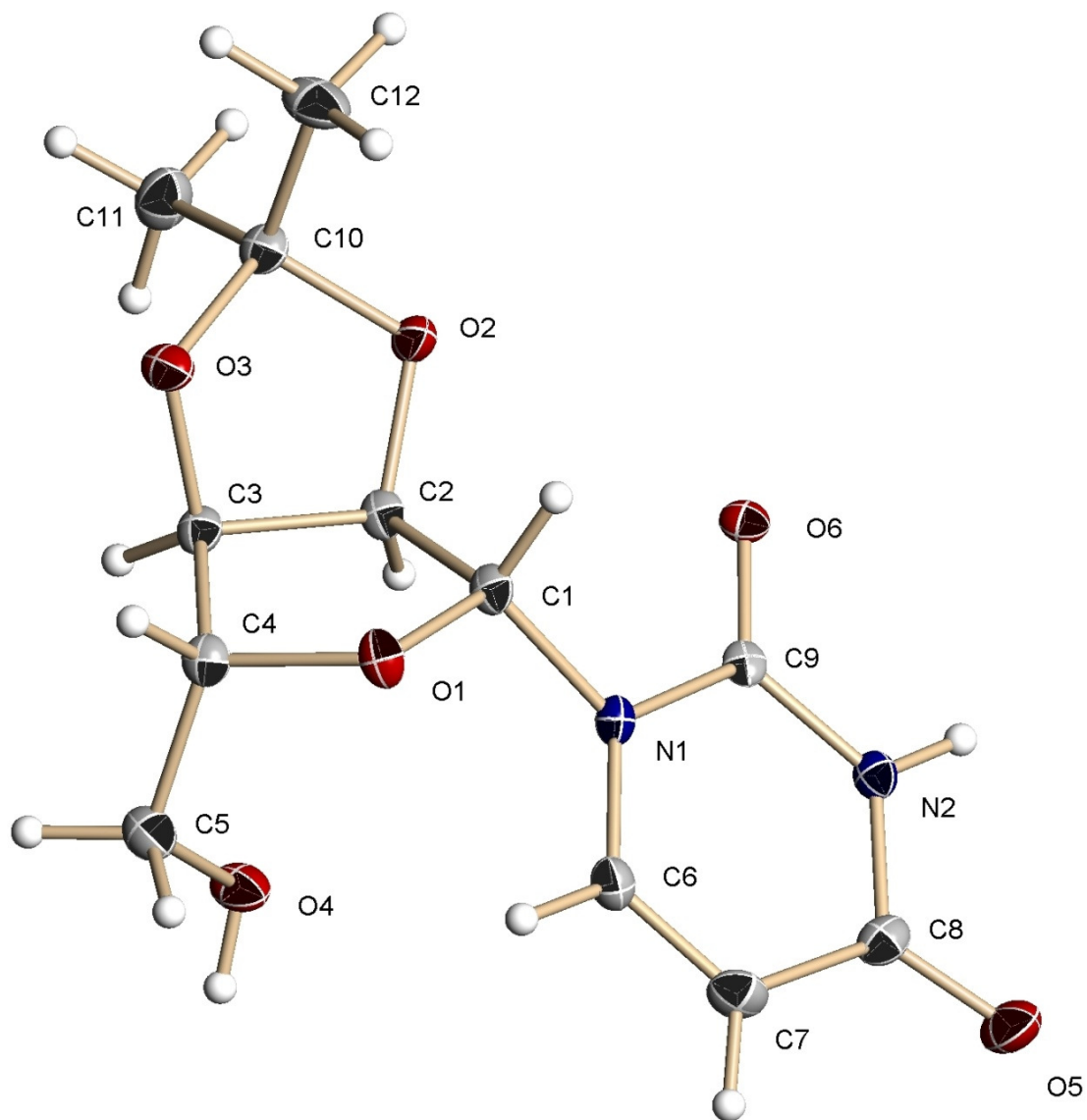


Figure 103: X-Ray crystal structure of 2',3'-*O*-isopropylidene uridine (**38**).

Table 1. Crystal data and structure refinement for 08mz108_0m:

Identification code: 08mz108_0m
 Empirical formula: C12 H16 N2 O6
 Formula weight: 284.27
 Temperature: 100(2) K
 Wavelength: 0.71073 Å
 Crystal system: Orthorhombic
 Space group: P2₁2₁2₁
 Unit cell dimensions:
 a = 5.1537(15) Å, α = 90°
 b = 12.598(4) Å, β = 90°
 c = 19.834(6) Å, γ = 90°
 Volume, Z: 1287.8(7) Å³, 4
 Density (calculated): 1.466 Mg/m³
 Absorption coefficient: 0.119 mm⁻¹
 F(000): 600
 Crystal size: 0.28 × 0.19 × 0.15 mm
 Crystal shape, colour: plate, colourless
 θ range for data collection: 1.91 to 28.28°
 Limiting indices: $-6 \leq h \leq 6$, $-7 \leq k \leq 16$, $-25 \leq l \leq 25$
 Reflections collected: 6408
 Independent reflections: 1850 (R(int) = 0.0554)
 Completeness to $\theta = 28.28^\circ$: 98.7 %
 Absorption correction: multi-scan
 Max. and min. transmission: 0.982 and 0.623
 Refinement method: Full-matrix least-squares on F^2
 Data / restraints / parameters: 1850 / 0 / 184
 Goodness-of-fit on F^2 : 1.096
 Final R indices [$I > 2\sigma(I)$]: R1 = 0.0531, wR2 = 0.1313
 R indices (all data): R1 = 0.0608, wR2 = 0.1377
 Largest diff. peak and hole: 0.425 and -0.354 e × Å⁻³

Refinement of F^2 against ALL reflections. The weighted R-factor wR and goodness of fit are based on F^2 , conventional R-factors R are based on F , with F set to zero for negative F^2 . The threshold expression of $F^2 > 2\sigma(F^2)$ is used only for calculating R-factors

Treatment of hydrogen atoms:

All hydrogen atoms were placed in calculated positions and were refined

with an isotropic displacement parameter 1.5 (methyl) or 1.2 times (all others) that of the adjacent carbon or nitrogen atom.

Table 2. Atomic coordinates [$\times 10^4$] and equivalent isotropic displacement parameters [$\text{\AA}^2 \times 10^3$] for 08mz108_0m. U(eq) is defined as one third of the trace of the orthogonalized U_{ij} tensor.

	x	y	z	U(eq)
C(1)	244(6)	5816(2)	666(1)	14(1)
C(2)	1307(6)	4873(2)	259(1)	14(1)
C(3)	-442(6)	3949(2)	465(1)	14(1)
C(4)	-1739(6)	4290(2)	1121(1)	16(1)
C(5)	-503(6)	3837(3)	1743(2)	20(1)
C(6)	2252(6)	6507(2)	1737(2)	17(1)
C(7)	3910(6)	7147(3)	2065(2)	19(1)
C(8)	5696(6)	7793(2)	1695(2)	17(1)
C(9)	4077(5)	6938(2)	662(1)	12(1)
C(10)	-1040(6)	4273(2)	-664(1)	16(1)
C(11)	354(7)	3352(3)	-995(2)	25(1)
C(12)	-2968(7)	4824(3)	-1113(2)	26(1)
N(1)	2276(5)	6406(2)	1051(1)	14(1)
N(2)	5646(5)	7632(2)	1006(1)	14(1)
O(1)	-1652(4)	5438(2)	1113(1)	16(1)
O(2)	844(4)	5032(2)	-438(1)	16(1)
O(3)	-2332(4)	3923(2)	-60(1)	17(1)
O(4)	2203(4)	4047(2)	1745(1)	20(1)
O(5)	7178(5)	8464(2)	1937(1)	24(1)
O(6)	4222(4)	6814(2)	54(1)	14(1)

All esds (except the esd in the dihedral angle between two l.s. planes) are estimated using the full covariance matrix. The cell esds are taken into account individually in the estimation of esds in distances, angles and torsion angles; correlations between esds in cell parameters are only used when they are defined by crystal symmetry. An approximate (isotropic) treatment of cell esds is used for estimating esds involving l.s. planes.

Table 3. Bond lengths [\AA] and angles [deg] for 08mz108_0m.

C(1)-O(1)	1.402(3)
C(1)-N(1)	1.495(4)
C(1)-C(2)	1.538(4)
C(1)-H(1)	0.9800
C(2)-O(2)	1.417(3)
C(2)-C(3)	1.528(4)
C(2)-H(2)	0.9800
C(3)-O(3)	1.426(3)
C(3)-C(4)	1.525(4)
C(3)-H(3)	0.9800
C(4)-O(1)	1.448(4)
C(4)-C(5)	1.500(4)
C(4)-H(4)	0.9800
C(5)-O(4)	1.420(4)
C(5)-H(5A)	0.9700
C(5)-H(5B)	0.9700
C(6)-C(7)	1.343(4)
C(6)-N(1)	1.366(4)
C(6)-H(6)	0.9300
C(7)-C(8)	1.432(4)
C(7)-H(7)	0.9300
C(8)-O(5)	1.236(4)
C(8)-N(2)	1.382(4)
C(9)-O(6)	1.218(3)
C(9)-N(2)	1.373(4)
C(9)-N(1)	1.380(4)
C(10)-O(2)	1.434(3)
C(10)-O(3)	1.440(3)
C(10)-C(12)	1.505(4)
C(10)-C(11)	1.515(4)
C(11)-H(11A)	0.9600
C(11)-H(11B)	0.9600
C(11)-H(11C)	0.9600
C(12)-H(12A)	0.9600
C(12)-H(12B)	0.9600
C(12)-H(12C)	0.9600
N(2)-H(2A)	0.8600
O(4)-H(4A)	0.8200
&E	
&D	
O(1)-C(1)-N(1)	109.5(2)
O(1)-C(1)-C(2)	108.5(2)
N(1)-C(1)-C(2)	113.8(2)
O(1)-C(1)-H(1)	108.3
N(1)-C(1)-H(1)	108.3
C(2)-C(1)-H(1)	108.3
O(2)-C(2)-C(3)	105.7(2)
O(2)-C(2)-C(1)	110.1(2)
C(3)-C(2)-C(1)	103.7(2)
O(2)-C(2)-H(2)	112.3
C(3)-C(2)-H(2)	112.3
C(1)-C(2)-H(2)	112.3
O(3)-C(3)-C(4)	109.3(2)
O(3)-C(3)-C(2)	102.9(2)
C(4)-C(3)-C(2)	105.9(2)
O(3)-C(3)-H(3)	112.7
C(4)-C(3)-H(3)	112.7

C(2)-C(3)-H(3)	112.7
O(1)-C(4)-C(5)	112.1(2)
O(1)-C(4)-C(3)	104.9(2)
C(5)-C(4)-C(3)	114.1(2)
O(1)-C(4)-H(4)	108.5
C(5)-C(4)-H(4)	108.5
C(3)-C(4)-H(4)	108.5
O(4)-C(5)-C(4)	110.4(3)
O(4)-C(5)-H(5A)	109.6
C(4)-C(5)-H(5A)	109.6
O(4)-C(5)-H(5B)	109.6
C(4)-C(5)-H(5B)	109.6
H(5A)-C(5)-H(5B)	108.1
C(7)-C(6)-N(1)	122.2(3)
C(7)-C(6)-H(6)	118.9
N(1)-C(6)-H(6)	118.9
C(6)-C(7)-C(8)	120.1(3)
C(6)-C(7)-H(7)	119.9
C(8)-C(7)-H(7)	119.9
O(5)-C(8)-N(2)	119.8(3)
O(5)-C(8)-C(7)	125.9(3)
N(2)-C(8)-C(7)	114.3(3)
O(6)-C(9)-N(2)	122.5(3)
O(6)-C(9)-N(1)	122.2(3)
N(2)-C(9)-N(1)	115.3(2)
O(2)-C(10)-O(3)	104.9(2)
O(2)-C(10)-C(12)	108.9(3)
O(3)-C(10)-C(12)	109.2(2)
O(2)-C(10)-C(11)	109.0(2)
O(3)-C(10)-C(11)	110.3(3)
C(12)-C(10)-C(11)	114.2(3)
C(10)-C(11)-H(11A)	109.5
C(10)-C(11)-H(11B)	109.5
H(11A)-C(11)-H(11B)	109.5
C(10)-C(11)-H(11C)	109.5
H(11A)-C(11)-H(11C)	109.5
H(11B)-C(11)-H(11C)	109.5
C(10)-C(12)-H(12A)	109.5
C(10)-C(12)-H(12B)	109.5
H(12A)-C(12)-H(12B)	109.5
C(10)-C(12)-H(12C)	109.5
H(12A)-C(12)-H(12C)	109.5
H(12B)-C(12)-H(12C)	109.5
C(6)-N(1)-C(9)	121.2(2)
C(6)-N(1)-C(1)	123.3(2)
C(9)-N(1)-C(1)	115.2(2)
C(9)-N(2)-C(8)	126.5(3)
C(9)-N(2)-H(2A)	116.7
C(8)-N(2)-H(2A)	116.7
C(1)-O(1)-C(4)	111.6(2)
C(2)-O(2)-C(10)	108.9(2)
C(3)-O(3)-C(10)	106.5(2)
C(5)-O(4)-H(4A)	109.5

Table 4. Anisotropic displacement parameters [$\text{\AA}^2 \times 10^3$] for 08mz108_0m. The anisotropic displacement factor exponent takes the form: $-2 \pi^2 [(h a^*)^2 U_{11} + \dots + 2 h k a^* b^* U_{12}]$

	U11	U22	U33	U23	U13	U12
C(1)	10(1)	14(1)	17(1)	2(1)	1(1)	-2(1)
C(2)	8(1)	15(1)	18(1)	1(1)	1(1)	-1(1)
C(3)	11(1)	14(1)	18(1)	0(1)	-2(1)	-1(1)
C(4)	12(1)	17(1)	18(1)	0(1)	2(1)	-1(1)
C(5)	16(2)	22(2)	22(2)	5(1)	-1(1)	-1(1)
C(6)	18(1)	14(1)	18(1)	1(1)	3(1)	-1(1)
C(7)	23(2)	22(2)	13(1)	-2(1)	4(1)	4(1)
C(8)	13(1)	18(1)	20(1)	-3(1)	-3(1)	2(1)
C(9)	7(1)	12(1)	17(1)	2(1)	-2(1)	2(1)
C(10)	11(1)	18(1)	18(1)	0(1)	-1(1)	-2(1)
C(11)	29(2)	22(2)	23(2)	-5(1)	5(1)	-3(1)
C(12)	19(2)	36(2)	23(2)	10(1)	-6(1)	-3(1)
N(1)	13(1)	12(1)	17(1)	0(1)	1(1)	-2(1)
N(2)	12(1)	15(1)	16(1)	2(1)	1(1)	-2(1)
O(1)	13(1)	14(1)	21(1)	2(1)	6(1)	1(1)
O(2)	18(1)	17(1)	14(1)	-1(1)	0(1)	-6(1)
O(3)	13(1)	22(1)	16(1)	3(1)	-2(1)	-4(1)
O(4)	15(1)	27(1)	19(1)	4(1)	-4(1)	-2(1)
O(5)	22(1)	31(1)	20(1)	-3(1)	-2(1)	-9(1)
O(6)	12(1)	17(1)	13(1)	1(1)	-1(1)	1(1)

Table 5. Hydrogen coordinates ($\times 10^4$) and isotropic displacement parameters ($\text{\AA}^2 \times 10^3$) for 08mz108_0m.

	x	y	z	U(eq)
H(1)	-586	6312	352	17
H(2)	3140	4733	356	16
H(3)	507	3278	509	17
H(4)	-3560	4065	1109	19
H(5A)	-1294	4149	2140	24
H(5B)	-793	3077	1758	24
H(6)	1048	6120	1985	20
H(7)	3898	7171	2534	23
H(11A)	1550	3042	-681	37
H(11B)	1287	3603	-1383	37
H(11C)	-890	2828	-1133	37
H(12A)	-2084	5117	-1496	39
H(12B)	-3803	5384	-867	39
H(12C)	-4246	4323	-1263	39
H(2A)	6705	8005	768	17
H(4A)	2812	3889	2113	30

Table 6. Torsion angles [deg] for 08mz108_0m.

O(1)-C(1)-C(2)-O(2)	119.5(2)
N(1)-C(1)-C(2)-O(2)	-118.4(3)
O(1)-C(1)-C(2)-C(3)	6.8(3)
N(1)-C(1)-C(2)-C(3)	129.0(2)
O(2)-C(2)-C(3)-O(3)	-19.5(3)
C(1)-C(2)-C(3)-O(3)	96.3(2)
O(2)-C(2)-C(3)-C(4)	-134.2(2)
C(1)-C(2)-C(3)-C(4)	-18.3(3)
O(3)-C(3)-C(4)-O(1)	-86.9(3)
C(2)-C(3)-C(4)-O(1)	23.4(3)
O(3)-C(3)-C(4)-C(5)	150.1(3)
C(2)-C(3)-C(4)-C(5)	-99.7(3)
O(1)-C(4)-C(5)-O(4)	-66.4(3)
C(3)-C(4)-C(5)-O(4)	52.7(4)
N(1)-C(6)-C(7)-C(8)	3.2(5)
C(6)-C(7)-C(8)-O(5)	174.6(3)
C(6)-C(7)-C(8)-N(2)	-4.3(4)
C(7)-C(6)-N(1)-C(9)	2.1(4)
C(7)-C(6)-N(1)-C(1)	-171.6(3)
O(6)-C(9)-N(1)-C(6)	175.9(3)
N(2)-C(9)-N(1)-C(6)	-5.6(4)
O(6)-C(9)-N(1)-C(1)	-9.9(4)
N(2)-C(9)-N(1)-C(1)	168.6(2)
O(1)-C(1)-N(1)-C(6)	2.1(4)
C(2)-C(1)-N(1)-C(6)	-119.5(3)
O(1)-C(1)-N(1)-C(9)	-171.9(2)
C(2)-C(1)-N(1)-C(9)	66.5(3)
O(6)-C(9)-N(2)-C(8)	-177.1(3)
N(1)-C(9)-N(2)-C(8)	4.3(4)
O(5)-C(8)-N(2)-C(9)	-178.5(3)
C(7)-C(8)-N(2)-C(9)	0.5(4)
N(1)-C(1)-O(1)-C(4)	-116.4(2)
C(2)-C(1)-O(1)-C(4)	8.3(3)
C(5)-C(4)-O(1)-C(1)	104.4(3)
C(3)-C(4)-O(1)-C(1)	-20.0(3)
C(3)-C(2)-O(2)-C(10)	-0.1(3)
C(1)-C(2)-O(2)-C(10)	-111.6(3)
O(3)-C(10)-O(2)-C(2)	19.7(3)
C(12)-C(10)-O(2)-C(2)	136.5(3)
C(11)-C(10)-O(2)-C(2)	-98.4(3)
C(4)-C(3)-O(3)-C(10)	144.1(2)
C(2)-C(3)-O(3)-C(10)	31.9(3)
O(2)-C(10)-O(3)-C(3)	-32.8(3)
C(12)-C(10)-O(3)-C(3)	-149.4(2)
C(11)-C(10)-O(3)-C(3)	84.4(3)

Table 7. Hydrogen bonds for 08mz108_0m [\AA and deg].

D-H...A	d(D-H)	d(H...A)	d(D...A)	<(DHA)
---------	--------	----------	----------	--------

N(2)-H(2A)...O(6)#1	0.86	2.10	2.882(3)	151.4
N(2)-H(2A)...O(2)#1	0.86	2.60	3.152(3)	123.3
O(4)-H(4A)...O(5)#2	0.82	1.96	2.734(3)	157.6

Symmetry transformations used to generate equivalent atoms:

#1 $x+1/2, -y+3/2, -z$ #2 $-x+1, y-1/2, -z+1/2$

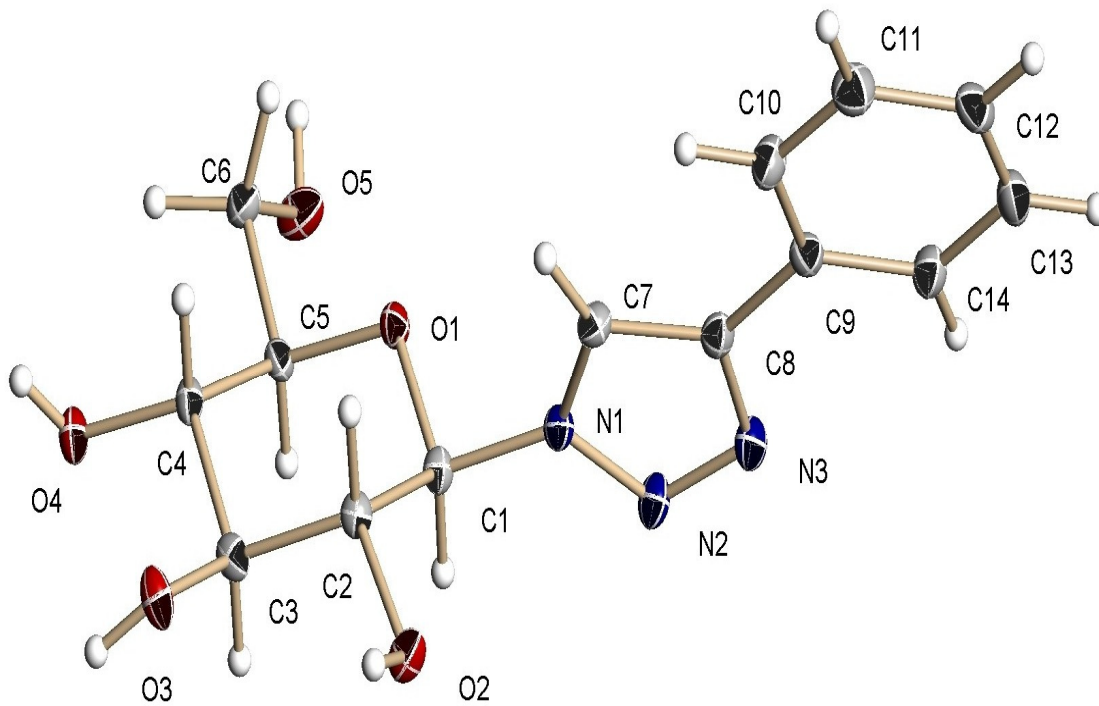


Figure 104: X-Ray crystal structure of deprotected phenyl triazole **47**.

Table 1. Crystal data and structure refinement for 08mz013_0m:

Identification code: 08mz013_0m
 Empirical formula: C₁₄ H₁₇ N₃ O₅
 Formula weight: 307.31
 Temperature: 100(2) K
 Wavelength: 0.71073 Å
 Crystal system: Orthorhombic
 Space group: P2₁2₁2₁
 Unit cell dimensions:
 a = 5.8104(8) Å, α = 90°
 b = 14.0117(18) Å, β = 90°
 c = 16.768(2) Å, γ = 90°
 Volume, Z: 1365.2(3) Å³, 4
 Density (calculated): 1.495 Mg/m³
 Absorption coefficient: 0.115 mm⁻¹
 F(000): 648
 Crystal size: 0.40 × 0.16 × 0.11 mm
 Crystal shape, colour: rod, colourless
 θ range for data collection: 1.89 to 28.28°
 Limiting indices: $-7 \leq h \leq 7$, $-15 \leq k \leq 18$, $-22 \leq l \leq 22$
 Reflections collected: 9293
 Independent reflections: 1971 (R(int) = 0.0302)
 Completeness to $\theta = 28.28^\circ$: 99.9 %
 Absorption correction: multi-scan
 Max. and min. transmission: 0.988 and 0.888
 Refinement method: Full-matrix least-squares on F^2
 Data / restraints / parameters: 1971 / 0 / 203
 Goodness-of-fit on F^2 : 1.050
 Final R indices [$I > 2\sigma(I)$]: R1 = 0.0327, wR2 = 0.0767
 R indices (all data): R1 = 0.0372, wR2 = 0.0793
 Largest diff. peak and hole: 0.257 and -0.190 e × Å⁻³

Refinement of F^2 against ALL reflections. The weighted R-factor wR and goodness of fit are based on F^2 , conventional R-factors R are based on F , with F set to zero for negative F^2 . The threshold expression of $F^2 > 2\sigma(F^2)$ is used only for calculating R-factors

Treatment of hydrogen atoms:

All hydrogen atoms were placed in calculated positions and were refined

with an isotropic displacement parameter 1.5 (hydroxyl, methyl) or 1.2 times (all others) that of the adjacent carbon or oxygen atom.

Table 2. Atomic coordinates [$\times 10^4$] and equivalent isotropic displacement parameters [$\text{\AA}^2 \times 10^3$] for 08mz013_0m. $U(\text{eq})$ is defined as one third of the trace of the orthogonalized U_{ij} tensor.

	x	y	z	U(eq)
C(1)	580(3)	3161(1)	2860(1)	13(1)
C(2)	-1967(3)	3377(1)	2959(1)	13(1)
C(3)	-2652(3)	3077(1)	3798(1)	14(1)
C(4)	-2106(3)	2020(1)	3894(1)	13(1)
C(5)	461(3)	1851(1)	3749(1)	13(1)
C(6)	1137(3)	814(1)	3819(1)	15(1)
C(7)	422(4)	3265(1)	1345(1)	15(1)
C(8)	1882(3)	3694(1)	812(1)	14(1)
C(9)	1714(4)	3778(1)	-64(1)	15(1)
C(10)	-255(4)	3470(1)	-464(1)	19(1)
C(11)	-425(4)	3570(2)	-1288(1)	22(1)
C(12)	1366(4)	3975(1)	-1715(1)	21(1)
C(13)	3337(4)	4276(1)	-1326(1)	22(1)
C(14)	3515(4)	4182(1)	-502(1)	18(1)
N(1)	1368(3)	3429(1)	2068(1)	13(1)
N(2)	3323(3)	3937(1)	1995(1)	16(1)
N(3)	3643(3)	4094(1)	1232(1)	17(1)
O(1)	1007(2)	2172(1)	2951(1)	14(1)
O(2)	-2312(2)	4364(1)	2823(1)	17(1)
O(3)	-5026(2)	3280(1)	3887(1)	18(1)
O(4)	-2715(2)	1707(1)	4678(1)	16(1)
O(5)	3543(2)	748(1)	3991(1)	22(1)

All esds (except the esd in the dihedral angle between two l.s. planes) are estimated using the full covariance matrix. The cell esds are taken into account individually in the estimation of esds in distances, angles and torsion angles; correlations between esds in cell parameters are only used when they are defined by crystal symmetry. An approximate (isotropic) treatment of cell esds is used for estimating esds involving l.s. planes.

Table 3. Bond lengths [\AA] and angles [deg] for 08mz013_0m.

C(1)-O(1)	1.415(2)
C(1)-N(1)	1.455(2)
C(1)-C(2)	1.520(3)
C(1)-H(1)	1.0000
C(2)-O(2)	1.416(2)
C(2)-C(3)	1.521(2)
C(2)-H(2)	1.0000
C(3)-O(3)	1.416(2)
C(3)-C(4)	1.523(3)
C(3)-H(3)	1.0000
C(4)-O(4)	1.430(2)
C(4)-C(5)	1.529(3)
C(4)-H(4)	1.0000
C(5)-O(1)	1.447(2)
C(5)-C(6)	1.510(3)
C(5)-H(5)	1.0000
C(6)-O(5)	1.430(2)
C(6)-H(6A)	0.9900
C(6)-H(6B)	0.9900
C(7)-N(1)	1.351(2)
C(7)-C(8)	1.371(3)
C(7)-H(7)	0.9500
C(8)-N(3)	1.363(3)
C(8)-C(9)	1.476(2)
C(9)-C(10)	1.395(3)
C(9)-C(14)	1.398(3)
C(10)-C(11)	1.393(2)
C(10)-H(10)	0.9500
C(11)-C(12)	1.384(3)
C(11)-H(11)	0.9500
C(12)-C(13)	1.383(3)
C(12)-H(12)	0.9500
C(13)-C(14)	1.393(3)
C(13)-H(13)	0.9500
C(14)-H(14)	0.9500
N(1)-N(2)	1.345(2)
N(2)-N(3)	1.313(2)
O(2)-H(2A)	0.8400
O(3)-H(3A)	0.8400
O(4)-H(4A)	0.8400
O(5)-H(5A)	0.8400
O(1)-C(1)-N(1)	107.27(14)
O(1)-C(1)-C(2)	110.74(15)
N(1)-C(1)-C(2)	110.78(14)
O(1)-C(1)-H(1)	109.3
N(1)-C(1)-H(1)	109.3
C(2)-C(1)-H(1)	109.3
O(2)-C(2)-C(1)	108.37(15)
O(2)-C(2)-C(3)	112.48(15)
C(1)-C(2)-C(3)	107.50(15)
O(2)-C(2)-H(2)	109.5
C(1)-C(2)-H(2)	109.5
C(3)-C(2)-H(2)	109.5

O(3)-C(3)-C(2)	107.27(15)
O(3)-C(3)-C(4)	112.76(16)
C(2)-C(3)-C(4)	108.20(15)
O(3)-C(3)-H(3)	109.5
C(2)-C(3)-H(3)	109.5
C(4)-C(3)-H(3)	109.5
O(4)-C(4)-C(3)	110.11(15)
O(4)-C(4)-C(5)	109.88(14)
C(3)-C(4)-C(5)	109.68(15)
O(4)-C(4)-H(4)	109.0
C(3)-C(4)-H(4)	109.0
C(5)-C(4)-H(4)	109.0
O(1)-C(5)-C(6)	108.26(14)
O(1)-C(5)-C(4)	108.23(14)
C(6)-C(5)-C(4)	112.97(16)
O(1)-C(5)-H(5)	109.1
C(6)-C(5)-H(5)	109.1
C(4)-C(5)-H(5)	109.1
O(5)-C(6)-C(5)	109.37(16)
O(5)-C(6)-H(6A)	109.8
C(5)-C(6)-H(6A)	109.8
O(5)-C(6)-H(6B)	109.8
C(5)-C(6)-H(6B)	109.8
H(6A)-C(6)-H(6B)	108.2
N(1)-C(7)-C(8)	104.94(17)
N(1)-C(7)-H(7)	127.5
C(8)-C(7)-H(7)	127.5
N(3)-C(8)-C(7)	107.97(16)
N(3)-C(8)-C(9)	122.05(17)
C(7)-C(8)-C(9)	129.96(18)
C(10)-C(9)-C(14)	119.12(16)
C(10)-C(9)-C(8)	120.52(18)
C(14)-C(9)-C(8)	120.36(18)
C(11)-C(10)-C(9)	120.29(19)
C(11)-C(10)-H(10)	119.9
C(9)-C(10)-H(10)	119.9
C(12)-C(11)-C(10)	120.0(2)
C(12)-C(11)-H(11)	120.0
C(10)-C(11)-H(11)	120.0
C(13)-C(12)-C(11)	120.28(17)
C(13)-C(12)-H(12)	119.9
C(11)-C(12)-H(12)	119.9
C(12)-C(13)-C(14)	120.02(19)
C(12)-C(13)-H(13)	120.0
C(14)-C(13)-H(13)	120.0
C(13)-C(14)-C(9)	120.26(19)
C(13)-C(14)-H(14)	119.9
C(9)-C(14)-H(14)	119.9
N(2)-N(1)-C(7)	110.68(15)
N(2)-N(1)-C(1)	118.99(14)
C(7)-N(1)-C(1)	130.32(16)
N(3)-N(2)-N(1)	107.23(14)
N(2)-N(3)-C(8)	109.18(16)
C(1)-O(1)-C(5)	111.47(13)
C(2)-O(2)-H(2A)	109.5
C(3)-O(3)-H(3A)	109.5
C(4)-O(4)-H(4A)	109.5

C(6)-O(5)-H(5A)

109.5

Table 4. Anisotropic displacement parameters [$\text{\AA}^2 \times 10^3$] for 08mz013_0m. The anisotropic displacement factor exponent takes the form: $-2 \pi^2 [(h a^*)^2 U_{11} + \dots + 2 h k a^* b^* U_{12}]$

	U11	U22	U33	U23	U13	U12
C(1)	12(1)	15(1)	11(1)	1(1)	-1(1)	0(1)
C(2)	12(1)	14(1)	13(1)	1(1)	-1(1)	0(1)
C(3)	9(1)	18(1)	14(1)	-2(1)	-1(1)	1(1)
C(4)	12(1)	17(1)	10(1)	1(1)	0(1)	-3(1)
C(5)	14(1)	14(1)	11(1)	0(1)	1(1)	1(1)
C(6)	14(1)	13(1)	19(1)	0(1)	0(1)	-1(1)
C(7)	15(1)	14(1)	16(1)	0(1)	-1(1)	-1(1)
C(8)	14(1)	12(1)	16(1)	1(1)	0(1)	1(1)
C(9)	18(1)	12(1)	14(1)	1(1)	1(1)	2(1)
C(10)	20(1)	19(1)	18(1)	2(1)	0(1)	-5(1)
C(11)	25(1)	21(1)	20(1)	-2(1)	-4(1)	-2(1)
C(12)	32(1)	18(1)	13(1)	1(1)	3(1)	4(1)
C(13)	25(1)	19(1)	20(1)	2(1)	9(1)	1(1)
C(14)	16(1)	18(1)	20(1)	0(1)	2(1)	-2(1)
N(1)	12(1)	14(1)	14(1)	0(1)	1(1)	-1(1)
N(2)	12(1)	19(1)	18(1)	2(1)	-1(1)	-3(1)
N(3)	17(1)	17(1)	15(1)	3(1)	0(1)	-1(1)
O(1)	16(1)	13(1)	12(1)	2(1)	2(1)	1(1)
O(2)	13(1)	14(1)	24(1)	3(1)	-1(1)	2(1)
O(3)	11(1)	28(1)	13(1)	2(1)	0(1)	3(1)
O(4)	15(1)	21(1)	13(1)	3(1)	1(1)	-2(1)
O(5)	16(1)	15(1)	34(1)	-1(1)	-3(1)	3(1)

Table 5. Hydrogen coordinates ($\times 10^4$) and isotropic displacement parameters ($\text{\AA}^2 \times 10^3$) for 08mz013_0m.

	x	y	z	U(eq)
H(1)	1477	3523	3269	15
H(2)	-2872	3000	2561	16

H(3)	-1750	3454	4196	17
H(4)	-3013	1648	3494	15
H(5)	1370	2233	4142	15
H(6A)	240	506	4249	18
H(6B)	796	479	3312	18
H(7)	-956	2926	1230	18
H(10)	-1486	3191	-173	23
H(11)	-1771	3360	-1558	26
H(12)	1241	4046	-2276	25
H(13)	4568	4547	-1622	26
H(14)	4866	4393	-236	21
H(2A)	-3722	4471	2757	25
H(3A)	-5364	3288	4374	26
H(4A)	-3919	1377	4656	24
H(5A)	4002	190	3900	32

Table 6. Torsion angles [deg] for 07mz075m.

O(1)-C(1)-C(2)-O(2)	-177.10(13)
N(1)-C(1)-C(2)-O(2)	-58.21(18)
O(1)-C(1)-C(2)-C(3)	61.08(18)
N(1)-C(1)-C(2)-C(3)	179.98(14)
O(2)-C(2)-C(3)-O(3)	60.81(19)
C(1)-C(2)-C(3)-O(3)	-179.97(15)
O(2)-C(2)-C(3)-C(4)	-177.27(15)
C(1)-C(2)-C(3)-C(4)	-58.06(18)
O(3)-C(3)-C(4)-O(4)	-61.78(19)
C(2)-C(3)-C(4)-O(4)	179.74(14)
O(3)-C(3)-C(4)-C(5)	177.18(14)
C(2)-C(3)-C(4)-C(5)	58.70(18)
O(4)-C(4)-C(5)-O(1)	179.78(13)
C(3)-C(4)-C(5)-O(1)	-59.05(18)
O(4)-C(4)-C(5)-C(6)	59.91(19)
C(3)-C(4)-C(5)-C(6)	-178.91(15)
O(1)-C(5)-C(6)-O(5)	82.88(18)
C(4)-C(5)-C(6)-O(5)	-157.27(15)
N(1)-C(7)-C(8)-N(3)	0.2(2)
N(1)-C(7)-C(8)-C(9)	-177.97(18)
N(3)-C(8)-C(9)-C(10)	-171.55(18)
C(7)-C(8)-C(9)-C(10)	6.4(3)
N(3)-C(8)-C(9)-C(14)	7.4(3)
C(7)-C(8)-C(9)-C(14)	-174.6(2)
C(14)-C(9)-C(10)-C(11)	-0.4(3)
C(8)-C(9)-C(10)-C(11)	178.61(19)
C(9)-C(10)-C(11)-C(12)	0.1(3)
C(10)-C(11)-C(12)-C(13)	0.4(3)
C(11)-C(12)-C(13)-C(14)	-0.7(3)
C(12)-C(13)-C(14)-C(9)	0.4(3)
C(10)-C(9)-C(14)-C(13)	0.1(3)
C(8)-C(9)-C(14)-C(13)	-178.88(18)
C(8)-C(7)-N(1)-N(2)	0.1(2)
C(8)-C(7)-N(1)-C(1)	178.98(17)
O(1)-C(1)-N(1)-N(2)	-106.33(17)
C(2)-C(1)-N(1)-N(2)	132.70(16)

O(1)-C(1)-N(1)-C(7)	74.8(2)
C(2)-C(1)-N(1)-C(7)	-46.1(2)
C(7)-N(1)-N(2)-N(3)	-0.34(19)
C(1)-N(1)-N(2)-N(3)	-179.39(15)
N(1)-N(2)-N(3)-C(8)	0.47(19)
C(7)-C(8)-N(3)-N(2)	-0.4(2)
C(9)-C(8)-N(3)-N(2)	177.92(17)
N(1)-C(1)-O(1)-C(5)	175.05(14)
C(2)-C(1)-O(1)-C(5)	-63.95(18)
C(6)-C(5)-O(1)-C(1)	-175.55(15)
C(4)-C(5)-O(1)-C(1)	61.66(18)

Table 7. Hydrogen bonds for 08mz013_0m [\AA and deg].

D-H...A	d(D-H)	d(H...A)	d(D...A)	<(DHA)
O(5)-H(5A)...N(3)#1	0.84	2.07	2.861(2)	157.0
O(4)-H(4A)...O(5)#2	0.84	2.05	2.804(2)	149.5
O(3)-H(3A)...O(4)#3	0.84	2.09	2.8681(18)	152.8
O(2)-H(2A)...N(2)#2	0.84	2.27	2.952(2)	138.9

Symmetry transformations used to generate equivalent atoms:

#1 $-x+1, y-1/2, -z+1/2$ #2 $x-1, y, z$ #3 $x-1/2, -y+1/2, -z+1$

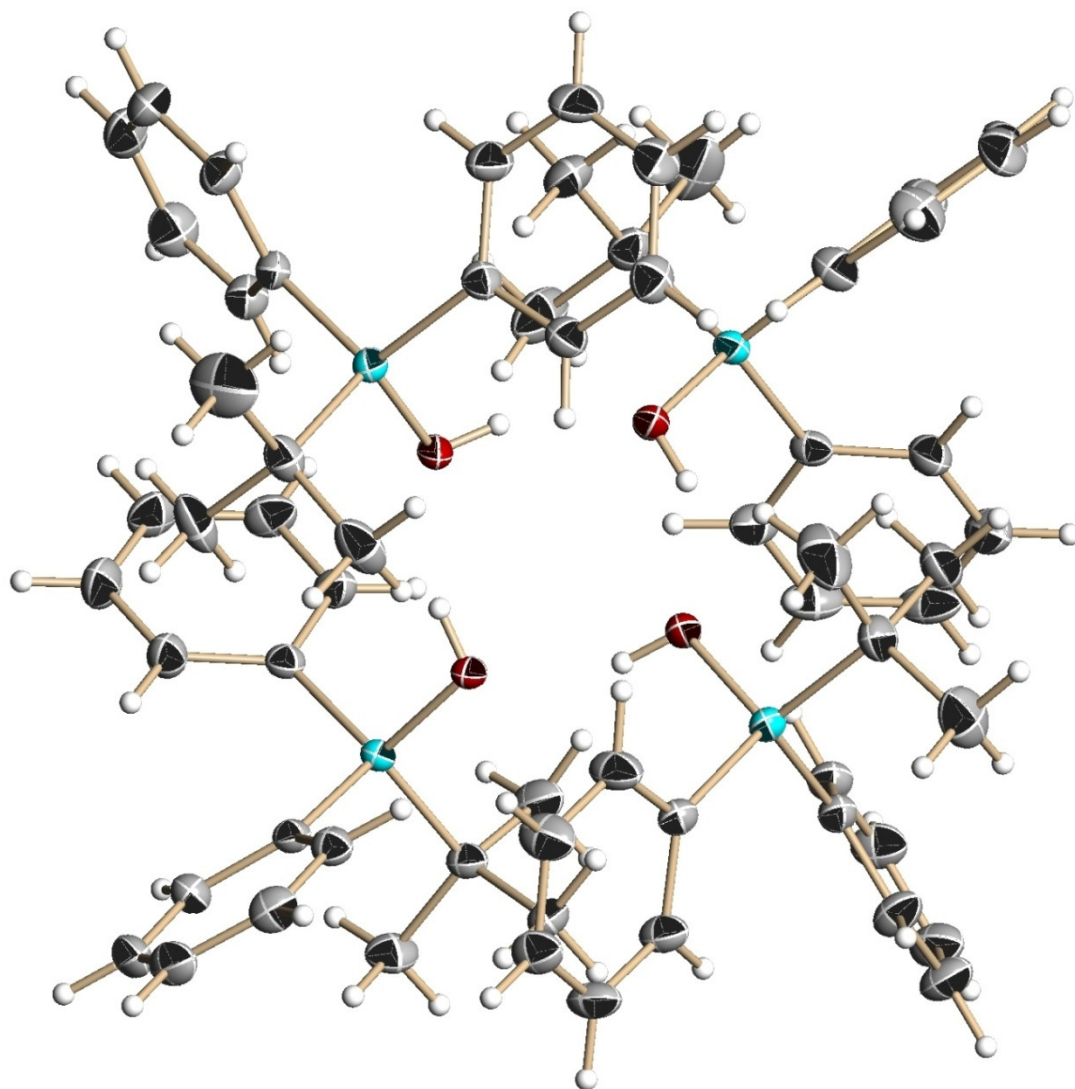


Figure 105: X-Ray crystal structure of *t*-butyl-diphenylsilanol tetramer **50**.

Table 1. Crystal data and structure refinement for 08mz220_0m:

Identification code: 08mz220_0m
 Empirical formula: C₁₆ H₂₀ O Si
 Formula weight: 256.41
 Temperature: 140(2) K
 Wavelength: 0.71073 Å
 Crystal system: Triclinic
 Space group: I-42d
 Unit cell dimensions:
 a = 13.3226(10) Å, α = 100.7140(10)°
 b = 14.5966(11) Å, β = 98.7060(10)°
 c = 15.9691(12) Å, γ = 93.6240(10)°
 Volume, Z: 3002.8(4) Å³, 8
 Density (calculated): 1.134 Mg/m³
 Absorption coefficient: 0.144 mm⁻¹
 F(000): 1104
 Crystal size: 0.53 × 0.52 × 0.20 mm
 Crystal shape, colour: plate, colourless
 θ range for data collection: 1.32 to 28.28°
 Limiting indices: $-17 \leq h \leq 17$, $-19 \leq k \leq 19$, $-20 \leq l \leq 21$
 Reflections collected: 30690
 Independent reflections: 14753 ($R(\text{int}) = 0.0158$)
 Completeness to $\theta = 28.28^\circ$: 98.9 %
 Absorption correction: multi-scan
 Max. and min. transmission: 0.972 and 0.876
 Refinement method: Full-matrix least-squares on F^2
 Data / restraints / parameters: 14753 / 0 / 665
 Goodness-of-fit on F^2 : 1.029
 Final R indices [$I > 2\sigma(I)$]: R1 = 0.0376, wR2 = 0.0973
 R indices (all data): R1 = 0.0465, wR2 = 0.1040
 Largest diff. peak and hole: 0.395 and -0.258 e × Å⁻³

Refinement of F^2 against ALL reflections. The weighted R-factor wR and goodness of fit are based on F^2 , conventional R-factors R are based on F , with F set to zero for negative F^2 . The threshold expression of $F^2 > 2\sigma(F^2)$ is used only for calculating R-factors

Treatment of hydrogen atoms:
 All hydrogen atoms were placed in calculated positions and were refined

with an isotropic displacement parameter 1.5 (methyl, hydroxyl) or 1.2 times (all others) that of the adjacent carbon or oxygen atom.

Table 2. Atomic coordinates [$\times 10^4$] and equivalent isotropic displacement parameters [$\text{\AA}^2 \times 10^3$] for 08mz220_0m. U(eq) is defined as one third of the trace of the orthogonalized U_{ij} tensor.

	x	y	z	U(eq)
C(1A)	4449(1)	8130(1)	2764(1)	23(1)
C(2A)	4114(1)	8564(1)	3515(1)	29(1)
C(3A)	3490(1)	8082(1)	3940(1)	34(1)
C(4A)	3178(1)	7147(1)	3623(1)	33(1)
C(5A)	3510(1)	6692(1)	2893(1)	39(1)
C(6A)	4138(1)	7174(1)	2473(1)	35(1)
C(7A)	5598(1)	10023(1)	2759(1)	24(1)
C(8A)	6604(1)	10430(1)	2993(1)	28(1)
C(9A)	6834(1)	11354(1)	3423(1)	35(1)
C(10A)	6055(1)	11898(1)	3626(1)	37(1)
C(11A)	5055(1)	11519(1)	3396(1)	37(1)
C(12A)	4827(1)	10594(1)	2965(1)	32(1)
C(13A)	4860(1)	8680(1)	1015(1)	31(1)
C(14A)	3858(1)	9142(1)	885(1)	47(1)
C(15A)	5680(1)	9215(1)	657(1)	40(1)
C(16A)	4710(2)	7665(1)	516(1)	59(1)
C(1B)	6809(1)	7046(1)	5151(1)	21(1)
C(2B)	7010(1)	6826(1)	5975(1)	26(1)
C(3B)	6280(1)	6325(1)	6291(1)	31(1)
C(4B)	5333(1)	6038(1)	5795(1)	33(1)
C(5B)	5107(1)	6258(1)	4986(1)	31(1)
C(6B)	5836(1)	6755(1)	4667(1)	25(1)
C(7B)	9048(1)	7355(1)	4889(1)	21(1)
C(8B)	9284(1)	6625(1)	5317(1)	30(1)
C(9B)	10259(1)	6333(1)	5424(1)	37(1)
C(10B)	11026(1)	6767(1)	5101(1)	35(1)
C(11B)	10813(1)	7477(1)	4655(1)	34(1)
C(12B)	9836(1)	7764(1)	4551(1)	28(1)
C(13B)	7663(1)	9039(1)	5174(1)	23(1)
C(14B)	7847(1)	9220(1)	6168(1)	32(1)
C(15B)	6576(1)	9271(1)	4858(1)	27(1)
C(16B)	8433(1)	9680(1)	4872(1)	36(1)
C(1C)	9189(1)	4816(1)	2114(1)	22(1)
C(2C)	9970(1)	5326(1)	2742(1)	29(1)
C(3C)	10923(1)	4991(1)	2898(1)	38(1)
C(4C)	11115(1)	4147(1)	2424(1)	40(1)
C(5C)	10359(1)	3625(1)	1804(1)	38(1)
C(6C)	9404(1)	3952(1)	1654(1)	31(1)
C(7C)	7439(1)	5218(1)	761(1)	23(1)
C(8C)	6520(1)	5583(1)	507(1)	28(1)
C(9C)	6143(1)	5571(1)	-352(1)	31(1)
C(10C)	6688(1)	5204(1)	-985(1)	38(1)
C(11C)	7609(1)	4859(1)	-757(1)	45(1)

C(12C)	7981(1)	4864(1)	106(1)	35(1)
C(13C)	6986(1)	4652(1)	2477(1)	28(1)
C(14C)	6795(2)	3618(1)	2041(1)	60(1)
C(15C)	7445(1)	4744(1)	3434(1)	42(1)
C(16C)	5967(1)	5094(1)	2436(1)	43(1)
C(1D)	8996(1)	9724(1)	1676(1)	23(1)
C(2D)	9339(1)	10036(1)	2565(1)	31(1)
C(3D)	9370(1)	10973(1)	2956(1)	37(1)
C(4D)	9055(1)	11624(1)	2475(1)	41(1)
C(5D)	8687(1)	11336(1)	1602(1)	42(1)
C(6D)	8657(1)	10399(1)	1210(1)	32(1)
C(7D)	8407(1)	8322(1)	-22(1)	23(1)
C(8D)	8851(1)	8815(1)	-572(1)	31(1)
C(9D)	8411(1)	8741(1)	-1430(1)	38(1)
C(10D)	7512(1)	8181(1)	-1757(1)	41(1)
C(11D)	7067(1)	7676(1)	-1234(1)	41(1)
C(12D)	7514(1)	7743(1)	-379(1)	30(1)
C(13D)	10188(1)	7916(1)	1304(1)	29(1)
C(14D)	10620(1)	7985(1)	2264(1)	49(1)
C(15D)	9999(1)	6873(1)	877(1)	37(1)
C(16D)	10972(1)	8376(1)	862(2)	58(1)
O(1)	6422(1)	8272(1)	2260(1)	26(1)
O(2)	7370(1)	7633(1)	3654(1)	23(1)
O(3)	8031(1)	6393(1)	2432(1)	23(1)
O(4)	8159(1)	7844(1)	1607(1)	23(1)
Si(1)	5333(1)	8763(1)	2203(1)	22(1)
Si(2)	7738(1)	7761(1)	4708(1)	18(1)
Si(3)	7912(1)	5281(1)	1939(1)	20(1)
Si(4)	8936(1)	8453(1)	1154(1)	20(1)

All esds (except the esd in the dihedral angle between two l.s. planes) are estimated using the full covariance matrix. The cell esds are taken into account individually in the estimation of esds in distances, angles and torsion angles; correlations between esds in cell parameters are only used when they are defined by crystal symmetry. An approximate (isotropic) treatment of cell esds is used for estimating esds involving l.s. planes.

Table 3. Bond lengths [\AA] and angles [deg] for 08mz220_0m.

C(1A)-C(2A)	1.3986(17)
C(1A)-C(6A)	1.4015(18)
C(1A)-Si(1)	1.8798(13)
C(2A)-C(3A)	1.3864(19)
C(2A)-H(2A)	0.9500
C(3A)-C(4A)	1.378(2)
C(3A)-H(3A)	0.9500
C(4A)-C(5A)	1.379(2)
C(4A)-H(4A)	0.9500
C(5A)-C(6A)	1.385(2)
C(5A)-H(5A)	0.9500
C(6A)-H(6A)	0.9500
C(7A)-C(8A)	1.3983(18)
C(7A)-C(12A)	1.4029(18)
C(7A)-Si(1)	1.8732(13)
C(8A)-C(9A)	1.387(2)
C(8A)-H(8A)	0.9500
C(9A)-C(10A)	1.387(2)
C(9A)-H(9A)	0.9500
C(10A)-C(11A)	1.378(2)
C(10A)-H(10A)	0.9500
C(11A)-C(12A)	1.389(2)
C(11A)-H(11A)	0.9500
C(12A)-H(12A)	0.9500
C(13A)-C(16A)	1.532(2)
C(13A)-C(14A)	1.537(2)
C(13A)-C(15A)	1.542(2)
C(13A)-Si(1)	1.8848(14)
C(14A)-H(14A)	0.9800
C(14A)-H(14B)	0.9800
C(14A)-H(14C)	0.9800
C(15A)-H(15A)	0.9800
C(15A)-H(15B)	0.9800
C(15A)-H(15C)	0.9800
C(16A)-H(16A)	0.9800
C(16A)-H(16B)	0.9800
C(16A)-H(16C)	0.9800
C(1B)-C(6B)	1.4012(18)
C(1B)-C(2B)	1.4021(17)
C(1B)-Si(2)	1.8711(12)
C(2B)-C(3B)	1.3899(18)
C(2B)-H(2B)	0.9500
C(3B)-C(4B)	1.380(2)
C(3B)-H(3B)	0.9500
C(4B)-C(5B)	1.382(2)
C(4B)-H(4B)	0.9500
C(5B)-C(6B)	1.3888(18)
C(5B)-H(5B)	0.9500
C(6B)-H(6B)	0.9500
C(7B)-C(8B)	1.3968(18)
C(7B)-C(12B)	1.4008(17)
C(7B)-Si(2)	1.8776(13)
C(8B)-C(9B)	1.3890(19)
C(8B)-H(8B)	0.9500

C(9B)-C(10B)	1.382(2)
C(9B)-H(9B)	0.9500
C(10B)-C(11B)	1.382(2)
C(10B)-H(10B)	0.9500
C(11B)-C(12B)	1.3872(19)
C(11B)-H(11B)	0.9500
C(12B)-H(12B)	0.9500
C(13B)-C(16B)	1.5342(18)
C(13B)-C(14B)	1.5389(18)
C(13B)-C(15B)	1.5389(18)
C(13B)-Si(2)	1.8900(12)
C(14B)-H(14D)	0.9800
C(14B)-H(14E)	0.9800
C(14B)-H(14F)	0.9800
C(15B)-H(15D)	0.9800
C(15B)-H(15E)	0.9800
C(15B)-H(15F)	0.9800
C(16B)-H(16D)	0.9800
C(16B)-H(16E)	0.9800
C(16B)-H(16F)	0.9800
C(1C)-C(2C)	1.3973(18)
C(1C)-C(6C)	1.4063(17)
C(1C)-Si(3)	1.8715(13)
C(2C)-C(3C)	1.393(2)
C(2C)-H(2C)	0.9500
C(3C)-C(4C)	1.381(2)
C(3C)-H(3C)	0.9500
C(4C)-C(5C)	1.378(2)
C(4C)-H(4C)	0.9500
C(5C)-C(6C)	1.389(2)
C(5C)-H(5C)	0.9500
C(6C)-H(6C)	0.9500
C(7C)-C(12C)	1.3993(18)
C(7C)-C(8C)	1.4016(18)
C(7C)-Si(3)	1.8741(13)
C(8C)-C(9C)	1.3836(19)
C(8C)-H(8C)	0.9500
C(9C)-C(10C)	1.381(2)
C(9C)-H(9C)	0.9500
C(10C)-C(11C)	1.380(2)
C(10C)-H(10C)	0.9500
C(11C)-C(12C)	1.389(2)
C(11C)-H(11C)	0.9500
C(12C)-H(12C)	0.9500
C(13C)-C(14C)	1.529(2)
C(13C)-C(15C)	1.535(2)
C(13C)-C(16C)	1.537(2)
C(13C)-Si(3)	1.8910(13)
C(14C)-H(14G)	0.9800
C(14C)-H(14H)	0.9800
C(14C)-H(14I)	0.9800
C(15C)-H(15G)	0.9800
C(15C)-H(15H)	0.9800
C(15C)-H(15I)	0.9800
C(16C)-H(16G)	0.9800
C(16C)-H(16H)	0.9800
C(16C)-H(16I)	0.9800

C(1D)-C(6D)	1.3979(19)
C(1D)-C(2D)	1.4030(18)
C(1D)-Si(4)	1.8783(13)
C(2D)-C(3D)	1.390(2)
C(2D)-H(2D)	0.9500
C(3D)-C(4D)	1.376(2)
C(3D)-H(3D)	0.9500
C(4D)-C(5D)	1.383(2)
C(4D)-H(4D)	0.9500
C(5D)-C(6D)	1.3902(19)
C(5D)-H(5D)	0.9500
C(6D)-H(6D)	0.9500
C(7D)-C(12D)	1.3943(18)
C(7D)-C(8D)	1.4048(17)
C(7D)-Si(4)	1.8726(13)
C(8D)-C(9D)	1.388(2)
C(8D)-H(8D)	0.9500
C(9D)-C(10D)	1.380(2)
C(9D)-H(9D)	0.9500
C(10D)-C(11D)	1.384(2)
C(10D)-H(10D)	0.9500
C(11D)-C(12D)	1.389(2)
C(11D)-H(11D)	0.9500
C(12D)-H(12D)	0.9500
C(13D)-C(16D)	1.534(2)
C(13D)-C(15D)	1.535(2)
C(13D)-C(14D)	1.536(2)
C(13D)-Si(4)	1.8895(14)
C(14D)-H(14J)	0.9800
C(14D)-H(14K)	0.9800
C(14D)-H(14L)	0.9800
C(15D)-H(15J)	0.9800
C(15D)-H(15K)	0.9800
C(15D)-H(15L)	0.9800
C(16D)-H(16J)	0.9800
C(16D)-H(16K)	0.9800
C(16D)-H(16L)	0.9800
O(1)-Si(1)	1.6553(9)
O(1)-H(1)	0.8400
O(2)-Si(2)	1.6521(9)
O(2)-H(2)	0.8400
O(3)-Si(3)	1.6534(9)
O(3)-H(3)	0.8400
O(4)-Si(4)	1.6551(9)
O(4)-H(4)	0.8400
C(2A)-C(1A)-C(6A)	116.37(12)
C(2A)-C(1A)-Si(1)	122.46(10)
C(6A)-C(1A)-Si(1)	121.06(10)
C(3A)-C(2A)-C(1A)	121.95(12)
C(3A)-C(2A)-H(2A)	119.0
C(1A)-C(2A)-H(2A)	119.0
C(4A)-C(3A)-C(2A)	120.12(13)
C(4A)-C(3A)-H(3A)	119.9
C(2A)-C(3A)-H(3A)	119.9
C(3A)-C(4A)-C(5A)	119.49(13)
C(3A)-C(4A)-H(4A)	120.3

C(5A)-C(4A)-H(4A)	120.3
C(4A)-C(5A)-C(6A)	120.30(13)
C(4A)-C(5A)-H(5A)	119.8
C(6A)-C(5A)-H(5A)	119.8
C(5A)-C(6A)-C(1A)	121.74(13)
C(5A)-C(6A)-H(6A)	119.1
C(1A)-C(6A)-H(6A)	119.1
C(8A)-C(7A)-C(12A)	117.06(12)
C(8A)-C(7A)-Si(1)	119.85(10)
C(12A)-C(7A)-Si(1)	123.09(10)
C(9A)-C(8A)-C(7A)	121.67(12)
C(9A)-C(8A)-H(8A)	119.2
C(7A)-C(8A)-H(8A)	119.2
C(10A)-C(9A)-C(8A)	119.86(13)
C(10A)-C(9A)-H(9A)	120.1
C(8A)-C(9A)-H(9A)	120.1
C(11A)-C(10A)-C(9A)	119.86(13)
C(11A)-C(10A)-H(10A)	120.1
C(9A)-C(10A)-H(10A)	120.1
C(10A)-C(11A)-C(12A)	120.12(13)
C(10A)-C(11A)-H(11A)	119.9
C(12A)-C(11A)-H(11A)	119.9
C(11A)-C(12A)-C(7A)	121.42(13)
C(11A)-C(12A)-H(12A)	119.3
C(7A)-C(12A)-H(12A)	119.3
C(16A)-C(13A)-C(14A)	110.11(15)
C(16A)-C(13A)-C(15A)	108.14(14)
C(14A)-C(13A)-C(15A)	109.03(12)
C(16A)-C(13A)-Si(1)	112.03(10)
C(14A)-C(13A)-Si(1)	110.18(10)
C(15A)-C(13A)-Si(1)	107.24(10)
C(13A)-C(14A)-H(14A)	109.5
C(13A)-C(14A)-H(14B)	109.5
H(14A)-C(14A)-H(14B)	109.5
C(13A)-C(14A)-H(14C)	109.5
H(14A)-C(14A)-H(14C)	109.5
H(14B)-C(14A)-H(14C)	109.5
C(13A)-C(15A)-H(15A)	109.5
C(13A)-C(15A)-H(15B)	109.5
H(15A)-C(15A)-H(15B)	109.5
C(13A)-C(15A)-H(15C)	109.5
H(15A)-C(15A)-H(15C)	109.5
H(15B)-C(15A)-H(15C)	109.5
C(13A)-C(16A)-H(16A)	109.5
C(13A)-C(16A)-H(16B)	109.5
H(16A)-C(16A)-H(16B)	109.5
C(13A)-C(16A)-H(16C)	109.5
H(16A)-C(16A)-H(16C)	109.5
H(16B)-C(16A)-H(16C)	109.5
C(6B)-C(1B)-C(2B)	117.30(11)
C(6B)-C(1B)-Si(2)	119.22(9)
C(2B)-C(1B)-Si(2)	123.37(10)
C(3B)-C(2B)-C(1B)	121.32(13)
C(3B)-C(2B)-H(2B)	119.3
C(1B)-C(2B)-H(2B)	119.3
C(4B)-C(3B)-C(2B)	120.06(13)
C(4B)-C(3B)-H(3B)	120.0

C(2B)-C(3B)-H(3B)	120.0
C(3B)-C(4B)-C(5B)	119.90(13)
C(3B)-C(4B)-H(4B)	120.0
C(5B)-C(4B)-H(4B)	120.0
C(4B)-C(5B)-C(6B)	120.17(13)
C(4B)-C(5B)-H(5B)	119.9
C(6B)-C(5B)-H(5B)	119.9
C(5B)-C(6B)-C(1B)	121.24(12)
C(5B)-C(6B)-H(6B)	119.4
C(1B)-C(6B)-H(6B)	119.4
C(8B)-C(7B)-C(12B)	116.83(12)
C(8B)-C(7B)-Si(2)	123.44(10)
C(12B)-C(7B)-Si(2)	119.67(10)
C(9B)-C(8B)-C(7B)	121.70(13)
C(9B)-C(8B)-H(8B)	119.1
C(7B)-C(8B)-H(8B)	119.1
C(10B)-C(9B)-C(8B)	119.98(14)
C(10B)-C(9B)-H(9B)	120.0
C(8B)-C(9B)-H(9B)	120.0
C(11B)-C(10B)-C(9B)	119.78(13)
C(11B)-C(10B)-H(10B)	120.1
C(9B)-C(10B)-H(10B)	120.1
C(10B)-C(11B)-C(12B)	119.89(13)
C(10B)-C(11B)-H(11B)	120.1
C(12B)-C(11B)-H(11B)	120.1
C(11B)-C(12B)-C(7B)	121.79(13)
C(11B)-C(12B)-H(12B)	119.1
C(7B)-C(12B)-H(12B)	119.1
C(16B)-C(13B)-C(14B)	109.22(11)
C(16B)-C(13B)-C(15B)	109.08(11)
C(14B)-C(13B)-C(15B)	108.61(10)
C(16B)-C(13B)-Si(2)	111.92(9)
C(14B)-C(13B)-Si(2)	110.80(9)
C(15B)-C(13B)-Si(2)	107.13(8)
C(13B)-C(14B)-H(14D)	109.5
C(13B)-C(14B)-H(14E)	109.5
H(14D)-C(14B)-H(14E)	109.5
C(13B)-C(14B)-H(14F)	109.5
H(14D)-C(14B)-H(14F)	109.5
H(14E)-C(14B)-H(14F)	109.5
C(13B)-C(15B)-H(15D)	109.5
C(13B)-C(15B)-H(15E)	109.5
H(15D)-C(15B)-H(15E)	109.5
C(13B)-C(15B)-H(15F)	109.5
H(15D)-C(15B)-H(15F)	109.5
H(15E)-C(15B)-H(15F)	109.5
C(13B)-C(16B)-H(16D)	109.5
C(13B)-C(16B)-H(16E)	109.5
H(16D)-C(16B)-H(16E)	109.5
C(13B)-C(16B)-H(16F)	109.5
H(16D)-C(16B)-H(16F)	109.5
H(16E)-C(16B)-H(16F)	109.5
C(2C)-C(1C)-C(6C)	117.15(12)
C(2C)-C(1C)-Si(3)	119.70(9)
C(6C)-C(1C)-Si(3)	123.13(10)
C(3C)-C(2C)-C(1C)	121.14(13)
C(3C)-C(2C)-H(2C)	119.4

C(1C)-C(2C)-H(2C)	119.4
C(4C)-C(3C)-C(2C)	120.19(14)
C(4C)-C(3C)-H(3C)	119.9
C(2C)-C(3C)-H(3C)	119.9
C(5C)-C(4C)-C(3C)	120.15(14)
C(5C)-C(4C)-H(4C)	119.9
C(3C)-C(4C)-H(4C)	119.9
C(4C)-C(5C)-C(6C)	119.71(14)
C(4C)-C(5C)-H(5C)	120.1
C(6C)-C(5C)-H(5C)	120.1
C(5C)-C(6C)-C(1C)	121.65(14)
C(5C)-C(6C)-H(6C)	119.2
C(1C)-C(6C)-H(6C)	119.2
C(12C)-C(7C)-C(8C)	116.79(12)
C(12C)-C(7C)-Si(3)	123.63(10)
C(8C)-C(7C)-Si(3)	119.50(9)
C(9C)-C(8C)-C(7C)	122.01(13)
C(9C)-C(8C)-H(8C)	119.0
C(7C)-C(8C)-H(8C)	119.0
C(10C)-C(9C)-C(8C)	119.78(13)
C(10C)-C(9C)-H(9C)	120.1
C(8C)-C(9C)-H(9C)	120.1
C(11C)-C(10C)-C(9C)	119.80(13)
C(11C)-C(10C)-H(10C)	120.1
C(9C)-C(10C)-H(10C)	120.1
C(10C)-C(11C)-C(12C)	120.29(14)
C(10C)-C(11C)-H(11C)	119.9
C(12C)-C(11C)-H(11C)	119.9
C(11C)-C(12C)-C(7C)	121.31(14)
C(11C)-C(12C)-H(12C)	119.3
C(7C)-C(12C)-H(12C)	119.3
C(14C)-C(13C)-C(15C)	109.76(14)
C(14C)-C(13C)-C(16C)	109.47(14)
C(15C)-C(13C)-C(16C)	107.77(12)
C(14C)-C(13C)-Si(3)	110.09(11)
C(15C)-C(13C)-Si(3)	108.60(9)
C(16C)-C(13C)-Si(3)	111.11(10)
C(13C)-C(14C)-H(14G)	109.5
C(13C)-C(14C)-H(14H)	109.5
H(14G)-C(14C)-H(14H)	109.5
C(13C)-C(14C)-H(14I)	109.5
H(14G)-C(14C)-H(14I)	109.5
H(14H)-C(14C)-H(14I)	109.5
C(13C)-C(15C)-H(15G)	109.5
C(13C)-C(15C)-H(15H)	109.5
H(15G)-C(15C)-H(15H)	109.5
C(13C)-C(15C)-H(15I)	109.5
H(15G)-C(15C)-H(15I)	109.5
H(15H)-C(15C)-H(15I)	109.5
C(13C)-C(16C)-H(16G)	109.5
C(13C)-C(16C)-H(16H)	109.5
H(16G)-C(16C)-H(16H)	109.5
C(13C)-C(16C)-H(16I)	109.5
H(16G)-C(16C)-H(16I)	109.5
H(16H)-C(16C)-H(16I)	109.5
C(6D)-C(1D)-C(2D)	116.62(12)
C(6D)-C(1D)-Si(4)	121.92(10)

C(2D)-C(1D)-Si(4)	121.39(10)
C(3D)-C(2D)-C(1D)	121.59(14)
C(3D)-C(2D)-H(2D)	119.2
C(1D)-C(2D)-H(2D)	119.2
C(4D)-C(3D)-C(2D)	120.35(14)
C(4D)-C(3D)-H(3D)	119.8
C(2D)-C(3D)-H(3D)	119.8
C(3D)-C(4D)-C(5D)	119.49(14)
C(3D)-C(4D)-H(4D)	120.3
C(5D)-C(4D)-H(4D)	120.3
C(4D)-C(5D)-C(6D)	120.17(15)
C(4D)-C(5D)-H(5D)	119.9
C(6D)-C(5D)-H(5D)	119.9
C(5D)-C(6D)-C(1D)	121.74(14)
C(5D)-C(6D)-H(6D)	119.1
C(1D)-C(6D)-H(6D)	119.1
C(12D)-C(7D)-C(8D)	117.20(12)
C(12D)-C(7D)-Si(4)	119.94(10)
C(8D)-C(7D)-Si(4)	122.83(10)
C(9D)-C(8D)-C(7D)	121.54(14)
C(9D)-C(8D)-H(8D)	119.2
C(7D)-C(8D)-H(8D)	119.2
C(10D)-C(9D)-C(8D)	119.86(14)
C(10D)-C(9D)-H(9D)	120.1
C(8D)-C(9D)-H(9D)	120.1
C(9D)-C(10D)-C(11D)	119.81(14)
C(9D)-C(10D)-H(10D)	120.1
C(11D)-C(10D)-H(10D)	120.1
C(10D)-C(11D)-C(12D)	120.22(15)
C(10D)-C(11D)-H(11D)	119.9
C(12D)-C(11D)-H(11D)	119.9
C(11D)-C(12D)-C(7D)	121.34(13)
C(11D)-C(12D)-H(12D)	119.3
C(7D)-C(12D)-H(12D)	119.3
C(16D)-C(13D)-C(15D)	107.94(13)
C(16D)-C(13D)-C(14D)	109.95(14)
C(15D)-C(13D)-C(14D)	107.90(12)
C(16D)-C(13D)-Si(4)	110.88(10)
C(15D)-C(13D)-Si(4)	108.23(10)
C(14D)-C(13D)-Si(4)	111.79(10)
C(13D)-C(14D)-H(14J)	109.5
C(13D)-C(14D)-H(14K)	109.5
H(14J)-C(14D)-H(14K)	109.5
C(13D)-C(14D)-H(14L)	109.5
H(14J)-C(14D)-H(14L)	109.5
H(14K)-C(14D)-H(14L)	109.5
C(13D)-C(15D)-H(15J)	109.5
C(13D)-C(15D)-H(15K)	109.5
H(15J)-C(15D)-H(15K)	109.5
C(13D)-C(15D)-H(15L)	109.5
H(15J)-C(15D)-H(15L)	109.5
H(15K)-C(15D)-H(15L)	109.5
C(13D)-C(16D)-H(16J)	109.5
C(13D)-C(16D)-H(16K)	109.5
H(16J)-C(16D)-H(16K)	109.5
C(13D)-C(16D)-H(16L)	109.5
H(16J)-C(16D)-H(16L)	109.5

H(16K)-C(16D)-H(16L)	109.5
Si(1)-O(1)-H(1)	109.5
Si(2)-O(2)-H(2)	109.5
Si(3)-O(3)-H(3)	109.5
Si(4)-O(4)-H(4)	109.5
O(1)-Si(1)-C(7A)	108.63(6)
O(1)-Si(1)-C(1A)	108.35(5)
C(7A)-Si(1)-C(1A)	109.99(6)
O(1)-Si(1)-C(13A)	105.67(6)
C(7A)-Si(1)-C(13A)	109.86(6)
C(1A)-Si(1)-C(13A)	114.12(6)
O(2)-Si(2)-C(1B)	108.90(5)
O(2)-Si(2)-C(7B)	107.61(5)
C(1B)-Si(2)-C(7B)	111.13(6)
O(2)-Si(2)-C(13B)	105.96(5)
C(1B)-Si(2)-C(13B)	108.25(5)
C(7B)-Si(2)-C(13B)	114.74(6)
O(3)-Si(3)-C(1C)	108.39(5)
O(3)-Si(3)-C(7C)	108.10(5)
C(1C)-Si(3)-C(7C)	111.25(6)
O(3)-Si(3)-C(13C)	106.20(6)
C(1C)-Si(3)-C(13C)	109.86(6)
C(7C)-Si(3)-C(13C)	112.80(6)
O(4)-Si(4)-C(7D)	109.08(5)
O(4)-Si(4)-C(1D)	108.63(5)
C(7D)-Si(4)-C(1D)	108.29(6)
O(4)-Si(4)-C(13D)	105.04(5)
C(7D)-Si(4)-C(13D)	110.82(6)
C(1D)-Si(4)-C(13D)	114.82(6)

Table 4. Anisotropic displacement parameters [$\text{\AA}^2 \times 10^3$] for 08mz220_0m. The anisotropic displacement factor exponent takes the form: $-2 \pi^2 [(h a^*)^2 U_{11} + \dots + 2 h k a^* b^* U_{12}]$

	U11	U22	U33	U23	U13	U12
C(1A)	21(1)	24(1)	25(1)	5(1)	6(1)	5(1)
C(2A)	31(1)	23(1)	33(1)	1(1)	13(1)	2(1)
C(3A)	37(1)	30(1)	38(1)	1(1)	20(1)	3(1)
C(4A)	29(1)	31(1)	39(1)	6(1)	14(1)	-2(1)
C(5A)	50(1)	25(1)	39(1)	-2(1)	15(1)	-7(1)
C(6A)	46(1)	27(1)	32(1)	-2(1)	16(1)	0(1)
C(7A)	24(1)	24(1)	27(1)	8(1)	8(1)	5(1)
C(8A)	24(1)	32(1)	32(1)	8(1)	10(1)	5(1)
C(9A)	29(1)	36(1)	41(1)	3(1)	12(1)	-3(1)
C(10A)	42(1)	25(1)	44(1)	1(1)	17(1)	-1(1)
C(11A)	35(1)	28(1)	52(1)	5(1)	18(1)	9(1)
C(12A)	24(1)	27(1)	47(1)	7(1)	11(1)	5(1)
C(13A)	34(1)	35(1)	26(1)	11(1)	3(1)	8(1)
C(14A)	28(1)	73(1)	46(1)	27(1)	0(1)	10(1)
C(15A)	39(1)	57(1)	33(1)	24(1)	12(1)	17(1)
C(16A)	99(2)	44(1)	27(1)	3(1)	-2(1)	1(1)

C(1B)	24(1)	19(1)	21(1)	3(1)	7(1)	4(1)
C(2B)	28(1)	28(1)	23(1)	7(1)	7(1)	4(1)
C(3B)	40(1)	31(1)	29(1)	13(1)	14(1)	6(1)
C(4B)	36(1)	25(1)	43(1)	10(1)	19(1)	0(1)
C(5B)	27(1)	26(1)	39(1)	4(1)	7(1)	-2(1)
C(6B)	26(1)	22(1)	25(1)	3(1)	5(1)	2(1)
C(7B)	22(1)	23(1)	18(1)	1(1)	4(1)	3(1)
C(8B)	26(1)	34(1)	33(1)	13(1)	7(1)	7(1)
C(9B)	34(1)	43(1)	40(1)	18(1)	5(1)	15(1)
C(10B)	23(1)	43(1)	38(1)	4(1)	3(1)	11(1)
C(11B)	25(1)	36(1)	42(1)	5(1)	12(1)	3(1)
C(12B)	27(1)	28(1)	32(1)	8(1)	11(1)	6(1)
C(13B)	24(1)	21(1)	23(1)	2(1)	7(1)	2(1)
C(14B)	32(1)	35(1)	24(1)	-5(1)	3(1)	3(1)
C(15B)	31(1)	24(1)	29(1)	4(1)	8(1)	9(1)
C(16B)	38(1)	23(1)	51(1)	7(1)	21(1)	0(1)
C(1C)	26(1)	20(1)	23(1)	7(1)	6(1)	5(1)
C(2C)	29(1)	28(1)	29(1)	6(1)	4(1)	2(1)
C(3C)	26(1)	47(1)	40(1)	12(1)	-1(1)	1(1)
C(4C)	30(1)	52(1)	46(1)	24(1)	11(1)	18(1)
C(5C)	45(1)	35(1)	41(1)	12(1)	14(1)	21(1)
C(6C)	35(1)	25(1)	32(1)	4(1)	4(1)	8(1)
C(7C)	27(1)	22(1)	20(1)	2(1)	3(1)	1(1)
C(8C)	29(1)	31(1)	24(1)	6(1)	5(1)	4(1)
C(9C)	30(1)	34(1)	28(1)	6(1)	-2(1)	4(1)
C(10C)	51(1)	39(1)	20(1)	1(1)	-2(1)	10(1)
C(11C)	56(1)	55(1)	22(1)	-1(1)	9(1)	23(1)
C(12C)	38(1)	42(1)	25(1)	3(1)	5(1)	16(1)
C(13C)	26(1)	33(1)	27(1)	12(1)	4(1)	-1(1)
C(14C)	73(1)	36(1)	73(1)	9(1)	28(1)	-18(1)
C(15C)	30(1)	68(1)	35(1)	32(1)	5(1)	4(1)
C(16C)	24(1)	76(1)	36(1)	28(1)	7(1)	5(1)
C(1D)	22(1)	24(1)	24(1)	3(1)	8(1)	0(1)
C(2D)	27(1)	38(1)	26(1)	2(1)	4(1)	6(1)
C(3D)	28(1)	45(1)	30(1)	-11(1)	5(1)	1(1)
C(4D)	46(1)	27(1)	46(1)	-8(1)	22(1)	-5(1)
C(5D)	65(1)	25(1)	41(1)	9(1)	23(1)	9(1)
C(6D)	46(1)	26(1)	26(1)	5(1)	12(1)	5(1)
C(7D)	28(1)	22(1)	20(1)	3(1)	9(1)	4(1)
C(8D)	40(1)	28(1)	26(1)	4(1)	13(1)	1(1)
C(9D)	61(1)	32(1)	24(1)	9(1)	17(1)	7(1)
C(10D)	60(1)	41(1)	20(1)	3(1)	3(1)	10(1)
C(11D)	43(1)	45(1)	29(1)	1(1)	-2(1)	-4(1)
C(12D)	34(1)	31(1)	25(1)	4(1)	6(1)	-2(1)
C(13D)	23(1)	31(1)	36(1)	9(1)	8(1)	6(1)
C(14D)	41(1)	55(1)	44(1)	1(1)	-9(1)	22(1)
C(15D)	38(1)	34(1)	44(1)	7(1)	14(1)	16(1)
C(16D)	29(1)	58(1)	101(2)	36(1)	30(1)	9(1)
O(1)	26(1)	32(1)	24(1)	12(1)	10(1)	13(1)
O(2)	28(1)	25(1)	17(1)	4(1)	6(1)	10(1)
O(3)	34(1)	20(1)	18(1)	4(1)	8(1)	7(1)
O(4)	24(1)	23(1)	26(1)	10(1)	12(1)	6(1)
Si(1)	20(1)	24(1)	23(1)	6(1)	7(1)	7(1)
Si(2)	20(1)	20(1)	16(1)	4(1)	5(1)	3(1)
Si(3)	22(1)	19(1)	18(1)	4(1)	4(1)	4(1)
Si(4)	20(1)	21(1)	20(1)	5(1)	7(1)	2(1)

Table 5. Hydrogen coordinates ($\times 10^4$) and isotropic displacement parameters ($\text{\AA}^2 \times 10^3$) for 08mz220_0m.

	x	y	z	U (eq)
H(2A)	4320	9209	3741	35
H(3A)	3278	8396	4451	41
H(4A)	2737	6819	3906	39
H(5A)	3307	6045	2678	47
H(6A)	4364	6847	1973	42
H(8A)	7143	10066	2854	34
H(9A)	7524	11614	3579	42
H(10A)	6210	12530	3923	44
H(11A)	4520	11892	3533	45
H(12A)	4134	10343	2806	39
H(14A)	3609	9078	266	71
H(14B)	3979	9808	1157	71
H(14C)	3349	8836	1151	71
H(15A)	6329	8939	758	60
H(15B)	5767	9874	951	60
H(15C)	5467	9173	35	60
H(16A)	4125	7335	674	88
H(16B)	5325	7353	661	88
H(16C)	4585	7657	-106	88
H(2B)	7659	7023	6324	31
H(3B)	6434	6180	6850	38
H(4B)	4837	5689	6008	40
H(5B)	4451	6069	4648	37
H(6B)	5672	6900	4109	29
H(8B)	8763	6320	5542	36
H(9B)	10400	5836	5719	45
H(10B)	11697	6578	5184	42
H(11B)	11334	7768	4421	40
H(12B)	9699	8252	4242	34
H(14D)	8513	9022	6376	48
H(14E)	7311	8865	6364	48
H(14F)	7836	9890	6396	48
H(15D)	6512	9934	5079	41
H(15E)	6082	8883	5070	41
H(15F)	6443	9144	4225	41
H(16D)	8315	10335	5069	54
H(16E)	8348	9537	4240	54
H(16F)	9127	9576	5116	54
H(2C)	9849	5910	3068	34
H(3C)	11442	5345	3332	46
H(4C)	11769	3927	2526	48
H(5C)	10489	3043	1479	46
H(6C)	8884	3583	1231	37
H(8C)	6143	5848	937	33
H(9C)	5511	5814	-506	38
H(10C)	6430	5189	-1576	45
H(11C)	7991	4616	-1191	53
H(12C)	8616	4624	253	42
H(14G)	7435	3323	2112	90
H(14H)	6537	3563	1424	90

H(14I)	6292	3304	2307	90
H(15G)	6975	4416	3720	63
H(15H)	7556	5408	3713	63
H(15I)	8098	4467	3479	63
H(16G)	5638	5012	1831	64
H(16H)	6093	5764	2691	64
H(16I)	5522	4788	2758	64
H(2D)	9556	9595	2907	37
H(3D)	9610	11166	3559	45
H(4D)	9090	12267	2741	49
H(5D)	8453	11780	1269	50
H(6D)	8400	10212	609	38
H(8D)	9466	9207	-351	37
H(9D)	8729	9075	-1791	45
H(10D)	7199	8143	-2340	49
H(11D)	6453	7283	-1461	49
H(12D)	7205	7386	-29	36
H(14J)	11219	7630	2316	73
H(14K)	10099	7726	2550	73
H(14L)	10817	8643	2538	73
H(15J)	9707	6810	265	56
H(15K)	9522	6558	1167	56
H(15L)	10646	6588	926	56
H(16J)	11607	8073	933	86
H(16K)	11107	9043	1125	86
H(16L)	10703	8305	245	86
H(1)	6578	8146	2753	39
H(2)	7647	7187	3396	34
H(3)	8126	6735	2077	35
H(4)	7656	8144	1700	34

Table 6. Torsion angles [deg] for 08mz220_0m.

C(6A)-C(1A)-C(2A)-C(3A)	-1.3(2)
Si(1)-C(1A)-C(2A)-C(3A)	-177.67(12)
C(1A)-C(2A)-C(3A)-C(4A)	-0.3(2)
C(2A)-C(3A)-C(4A)-C(5A)	1.6(2)
C(3A)-C(4A)-C(5A)-C(6A)	-1.2(3)
C(4A)-C(5A)-C(6A)-C(1A)	-0.5(3)
C(2A)-C(1A)-C(6A)-C(5A)	1.7(2)
Si(1)-C(1A)-C(6A)-C(5A)	178.12(13)
C(12A)-C(7A)-C(8A)-C(9A)	1.1(2)
Si(1)-C(7A)-C(8A)-C(9A)	-178.48(11)
C(7A)-C(8A)-C(9A)-C(10A)	-0.5(2)
C(8A)-C(9A)-C(10A)-C(11A)	-0.2(2)
C(9A)-C(10A)-C(11A)-C(12A)	0.2(2)
C(10A)-C(11A)-C(12A)-C(7A)	0.5(2)
C(8A)-C(7A)-C(12A)-C(11A)	-1.1(2)
Si(1)-C(7A)-C(12A)-C(11A)	178.44(12)
C(6B)-C(1B)-C(2B)-C(3B)	1.10(18)
Si(2)-C(1B)-C(2B)-C(3B)	177.31(10)
C(1B)-C(2B)-C(3B)-C(4B)	-0.4(2)
C(2B)-C(3B)-C(4B)-C(5B)	-0.7(2)

C(3B)-C(4B)-C(5B)-C(6B)	1.0(2)
C(4B)-C(5B)-C(6B)-C(1B)	-0.3(2)
C(2B)-C(1B)-C(6B)-C(5B)	-0.79(18)
Si(2)-C(1B)-C(6B)-C(5B)	-177.17(10)
C(12B)-C(7B)-C(8B)-C(9B)	1.6(2)
Si(2)-C(7B)-C(8B)-C(9B)	178.76(11)
C(7B)-C(8B)-C(9B)-C(10B)	-0.1(2)
C(8B)-C(9B)-C(10B)-C(11B)	-1.4(2)
C(9B)-C(10B)-C(11B)-C(12B)	1.4(2)
C(10B)-C(11B)-C(12B)-C(7B)	0.2(2)
C(8B)-C(7B)-C(12B)-C(11B)	-1.6(2)
Si(2)-C(7B)-C(12B)-C(11B)	-178.91(11)
C(6C)-C(1C)-C(2C)-C(3C)	0.5(2)
Si(3)-C(1C)-C(2C)-C(3C)	178.86(11)
C(1C)-C(2C)-C(3C)-C(4C)	0.7(2)
C(2C)-C(3C)-C(4C)-C(5C)	-1.1(2)
C(3C)-C(4C)-C(5C)-C(6C)	0.3(2)
C(4C)-C(5C)-C(6C)-C(1C)	0.9(2)
C(2C)-C(1C)-C(6C)-C(5C)	-1.3(2)
Si(3)-C(1C)-C(6C)-C(5C)	-179.59(11)
C(12C)-C(7C)-C(8C)-C(9C)	2.1(2)
Si(3)-C(7C)-C(8C)-C(9C)	178.82(11)
C(7C)-C(8C)-C(9C)-C(10C)	-1.1(2)
C(8C)-C(9C)-C(10C)-C(11C)	-0.5(2)
C(9C)-C(10C)-C(11C)-C(12C)	1.1(3)
C(10C)-C(11C)-C(12C)-C(7C)	-0.1(3)
C(8C)-C(7C)-C(12C)-C(11C)	-1.5(2)
Si(3)-C(7C)-C(12C)-C(11C)	-178.08(13)
C(6D)-C(1D)-C(2D)-C(3D)	-1.9(2)
Si(4)-C(1D)-C(2D)-C(3D)	-179.00(11)
C(1D)-C(2D)-C(3D)-C(4D)	0.3(2)
C(2D)-C(3D)-C(4D)-C(5D)	1.4(2)
C(3D)-C(4D)-C(5D)-C(6D)	-1.4(2)
C(4D)-C(5D)-C(6D)-C(1D)	-0.2(2)
C(2D)-C(1D)-C(6D)-C(5D)	1.8(2)
Si(4)-C(1D)-C(6D)-C(5D)	178.90(12)
C(12D)-C(7D)-C(8D)-C(9D)	1.1(2)
Si(4)-C(7D)-C(8D)-C(9D)	-176.56(11)
C(7D)-C(8D)-C(9D)-C(10D)	0.7(2)
C(8D)-C(9D)-C(10D)-C(11D)	-1.8(2)
C(9D)-C(10D)-C(11D)-C(12D)	1.0(2)
C(10D)-C(11D)-C(12D)-C(7D)	0.8(2)
C(8D)-C(7D)-C(12D)-C(11D)	-1.8(2)
Si(4)-C(7D)-C(12D)-C(11D)	175.86(12)
C(8A)-C(7A)-Si(1)-O(1)	11.49(12)
C(12A)-C(7A)-Si(1)-O(1)	-168.07(11)
C(8A)-C(7A)-Si(1)-C(1A)	129.92(11)
C(12A)-C(7A)-Si(1)-C(1A)	-49.64(13)
C(8A)-C(7A)-Si(1)-C(13A)	-103.65(11)
C(12A)-C(7A)-Si(1)-C(13A)	76.78(13)
C(2A)-C(1A)-Si(1)-O(1)	115.11(11)
C(6A)-C(1A)-Si(1)-O(1)	-61.05(13)
C(2A)-C(1A)-Si(1)-C(7A)	-3.50(13)
C(6A)-C(1A)-Si(1)-C(7A)	-179.65(11)
C(2A)-C(1A)-Si(1)-C(13A)	-127.48(12)
C(6A)-C(1A)-Si(1)-C(13A)	56.36(13)
C(16A)-C(13A)-Si(1)-O(1)	58.56(14)

C(14A)-C(13A)-Si(1)-O(1)	-178.49(11)
C(15A)-C(13A)-Si(1)-O(1)	-59.95(11)
C(16A)-C(13A)-Si(1)-C(7A)	175.57(12)
C(14A)-C(13A)-Si(1)-C(7A)	-61.48(12)
C(15A)-C(13A)-Si(1)-C(7A)	57.06(11)
C(16A)-C(13A)-Si(1)-C(1A)	-60.38(14)
C(14A)-C(13A)-Si(1)-C(1A)	62.57(12)
C(15A)-C(13A)-Si(1)-C(1A)	-178.89(9)
C(6B)-C(1B)-Si(2)-O(2)	-18.92(11)
C(2B)-C(1B)-Si(2)-O(2)	164.94(10)
C(6B)-C(1B)-Si(2)-C(7B)	-137.29(10)
C(2B)-C(1B)-Si(2)-C(7B)	46.57(12)
C(6B)-C(1B)-Si(2)-C(13B)	95.84(10)
C(2B)-C(1B)-Si(2)-C(13B)	-80.30(11)
C(8B)-C(7B)-Si(2)-O(2)	-120.42(11)
C(12B)-C(7B)-Si(2)-O(2)	56.66(11)
C(8B)-C(7B)-Si(2)-C(1B)	-1.27(13)
C(12B)-C(7B)-Si(2)-C(1B)	175.81(10)
C(8B)-C(7B)-Si(2)-C(13B)	121.95(11)
C(12B)-C(7B)-Si(2)-C(13B)	-60.97(12)
C(16B)-C(13B)-Si(2)-O(2)	-65.60(11)
C(14B)-C(13B)-Si(2)-O(2)	172.23(9)
C(15B)-C(13B)-Si(2)-O(2)	53.91(9)
C(16B)-C(13B)-Si(2)-C(1B)	177.71(10)
C(14B)-C(13B)-Si(2)-C(1B)	55.54(10)
C(15B)-C(13B)-Si(2)-C(1B)	-62.78(10)
C(16B)-C(13B)-Si(2)-C(7B)	52.96(12)
C(14B)-C(13B)-Si(2)-C(7B)	-69.21(10)
C(15B)-C(13B)-Si(2)-C(7B)	172.48(8)
C(2C)-C(1C)-Si(3)-O(3)	13.94(12)
C(6C)-C(1C)-Si(3)-O(3)	-167.81(10)
C(2C)-C(1C)-Si(3)-C(7C)	132.66(10)
C(6C)-C(1C)-Si(3)-C(7C)	-49.08(12)
C(2C)-C(1C)-Si(3)-C(13C)	-101.71(11)
C(6C)-C(1C)-Si(3)-C(13C)	76.55(12)
C(12C)-C(7C)-Si(3)-O(3)	118.96(12)
C(8C)-C(7C)-Si(3)-O(3)	-57.57(11)
C(12C)-C(7C)-Si(3)-C(1C)	0.06(14)
C(8C)-C(7C)-Si(3)-C(1C)	-176.47(10)
C(12C)-C(7C)-Si(3)-C(13C)	-123.92(12)
C(8C)-C(7C)-Si(3)-C(13C)	59.55(12)
C(14C)-C(13C)-Si(3)-O(3)	177.91(12)
C(15C)-C(13C)-Si(3)-O(3)	-61.90(11)
C(16C)-C(13C)-Si(3)-O(3)	56.47(11)
C(14C)-C(13C)-Si(3)-C(1C)	-65.07(13)
C(15C)-C(13C)-Si(3)-C(1C)	55.12(12)
C(16C)-C(13C)-Si(3)-C(1C)	173.49(10)
C(14C)-C(13C)-Si(3)-C(7C)	59.68(14)
C(15C)-C(13C)-Si(3)-C(7C)	179.86(10)
C(16C)-C(13C)-Si(3)-C(7C)	-61.77(12)
C(12D)-C(7D)-Si(4)-O(4)	-2.65(12)
C(8D)-C(7D)-Si(4)-O(4)	174.91(10)
C(12D)-C(7D)-Si(4)-C(1D)	-120.70(11)
C(8D)-C(7D)-Si(4)-C(1D)	56.85(12)
C(12D)-C(7D)-Si(4)-C(13D)	112.52(11)
C(8D)-C(7D)-Si(4)-C(13D)	-69.93(12)
C(6D)-C(1D)-Si(4)-O(4)	-116.88(11)

C(2D)-C(1D)-Si(4)-O(4)	60.08(12)
C(6D)-C(1D)-Si(4)-C(7D)	1.46(13)
C(2D)-C(1D)-Si(4)-C(7D)	178.43(10)
C(6D)-C(1D)-Si(4)-C(13D)	125.88(11)
C(2D)-C(1D)-Si(4)-C(13D)	-57.15(12)
C(16D)-C(13D)-Si(4)-O(4)	176.48(12)
C(15D)-C(13D)-Si(4)-O(4)	58.27(11)
C(14D)-C(13D)-Si(4)-O(4)	-60.43(12)
C(16D)-C(13D)-Si(4)-C(7D)	58.82(13)
C(15D)-C(13D)-Si(4)-C(7D)	-59.40(11)
C(14D)-C(13D)-Si(4)-C(7D)	-178.09(11)
C(16D)-C(13D)-Si(4)-C(1D)	-64.26(14)
C(15D)-C(13D)-Si(4)-C(1D)	177.52(9)
C(14D)-C(13D)-Si(4)-C(1D)	58.83(13)

Table 7. Hydrogen bonds for 08mz220_0m [\AA and deg].

D-H...A	d(D-H)	d(H...A)	d(D...A)	<(DHA)
O(4)-H(4)...O(1)	0.84	1.99	2.7393(12)	148.1
O(3)-H(3)...O(4)	0.84	1.91	2.7025(12)	157.8
O(2)-H(2)...O(3)	0.84	1.90	2.6955(12)	156.5
O(1)-H(1)...O(2)	0.84	1.95	2.7370(12)	156.6
